Kimberlite Weathering: Mineralogy and Mechanism

By

JACQUELINE MORKEL

A dissertation submitted in partial fulfilment of the requirements for the degree

PHILOSOPHIAE DOCTOR
(METALLURGICAL ENGINEEERING)

in the

Faculty of Engineering, Built Environment and Information Technology

University of Pretoria

Pretoria

2006

Kimberlite Weathering: Mineralogy and Mechanism

STUDENT: **JACQUELINE MORKEL**

SUPERVISORS: **M.K.G. VERMAAK AND P.C. PISTORIUS**

DEPARTMENT: **MATERIALS SCIENCE AND METALLURGICAL ENGINEERING**

DEGREE: **PHILOSOPHIAE DOCTOR (METALLURGICAL ENGINEERING)**

ABSTRACT

The aim of this study was to arrive at a fundamental understanding of kimberlite weathering and of factors which affect the rate and extent of weathering. Weathering was evaluated by measuring the change in size distribution after immersing crushed kimberlite in solutions of various compositions. Reproducibility of the measurements was found to be good, with the cumulative mass passing a given size differing by 7% or less, as tested for various weathering conditions.

Kimberlite mineralogy, specifically the swelling clay content, was found to play a central role: kimberlite ores containing no swelling clay were not prone to weathering under any of the conditions tested.

The cation exchange capacity (CEC) correlates well with the swelling clay content and with the weathering behaviour. The cation exchange capacity may be used in conjunction with the swelling clay content, as a predictor of possible kimberlite behaviour; however, given the relative complexity and cost of measuring swelling clay content (by X-ray diffraction), the CEC is the preferred parameter for practical use.

Cations in the weathering solution have a strong effect on kimberlite weathering; the strength of the effect followed the series $Cu^{2+} > Li^+ > Fe^{2+} > Ca^{2+} > Fe^{3+} > Mg^{2+}$, whereas K^+ and NH_4^+ stabilised the kimberlite somewhat against weathering. This sequence was in reasonable

correlation with the ionic potential (ratio of valency to ionic radius), but with exceptionally strong weathering effects of Cu^{2+}, and (to a lesser extent) of Li^+ and Fe^{2+}. The strong effect of the latter group of cations may be related to their tendency to adsorb onto other crystal sites in addition to the interlayer – the associated change in surface energy can change the fracture behaviour of the kimberlite.

Measurement of the layer spacing of the swelling clay (by X-ray diffraction) showed no correlation between the weathering effect of a cation and the associated thickness of the interlayer. For solutions of cupric ions, the identity of the anion (chloride or sulphate) has little effect on weathering. The size of the crushed kimberlite ore similarly has little effect on the relative extent of size degradation by weathering.

The concentration of cupric ions affects weathering, as does the weathering time – although 85% of the weathering caused by 30 days' exposure was found to occur within the first 24 hours. Increasing the temperature to 40°C (in a magnesium chloride solution) also increased weathering strongly. The kinetics of exchange of cuprous and potassium ions was measured (for two different kimberlites); the apparent reaction order (with respect to the concentration of exchanging cations in solution) varied between 1 and 3.5, and exchange of potassium was more rapid.

This work has practical implications for in-plant processing of kimberlite, possible alternative kimberlite processing routes which eliminate one or more crushing steps, and for the stability of mine tunnels which pass through kimberlite.

KEYWORDS: Kimberlite, weathering, swelling, mineralogy, clay minerals, accelerated weathering, cation exchange

ACKNOWLEDGEMENT

Firstly I thank the Lord Jesus Christ for the abilities and talents He blessed me with. Also for His divine inspiration and for giving me hope in the times it felt that there was none.   I thank my husband for his continued support and understanding and for always being there. I thank Dr. Thys Vermaak for his technical support and also friendship during this time. I would also like to thank the University of Pretoria colleaques, especially Sarah Havenga for her administrative functions and her friendship. I am grateful to my parents for the opportunities they provided, for always being there and supporting me.   I am grateful to De Beers, especially Mr. Pete Sergeant for his contributions and Richard Kekana for the supply of ore resources. Other De Beers colleques that contributed are Leon Kruger and Serkan Saydam. Thanks to Fanie Kruger at Mintek for the hours spent on XRD work to characterise the mineralogy and also Sabine Verryn at the University of Pretoria. Prof Pistorius deserves a special acknowledgement for his time, technical guidance, editing and contributing to my personal growth.

My wish is that this study will really improve the understanding of weathering and the impact thereof on kimberlite material. I hope wholeheartedly that this goal was achieved.

Heb 13:21 May God make you perfect in every good work to do his will, working in you that which is wellpleasing in his sight, through Jesus Christ; to whom *be* glory forever and ever.

LIST OF FIGURES

Figure 75. Venetia K1 Hypabyssal South kimberlite unweathered (left) compared to the weathered product (right). Weathering was done in a 0.05 M cupric sulphate solution for 6 days.

Figure 76. Venetia K1 TKB East kimberlite unweathered (left) compared to the weathered product (right). Weathering was done in a 0.05 M cupric sulphate solution for 6 days.

Figure 77. Venetia K2 South kimberlite unweathered (left) compared to the weathered product (right). Weathering was done in a 0.05 M cupric sulphate solution for 6 days.

Figure 78. Venetia K2 North East kimberlite unweathered (left) compared to the weathered product (right). Weathering was done in a 0.05 M cupric sulphate solution for 6 days.

Figure 79. Venetia K2 West kimberlite unweathered (left) compared to the weathered product (right). Weathering was done in a 0.05 M cupric sulphate solution for 6 days.

Figure 80. Venetia K8 unweathered (left) compared to the weathered product (right). Weathering was done in a 0.05 M cupric sulphate solution for 6 days.

Figure 81. Venetia Red kimberlite unweathered (left) compared to the weathered product (right). Weathering was done in a 0.05 M cupric sulphate solution for 6 days.

Figure 82. Results of weathering tests performed on Venetia kimberlites (- 26.5 + 22.4 mm) in a 0.05 M cupric sulphate solution for 6 days.

Figure 83a. Comparing weathering results with the smectite content of Venetia ores. Weathering is shown as log cumulative % passing at 10.3 mm from figure 82 (6 days' weathering in 0.05 M copper sulphate).

Figure 83b. Comparing weathering results with cation exchange capacity of Venetia ores. Weathering is shown as log cumulative % passing at 10.3 mm from figure 82 (6 days' weathering in 0.05 M copper sulphate).

Figure 84. Repeatability of the weathering tests were evaluated by triplicate tests at 0.025, 0.1 and 0.5 M copper concentration. Tests were done on 300 g, -16 + 13.2 mm Dutoitspan kimberlite.

Figure 85. ICP analysis results displaying the steady decrease of the concentration of copper in the weathering solution as a function of time. The lines are fitted curves for simple n^{th} - order kinetics (parameters of curve fits in table 25).

Figure 86. ICP analysis results displaying the release of sodium, potassium, calcium and the sum of minor cations (K^+, Ca^{2+}, Mg^{2+} and Al^{3+}) from the kimberlite into the 0.025 M copper solution.

Figure 87. ICP analysis results displaying the release of sodium, potassium, calcium and the sum of minor cations (K^+, Ca^{2+}, Mg^{2+} and Al^{3+}) from the kimberlite into the 0.1 M copper solution.

Figure 88. ICP analysis results displaying the release of sodium, potassium, calcium and the sum of minor cations (K^+, Ca^{2+}, Mg^{2+} and Al^{3+}) from the kimberlite into the 0.5 M copper solution.

Figure 89. ICP analysis results displaying the release of sodium from the kimberlite into the solution at 0.025, 0.1 and 0.5 M copper concentration.

Figure 90. ICP analysis results displaying the release of the sum of other cations (K^+, Ca^{2+}, Mg^{2+} and Al^{3+}) from the kimberlite into the solution at 0.025, 0.1 and 0.5 M copper concentration.

Figure 91. A plot of log dC/dt vs. log (C-C_∞) for the 0.025 M copper weathering test. Time in hours, (C-C_∞) in mmol/l and dC/dt in mmol/(lxh).

LIST OF TABLES

ABBREVIATIONS

XRD: X-Ray Diffraction

XRF: X-Ray Fluorescence

Cpht: Carats per hundred tons of ore

ESP: Exchangable Sodium Percentage

CEC: Cation Exchange Capacity

REE: Rare Earth Elements

TKB: Tuffisitic Kimberlite Breccia

HYP: Hypabyssal Kimberlite

ppm: Parts per million

s: Seconds

μm: micrometer

LIST OF APPENDIXES

Appendix A: Specifications on XRD work done at University of Pretoria and Mintek

Appendix B: Original XRD Data

Appendix C: Size distribution data

Appendix D: Slake Durability data

1   BACKGROUND

1.1   Project Definition

Weathering in the context of this study refers to the rapid breakdown of kimberlite material with a specific mineralogy when exposed to water. Kimberlite weathering/degradation is often neglected in process design, plant operation, maintenance, modelling and simulation. This can have serious process implications, since some kimberlites can be totally reduced to fines within minutes of contact with water while others are not prone to weathering degradation at all. These distinctly different types of material influence many plant operations, including crushing, desliming, dense medium separation and settling. If the behaviour of kimberlite material can be anticipated it will allow for preventative measures in managing and controlling the treatment plant. Understanding of the kimberlite weathering mechanism also creates opportunities of accelerating the weathering process and possibly developing new processing options.

The project initiated by De Beers firstly aimed to define the mineralogy of kimberlite, especially the clay systems which are present in kimberlite. The study then focused on identifying the critical parameters in the weathering process. With this understanding, new work on accelerating the weathering process can be suggested and feasibility of such processes investigated. On the other hand, weathering of kimberlite poses risks underground due to unstable tunnels and the knowledge on the weathering mechanism might provide means of decelerating or preventing weathering.

1.2   Diamond Processing

A generalised flow sheet for diamond extraction is shown as figure 1 (Hodgson, 1981). It consists of two groups of techniques namely liberation and concentration. The processing starts with the run of mine ore being crushed in two or three stages of primary comminution. The material is then fed to a scrubbing section where the fine material (< 1mm) is washed off and removed by screening. The fine material is thickened and dumped as tailings with the water being recovered and recycled. The washed ore is usually sized by screening and sent for further treatment in these size fractions. The primary concentration is usually by dense medium separation and then final concentration typically occurs by grease tables followed by X-ray sorting machines. The waste material of the fines processing stream is dumped as tailings whereas the waste material from the coarse stream is usually re-crushed to ensure that smaller diamonds are liberated before discarding the material.
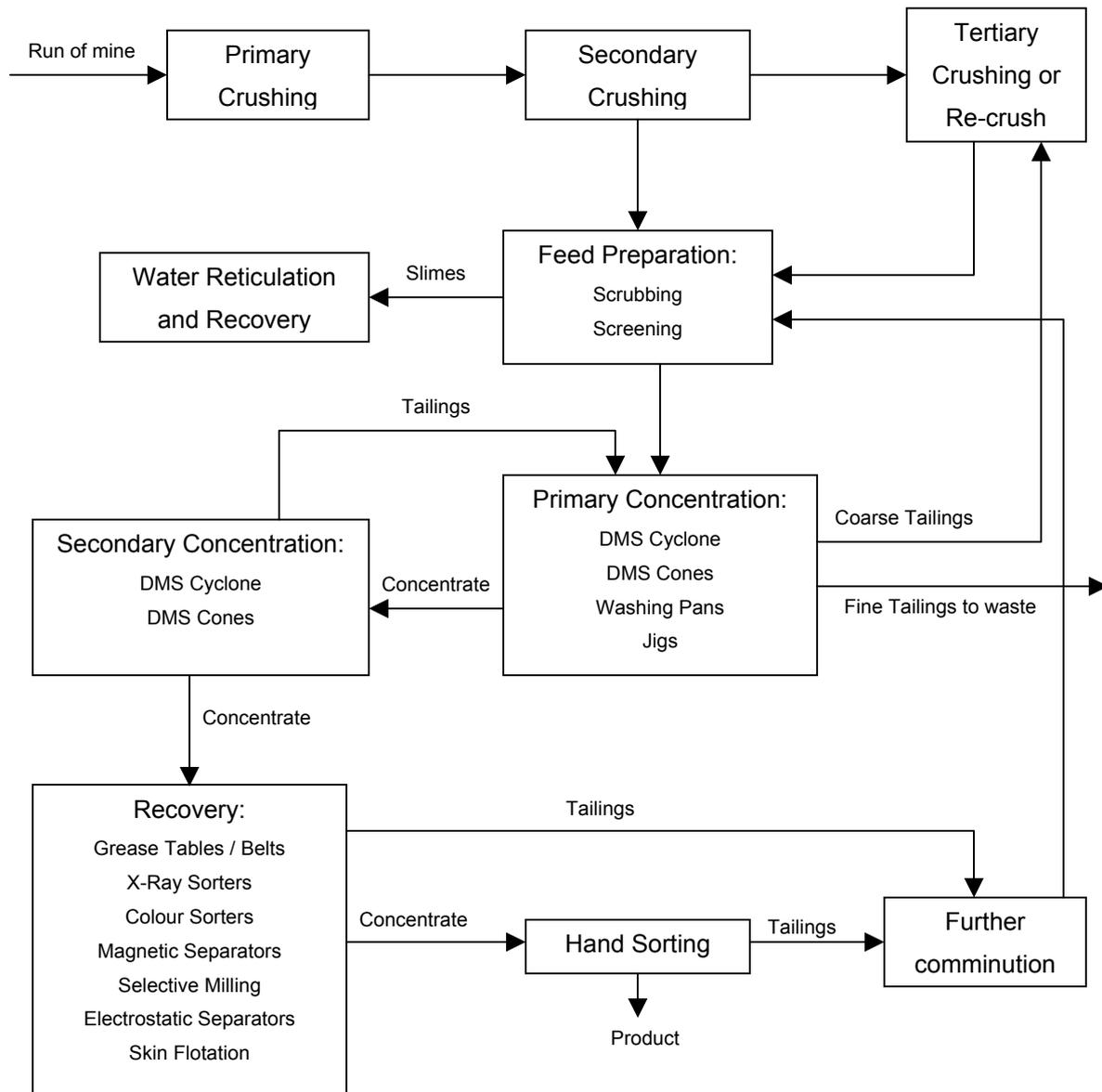
Figure 1. Generalised flowsheet for diamond extraction (Hodgson, 1981).

Weathering affects several aspects of diamond processing. Firstly because weathering causes decreased bulk strength the crushing requirement differs according to the mineralogy and state of weathering of the kimberlite. Therefore overcrushing of softer, more weathered material can occur and can also imply that diamond breakage can occur. Weathering on some ores can cause total failure with predominantly fine material as product. This increases the required capacity to handle slimes and influences the water regeneration and flocculation circuits. In terms of concentration, weathering can impact on the dense medium separation. There are also other implications for example the stockpiling and transport of material on conveyer belts can cause breakdown of ore after some weathering has taken place.

2

A map of the De Beers operations is shown in figure 2. It is shown here for reference, since kimberlite samples from different South African origins were tested.

Figure 2.   De Beers Operations in Southern Africa (From the De Beers website: www.debeersgroup.com)

2   LITERATURE STUDY

2.1   *KIMBERLITE MINERALOGY*

The diamond bearing ore is referred to as kimberlite and is a rare type of volcanic rock. The kimberlite volcanoes are known as pipes due to their inverted-cone shape (Harlow, 1998). It is suggested that kimberlite pipes form by viscous magma travelling upward through cracks in the rock. The magma continues to dilate and fracture the crust whilst gases dissolved in the kimberlite dissociate from the matrix and expand, thus driving the magma and entrained rocks and diamonds up to the surface at ultrahigh velocities. The swirling fluid consisting of rock, mineral fragments and expanding gases breaks through the surface and forms the characteristic shape called a diatreme. At the top of the kimberlite pipe a crater zone is formed which is quickly stripped away by rain and weathering (Harlow, 1998).

Kimberlites are diverse and complex hybrid rocks consisting of crystals originating from mantle-derived xenoliths, the discrete nodule suite and primary phases crystallizing from the kimberlite magma as described by Mitchell (1986). These volatile rich (CO_2 predominantly) potassic ultrabasic igneous rocks can occur as small volcanic pipes, dykes and sills. Kimberlite is further defined by Mitchell (1986) as inequigranular alkalic peridotites containing rounded and corroded megacrysts, which can include olivine, phlogopite, magnesian ilmenite and pyrope. See table 1 for the chemical composition of these minerals. These macrocrysts (0.5 - 10 mm) are relatively large compared to the fine-grained groundmass and cause the inequigranular nature of kimberlites. These macrocrysts are set in a fine-grained matrix (groundmass) of second generation primary olivine and/or phlogopite together with serpentine, perovskite, calcite and/or dolomite (carbonates) and spinels. Other minerals include diopside, rutile, apatite, monticellite and nickeliferous sulphides. Weathering processes such as serpentization and carbonation commonly alters the early-formed matrix minerals as discussed under section 2.2. This causes replacement of early-formed olivine, phlogopite, monticellite and apatite by serpentine, calcite and chlorite as shown in figure 3. Highly weathered kimberlite can be composed of essentially calcite, serpentine, chlorite, smectite and magnetite together with minor phlogopite, apatite and perovskite. The changes in the crystal structure when clay minerals form, are discussed in section 2.2.5.

Clay minerals formed during the weathering process are classified under the phyllosilicates mineral group (see section 2.2.4.5) and consist of extended sheets of SiO_4^{4-} tetrahedra. The members of this mineralogical group are soft and flaky and have a relatively low specific gravity. Smectite (e.g. montmorillonite and saponite) and vermiculite are swelling clays

4

commonly present in kimberlite. These clay minerals can generate internal pressures due to their swelling nature therefore decreasing the overall strength of the rock. The nature of clay minerals is discussed further in section 2.2.4.

Not all kimberlites contain diamond and if diamonds are present it is a very rare constituent at 5 - 140 carats per hundred tons (cpht) where 1 carat = 0.2 g (Wilson and Anhaeusser, 1998).

Mineralogical classification of kimberlites has been attempted by different authors and is reviewed below.

Wilson and Anhaeusser (1998) proposed classification into two groups. Group I is the olivine rich monticellite-serpentine-calcite kimberlites (< 5 % mica), which correspond to the basaltic kimberlites. Group II is the micaceous kimberlites (> 50 % mica) corresponding to the micaceous lamprophyric kimberlites.

Mitchell (1986) rather suggested three groups based upon the predominance of olivine, phlogopite and calcite e.g. kimberlite (equivalent to basaltic kimberlite), micaceous kimberlite (equivalent to lamprophyric kimberlite), and calcite or calcareous kimberlite.

Skinner and Clement (1979) derived five varieties of kimberlite based upon the predominance of diopside, monticellite, phlogopite, calcite and serpentine.

For this study the approach is to identify the mineralogy of kimberlites and relate it to the mechanism and rate of weathering in the simplest possible way. The mineralogy is therefore rather described in terms of the main mineral groups with little focus on subgroups, cation substitution ratios etc. The focus is also not on the lesser constituents of kimberlites (e.g. garnets, spinels etc.) and further reading, if required, is directed to the work of Mitchell (1986).

The mineral phases commonly present in kimberlites are discussed in the next section.
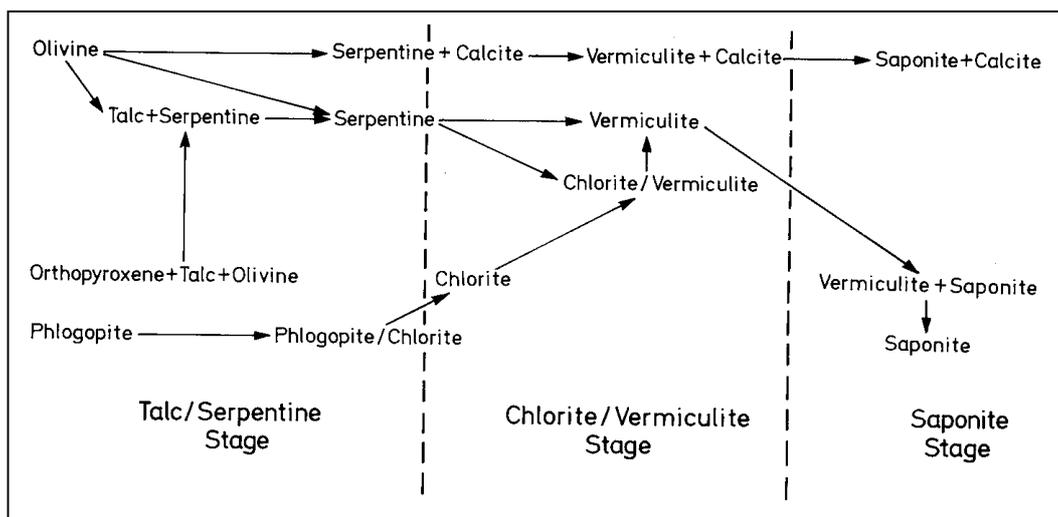
Figure 3. Schematic diagram showing the alteration of olivine, pyroxene and mica (Dawson, 1980).

Table 1. Kimberlite mineral phases (Composed from Klein and Hurlbut, 1993).

Mineral Name	G Specific Gravity	H Hardness	Composition	Comments
Apatite	3.15 - 3.2	5	$Ca_5(PO_4)_3(F,Cl,OH)$	-
Calcite	2.71	3	$CaCO_3$	-
Chlorite	2.6 – 3.3	2 – 2.5	$(Mg,Fe)_3(Si,Al)_4O_{10}(OH)_2 \cdot (Mg,Fe)_3(OH)_6$	Green colour
Diopside	3.2	5 - 6	$CaMgSi_2O_6$	White to light green pyroxene
Dolomite	2.85	3.5 - 4	$CaMg(CO_3)_2$	-
Halloysite	2.0-2.2	1-2	$Al_2Si_2O_5(OH)_4 \cdot 2H_2O$	
Ilmenite	4.7	5.5 - 6	$FeTiO_3$	-
Kaolinite	2.6	2	$Al_2Si_2O_5(OH)_4$	-
Magnetite	5.18	6	Fe_3O_4	Spinel group
Monticellite	3.2	5	$CaMgSiO_4$	Rare olivine alteration product
Montmorillonite	2.5	1 – 1.5	$(Al,Mg)_8(Si_4O_{10})_4(OH)_8 \cdot 12H_2O$	Al rich - Smectite
Olivine	3.27 – 4.37	6.5 - 7	$(Mg,Fe)_2SiO_4$	Green ground-mass mineral
Perovskite	4.03	5.5	$CaTiO_3$	-
Phlogopite	2.86	2.5 - 3	$KMg_3(AlSi_3O_{10})(OH)_2$	Yellow brown Mica
Pyrope	3.58	7	$Mg_3Al_2Si_3O_{12}$	Garnet
Rutile	4.18 – 4.25	6 – 6.5	TiO_2	Reddish brown
Serpentine	2.3	3 - 5	$Mg_3Si_2O_5(OH)_4$	Green to yellow
Spinel	3.5 – 4.1	8	$MgAl_2O_4$	-
Talc	2.7 – 2.8	1	$Mg_3Si_4O_{10}(OH)_2$	-
Vermiculite	2.4	1.5	$(Mg,Ca)_{0.3}(Mg,Fe,Al)_{3.0}(Al,Si)_4O_{10}(OH)_4 \cdot 8H_2O$	Altered (biotite) mica

6

2.1.1 Olivine

Olivine ((Mg,Fe)$_2$SiO$_4$) is originally the commonest and most characteristic mineral in kimberlite, according to Mitchell (1986). As groundmass constituent olivine occurs as single crystals smaller than 0.5 mm with the colour ranging from pale green to pale yellowish-brown with increasing iron (Mitchell, 1986). Magnesian ilmenite, chrome spinel and rutile can be present in some olivine groundmass as inclusions. Primary olivines richer in iron than Fo$_{85}$ are not characteristic of kimberlites. Forsterite ("Fo") refers to the end member of olivine Mg$_2$SiO$_4$, thus Fo$_{100}$ means no substitution of the Mg^{2+} by Fe^{2+} has occurred. Therefore in kimberlites the highest substitution of iron for magnesium in forsterite is 15 %, but is seldom this high.

Due to its high weatherability, olivine is commonly altered along margins and fractures to several varieties (pseudomorphs) of serpentine with or without magnetite (see figure 3). The formation of magnetite when olivine is weathered to serpentine is discussed in section 2.2.2.7. Secondary processes can locally form less prominent alteration minerals e.g. brucite, serpentine, chlorite, calcite, talc, pyrite and other clay minerals (Mitchell, 1986).

Megacrystal olivines, single crystals of 2 – 5 cm in diameter, are present in a few localities but are very rare. Macrocrystal olivines are 0.5 – 1 cm in diameter and occur as round to elliptical single crystals.   The ratio of macrocrystal to groundmass olivines can vary widely. Macrocrysts (fragmented megacrysts) are commonly intergrown with enstatite, Cr-pyrope, ilmenite, diopside, chromite, phlogopite, Cu-Ni sulphides and rutile.   Macrocrysts can commonly be identified by CO$_2$ fluid inclusions.

In this study very little olivine was identified suggesting that weathering has progressed past this point in these specific South African kimberlites.

2.1.2 Phlogopite / Micas

Phologopite (KMg$_3$(AlSi$_3$O$_{10}$)(OH)$_2$) is a silvery bronze mineral consisting of single crystals around 5 mm – 10 cm in diameter. It is often replaced by calcite, chlorite and serpentine especially along cleavage planes. Micas are defined as the finer size fraction of phlogopite (- 5 mm).   Micas are found in the groundmass as well as megacrysts / macrocrysts. Groundmass micas are usually 0.05 – 1 mm large rounded, corroded and distorted crystals. Intergrowth with diopside is found at an extremely fine grain size. Groundmass micas can contain inclusions of spinel and perovskite and can commonly be found within calcite-serpentine segregations. In some kimberlites megacrystal or macrocrystal micas can account for the bulk of the minerals present (> 50 %) and in other cases can be as low as 1%.

7

Dawson and Smith (1977) categorized South African micas into two types as given in table 2.

Table 2. The mica types present in South Africa according to Dawson and Smith (1977), (compositions are in mass percentage).

Mica Type	Mg / (Mg + Fe)	% Al_2O_3	% TiO_2
Type I (Fe rich)	0.45 - 0.65	14 - 16	3 - 6
Type II (Mg rich)	0.82 - 0.93	6.8 - 14.2	0.07 - 0.4

2.1.3 Serpentine

Serpentine ($Mg_3Si_2O_5(OH)_4$) can account for up to 50 % of the groundmass minerals. It is usually very fine grained and finely intergrown with other phases. Serpentine is usually classified according to different pseudomorphs of serpentine called lizardite, antigorite and chrysotile. These subgroups of serpentine have characteristic features of appearance e.g. antigorite is flaky and lamellar whilst chrysotile is fibrous. These subgroups of serpentine cannot be detected by conventional XRD due to the poor crystallinity of serpentine.

2.1.4 Monticellite

Monticellite ($CaMgSiO_4$) occurs as very fine particles (0.005 – 0.08 mm), from trace to 60 – 80 % of the groundmass of kimberlites. This mineral is very difficult to identify, as it is colourless and finely dispersed. It is very easily replaced by calcite in the weathering process, which could account for its absence in some kimberlites. The mineral is relatively pure in kimberlites (close to $CaMgSiO_4$ in composition) although in some cases a trend for solid solution towards forsterite (Mg_2SiO_4) can occur.

2.1.5 Perovskite

Perovskite ($CaTiO_3$) usually accounts for trace amounts up to 10 % in kimberlites. In rare occasions where perovskite and spinel have been concentrated in the kimberlite due to magmatic processes it can rise up to 25 %. The crystals range from 0.05 – 0.2 mm in size and can be scattered throughout the groundmass or concentrated together with spinel phases.   The colour can range from yellow-brown through brown to reddish-brown. Perovskite in kimberlite is relatively pure $CaTiO_3$ and very little substitution takes place. Small amounts of rare earth elements (REE) can report in this mineral phase.

2.1.6 Carbonates (calcite and dolomite)

Calcite ($CaCO_3$) is the predominant carbonate in kimberlites and can report at trace levels to over 50 % in calcite rich kimberlites. It is usually pure with low MgO and FeO impurities. Dolomite is present as an accessory phase in small quantities. A few other carbonates can occur in minute quantities e.g. aragonite ($CaCO_3$) and strontianite ($SrCO_3$).

2.1.7 Chlorite

Chorite has been found in four parageneses according to Mitchell (1986):

1. *Replacing serpentinized olivine.* Olivines are initially transformed to serpentine, which is transformed to chlorite and ultimately to vermiculite as shown by figure 3.
2. *Discrete nodules of chlorite* are 1 – 4 cm in size and can be categorized according to the iron content into high, intermediate and low iron chlorites. In kimberlites it is typically the low iron chlorites that are predominant.
3. *Replacing phlogopites*. Chlorite readily replaces phlogopites along cleavage planes and grain boundaries. These chlorites vary from colourless to pale green to bright emerald green in highly weathered micaceous kimberlites.
4. *Primary groundmass chlorites* are identified by blue-green platelets of ~ 0.05 mm and are only found in calcite rich samples. It is very rare in phlogopite and serpentine rich kimberlites.

2.1.8 Clay minerals

A wide variety of clay minerals has been reported in kimberlites such as montmorillonite, halloysite, kaolinite, sepiolite, vermiculite, talc, saponite etc. (Mitchell, 1986). Classification of clay minerals is not consistent and differs from author to author. Predominant clay minerals in kimberlite are discussed further in section 2.2.5.

2.1.9 Spinel

Groundmass spinel (0.001 - 0.1 mm) can typically comprise 1 – 30 weight % of the kimberlite. The composition of most kimberlite spinels fall within the eight-component system: $MgCr_2O_4$ (magnesiochromite), $FeCr_2O_4$ (chromite), $MgAl_2O_4$ (spinel), $FeAl_2O_4$ (hercynite), Mg_2TiO_4 (maganoan ulvöspinel), Fe_2TiO_4 (ulvöspinel), $MgFe_2O_4$ (magnesioferrite), Fe_3O_4 (magnetite). For further information on the spinel groups the reader is referred to Mitchell (1986) for extensive coverage of these mineral phases.

2.1.10 Magnesian Ilmenite

Magnesian ilmenite is a solid solution combination of ilmenite ($FeTiO_3$) and geikielite ($MgTiO_3$). This mineral is relatively resistant to chemical and physical weathering and is easily recognizable by its bright metallic luster. It can account for trace to ~ 10 weight % of kimberlites. Some kimberlites e.g. Koffiefontein and Finsch seem to be devoid of this mineral. It can again occur as a groundmass constituent or as megacrysts/macrocrysts and is largely intergrown with other minerals e.g. olivine, phlogopite and spinel. It can occur in the groundmass as grains smaller than 0.5 mm and can be as large as 10 cm. The ilmenites in South Africa are quite enriched in magnesium with 4 – 20 % as MgO.

2.1.11 Pyroxene

Clinopyroxenes are common as megacrysts and groundmass phases compared to orthopyroxenes, which are relative rare due to high weatherability. Most of the clinopyroxenes in kimberlites are chromium poor according to the classification of Mitchell (1986). This specific group is distinguished by a grey-green to dark, bottle-green colour and is usually coated by a fine white alteration product consisting of serpentine, calcite and chlorite. Pyroxene minerals that have been identified are diopside, omphacite and hedenbergite.

2.1.12 Apatite

This phosphate mineral as groundmass constituent (< 0.01 mm grains) can account for as little as 1 % or as much as 10 weight % of the kimberlite. Apatites are usually found in carbonate or calcite rich kimberlites. It is not very stable and is often replaced by calcite. It is considered to be very pure fluoro-hydroxy apatite although significant replacement of the phosphor by silicon can occur.

2.1.13 Garnet

Garnet is a trace kimberlite mineral but characteristic of kimberlites. Its distinctive lilac or purple red pyrobes are easily distinguished and are very resistant to weathering. Therefore this mineral is central in the exploration process. In terms of weathering it is considered insignificant.

2.1.14 Conclusion

The aim of this project is to relate the mineralogy of kimberlites to the weathering process, which is accompanied by a decrease in mechanical properties of the kimberlite rock together with an increase in fines generation and increased stickiness. A simple relationship between the mineralogy and the weathering process is proposed and therefore the mineralogical focus of this study is on the predominant mineral groups rather than detailed, complex and very accurate geological description of the mineralogy. If detailed geological and mineralogical information is required, the reader is referred to Mitchell (1986).

2.2   WEATHERING PRINCIPLES

The weathering mechanisms present can be mechanical, chemical and / or biological. These different mechanisms will be discussed separately although the weathering mechanism in realistic terms is a combination of all the above.

2.2.1 Mechanical Weathering

Mechanical weathering, also termed physical weathering, involves the disintegration of rock without any chemical alteration, although chemical and mechanical weathering usually occur in parallel, enhancing the effects of weathering. Bland and Rolls (1998) suggest the following mechanisms of mechanical weathering:

2.2.1.1   Low temperature, water based weathering

• Freezing of in-place water

Freeze-thaw weathering represents the disintegration of rock when water freezes and expands within the rock. The volumetric expansion of ~ 9 % is due to the hexagonal arrangement that frozen water acquires. Associated with the expansion is internal pressure against walls where Bland and Rolls (1998) quote a pressure of 207 MPa at - 22 °C (under constraint). Even though these temperatures are rarely reached in South Africa, any force larger than 10 MPa can already exceed the tensile strength of some rocks and cause breakdown.

• Water migration and ice growth

This refers to the movement of water to a freezing zone rather than in-place freezing. At temperatures even below 0 °C water can coexist with ice, as the freezing point can be reduced by the presence of salts or by a thin adsorbed water layer or by capillary effects. Factors that modify the behaviour of freezing water include rock properties and environmental conditions. The migration of water is energetically driven by a free energy gradient, which is influenced by rock permeability, temperature and water availability.

2.2.1.2   Hydration shattering

Hydration is in fact a chemical process and discussed in section 2.2.2.1.   However, this chemical process can imply mechanisms for mechanical weathering.   Due to their polarity water molecules are attracted to charged mineral surfaces and an adsorbed layer is formed. The attraction occurs in a certain orientation, which decreases the ability of the water to freeze (even at subzero temperatures), as the energy required to re-orientate may be insufficient.   This can also cause repulsion forces between molecules in small cracks.   This mechanism of weathering is common for carbonates and schists and clay minerals may also be susceptible.

2.2.1.3   Salt weathering

Salts are chemical compounds which form from the reaction between acids and bases.   Salts are important in the weathering process because of the expansionary forces upon thermal expansion, hydration and crystallisation.

Thermal expansion

The thermal expansion coefficient of the salt should exceed that of the surrounding rock for weathering to take place.   For sodium chloride a volumetric expansion of 1 % occurs on a temperature rise of 50 °C, which is greater than any rock.   The internal stresses produced by thermal expansion are less significant than hydration and crystallisation pressures.

Hydration pressure

When salts are hydrated, volumetric expansions of 100 - 300 % can occur generating pressures of 20 - 200 bar.   Sulphates are of particular interest as they can pass through a full hydration - dehydration cycle in 24 hours, if the temperature reaches the transition point at which salts become fully hydrated and then the temperature falls for the dehydration cycle. The chemical process of hydration is discussed in section 2.2.2.1.

13

Crystallisation pressure

Crystallisation can occur when the concentration of a solution is increased at a constant temperature (usually by evaporation) or when the temperature of an almost saturated solution is decreased. Crystallisation is not possible if the solution does not reach saturation. After saturation the salt can crystallise slowly around nuclei or the solution can become super saturated and crystallisation is postponed, but the rate of crystallisation is much higher when it eventually starts. When crystals grow during crystallisation a pressure is generated which is well in excess of the tensile strength of rocks.

Experimental work

Salt weathering can be studied under controlled laboratory conditions where the most common method is to expose different rock types to a range of aqueous salt solutions. A climatic cabinet is usually used to simulate climatic conditions. Such a cabinet allows for the temperature and humidity to be artificially controlled. The weathering tests can thus be accelerated in order to produce results rapidly and to allow for monitoring of the process with a precision that is not possible in field investigations. Bland and Rolls (1998) discuss the weaknesses of the laboratory approach:

- Reproduction of natural climatic conditions is complex

Simulation of the natural heat and humidity as well as climatic cycles is difficult and can not be closely related due to the limitations of experimental equipment and the complexity of natural climatic conditions.

- Representativeness of rock samples

Does the sample used for testing relate to the field conditions in terms of composition, size and shape? The natural stress conditions present in the environment are developed by several mechanisms and are therefore difficult to reproduce.

- Nature of the solutions used in the laboratory experiments

In laboratory experiments single salt-hydrate solutions are usually used whereas complex mixtures are most common in nature.

14

2.2.1.4   Wetting and drying

When wetting and drying occur in cycles e.g. rain followed by evaporation, weathering can occur. When a crack or exposed rock surface is wetted, an adsorbed water layer is formed. The addition of more water may cause swelling pressure. If evaporation now occurs the water not adsorbed will be removed which will now cause attractive forces between residual water molecules on opposing wall surfaces. These expansion and contraction forces give rise to cracking and flaking of rocks. Shale is particularly susceptible to this process as are other rocks such as sandstone, limestone, granite, basalt and schist. The following rock properties cause vulnerability to wetting and drying weathering, as defined by Bland and Rolls (1998).

-       the presence of clay minerals with water adsorption ability
-       structural weaknesses which encourage water entry e.g. cleavage planes
-       low tensile strength
-       pore size and distribution

2.2.1.5   Insolation weathering

This mechanism refers to the influence of temperature change on the physical breakdown of rocks. Rock surfaces expand when exposed to the sun or other heat sources and contract when the heat source is removed. The expansion and contraction cause stresses, which can cause breakage if these exceed the elastic limit of the rock. Infrequent bush fires cause temperatures as high as 800 °C, with subsequent cooling within 10 minutes, which expose rocks to extreme thermal shock with destructive results. The rock properties play a large role in this mechanism of weathering such as albedo (reflection of heat, thus a measure of the ability to absorb heat), thermal conductivity (ability to conduct heat) and the coefficient of thermal expansion. The thermal conductivity of rocks is usually low and causes marked temperature gradients, which cause steep stress gradients in the upper layers because of the changes in the amount of expansion. The coefficient of thermal expansion is an important characteristic as far as weathering is concerned, as expansion can generate very high stresses.

2.2.1.6   Pressure release weathering

The presence of sheet joints parallel to the local land surface weakens the bulk strength of the rock. Such joints are usually formed by land erosion. Due to the weight of the overlying rocks, the rocks just below the surface experience high compressive stress. Erosion now occurs by removing overlying rock, which reduces the compressive stress on the rock and expansion in the direction of the stress reduction occurs. Failure usually begins with the extension of an initial crack and continues with the development of sheet jointing parallel to the unloading surface. This type of weathering is most effective in brittle, crystalline rocks of high elasticity e.g. granites and massive sandstones. The Griffith theory can be used as guidance to crack propagation (Bland and Rolls, 1998).

2.2.2 Chemical weathering

Agents that can cause chemical weathering are water, carbon dioxide and oxygen. Carbon dioxide will alter the pH when dissolved in water and can drastically influence the dissolution of calcite and silica as well as minerals containing iron and aluminium. Oxygen plays an important role especially in oxidation processes.

The mechanisms of chemical weathering are hydration, solution, oxidation (redox reactions), hydrolysis and complex formation (chelation).

2.2.2.1   Hydration

All ions, whether positively or negatively charged, are hydrated to varying extents in water. Ionic hydration is an exothermic process releasing energy defined as the hydration energy (enthalpy). The degree of hydration is dependent on the ionic size and charge density, with the relationship of a direct increase in hydration enthalpy exothermicity with decreasing size and increasing charge density as shown in figure 5 (Greenwood and Earnshaw, 1997). In figure 5 the effective ionic radius of the cation plus a constant value of 85 pm is used (r_{eff}). The hydration of cations is of particular interest in the kimberlite weathering process due to the swelling process that takes place in kimberlite. Figure 4 shows the effect of hydration size for monovalent cations Li, Na and K. The hydration enthalpy (exothermicity) decreases with increasing cation hydration size. From figure 5 it is concluded that trivalent cations are the highest in hydration enthalpy, then divalent cations and lastly monovalent cations. Hydration data for some mono-, di- and trivalent cations are given in table 3. Latimer derived an equation for the hydration energy (equation 1), which is a function of the charge of the cation (Z) and the cationic radius (r in pm). This equation holds when the electronegativity of the

16

metal is not too great (< 1.5). Cations with electronegativies >1.5 have substantially higher hydration energies than more electropositive cations of comparable radius and charge. These electronegative metals have some degree of covalent bonding in their interaction with the oxygen atom of the water molecule, i.e., oxygen's unshared pair of electrons is shared with the metal atom. As the interaction between the metal ion and the coordinated water molecules increases, the oxygen further polarises the oxygen, hydrogen bond. This increases the acidity of the complex ultimately leading to hydrolysis. Z^2/r is used as an indication of the acidity. $Z^2/r < 0.01$, with r in pm, is non acidic e.g. Cs^+ and Rb^+. Li^+, Ba^{2+} and Ca^{2+} are defined as feebly acidic, falling in the range $0.01 < Z^2/r < 0.04$. Mg^{2+} is weakly acidic, lying in the range $0.04 < Z^2/r < 0.1$, and Al^{3+} lies in the moderately acidic range of $0.1 < Z^2/r < 0.16$. Strongly acidic cations ($Z^2/r > 0.22$) are not able to exist in water. (Note that the hydration enthalpy data in figure 5 are plotted against Z^2/r_{eff}, where $r_{eff} = r + 50$ pm, and hence these do not correspond to the Z^2/r values quoted above.)

$$\Delta H_{hyd} = -\frac{60900Z^2}{r+50} \text{ [kJ/mol]} \tag{1}$$

Where Z is the charge of the cation and r is the cationic radius in pm.

Table 3. Metal and ionic radii from Greenwood and Earnshaw (1997) and hydration bond size from Richens (1997).

Element	Cation Charge	Metal radius	Ionic radius	M-OH bond size	Hydration Enthalpy
		pm	pm	pm	kJ/mol
Ag	+ 1	144	115	240	-475.3
Li	+ 1	152	76	195-228	-514.1
Na	+ 1	186	102	240-250	-405.4
K	+ 1	227	138	260-295	-320.9
Ca	+ 2	197	100	241-246	-1592.4
Cr	+ 2	128	80	230	-1849.7
Cu	+ 2	128	77	196-200	-2100.4
Fe	+ 2	124	78	213	-1920
Mg	+ 2	112	27[a]	200-215	-1922.1
Mn	+ 2	118	83	218	-1845.6
Al	+ 3	143	53.5[b]	187-190	-4659.7
Cr	+ 3	128	80	196	-4401.6
Fe	+ 3	124	78	200	-4376.5
Ga	+ 3	135	62	215	-4684.8

[a] For a coordination of 4, [b] For a coordination of 6
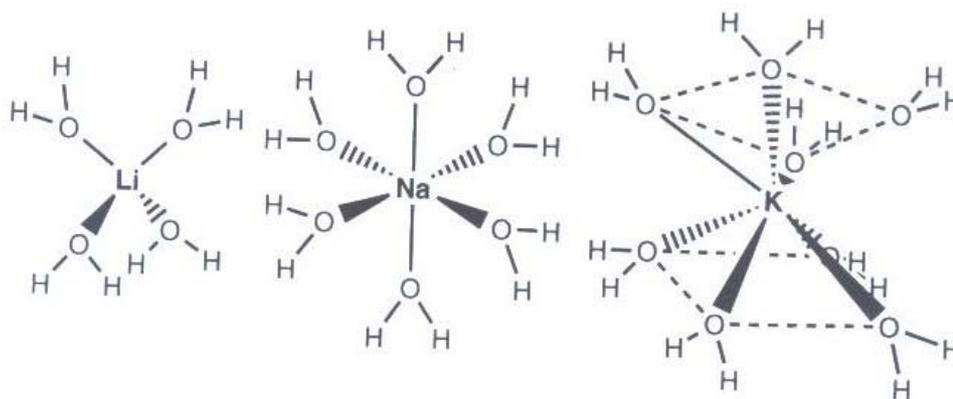
Figure 4. Hydration structures of lithium, sodium and potassium (Richens, 1997).
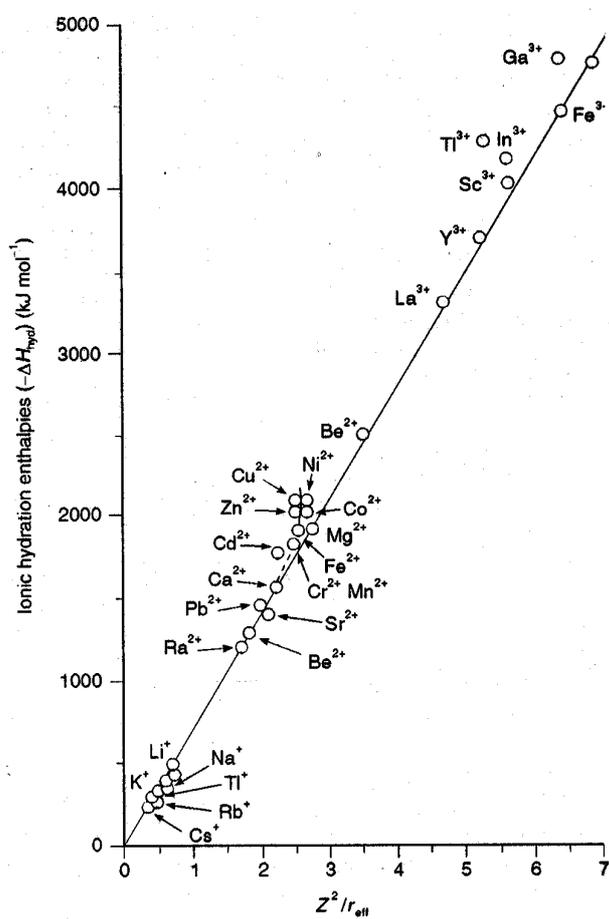
Figure 5. Hydration energy as a function of size and charge of the cation (Greenwood and Earnshaw, 1997).

2.2.2.2 *Water exchange rates on hydrated ions*

The rate of water exchange on aqua ions gives an indication of the stability of ion–water complexes. Figure 6 gives water exchange rate constants and mean residence times for aqua metal ions at 25 °C (Richens, 1997). These water exchange rates may give an indication of ion exchange rates between the interlayer cations in swelling clays and hydrated cations in the bulk solution.
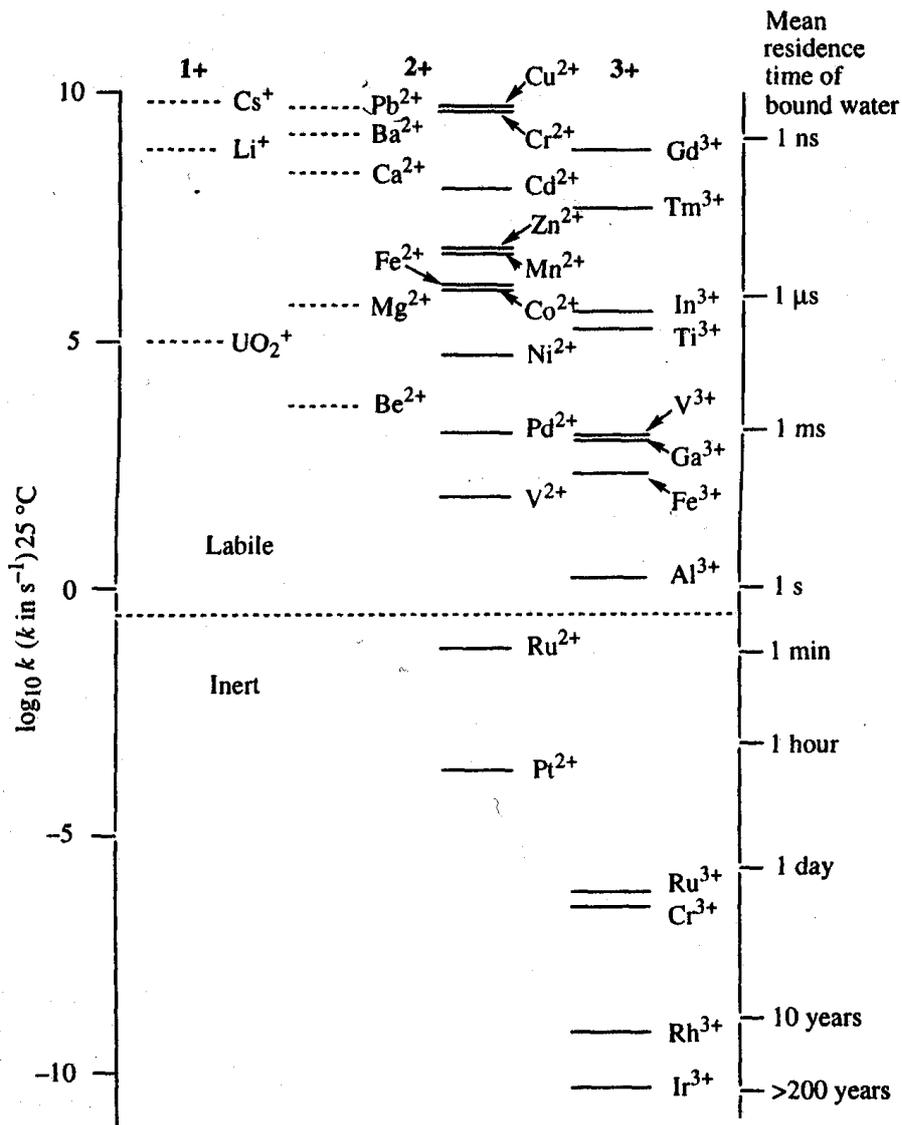
Figure 6. Water exchange rate constants and mean residence times for aqua metal ions at 25 °C (Richens, 1997).

19

2.2.2.3   Solution

Ionic salt added to a solution will initially dissolve until the solution becomes saturated. Super saturation can occur, usually when the conditions change, and if there are no nucleation sites available for crystallization to start. As mentioned previously the rate of crystallization when it finally starts will be much greater than for saturated-solution crystallization.

The ionic potential can be an indication of weathering as it reflects the measure of ease with which an ion can be removed from a mineral in solution. Ions with low ionic potential are the main components of weathering solutions as they are more mobile (easily dissolved and carried away). The ionic potential can be calculated by dividing the charge of the ion by its radius in angstrom units. Tabulated values are available in (Richens, 1997). The solubility product (K_{SP}) can also be used as an indication of weathering for solids. The higher the solubility product, the higher the tendency for the rock to dissolve and the greater is the likelihood of weathering. For an exothermic dissolution a higher temperature will lower the solubility, whereas a higher temperature will increase the solubility for an endothermic process.

2.2.2.4   Acids and Bases

Silica is a mineral of interest as far as weathering is concerned as it can form silicic acid in the presence of water by equation 2. The extent to which this reaction can occur however depends on the stable form of silica, where quartz is slow to react with water while amorphous silica is more reactive. The weathering of aluminosilicates, e.g. feldspars and micas, can form silica. Water becomes acidic with dissolved CO_2, which can cause the solubility of SiO_2 to be exceeded, resulting in the precipitation of amorphous silica. The amorphous silica can slowly expel water by the ageing process to first form opal or cristobalite (~10 % water), then chalcedony (~ 1 % water) and lastly quartz, with an associated increase in density from 2.1 - 2.7 g/cm^3.

$$SiO_2\,(s) + 2H_2O = Si(OH)_4\,(aq) \tag{2}$$

2.2.2.5   Hydrolysis

Hydrolysis in contrast with hydration involves a chemical reaction with water causing one O-H bond of H_2O to be broken. Hydrolysis can occur under acidic, neutral or basic conditions and occurs with compounds in which either the cations or anions or both give rise to the formation of a weak acid or base. The resulting pH (see table 4) is of interest when weathering is concerned. Different methods of determining the hydrolysis potential and hydrolysis constant values for ions are discussed in Richens (1997).

20

Table 4. Hydrolysis of salts as in Bland and Rolls (1998).

Type of salt	Example	pH of resulting solution
Strong acid - strong base	$CaSO_4$, Na_2SO_4	7
Weak acid - strong base	$CaCO_3$, Na_2CO_3	> 7 (basic)
Strong acid - weak base	$(NH_4)_2SO_4$	< 7 (acidic)
Weak acid - weak base	$(NH_4)_2CO_3$	Close to 7 depending on strength of the acid and base

2.2.2.6   Carbonation

The weathering effects of CO_2 in aqueous solutions are described as the Earth's commonest weathering mechanism. As previously discussed dissolved CO_2 causes water to become acidic (equation 3) due to the formation of carbonic acid. The pH of water in equilibrium with the atmosphere (containing 0.03 - 0.04 % CO_2 by volume) is ~ 5.6, but the concentration of CO_2 can be up to 20 % higher in groundwater because of biological activity that generates CO_2 (Bland and Rolls, 1998).

$$CO_2\,(g) + H_2O\,(l)\ = H_2CO_3\,(aq) \tag{3}$$

This weak acid can dissociate further:

$$H_2CO_3\,(aq) = H^+\,(aq) + HCO_3^-\,(aq) \tag{4}$$

The interaction of calcium carbonate (limestone) is also of interest under the carbonation subject. Calcium carbonate is soluble to a limited extent in water according to equation 5 whereafter hydrolysis can occur (equation 6) to alter the water to a calcium rich basic solution. The dissolution of calcium carbonate increases as the pH decreases. The weathering of pyrite (FeS_2) causes the production of sulphuric acid, which can cause the breakdown of limestone as shown in equation 7. Limestone can also be weathered by carbonic acid, which is formed when CO_2 is dissolved in water as shown by equation 8.

$$CaCO_3\,(s) = Ca^{2+}\,(aq) + CO_3^{2-}\,(aq) \tag{5}$$

$$CO_3^{2-}\,(aq) + H_2O(l) = HCO_3^-\,(aq) + OH^-\,(aq) \tag{6}$$

$$CaCO_3\,(s) + 2\,H^+\,(aq) = Ca^{2+}\,(aq) + H_2O\,(l) + CO_2\,(g) \tag{7}$$

$$CaCO_3\,(s) + H_2CO_3\,(aq) = Ca^{2+}\,(aq) + 2\,HCO_3^-\,(aq) \tag{8}$$
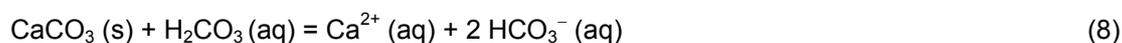
2.2.2.7   Redox reactions

- Oxidation

Dissolved oxygen acts as oxidising agent, and can also affect ions in solution with iron as the most commonly oxidised material. Ferrous iron [Fe(II)] with a yellowish colour is oxidised to ferric iron [Fe(III)] which has a reddish colour. An example of direct oxidation from the mineral and the influence on weathering is, for example, comparison of the micas, biotite $[K(Mg,Fe)_3(AlSi_3O_{10})(OH)_2]$ and muscovite $[KAl_2(AlSi_3O_{10})(OH)_2]$. Biotite is much more easily weathered due to the oxidation of iron that can occur. Another mechanism of iron oxidation is where the Fe^{2+} is first released from the mineral and then oxidised e.g. the release of ferrous oxide upon hydrolysis of olivine to serpentine shown by equation 9. Oxidation then occurs and forms goethite (equation 10). The oxidation can also produce ferric iron in the hematite form (Fe_2O_3). Manganese is also a susceptible element for oxidation due to the Mn^{2+} and Mn^{4+} oxidation states.

$$3\ MgFeSiO_4 + 2\ H_2O \rightarrow H_4Mg_3Si_2O_9 + SiO_2 + 3\ FeO \tag{9}$$

$$2\ FeO + \tfrac{1}{2}\ O_2 + H_2O \rightarrow 2\ FeOOH \tag{10}$$
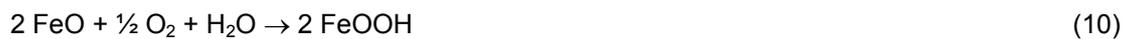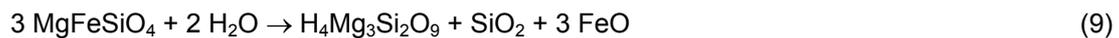
- Reduction

Weathering products due to reduction reactions are less prominent, although reduction can occur in oxygen free environments e.g. waterlogged soils. Such soils are characteristically green/grey due to the reduced form of iron that is stable. Organic matter commonly functions as reducing agents.

2.2.2.8   Cation Exchange

Fine soil particles (< 0.2 μm diameter clay or humus colloidal particles) produced by weathering can provide a reservoir of exchangeable cations and anions, which may be involved in further weathering processes. Exchangeable cations are more common than exchangeable anions and include H^+, K^+, Na^+, Mg^{2+} and Al^{3+}. Of particular interest in clays is that the replacement of Si^{4+} with Al^{3+} in tetrahedral sheets causes a negative charge of one, attracting monovalent cations to be adsorbed onto the surface. The octahedral sheet, in the way it links with other layers, also causes a –2 negative charge allowing for cations to be absorbed in the structure. The ability of an ore or soil to absorb cations is described by the cation exchange capacity (CEC), which can be as high as 60 [cmol/kg] for clay soils according to Bland and Rolls (1998). The units describe the number of centimoles (0.01 Mol)

of cations replaced per kilogram of ore or soil. Therefore if a soil has a CEC of 10 cmol/kg, 1 kg of this soil can absorb 10 cmol of H^+ (for example) and can exchange it for 10 cmol of another cation. The focus is on the charge exchanged rather than number of ions or molecules (Brady and Weil, 1999). Vermiculite is the clay mineral with the highest CEC with values of 100-180 while smectites vary from 80 – 140.

The CEC can be determined at ARC (Agricultural Research Council, South Africa) using the standard method as described by the Soil Science Society of South Africa (1990). The method uses 1 M of ammonium acetate as extractant measuring the extracted calcium, magnesium, potassium and sodium.   Brady and Weil (1999) give general information on determining the CEC and the different methods that can be used.

In the case where a kimberlite or clay mineral has a tendency to exchange cations, the properties of the ore can be altered by the type of cation present. Each cation will alter the clay structure and properties differently due to its unique properties e.g. valence, effective radius and absorption mechanism. A considerable amount of work has been done on the influence of cations on swelling clays and their properties e.g. Cases *et al* (1997); Rytwo *et al* (1996); Badreddine *et al* (2002); Prost (1981); Czimerova *et al* (2004).   This subject is discussed in more detail in section 3.2.

2.2.3 Biological weathering

Living organisms are not usually part of the immediate causes of breakdown but are agents of the physical and chemical weathering mechanisms. The zone of activity of these organisms is called the biosphere and includes biological agents such as bacteria, lichens, algae, fungi, plant roots and organic matter in a state of decay. These organisms contribute to weathering by either exerting a physical stress or by emitting substances e.g. carbon dioxide, as part of their life processes.

2.2.3.1   *Production of organic and inorganic acids*

The production of acid is perhaps the biggest contribution that biological agents can make to weathering. The inorganic acid largely arises from oxidation processes e.g. sulphuric acid is produced when bacterial oxidation of sulphur compounds occurs. Organic acids can be produced as by-products of organic decomposition or by biological agents as part of their existence. The influence of organic acids depends on specific materials e.g. olivine responds more rapidly to organic acid attack than to weathering under sterile conditions.

23

The main biological agents are:

Bacteria

Bacteria contribute to weathering in a number of ways as listed below.

- Releasing carbon dioxide

The increase in the proportion of carbon dioxide due to the activity of microorganisms has been estimated at 0.5 - 20 % compared to the atmosphere average of 0.03 %. As mentioned previously this can give rise to weakly acid solutions with pH ~ 5 - 6, which enhance chemical weathering.

- Nitrification process

The nitrobacteria are involved in the nitrification process, which is the term for conversion of ammonium ions (products of the bacterial processing of dead plant and animal matter) to nitrates (NO_3^-, process of nitratation) and nitrites (NO_2^-, process of nitritation). This process is of importance to weathering as it entails the release of protons as shown by equation 11, and particularly 2 hydrogen ions are produced for every ammonium ion resulting in acidic conditions.

$$NH_4^+ + 2\,O_2 \rightarrow NO_3^- + 2\,H^+ + H_2O \tag{11}$$

Experimental tests on vermiculite clay as quoted in Bland and Rolls (1998) show the removal of Mg^{2+} from this mineral in a bacterial environment compared to a sterile environment. In the bacterial environment the removal of the magnesium ions was twice as much as for the sterile environment, confirming that weathering mechanisms interact and cannot be evaluated as separate entities.

- Oxidation of metals

Many bacteria are capable of oxidising metals, which can then be removed from the host structure and subsequently precipitated. This microbial alteration is most effective under acidic conditions. At pH values of 2 - 4.5, these bacteria can raise oxidation rates by factors of 10^5 - 10^6 compared to non-biological environments.

24

Lichens

Lichens are compound organisms, which are capable of carrying out biophysical and biochemical weathering.

Biophysical weathering can be brought about by penetration of hyphae (fungal ligaments) along microcracks, which may generate considerable tensile stresses in excess of rock tensile strength and cause breakdown. Another form of biophysical breakdown is due to the expansion of thalli (plant bodies) and hyphae due to water absorption. Bland and Rolls (1998) discuss that lichens can increase their water content by 150 - 300 % under specific conditions, with enormous associated stresses due to the expansion that takes place.

Biochemical weathering of lichens again refers to the emission of organic acids, which contribute to chemical weathering as discussed under section 2.2.3.

Algae and cyanobacteria as biological weathering agents

These agents can also produce biophysical weathering due to the ability to absorb water, which generates expansion forces. Algae contribute to biochemical weathering through their ability to dislocate and precipitate metals at rock surfaces. Manganese-oxidising cyanobacteria can remove manganese from wind-blown dust by oxidation; the manganese is almost immediately precipitated under damp conditions to form a varnish on desert rocks.

Plant roots

The upper zone of the regolith dominated by plant roots is called the rhizosphere and in this region chemical breakdown can occur by plant roots. The substances emitted from plant roots as part of their life cycle are organic acids, protons and electrons (Bland and Rolls, 1998). These substances contribute mostly to chelation (complex formation) as weathering mechanism.

Decaying plant and animal matter

Humus acts as contributor to weathering through essentially oxidation which yields large amounts of carbon dioxide and humic and fulvic organic acids. These acids operate through proton and complexation reactions. These chelates that are formed are soluble and are removed from the weathering environment.

25

2.2.4   Silicate weathering

Silicates make up over 90 % of the earth's crust and about 75 % of the exposed surface rocks (Bland and Rolls, 1998). The weathering of minerals by aqueous solutions can be influenced by the compositions and lattice structure of the mineral and also the nature and behaviour of the weathering process. Silicates occur in numerous structural orientations, which allow for categorising of these minerals (see table 5). This mineralogical group is of particular importance in the study of kimberlite weathering as it includes the clay and mica groups, which is the focus point of this study.

Table 5. Types of silicates from Bland and Rolls (1998).

Name of Silicate	Structural Group	General formula	Number of oxygen atoms shared
Nesosilicates (Orthosilicates)	Tetrahedra	SiO_4^{4-}	0
Sorosilicates	Double tetrahedra	$Si_2O_7^{2-}$	1
Cyclosilicates	Closed rings of tetrahedra	$(SiO_3^{2-})_n$ $n = 3, 4, 6$	2
Inosilicates	(1) Chains of tetrahedra (2) Double chains of tetrahedra	$(SiO_3^{2-})_n$ $(Si_4O_{11}^{2-})_n$	2 2 and 3
Phyllosilicates	Sheets of tetrahedra	$(Si_2O_5^{2-})_n$	3
Tectosilicates	3 D framework of tetrahedra	SiO_2	4

2.2.4.1   Nesosilicates

Nesosilicates are typically ionic solids which are hard and brittle e.g. zircon and garnet ($Ca_3Al_2(SiO_4)_3$). The olivine group of this category contains divalent cations, e.g. Mg^{2+}, Fe^{2+}, Mn^{2+} and Ca^{2+} with the general formula M_2SiO_4. The olivine group is easily weathered due to the simple structure and low lattice energy. Zircon ($ZrSiO_4$) has a very high lattice energy and is one of the most inert silicates. It has been used as a standard to rate the weathering of other silicates against.

In this category of silicates the minerals containing iron e.g. forsterite ($MgFeSiO_4$) are important when discussing weathering, as oxidation of the Fe^{2+} takes place readily. The weathering of these minerals is modified by environmental conditions. Under tropical conditions with good drainage the silicon and magnesium are lost while the Fe^{2+} is oxidised and the iron redistributed as goethite or hematite along fractures. Under less extreme conditions only magnesium is initially removed resulting in an iron-silicon rich framework. The silicon will eventually be removed and the iron rich network remains. Forsterite (Mg_2SiO_4) is an example of a mineral that is first weathered by hydrolysis and the oxygen atoms are protonated resulting in the release of silicic acid by equation 12.

$$Mg_2SiO_4 + 4\,H^+ \rightarrow 2\,Mg^{2+} + H_4SiO_4 \tag{12}$$

2.2.4.2 *Sorosilicates*

These ionic solids are very rare minerals and are of little significance in the weathering processes.

2.2.4.3 *Cyclosilicates*

In this structure SiO_4 tetrahedra are shared to form a closed ring. Cyclic metasilicates occur with three, four, six or eight shared tetrahedra. An example is benitoite ($BaTiSi_3O_9$). This group is again rare and not very important in terms of kimberlite and weathering.

2.2.4.4 *Inosilicates*

Inosilicates are characterised by tetrahedra joined to form chains. Minerals included in this group are pyroxenes and amphiboles and their weathering is aided by their good cleavage. When slow leaching takes place, weathering produces smectites along cleavage planes and fissures. Stronger leaching of pyroxenes and amphiboles dissolves residues congruently, resulting in iron rich smectites as weathering product. Tropical weathering with good drainage totally removes Ca^{2+}, Mg^{2+} and Si^{4+} leaving mainly oxohydroxides e.g. goethite.

2.2.4.5 *Phyllosilicates*

These sheet structure minerals are of utmost importance to weathering as these include most of the clay minerals e.g. kaolinite, montmorillonite, vermiculite. Mica is included under this category as the commonest phyllosilicate. In the mica structure, Al^{3+} can replace the Si^{4+} at the centre of some of the tetrahedra to give a layered structure. This mineral is hard but has pronounced cleavage planes making it mechanically weak as it can be split into sheets. Mica minerals include biotite, muscovite, phlogopite and annite. The cleavage planes allow for

27

effective weathering e.g. in the case of biotite, which goes through several alterations during weathering in that it can be converted to chlorite or vermiculite and other clay minerals. Conversion of biotite to clay minerals can for example form kaolinite and gibbsite as shown in equation 13.

$$2 \ KAl_3Si_3O_{10}(OH)_2 + 18 \ H_2O + 2 \ H^+ \rightarrow 3 \ Al_2O_3 \cdot 3 \ H_2O + 6 \ H_4SiO_4 + 2 \ K^+ \tag{13}$$
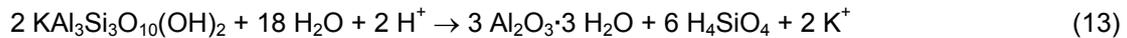
2.2.4.6   *Tectosilicates*

Tectosilicates have a characteristic framework structure such as silica and aluminosilicates, of which the most important group is the feldspars. Feldspars are also the most important single group of rock-forming silicate minerals. In these groups up to 50 % of the Si^{4+} ions have been replaced by Al^{3+}, causing extra cations to be added to maintain the charge balance. The feldspars are divided into alkali feldspars (replacement by monovalent cations) and plagioclase feldspars (replacement by divalent cations). In for example albite, the Na^+ can be replaced by K^+ (monovalent cation, thus alkali feldspars) ending up as orthoclase, as illustrated in equation 14. Alternatively the Na^+ in albite can be replaced by Ca^{2+} (divalent cation thus plagioclase feldspars) ending up as anorthite, as shown by equation 15.

$$NaAlSi_3O_8 \rightarrow Na_xK_{1-x}AlSi_3O_8 \rightarrow KAlSi_3O_8 \tag{14}$$

$$NaAlSi_3O_8 \rightarrow Na_xCa_{1-x}Al_{2-x}Si_{2+x}O_8 \rightarrow CaAlSi_2O_8 \tag{15}$$
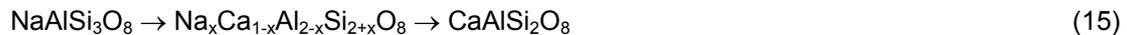
The ternary phase diagram, shown as figure 7, illustrates the variation in make up of feldspars.

Feldspars show very good cleavage planes and weathering typically takes place along fracture surfaces. The main weathering alteration reactions (equations 16 and 17) transform orthoclase to kaolinite and mica as the weathered products (Bland and Rolls, 1998).

$$4 \ KAlSi_3O_8 + 22 \ H_2O \rightarrow Al_4Si_4O_{10}(OH)_8 + 8 \ H_4SiO_4 + 4 \ K^+ + 4 \ OH^- \tag{16}$$
orthoclase   kaolinite

$$4 \ KAlSi_3O_8 + 12 \ H_2O + 2 \ H^+ \rightarrow KAl_3Si_3O_{10}(OH)_2 + 6 \ H_4SiO_4 + 2 \ K^+ \tag{17}$$
orthoclase   mica
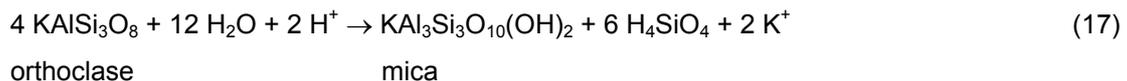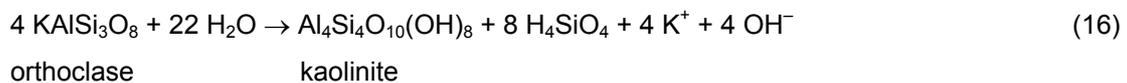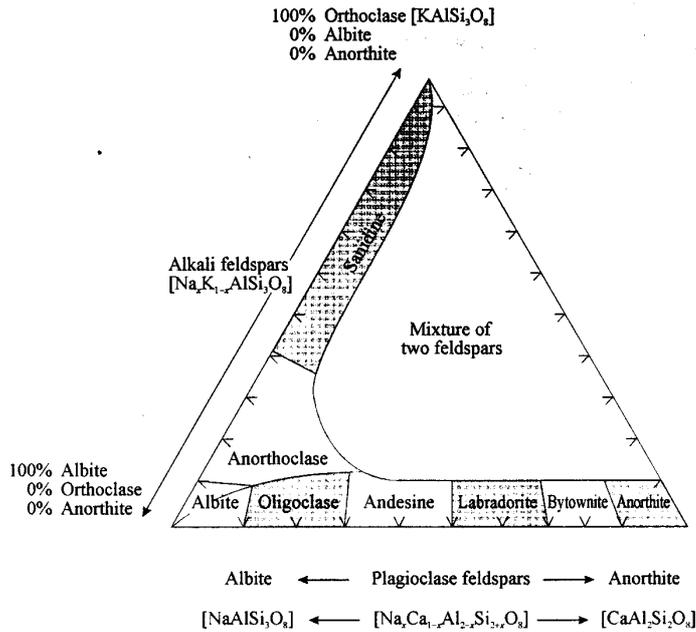
Figure 7. Ternary phase diagram showing the make up of feldspars (Bland and Rolls, 1998).

2.2.5 Products of weathering

2.2.5.1 *Crystalline phyllosilicate clays*

Clay minerals are the largest group of alteration products. The alteration sequence (Dawson, 1980) from olivine, pyroxene and mica is shown as figure 3 (section 2.1), to illustrate the formation of some clays. Clays are characterized by their small size and crystalline nature i.e. platelike structure. These minerals can be classified by the structure of the sheets or by the linkage between sheets.

2.2.5.1.1 *Structure of the sheets*

These minerals are formed from linked SiO_4^{4-} tetrahedra or octahedra.

- The tetrahedral sheet

Figure 8 illustrates the tetrahedral sheets where each tetrahedron is linked with its neighbours by sharing its basal oxygens. The enclosed ion of each tetrahedron is normally Si^{4+}, but this can be replaced by Al^{3+} or Fe^{3+}.
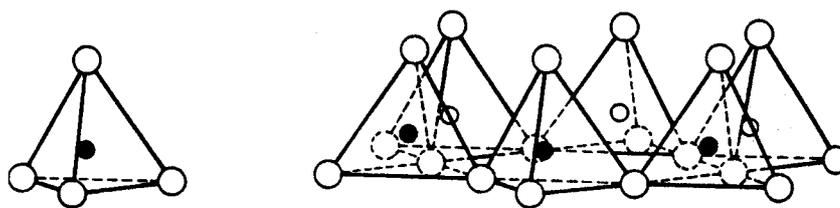
Figure 8. Illustration of a single SiO_4 tetrahedron and the sheet structure of SiO_4 tetrahedra (Bland and Rolls, 1998).

- The octahedral sheet

Figure 9 illustrates that each octahedron consists of six oxygen or hydroxyl ions which link by sharing the octahedral edges resulting in a nett charge of -2. In the basic form of the structure, two out of every three cation positions are filled by Al^{3+}, giving a (gibbsite) dioctahedral sheet. In some cases, all cation positions are filled by divalent cations such as Mg^{2+}, to give a trioctahedral sheet (brucite, if the cation is Mg^{2+}).
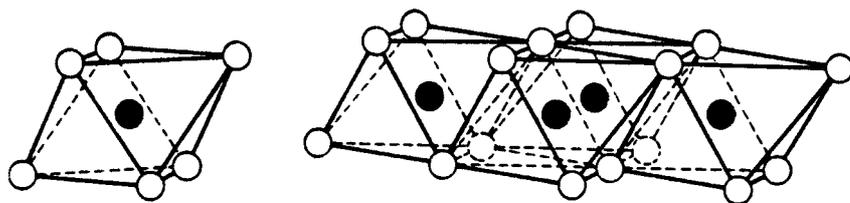
Figure 9. Illustrating a single octahedron and the sheet structure of linked octahedral (Bland and Rolls, 1998).

2.2.5.1.2 Linkage between sheets

Sheets are linked to form layers and how these are combined to form unit structures is of importance.

- Linkage to form 1:1 layers

A 1:1 layer refers to the linkage of a single octahedral sheet and a single tetrahedral sheet by weak intermolecular forces (induced dipole-dipole forces). This paired structure is about 7 Å thick (Bland and Rolls, 1998). The oxygens at the tips of the tetrahedra project into a plane of hydroxyls in the octahedral sheet, thus the oxygens replace two-thirds of the hydroxyls. Kaolinite ($Al_2Si_2O_5(OH)_4$) is considered the most important 1:1 clay type, shown in figure 10. Water cannot enter between these layers and therefore kaolinite is non-swelling. The other clay mineral categorised in this group is serpentine ($Mg_3Si_2O_5(OH)_4$), which is very similar to

30

kaolinite except that a sheet of brucite ($Mg(OH)_2$) is present rather than the gibbsite layer ($Al(OH)_3$). Serpentine is also non-swelling due to its similar structure. Halloysite on the other hand has a single layer of water molecules between the structural sheets to form hydrogen bonds and is therefore a swelling clay (see figure 10).

- Linkage to form 2:1 layers

This structure typically consists of three sheets, an octahedral sheet between two silica tetrahedral sheets on both sides. This layer is about 10 Å thick. The oxygens of the tetrahedral sheet point towards the central octahedral sheet and replace two-thirds of the hydroxyls of the octahedral. The layers are bonded by cations e.g. illite and vermiculite or by a brucite sheet in chlorite. The 2:1 clay group is divided into 4 groups namely illite, smectite, vermiculite and chlorite as is shown in figure 10.

Illite

In this mineral about one-sixth of the Si^{4+} in the tetrahedral layer is substituted by Al^{3+}, resulting in a high silicon to aluminium ratio and a reduced net charge deficiency. The interlayer cations (K^+, Ca^{2+}, Mg^{2+} or H^+) are relatively few thus the forces between layers are weaker. If potassium cations are present these will prevent the entrance of water and other cations, therefore illite generally has a low cation exchange capacity.

Smectite group

The central sheet of gibbsite is altered in this mineral group, in that oxygens replace two of every three hydroxide ions. Substitution by low valence cations in the octahedral (Al^{3+} replaced by Fe^{2+}, Mg^{2+} replaced by Zn^{2+}) and tetrahedral sites (Si^{4+} by Al^{3+}) causes electronic imbalance, which is usually corrected by the presence of interlayer cations e.g. Na^+, Ca^{2+}, Mg^{2+}. For montmorillonite the replacement of Al^{3+} by Mg^{2+} in the octahedral sheet is common with the occurrence of Na^+ as the interlayer cation. This group is called 'swelling clays' because water is readily absorbed between the layers therefore the basal spacing varies between 10 – 21 Å. The swelling of smectites is due to their small layer charge. It is suggested that the primary cause is because there is not a large enough attraction from the interlayer cations to keep the layers together (Moore and Reynolds, 1989).

Vermiculite

Vermiculite consists of a central sheet of brucite with octahedrally coordinated Mg^{2+} and Fe^{2+}. Extensive substitution of Si^{4+} by Al^{3+} and Fe^{3+} occurs. The charge imbalance is compensated by the introduction of Mg^{2+} interlayer cations. Water is also present between the layers thus making it a swelling clay. It is the clay mineral with the highest cation exchange capacity.

Chlorite minerals

An extra brucite-like layer is introduced as an octahedral sheet, which is electrostatically bonded. Due to the strong bond no hydration or swelling of this mineral can take place.

Figure 10 and table 6 illustrates the structural groups with examples.
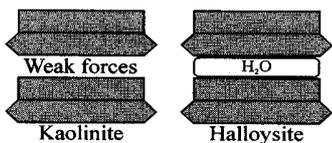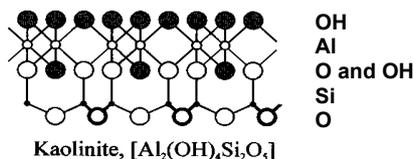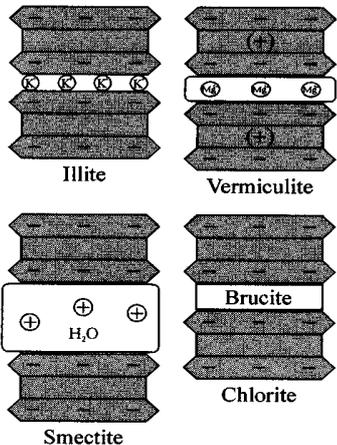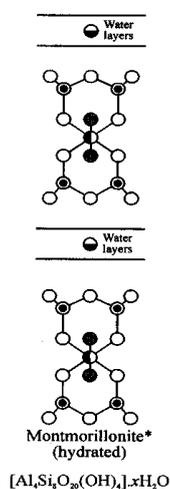
Figure 10. Structures of the clay minerals (Bland and Rolls, 1998).

Table 6. The layered silicates (Bland and Rolls, 1998).

Main group	Subgroup	Examples
Two layers (1:1)		
Kaolinite	Kaolinite	Kaolinite, halloysite
Kaolinite	Serpentine	Chrysotile, greenalite
Three layers (2:1)		
Pyrophyllite	Pyrophyllite, talc	Pyrophyllite, talc
Smectite	Dioctahedral	Montmorillonite, beidelite
	Trioctahedral	Saponite, saucinite
Vermiculite	Dioctahedral	Vermiculite
	Trioctahedral	Vermiculite
Mica	Dioctahedral	Illite, muscovite, sericite
	Trioctahedral	Biotite
Chlorite	Trioctahedral	Corundophite, pseudothuringite, talc-chlorite

Information on the unit layer formulas, octahedral and tetrahedral cations, charge per unit formula and exchangeable cations are shown in table 7 (from Brady and Weil, 1999).

Table 7. Unit layer formula, octahedral and tetrahedral cations, charge per unit formula and fixed and exchangeable interlayer components (Brady and Weil, 1999).

Mineral	Octahedral sheet	Tetrahedral Sheet	Coordinating Anions	Charge per unit formula	Interlayer components	
					Fixed	Exchangeable
1:1 Type						
Kaolinite	Al_2	Si_2	$O_5(OH)_4$	0	None	None
Serpentine	Mg_3	Si_2	$O_5(OH)_4$	0	None	None
2:1 Type Dioctahedral						
Pyrophyllite	Al_2	Si_4	$O_{10}(OH)_2$	0	None	None
Montmorillonite	$Al_{1.7}Mg_{0.3}$	$Si_{3.9}Al_{0.1}$	$O_{10}(OH)_2$	-0.4	None	$M^+_{0.4}$
Beidellite	Al_2	$Si_{3.6}Al_{0.4}$	$O_{10}(OH)_2$	-0.4	None	$M^+_{0.4}$
Nontronite	Fe_2	$Si_{3.6}Al_{0.4}$	$O_{10}(OH)_2$	-0.4	None	$M^+_{0.4}$
Vermiculite	$Al_{1.7}Mg_{0.3}$	$Si_{3.6}Al_{0.4}$	$O_{10}(OH)_2$	-0.7	xH_2O	$M^+_{0.7}$
Fine mica (Illite)	Al_2	$Si_{3.2}Al_{0.8}$	$O_{10}(OH)_2$	-0.8	$K^+_{0.7}$	$M^+_{0.1}$
Muscovite	Al_2	Si_3Al	$O_{10}(OH)_2$	-1.0	K^+	None
2:1 Type Trioctahedral						
Talc	Mg_3	Si_4	$O_{10}OH)_2$	0	None	None
Vermiculite	$Mg_{2.7}Fe^{3+}_{0.3}$	$Si_3\ Al$	$O_{10}(OH)_2$	-0.7	xH_2O	$M^+_{0.7}$
Chlorite	$Mg_{2.6}Fe^{3+}_{0.4}$	$Si_{2.5}(Al,Fe)_{1.5}$	$O_{10}(OH)_2$	-1.1	$Mg_2Al(OH)_6^+$	$M^+_{0.1}$

2.2.6   Intensity of weathering

Intensity refers to the degree of weathering or decomposition at a specific point in time, whilst the rate refers to the amount of change per unit time.

2.2.6.1   Controls of intensity

The controlling factors are categorised according to intrinsic and extrinsic factors.   The intrinsic factors are the properties related to the parent material.

Intrinsic factors

- Pores and fractures

These physical properties guide the entry of weathering fluids and therefore also the intensity of weathering. Weathering targets the fractures, cracks, fissures, cleavage planes and other surface weaknesses.

- Mineralogy

An arrangement of minerals in their order of stability is shown by Bland and Rolls (1998) where the method to determine the stability was to arrange them by the frequency of their occurrence in sedimentary rocks of increasing age, therefore an arrangement by their order of persistence. The version of Pettijohn (1941) is shown as table 8. However, the version published by Goldich (1938) is the more accepted version (figure 11). However this only includes the igneous rock-forming minerals. Some conflicting data has been reported especially in considering the environmental conditions when interpreting the mineral stability.

Table 8. Sequence of mineral persistence or Bowen's reaction series (Pettijohn, 1941).

Mineral	Persistence
Anatase	-3*
Muscovite	-2*
Rutile	-1*
Zircon	1
Tourmaline	2
Monazite	3
Garnet	4
Biotite	5
Apatite	6
Ilmenite	7
Magnetite	8
Staurolite	9
Kyanite	10
Epidote	11
Hornblende	12
Andalusite	13
Topaz	14
Sphene	15
Zoisite	16
Augite	17
Sillimanite	18
Hypersthene	19
Diopside	20
Actinolite	21
Olivine	22

Decreasing Stability

* Negative numbers indicate a tendency to formation rather than disappearance during long periods of burial.

Olivine	Calcic plagioclase	
Augite	Calci-alkalic plagioclase	
	Alkali - calcic plagioclase	
Hornblende	Alkalic plagioclase	Increasing Stability
Biotite		
	Potash Feldspar	
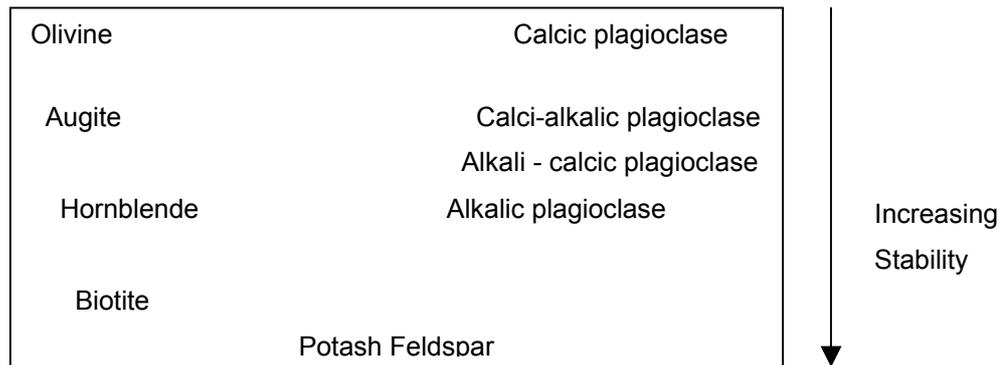
Figure 11. Sequence of mineral stability (Goldich, 1938).

Extrinsic factors (Environmental)

● Temperature

Temperature greatly influences the weathering rate because it influences the rates of chemical reactions. Bland and Rolls (1998) generalise it to an increase of 10 °C, which doubles the rate of the reaction. Changes in temperature can also cause the mechanism of weathering to change. Temperature will play a big role if the reaction is activation controlled. Temperature can be used to determine whether mass transfer of the reagent or product species is controlling the rate of the reaction or whether it is the rate of the chemical reaction itself. A very strong dependence on temperature indicates a chemically controlled reaction.

● Chemistry of weathering solutions

The characteristics of the weathering solution that determine the weathering activity are ion concentration, pH and temperature. As discussed previously, the content of CO_2 and biological agents largely influence the pH. The influence of specific ions on weathering is discussed in section 3.2.

● Hydrodynamics

Igneous rocks are highly permeable allowing for efficient water circulation and therefore high weathering possibilities compared to sedimentary rocks, which are slightly permeable and therefore higher in resistance. At mineral scale, water can enter at fractures and cleavage planes, whilst at a larger scale the joints, bedding planes and faults are weaknesses exploited by the weathering solution. Therefore the density and patterns of these fractures determine the efficiency of weathering.

37

In the regolith region the pathway of water is generalised to three distribution methods:

- Groundwater flow
- Shallow, saturated flow in soil.
- Saturation overland flow, which occurs where subsurface water returns to the land surface or where precipitation falls onto saturated areas, usually near surface channels.

The organised flow of water through rocks and the regolith contribute to weathering in that the fresh water comes into contact with minerals, which may accelerate weathering. Flushing carries the products of weathering away relating to the rate of weathering. Usually flushing speeds up the dissolution of minerals up to a limiting point after which dissolution is controlled by the solubility of the minerals.

2.2.6.2   Verbally descriptive approach to the intensity of weathering

Usually this appraisal is based on observation leading to verbal description for example as shown in table 9, which was obtained from Bland and Rolls (1998).

Table 9. Scheme of weathering grades for engineering purposes (Bland and Rolls, 1998).

Term	Grade	Description of weathering intensity
Fresh	I	No visible sign of rock material weathering; perhaps slight discolouration of major discontinuity surfaces
Slightly weathered	II	Discoloration indicates weathering of rock material and discontinuity surfaces. Weathering may discolour some of the rock material; yet it is not noticeably weakened.
Moderately weathered	III	Less than half of the rock material is decomposed or fragmented. Discoloured but unweakened rock is present either as a continuous framework or as corestones.
Highly weathered	IV	More than half of the rock material is decomposed or disintegrated. Fresh or discoloured or weakened rock is present either as a discontinuous framework or as corestones within the soil
Completely weathered	V	All rock material is decomposed and/or disintegrated to soil. The original mass structure and material fabric are still largely intact.
Residual soil	VI	All rock material is converted to soil. The mass structure and material fabric are destroyed. There is a large change of volume, but the soil has not been significantly transported. Can be divided into an upper A horizon of eluviated soil and a lower B-horizon of illuviated soil.

A five-point scale of friability is shown as table 10, which utilises simple equipment such as a boot or hammer to make an easy assessment of the strength or friability of the rock. This is mostly used where an assessment is made on site.

Table 10. A five-point scale of friability (Ollier, 1965).

1.	Fresh: a hammer tends to bounce off the rock
2.	Easily broken with a hammer
3.	The rock can be broken by a kick (with boots) but not by hand
4.	The rock can be broken apart in the hands, but does not disintegrate in water
5.	Soft rock that disintegrates when immersed in water.

2.2.7 Rate of weathering

Weathering rates can be described in different units of volume, of distance per unit time or mass per unit time, etc. The major problem in describing weathering is the difficulty of arriving at an accurate number due to the complexity concerning the different mechanisms and variables that influence weathering.

2.2.7.1   Units for measuring weathering rates

Units for measuring alteration by ionic loss:

- meq / m^2 (milliequivalents per square metre)
- mol / ha or mol/cm^2 (moles per hectare, or per square centimeter)
- mol / g (moles per gram)

Units for expressing loss/change:

- μm (micrometer)
- mm (millimeter)

Units for weathering rates where alteration is <u>uniform</u> (linear over time):

- meq / ($m^2 \times$ a) (milliequivalents per square metre per year)
- mol / (ha $\times$ a) (moles per hectare (or square centimeter) per year (or per second)))
- μm / ka (micrometers per 1000 years)
- mol / (g $\times$ h) (moles per gram per hour)
- t / ($km^2 \times$ a) (tonnes per square kilometer per year)

Units for weathering rates where alteration over time is <u>non-uniform</u> and may be expressed as a regression equation:

For example the rate of accumulation of clay in the B-horizon of an Antarctic soil has been expressed as:

$$Y = a + (b \log X) \tag{18}$$

where Y is the clay present as a percentage, a and b are regression coefficients and X is the time in years.

2.2.7.2   Experimental determination of weathering rates

This allows for research of the influence of time, mineralogy, temperature, solution concentration, surface area of substance etc. It does however involve simplification of this complex subject and care should be taken to ensure representation of the true conditions to be simulated. Laboratory testing is usually time limiting and the active agents in weathering solutions are usually present in much higher concentrations than in the environment. Bland and Rolls (1998) discuss that experimentally determined rates are usually one to three times higher than weathering rates in the field. This can be due to differences in temperatures and reduced contact between water and minerals in field situations.

The following variables have been identified to influence the weathering rate:

- The mineral composition

Specified weathering rates are given by Bland and Rolls (1998) e.g. the weathering rate of olivine was determined by two methods. The first used the release rate of Mg from forsterite and calculated a rate of 3.98×10^{-15} mol/cm^{2}s, the second was calculated from the Si release rate and resulted in a rate of 5.01×10^{-16} mol/cm^{2}s.

- The mineral structure

The original and developing structure have been found to influence weathering. Weathering is most rapid at reactive sites such as crystal defects, dislocations, twin boundaries and micro fractures. As weathering develops, these weaknesses can become enlarged (weathering rate maintained or increased) or blocked with secondary products, causing the weathering rate to drop rapidly. Diffusion paths have been found to block if the structures of the weathered material and the secondary product are similar. For example Bland and Rolls (1998) discuss the formation of clays when olivine weathers, where the structural units of the clays are too large to occupy diffusion avenues, therefore resulting in a high weathering rate. On the other hand the hydration of pyroxene results in a talc-like silicate product of which the lattice dimensions almost perfectly fit pyroxene resulting in blocking of the diffusion channels.

- Time

The weathering rate is usually found to decrease over time. This can be explained by either a precipitated layer at the mineral surface or due to preparation of the sample where grinding leaves a fine powder at the mineral surface, which will react rapidly with weathering fluids until it is dissolved. The high initial rate of mineral dissolution will fall away as the fine particles are dissolved.

- Weathering solution

The pH of the solution can largely influence the weathering rate of especially aluminium, magnesium and silicon. The presence of chelating agents for example fulvic acid can also influence the weathering rate. The concentration of salts in solution will also influence the weathering rate mechanically as discussed in section 2.2.1.3. Specifically the presence of certain cations should influence the weathering as discussed in section 3.2. The test work incorporated this property.

41

2.3   QUANTIFICATION / MEASUREMENT OF KIMBERLITE WEATHERING

2.3.1 Expressing kimberlite weathering

A few possibilities of expressing kimberlite weathering were considered:

- The mineral phases in the kimberlite could give an indication of the weatherability e.g. different clay minerals present.

- The chemical properties of the ore change e.g. the release of Fe or Na from the ore and uptake of other cations in the clay structures.

- The chemical properties of the weathering solution change as ions are released and used for clay formation.

- If swelling clays form, water uptake during absorption can be measured.

- Bulk strength of the ore decreases which can be determined by mechanical rock tests.

- Clays tend to form fines (slime), which can be determined by the weight loss of the sample.

- The slake durability test is a test mainly used in the mining industry and measures the weight loss of sample as a function of cyclic wetting (Saydam *et al*, 2003).

2.3.1.1   Changes in chemical or mineralogical properties of the ore

2.3.1.1.1   X-Ray Fluorescence analysis

The chemical composition of the ore can be determined by XRF (X-Ray Fluorescence) analysis. This analysis method is also called X-ray emission spectrography. The material is ground into a powder and compressed into a pellet using a binder. In the analysis procedure the pellet is irradiated with X-rays, which are generated in a high-intensity X-ray tube. The X-ray energy that is absorbed in the sample results in the generation of an X-ray emission spectrum that is characteristic for each element in the sample. This spectrum is then resolved into spectral lines, which can be identified by wavelengths that are specific to the

42

element that is producing the spectral line. This is then compared to standards to enable quantification. For more information on the analysis method and equipment the reader is referred to Klein and Hurlbut (1993). This analysis method allows for accurate determination of the chemical composition of inorganic matter. It is however very important to notice that this method cannot give any information on the mineral phases present or quantification thereof. Therefore this analysis method is optimally useful when used in conjunction with X-Ray Diffraction (XRD) analysis, which determines the minerals present.

In theory, XRF can be used as in section 2.2.7.2 to calculate the weathering rate by the release rate of Mg or Si from the ore. This approach will however be invalid if Mg is redeposited in another mineral e.g. a clay mineral. Therefore the approach is rather to follow the alteration to clay minerals (mineral phase analysis).

2.3.1.1.2   X-Ray Diffraction analysis

X-ray diffraction is a useful technique in identifying the minerals present. It is only applicable to crystals as they consist of an ordered three-dimensional structure with characteristic identity periods along crystallographic axes. When an X-ray beam strikes such a three-dimensional arrangement it causes the electrons in its path to vibrate with a frequency of the incident X-radiation. These electrons absorb some of the X-ray energy and emit (scatter) this energy as X-radiation of the same frequency and wavelength. Usually these scattered waves interfere destructively but in some conditions (when the Bragg law is fulfilled), these waves reinforce one another producing a cooperative scattering effect known as diffraction. Again more detailed discussions can be obtained from Klein and Hurlbut (1993). Quantitative analysis using XRD analysis is limited and only minerals in excess of ~ 5 % can be reported.

X-Ray Diffraction of clay minerals

The work by Bühmann (1998) and Moore and Reynolds (1989) discuss in detail the XRD analysis of clay minerals and how to determine the clay minerals accurately. Other authors on the X Ray Diffraction of clays are Brindly (1955) and Thorez (1975). Identification of clay minerals can become a cumbersome process due to overlapping reflections. This can be overcome by treating the ore. Firstly concentration of the clay mineral fraction (< 2 μm) is suggested for optimal XRD results. This will however not give an indication of the total sample mineralogy. A normal air-dry scan is then recorded. The ore can subsequently be treated firstly with ethylene glycol and / or glycerol to aid identification of the smectites and vermiculites (the procedure is discussed in Bühmann, 1998 and Moore and Reynolds, 1989). The XRD scan is again recorded before the sample is further treated with hydrazine and formamide which helps in identification of kaolinites. The sample is lastly treated at 500 °C to

collapse the swelling clays and this destroys or transforms minerals such as kaolinites and chlorites respectively. The XRD scans from the different treatments can now be compared and will allow identification of the main clay groups. Further treatments like saturation with Na, K, Ca and Mg can be considered if more accurate identification of the swelling clays is required. Other more specific applications are discussed by Bühmann (1998) and Moore and Reynolds (1989) if more information is required. From these treatments, comparison of the XRD scans will allow for identification of the clay groups.

For example the minerals in the kaolinite/serpentine group are both characterised by a 7 Å reflection in the normal scan but koalinite will collapse in the 500 °C treated scan whereas serpentine will be unaffected. Hydrazine treatment will expand kaolinites to 10.4 Å.

Smectite and vermiculite can both have a first basal spacing at 14 Å. The smectite spacing will expand to ~ 17 Å after glycol treatment whilst the vermiculite will show a peak at 14.2 Å after glycerol treatments. Heat treatment will shift smectite and vermiculite to 10 Å. The swelling clays are distinguished with certainty by saturation with K and Mg. Chlorite minerals will remain at 14 Å with glycol, glycerol and heat treatment.

For more information the reader is referred to Bühmann (1998), Moore and Reynolds (1989), Weaver (1989) and Poppe *et al* (2001).

The document by Bühmann (1998) also discusses optimal usage of the XRD equipment when working with clay minerals, to achieve the best results.

The smectite lattice parameter (the d value of the smectite 001 peak on a XRD scan) is called the interlayer spacing; i.e. the c axis spacing between the clay interlayers. It therefore gives an indication of the amount of swelling that has taken place. An interlayer spacing below 10 Å is associated with 0 water layers, 12.6 Å with 1 water layer, 15.6 Å with 2 layers, 18.6 Å with 3 layers, 21.6 Å with 4 layers and above that with more water layers (Tessier *et al*, 2004). Some authors have used this property to relate to the swelling. This is discussed further in section 3.2.

2.3.1.1.3   *Chemical indices as an indication of the intensity*

Combining XRD and XRF analysis, a few possibilities arise of quantifying weathering. The degree of alteration can be determined by either comparing the constitution of the parent material (if known) with the weathered material, or another approach is to work out the ratio between a highly resistant material e.g. quartz and other more easily weathered materials, which can then be used as an index.

44

- Absolute methods

Absolute methods are based on the approach that a quantifiable relationship exists between the unweathered and weathered material.

Isovolumetric method

This simple method is based on the assumption that no rock volume change occurs during the weathering process, and therefore the mass loss is an indication of the weathering that took place. This assumption is valid if the original petrographic textures and geological structure are still intact, which can be valid in some cases of low weathering rates. Kimberlite weathering however does not fit this assumption.

Benchmark mineral method

A resistant mineral is selected as benchmark and other minerals compared to it. Alumina is sometimes used because it is quite insoluble at pH values down to ~ 5.5 and is still retained in clay mineral weathered products. The approach is that the ratio between the alumina content of the parent rock and of the regolith is used to calculate the loss of the other compounds. This approach may prove useful if the material contains a highly weathering resistant mineral at relative high concentrations.

- Relative methods

In some cases the composition of the parent material is unknown or uncertain. In these cases the degree of weathering can be assessed by calculating the ratio between more stable and the less stable oxides, which is again expressed as an index. Two main groups exist, where the first one is based on alumina as the immobile mineral (the more general approach) and the other assumes that tourmaline is the most resistant mineral. For the second approach two weathering ratios (WR) are used, for heavy (h) and light (l) minerals:

$$WR(h) = \frac{zircon + tourmaline}{amphiboles + pyroxenes} \tag{19}$$

$$WR(l) = \frac{quartz}{feldspars} \tag{20}$$

These relative methods do however have the shortcoming that the various elements are assumed to be oxides, which is not entirely reliable as for example sodium oxide will rapidly react to form sodium hydroxide.

Table 11 below shows weathering indices that rely on the assumption that aluminium remains immobile during weathering and each ratio is suited for specific conditions (Bland and Rolls, 1998). This assumption is that Al is in the alumina form and does not take into account Al in other minerals e.g. feldspars. These indices again assume all elements as oxides, which are not necessary valid.

Table 11.   Weathering indices as published by Bland and Rolls (1998).

Chemical index of weathering (Harnois, 1988):

$$CIW = [Al_2O_3 / (Al_2O_3 + CaO + Na_2O)] \times 100 \tag{21}$$

Chemical index of alteration (Nesbitt and Young, 1982):

$$CIA = [Al_2O_3 / (Al_2O_3 + CaO + Na_2O + K_2O)] \times 100 \tag{22}$$

Weathering Index (Parker, 1970):

$$WI = [(2\, Na_2O / 0.35 + (MgO / 0.9) + 2\, K_2O / 0.25) + CaO / 0.7] \times 100 \tag{23}$$

Weathering index Vogel (1973):

$$MWPI = [(Na_2O + K_2O + CaO + MgO) /$$
$$(Na_2O + K_2O + CaO + MgO + SiO_2 + Al_2O_3 + Fe_2O_3)] \times 100 \tag{24}$$

46

2.3.1.1.4   Changes in chemical properties of the weathering solution

Ca, Mg and Fe release into the weathering solution was evaluated as functions of time by Hodgson (1981). The tests were done on Cullinan kimberlites in a 9 M sulphuric acid solution at 70 ˚C. All three cation concentrations were found to increase with time and reached constant levels around 24 hours. The highest concentration was for Mg, although Mg and Fe in solution were found to be very similar, in concentrations twice as high as Ca. Specific values are not quoted as this is very much determined by the type of ore and specific testing conditions, but this method could be used to evaluate the changes taking place during weathering.

2.3.1.1.5   Adsorption of water to form swelling clays

An extensive study by Erguler and Ulusay (2003) explored the methods that have been developed to determine swelling. This includes the free swell index, modified free swell index, methylene blue, $Wmax_{24,72}$ and direct measurement of volume change by the odometer. The free swell test as suggested by Holtz and Gibbs (1956) uses a 100 cm^3 water filled beaker. 10 cm^3 dry soil is sieved through a 0.42 mm aperture size and the undersize poured into the water.   The swollen volume of the soil after it comes to rest is noted. The free swell is given as %. Holtz and Gibbs also discuss the modified free swell index which is a non-dimensional index developed from the free swell test to overcome its limitations, for example a negative swell percentage for kaolinite clay and measurement errors in reading off the volume. The methylene blue test gives a relative measure of the CEC as methylene blue is preferentially adsorbed on the negatively charged sites.   The $Wmax_{24,72}$ parameter suggested by Erguler and Ulusay uses 400 g of ore adding water up to 300 mL. The slurry is stirred for ~ 5 minutes and then left for 24 and 72 hours respectively. After 24 hours the beaker is laid down for 15 minutes for the water to flow out. The water content of the sample is now determined and reported as W_{24} or W_{72}.

The results from these authors did not show good correlation between the free swell, modified free swell or methylene blue tests. They therefore introduced the new parameter $Wmax_{24, 72}$, which showed better predictive ability.

Stephens (1975) also did experimental work on the swelling characteristics of clays. This study included drying of weathered material at 150, 750 and 800 °C. All the dehydration and dehydroxylation in clays will be complete at 800 °C, thus higher temperature tests should not prove useful. The amount of water was evaluated by the mass loss of the sample. This investigation concluded that the water loss (in mass unit) from clays was too small for

sufficient differentiation. This study did not take into account the type of kimberlite or any mineralogical properties and whether swelling clay was present is not known.

2.3.1.2   Assessment based on the mechanical properties of the ore

2.3.1.2.1   Single particle breakage tests

Napier Munn *et al* (1996) discussed the different single particle breakage tests and concluded slow compression, drop weight and pendulum tests to be very similar. The disadvantage of single particle breakage tests is the large number of particles that needs to be assessed for a statistically representative analysis. These methods are discussed below.

- Schmidt hammer

More advanced equipment such as the Schmidt hammer measures the changes in the mechanical strength of the material, but avoids possible operator bias (Bland and Rolls, 1998). This test does however yield questionable results when applied to clay bearing rocks.

- Pendulum test

This apparatus is constructed in such a way that the input pendulum is released from a known height to swing down and break a particle attached to the rebound pendulum. It allows for study of the effect of velocity on the single particle, determination of the size distribution and new surface of the comminuted products. A correlation can be made of the specific fracture energy with the new surface area created. Bond (1954) used the pendulum under controlled crushing conditions on specific sized particles, which became known as the crushability test. Napier-Munn *et al* (1996) consider irregular specimens better than spherical particles for a wide range of input energy.

A technological twin pendulum test was developed by the JKMRC institute. This specific development of the twin pendulum test consists of an input and rebound pendulum suspended from a rigid frame. The single particle is fixed to the rebound pendulum and the input pendulum is released from a known height to swing down and collide with the particle. The rebound pendulum swings between a laser source and detector. The detector is mounted at right angles to the plane of swing on an optical bench and a computer records the motion (Napier-Munn *et al*, 1996).

The pendulum test was used by Stephens (1975) as a possible kimberlite weathering output but this produced severely scattered results. It was also suggested that the particles break on

weakened planes and therefore the measurement does not reflect the reduced bulk strength due to weathering.

- Drop weight test

This test is considered the most suited for characterizing the breakage of soft materials e.g. simulating of the handling of ores. The test works on the principle that a particle is dropped from a known height and the size distribution of the broken product is measured. The energy can be calculated simply as the potential energy in Joules (equation 25), with m the mass of the particle in kg, g is the gravitational acceleration equal to 9.81 m/s^2 and h is the drop height in m. Conversion gives 1 kWh/t = 3600 J/kg resulting in a height of 367 m required to apply 1kWh/t, which is the typical crushing energy. Therefore this test was altered for a more convenient but similar test where a suitable weight is dropped on to the particle, where distances of less than 1 m are required.

$$E = mgh \tag{25}$$

The altered test can be used to establish the relationship between surface area produced and the input energy. The size distribution of the resulting particles can be described by the Schuhmann linear equation (equation 26).

$$Eis = Ak^{(1-n)} \tag{26}$$

Eis is the specific energy input [Joules / kg], A and n are constants and k is the size modulus.

Further modifications have been made to this test to fit the specific application as discussed by Napier-Munn *et al* (1996). Again a more technological version of this test was developed by the JKMRC. This test allows for drop weights of 20 – 50 kg to be released by a pneumatic switch at drop heights of 0.05 – 1 m. The particles used are 10 – 50 mm in diameter and the test was designed for ores with specific gravities of 2.8 – 4 g/cm^3. These conditions represent operating energy ranges of 0.01 – 50 kWh/t. For softer material it is suggested that smaller breakage heads ~ 2 kg be used at a height of ~ 0.35 m (0.001 kWh/t). During the test the rebound of the breakage head should be minimized as this allows for loss of energy that is not measured.

The JKMRC comminution handbook by Napier-Munn *et al* (1996) regards the drop weight test to be superior to the pendulum test as it allows for extended input energy ranges, requires shorter testing times, can use an extended particle range and has greater precision.

The outputs of a pendulum/drop weight or any other breakage test will have to accommodate the product size distribution. To relate this to the mineralogy or rate of weathering will require the reduction of the size distribution to a single breakage ratio or index. JKMRC has developed the characteristic breakage index (t_{10}) for this reason. This index simply refers to the cumulative % passing at 10 % of the original ore particle size (See figure 12). Y is the geometric mean of the size interval for the test particles.
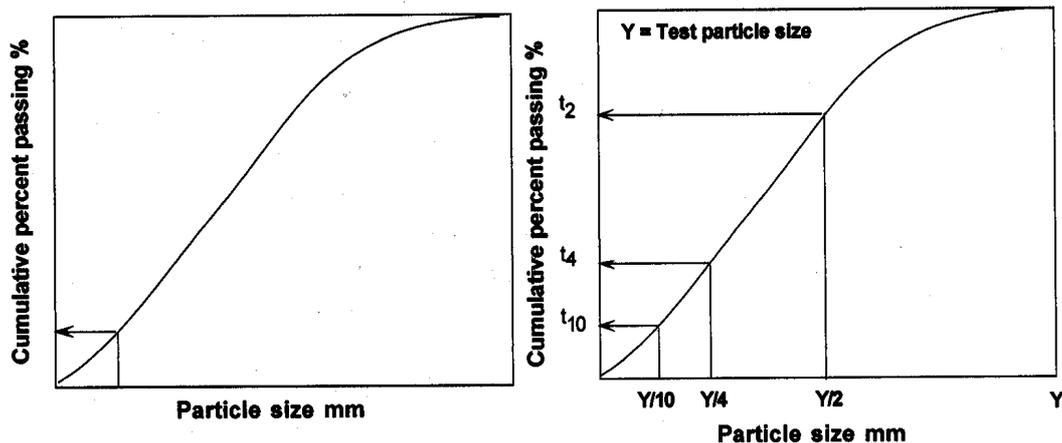
Figure 12. Normal size distribution curve illustrating the t_{10} from Napier-Munn *et al* (1996).

Another index rather than t_{10} can be used in a similar way from the size distribution curve e.g. t_4 and t_2 as shown in figure 12.

- Compression test

Compression testing was done by Stephens (1975) in a vice as a possible kimberlite weathering evaluation. As with the pendulum test it was found that consistent results could not be found due to irregularities of the testing specimen [i.e. weakened planes, mineralogy, surface characteristics (machining), size of the specimen etc.]

2.3.1.2.2   Batch tests

- Autogeneous milling

Autogeneous milling tests as indicator of the reduced bulk strength of the material were applied by Stephens (1975) and Hopwood and Webb (1975); both found this method very suitable. Hopwood and Webb (1975) used an 8-inch batch mill at 50 % critical speed for 30 minutes. The size distribution of the product can be used as a weathering index or a specific

50

point on the curve e.g. t_{10}, d_{10} (particle size where 10 % of the cumulative % of ore passed) or d_{80} (particle size where 80 % of the cumulative % of ore passed) as a function of time.

The major advantage of this test is that it can accommodate larger samples, which increases representativeness and the ease of obtaining a representative sample. It is not as sensitive to mineralogical and physical properties of the ore as single particle breakage tests. This type of test should require fewer tests for repeatability due to the increased size of the sample.

Both of the investigations mentioned above used the median size (d_{50}) as the output parameter, as a meaningful difference could be reported for small variation in the weathering. The difference between the reports is that Stephens (1975) found the product size distribution to be a normal distribution for fully weathered material but found that unweathered material lacked intermediate sizes (milling rounded the unweathered rock leaving large and fine particles). Hopwood and Webb (1975) on the other hand found weathered kimberlite material to lack intermediate sizes and concluded the weathering process to be surface limited. For these investigations the geology or mineralogy of the kimberlite material was not at all considered and it is suggested that the mineralogy of the kimberlites for the two studies might have been very different. The study by Hopwood and Webb (1975) was done on Cullinan kimberlite whilst the study by Stephens (1975) was done on Kimberley kimberlites. The type of milling (energy applied) will also have an influence on the product size distribution. The present study showed that the type of ore would determine this parameter. An ore like Koffiefontein, which is highly weatherable, generates a lot of fines in a very short time whereas a medium weatherable ore will not really generate fines but the size distribution curve will move to smaller sizes.

t_{10} as an output parameter seemed very suitable as it is already used in De Beers for modelling and simulation of crushing units. This model can then determine the influence of weathering on t_{10} and on the product size distribution. The t_{10} for crusher breakage is usually 10 – 20 % and can range between 20 – 50 % for tumbling mills.

Using an ore abrasion test (Napier-Munn *et al*, 1996) might also prove useful in terms of the fines generation during weathering and clay formation. The output parameter is now defined as t_a. t_a is defined as one tenth of t_{10} and therefore is one tenth of the cumulative percentage passing at Y/10 (see figure 12). t_a can be as low as 0.2 for very hard ores to above 2 for very soft ores and gives an indication of the resistance to abrasion that a specific ore has. This abrasion test uses a 300 mm diameter x 300 mm long tumbling mill with four 10 mm lifter bars. A 3 kg sample of size – 55 + 38 mm is then ground for 10 minutes at 70 % critical speed (~ 53 rpm).

Ultimately the choice of parameter depends on whether much fines would be generated after weathering (greater part of the size distribution curve similar to unweathered state) or whether the whole size distribution curve would shift to smaller sizes. Based on this, the output parameter could be chosen.

- Comminution Energy

The parameter t_{10} as discussed under the drop weight test was adapted for autogeneous or semi-autogeneous milling, to incorporate the comminution energy (Napier Munn *et al*, 1996). This adaptation included fitting of a function, given as equation 27.

$$t_{10} = A\left[1 - e^{(-b \times E_{CS})}\right] \tag{27}$$

t_{10}: The percent passing 1/10 th of the initial mean particle size

E_{CS}: The specific comminution energy (kWh/t)

A,b: The ore impact breakage parameters

The influence of comminution energy can therefore be determined by plotting t_{10} vs. E_{CS}.

2.3.1.3   Fines generation or mass loss of the sample

Some form of fines generation or mass loss of the sample due to fines generation was used as a quantitative measure by Stephens (1975), Hodgson (1981) and Clark (1982). Stephens (1975) concluded that too little fines generation took place for quantitative analysis without attrition or without accelerated weathering tests. He concluded that this might be a useful parameter if the tests could be altered to produce ~ 50 % slimes. Clark (1982) simply used the % slimes defined as the % -1 mm material, which was a useful tool to compare weathering at different times of 1, 2, 4 and 6 months where a maximum of 20 % of the feed material reported to the fines. Hodgson (1981) used the % - 75 μm material after weathering (which was in the order of 20 % after one day) but at increased temperatures around 70 °C. Again the mineralogy of these ores can not be compared to link the fines generation to the mineralogical properties.   Fines generation could be a useful parameter on highly weatherable ores.

2.3.1.4   The slake durability test

Towards the end of this study the slake durability test (figure 13) which is mainly utilised in the mining industry was recognised as an alternative weathering test. This test combines the effect of cyclic swelling and abrasion to accelerate the rate of weathering. This test was

52

standardized by the American Society for testing and materials (ASTM D4644-04). The test uses ~ 10 pieces of rock weighing 40 – 60 g each.   The sample is rotated in a steel mesh drum partially immersed in water for 10 minute cycles with oven drying between cycles at ~ 80 °C for 8 – 12 hours. The steel drums are made of sieve mesh at 2 mm allowing all particles smaller than this to pass into the water bath. The slake durability index (see table 12) is then used as the output which is defined as the percentage of the final weight to initial dry weight after each cycle. Usually at least four cycles are required for characterisation of a clay rich material (Gökceoğlu *et al*, 2000).

Table 12.   Weathering Description of the Slake durability index.

Amount of slaking / Weatherability of the ore	Slake durability index (%)
Very low	0 – 25
Low	25 – 50
Medium	50 - 75
High	75 – 95
Very High	95 - 100
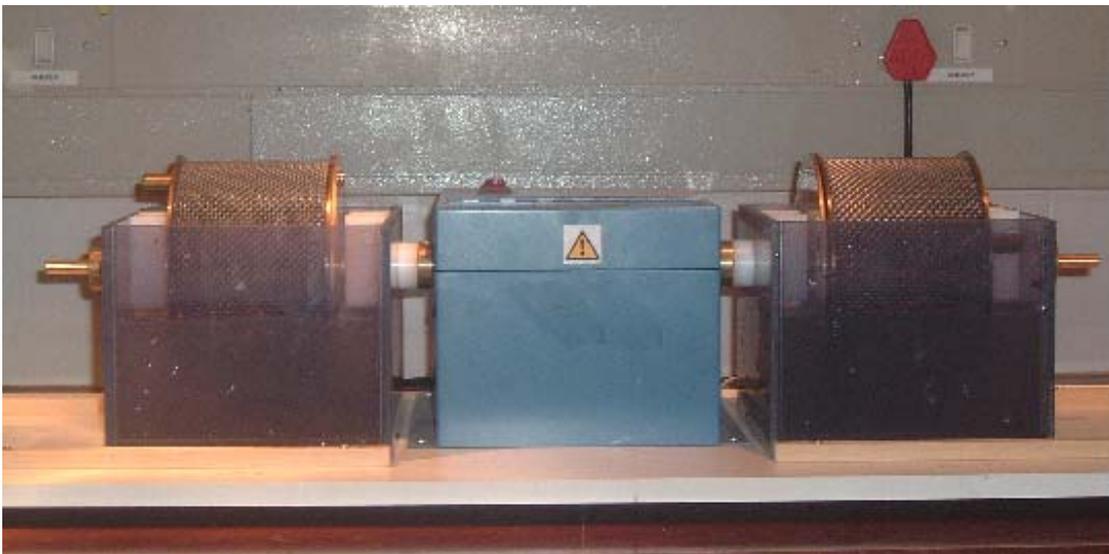
Figure 13. Slake durability test equipment.

53

2.3.1.5   Conclusion

From the discussion above it was concluded that one single parameter could not sufficiently describe weathering. It was decided to use a combination of chemical and mineralogical properties of the ore together with a mechanical test to represent the reduced bulk strength after weathering.

XRF analysis was used to obtain the chemical composition of the ore. XRD with the clay sub treatments as discussed in section 2.3.1.1.2 was used to identify the mineral phases present on a semi-quantitative basis. The interlayer spacing (d) from XRD was used as an indication of the amount of swelling.

For the mechanical test the autogeneous batch mill test was initially used, as the applicability of this test with South African kimberlites has been proven and repeatability should be better with batch tests than single particle breakage tests. The output parameter of weathering tests was therefore chosen as the size distribution of the weathered and milled ore as compared to the non-weathered milled ore (base case).   For reduction of the size distribution graph to a single output t_{80} was mostly used. t_{10} was found not to be suitable as the most significant changes in the size distribution graphs took place at 70 – 80 % of the starting size. Later on the slake durability test was also used.

54

2.4   PARAMETERS THAT INFLUENCE KIMBERLITE WEATHERING

2.4.1   Accelerated weathering

Weathering can occur in as little as a few seconds but can sometimes take months or even years before it becomes visible. The controlling variables that can cause these differences in kimberlite ores need to be studied and how the weathering environment can impact on this process need to be defined and understood.   Previous work on accelerated kimberlite weathering is summarised below.

2.4.2   Ion concentration

Accelerated weathering tests by Hopwood and Webb (1975) concluded that the presence of aluminium in solution led visually to the breakdown of a Cullinan kimberlite. The mineralogy of the sample used is unknown.

Hodgson (1981) did a study on the hydrothermal alteration of kimberlite. He found the combination of H^+, Al^{3+} and temperature determined the clay minerals that will form.

No other literature utilising cations as accelerator for the weathering process was found. Other literature on the influence of cations on the smectite structure and swelling is however available and discussed in section 3.2.

2.4.3   Acid concentration

As discussed under section 2.4.2 above, Hodgson (1981) found that the temperature, acid and aluminium concentration determine the type of clays formed as alteration products. Hodgson also tested the influence of different acids at different concentrations (1-16 M) and temperatures (70 and 100 °C) separately. He found sulphuric acid a little more aggressive than hydrochloric acid.

In practice the weathering solution pH can be as low as 5 as discussed under section 2.2.3.1 depending on the dissolved CO_2 and bacteria present. Mine recycle water on the other hand can be as high as pH 9 – 10.

2.4.4 Temperature

Hopwood and Webb (1975) tested the effect of temperature on weathering between 50 and 900 °C and also used heating and cooling/quenching cycles. The conclusions were that above 800 °C the kimberlite became brown and very tough and would not weather under any conditions. They found no other effect of temperature on the weathering process under normal heating and cooling, heating and quenching and cyclic variation. Again the mineralogy of the sample used is unknown.

In contrast to the findings of Hopwood and Webb (1975), Hodgson (1981) found that temperature definitely influenced weathering. He concluded that the combination of temperature, acid and aluminium concentration determines the clay product and cannot be studied separately. The influence of the type of clay product on the rate and degree of weathering has not been tested.

With South African diamond mines the temperature limits in different geological areas can be between - 5 and 40 °C.

2.4.5 Wetting and drying cycles

Cyclical wetting and drying is important for mechanical weathering as discussed in section 2.2.1.4. Swelling clays especially should be vulnerable to cyclic wetting and drying and this could be a parameter utilised when accelerated weathering is required. Cyclic wetting and drying is utilised by the slake durability test discussed in section 2.3.1.4.

2.4.6 Other parameters

Hopwood and Webb (1975) tested microwave heating as a possible weathering accelerator but found that the kimberlite exploded without any prior softening. It was concluded that breakage occurred by differential expansion and not chemical weathering of the material. The same investigation tested ultrasonic breaking as a possible influential factor but found no physical degradation of the kimberlite even at very high ultrasonic sound intensity. It was however found that the ultrasonic breaking could break down products that formed on the surface and in this regard improve weathering. They also tested ultraviolet and infrared light and found no influence on kimberlite weatherability.

56

3.   MECHANISMS   CONTROLLING   KIMBERLITE WEATHERING

This study suggests that kimberlite weathering is mainly due to the presence of swelling clays. In that case the cations present play a large role, as swelling clays can exchange especially interlayer cations to a large extent. Each cation influences the clay structure and properties in a unique way depending on the cation and clay properties as well as the mechanism of cation absorption.

3.1   Swelling as the weathering mechanism

Two types of distinctly different swelling mechanisms have been identified and are discussed by Madsen and Müller-Vonmoos (1989). According to this study the swelling is determined by the type of clay minerals, amount of clays, surface charge and valence of cations present in the double layer. The first phase termed crystalline swelling is due to the hydration of exchangeable cations of the initially dry clay. Phase two termed osmotic swelling occurs due to large differences in ion concentrations close to the surface and the pore water. Figure 14 shows the layer structure of the swelling smectite, montmorillonite. The adsorption of cations takes place for the structure to acquire charge balance.   In the dry state the montmorillonite layers lie so close together (0.96 – 1 nm) that they are almost in contact (Madsen and Müller-Vonmoos, 1989). These negatively charged layers are held together strongly by coulombic forces but also weak van der Waals attraction. These cations hydrate upon contact with water (see table 3) and cause a widening of the spacing between the layers (as much as double the initial volume).   Madsen and Müller-Vonmoos (1989) quote pressures of 100 MPa due to the crystalline swelling. They also show that this mechanism causes stepwise swelling (widening) where each step is associated with the addition of one more water layer up to a maximum water adsorption. This swelling mechanism is concluded the predominant of the two types.

Osmotic swelling is associated with a large concentration difference between the ions electrostatically bonded to the surface and the ions in the pore water of the rock. This excess negative charge must be corrected by positive ions close to the surface, giving very high concentrations of positive ions close to the surface. This negatively charged surface and cloud of positive ions form the diffuse electric double layer. Pressures associated with this type of swelling are normally less than 2 MPa (Madsen and Müller-Vonmoos, 1989).

57
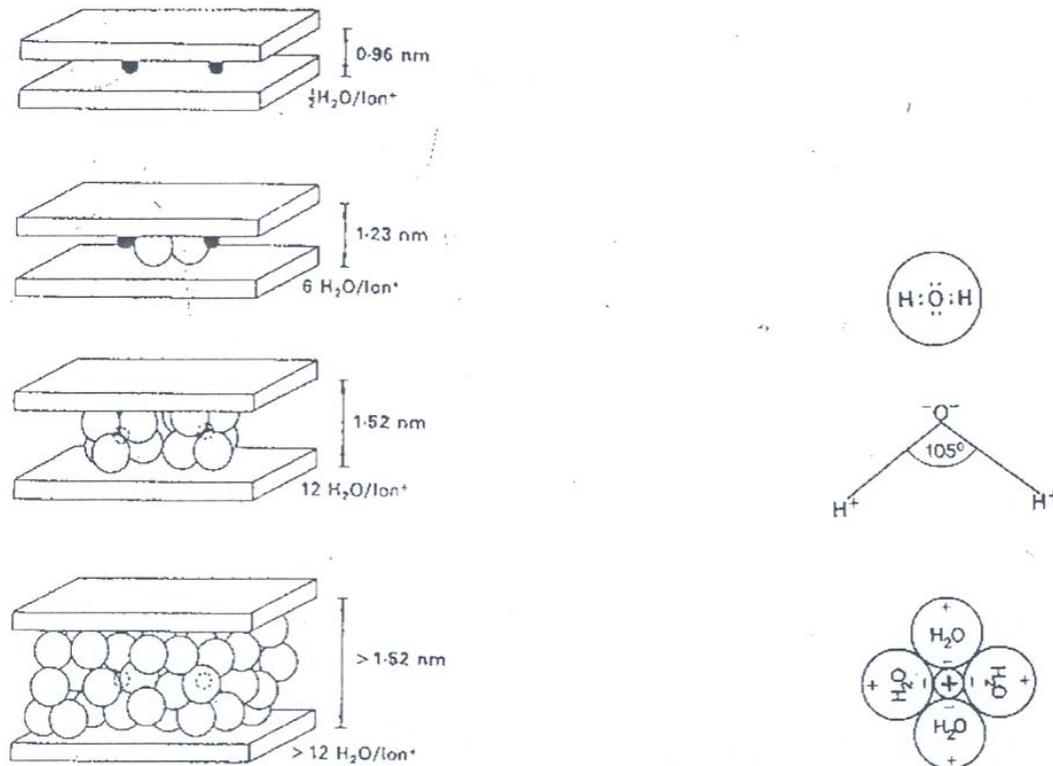
Figure 14. Innercrystalline swelling of montmorillonite (Madsen and Müller-Vonmoos, 1989).

3.2   The effect of cations on swelling behaviour

In the case where a kimberlite contains swelling clays (e.g. montmorillonite or saponite), it will also exhibit cation exchanging. The properties of the kimberlite can be altered by the type of cation/s present, because each cation has unique properties. One method used to indicate the extent of swelling taking place is the XRD interlayer spacing (see section 2.3.1.1.2), which is simply the d value of the smectite 001 peak on a XRD scan. An interlayer spacing below 10 Å is associated with 0 water layers, 12.6 Å with 1 water layer, 15.6 Å with 2 layers, 18.6 Å with 3 layers, 21.6 Å with 4 layers and above that with more water layers (Tessier *et al*, 2004). Ferrage *et al* (2005) show that the interlayer spacing under ambient conditions (approximately 25 °C and 35 % relative humidity) are very similar and rarely above two water layers. This study showed that the interlayer spacing of montmorillonite is correlated with the ionic potential of the cations (the effective cation radius and charge). This is investigated in section 6.6.

58

- *CATIONS THAT SWELL CLAY INTERLAYERS*

Absorption and desorption studies on the Mg^{2+}, Ca^{2+}, Sr^{2+} and Ba^{2+} montmorillonite exchanged forms by Cases *et al* (1997) have shown that these cations have a swelling effect on montmorillonite.   Other studies on Na^+, Ca^{2+} and Mg^{2+} exchanged swelling clays confirm the swelling capability of these cations. (Rytwo *et al*, 1996; Badreddine *et al*, 2002; Prost, 1981). Ferrage *et al* (2005) shows that for room temperature the relative humidity around 35% results in primarily 2 water layer spacings for Mg^{2+} and Ca^{2+}. Na^+ and Li^+ on the other hand will display primarily 1 water layer spacing, and K^+ predominantly 0 water layers.

- *CATIONS THAT COLLAPSE SWELLING CLAY INTERLAYERS*

Collapsing the interlayer of swelling clays has been shown to be possible with NH_4^+, Cs^+, K^+, Rb^+ (Czimerova *et al*, 2004). K^+, Cs^+ and Rb^+ clays were also investigated by Badreddine *et al* (2002). Grim (1968) show that vermiculite saturated with K^+, NH_4^+, Rb^+ and Cs^+ showed no expansion of the lattice. The selectivity of potassium in montmorillonite was studied by Carson and Dixon (1972). These cations are unique in their large ionic sizes K^+ (1.33 Å), NH_4^+ (1.43 Å), Cs^+ (1.69 Å).

The collapsing capability of potassium was studied by Malla and Douglas (1985). This study showed that the smectite interlayer can be collapsed to 10.6 – 12.8 Å depending on the layer charge of the original smectite layer. Carson and Dixon (1972) showed collapse of calcium montmorillonite from 23 Å to 14 Å with potassium. Ferrage *et al* (2005) showed that under ambient conditions K^+ exchanged montmorillonite results in predominantly 0 water layers. The possibility of slowing down weathering has merit within underground mines as it could be used to improve tunnel wall stability. This opportunity is discussed in section 7.2.

- *CATION EXCHANGE MECHANISM*

From literature it is also shown that cation exchange is influenced by a selectivity order which refers to the ease of replacing an existing cation in the interlayer spacing.   Wu and Li (1998) show a selectivity order as follows: $Na^+ < K^+ < Cd^{2+} < Zn^{2+} < Mg^{2+} < Cu^{2+} < Ca^{2+} < Pb^{2+}$. Eberl (1980) include different cations and show a selectivity order of: $H^+ < Li^+ < Na^+ < K^+ < Rb^+ < Cs^+$. The selectivity order of Wu and Li (1998) suggests that if the interlayer is collapsed by potassium, the potassium could easily be replaced by magnesium or calcium if available and energetically favourable. Grim (1968) show the replacement order of Ba saturated clays: $Li^+ < Na^+ < NH_4^+ < K^+ < Mg^{2+} < Rb^+ < Ca^{2+}$. The selectivity order is however determined by the type of smectite or vermiculite, the layer charge and also the type of replaceable cations.

Anderson *et al* (1989) suggest that cation selectivities are determined by the cation valence, hydrated radii, hydration energies and polarizability. The cation valence and hydrated radii has been combined in what is called the ionic potential (z/r_{eff}) as used by Ferrage *et al* (2005) to model the XRD interlayer spacing. The ionic potential is investigated further in section 6.2.5.

Cation exchange data can be expressed by the selectivity coefficient K_N also referred to as the cation exchange constant. Bruggenwert and Kamphorst (1982) report the cation exchange data as follows (equation 28):

$$K_N = \frac{N_B^{1/z_B} \, c_A^{1/z_A}}{N_A^{1/z_A} \, c_B^{1/z_B}} \tag{28}$$

where N_i is the equivalent fraction adsorbed in the clay, c_i is the concentration in the solution, and z_i is the valence of cation *i*. *A* is the cation in the clay at the start of the reaction, and *B* is the exchanging cation.

For cations of equal valence (e.g. exchange of Na^+ in the clay with K^+ in the solution), the equation shows that there will be a preference for the exchanging cation (i.e. $c_A/c_B > N_A/N_B$) if $K_N > 1$ (i.e. $\ln K_N > 0$).

For the exchange of cations where the valence is not equal, the situation is not so simple (because of the exponent $1/z$ in the equilibrium constant expression). In that case, the ratio c_A/c_B is given by:

$$\frac{c_A}{c_B} = K_N^{z_A} \frac{N_B^{z_A/z_B}}{N_A} c_B^{(z_A/z_B - 1)} \tag{29}$$

The "preference" of the clay for cation *B* hence depends on its concentration in the solution, and also the degree of loading of *B* onto the clay (N_B).

If one takes the arbitrary situation of $N_B = N_A = 0.5$, we then find:

$$\frac{c_A}{c_B} = K_N^{z_A} \left(0.5 c_B\right)^{(z_A/z_B - 1)} \tag{30}$$

Hence $c_A/c_B > 1$ if:

$$K_N \left(0.5c_B\right)^{\left(1/z_B - 1/z_A\right)} > 1 \tag{31}$$

The data from Bruggenwert and Kamphorst (1982) is compared with experimental work in section 6.5.

From studies on cation exchange it seems that the absorption mechanism differs for different cations. Strawn *et al* (2004) showed that copper tends to adsorb not only on the interlayer but also sorb on aluminol function groups. Adsorption at positions other than the interlayer – such as crystal edges - has also been shown true for Li^+ (Anderson *et al*, 1989) and Fe^{2+} (Hofstetter *et al*, 2003). On the other hand trivalent cations especially Al^{3+} and Fe^{3+} tend to form hydroxy species in the clay interlayer as utilised in pillared clay formation (Belver *et al*, 2004; Newman, 1987). It is clear that cation exchange in clays does not follow a simple mechanism but is rather unique for different clays, different cations and different environments.

4. PROBLEM STATEMENT

The main hypothesis states that the swelling clays present in the ore will determine whether a kimberlite will be prone to weathering. The reason is that the swelling action generates internal pressure and causes rapid breakdown of the material. The idea originated from initial observations on the Koffiefontein ore sample, which showed rapid breakdown in seconds compared to Wesselton ore, which could not be weathered under any reasonable conditions. The main difference between these ores was their swelling clay content; Koffiefontein contains ~ 50 – 60 % smectite compared to none detected in Wesselton. Smectite is the main swelling clay group present in kimberlite ores, being sub-classified as principally montmorillonite, nontronite and saponite. Swelling clays also allow for extensive cation exchange, which can enhance and accelerate the weathering process.

The driving force behind the exchange of cations was explained by Madsen and Müller-Vonmoos (1989). As discussed, clay minerals are part of the phyllosilicate group (layered silicates) and consist of SiO_4^{4-} tetrahedra and octahedra. In the tetrahedral arrangement a trioctahedral cation (e.g. Fe^{3+} or Al^{3+}) can replace Si^{4+} and cause negatively charged layers. The octahedral layers consist of six oxygens or six hydroxyl ions and are linked with the other layers by sharing the octahedral edges resulting in a –2 negative charge. These negatively charged layers cause the incorporation of an interlayer of cations between two negatively charged surfaces bonded by coulombic forces. Upon water contact the cations become

61

hydrated (some cations have a higher tendency towards hydration than others), incorporate water into the structure and cause widening of the interlayer. This mechanism causes the breakdown during weathering but also allows for enhanced and accelerated weathering by exchanging some of the existing cations with more 'aggressive' cations. This study suggests that the effect of a cation is determined by its valence and effective ionic radius, also called the ionic potential as discussed by Ferrage *et al* (2005), although other factors such as the type of clay, layer charge and absorption properties also influence the clay behaviour. This is discussed further in section 6.2.5.2.

The property of ores to exchange cations is reported as the CEC (cation exchange capacity) and is an inherent property of each ore. This property was found to complement the swelling clay hypothesis as ores with a high CEC show high weathering and ores with a very low CEC show no signs of degradation.

In summary the hypothesis is that a kimberlite is rendered weatherable if swelling clay is present in the ore. The rate of weathering will depend on the amount of swelling clay present and the type of cations present in the ore and in the weathering medium, as these will determine the extent of swelling, the cation adsorption mechanism and rate of cation exchange. The effect of different cations on weathering behaviour is investigated in this study to aim at defining this exchange process better for kimberlite.

5. EXPERIMENTAL PROCEDURE

Thirteen different types of kimberlite samples were received and labelled according to their origin. These samples were Geluk Wes (Tuffisitic Wesselton ore), Koffiefontein, Wesselton (Hypabyssal kimberlite ore), Cullinan TKB (Tuffisitic Kimberlite Breccia), Dutoitspan and eight samples from Venetia named: K1 Hypabyssal North East, K1 Hypabyssal South, K1 TKB East, K2 South, K2 West, K2 North East, K8 and Red Kimberlite. See figure 2 for a map of the South African De Beers mines. For more information on Venetia kimberlites see Doorgapershad *et al* (2003).

These ores were in the nominal size range of 50 – 100 mm. The ore was subsequently crushed in a laboratory jaw crusher to – 26 mm. The sample sizes ranged from 80 – 300 kg per sample.

5.1 Mineralogy

Ore in the – 9 + 8 mm size fraction was riffled to a ± 500 g sample and milled fine in a swingmill to around 50 μm for XRF and XRD analysis.

5.1.1 XRF ANALYSIS

XRF analysis was done at Mintek Analytical Services, South Africa. They use a X-lab 2000 instrument by Spectro. All the samples were analysed as powder briquettes. The briquettes were made with a wax binder and pressed under 10 tons of pressure. Except for milling in a WC bowl on rare occasions, the samples were analysed as received.

5.1.2 XRD ANALYSIS

The theory behind XRD analysis is discussed in section 2.3.1.1.2. It was mentioned that clay minerals can produce overlapping peaks on the XRD scan and therefore can require more work for accurate analysis. Therefore, the sub-treatment of clay minerals as discussed in this section was used in some cases to obtain more accurate results. To ensure the validity of the results, the samples were analysed at three different institutions as discussed below.

Agricultural Research Council

ARC (Agricultural Research Council) uses a Philips 1840 XRD instrument with a Co lamp over a range of 2 – 45 ° 2θ. Their procedure involves the removal of the –2 μm fraction and performing clay treatments on this fraction. The clay treatments involve glycol, glycerol and thermal treatments followed by the XRD scan. The % of -2 μm material is also determined by particle settling.   An air-dry scan of the total sample was also done compared to other work only on the clay fraction.

One drawback of this procedure is that the clay minerals are not accurately determined on the whole sample. The typical sub -2 micron fraction of these kimberlite samples is less than 30 %, so the clay XRD analysis could not represent the total mineralogy of the ore. Mineral identification results showed incorrect identification of minerals on some samples especially on overlapping clays e.g. smectite and chlorite both with lattice spacings at 14 Å. All De Beers' samples had previously been analysed at ARC and it is suggested that their procedure should be re-evaluated.

63

University of Pretoria

University of Pretoria XRD analysis was done on a Siemens D501 instrument utilising a copper lamp and a 4 – 70 ° 2θ range. The other specifications are given in Appendix A. The treatment of the sample included an air-dry, glycol and temperature treatment on selected samples. For quantification purposes the software program Topaz was used.

Mintek

Mintek XRD analysis is done on a Siemens D500 instrument with a Cu lamp and a 5 – 80 ° 2θ range. The other specifications on the instrument are given in Appendix A.

The kimberlite samples as received were milled for ten minutes in a McCrone micronizing mill with the purpose to reduce all mineral particles to a relatively small size (~ 50 μm). Size differences may have an influence on the XRD peak intensities of the different mineral components of this rock type. The samples were also side-mounted to minimise the effect of preferred orientation (Moore and Reynolds, 1989).

From the micronized material three representative sub-fractions were obtained for the following purposes:

1]   XRD on the first fraction was done on the material after micronizing and labelled "untreated".

2]   The second fraction was treated with ethylene glycol — this is used as an auxiliary treatment to expand swelling clays if present. Swelling clays include smectites (e.g. montmorillonite, nontronite), and some mixed-layer clays, and vermiculite. The sample was directly loaded into the XRD sample holder and placed in a desiccator where it was exposed to ethylene glycol fumes for 12 hours at 60°C. Thereafter XRD analysis was carried out on the sample.

3]   The third fraction was loaded into a porcelain crucible and heated for 2 hours in a muffle furnace at 550°C in air. XRD analysis was carried out on the product. This was followed by a consecutive session of another two hours heat treatment under the same conditions and XRD analysis repeated.

In the untreated XRD scan the mineral groups / minerals were identified. Certain minerals could only be identified with certainty within the broad basis of their mineral groups (e.g. smectite, mica, chlorite, amphibole, and pyroxene), while other minerals could be identified with certainty (e.g. talc and quartz). The mineral species identified in the untreated sample and their measured 2θ and d-values are presented in table 13. Table 14 contains the

64

literature 2θ and d-values of these minerals (Bühmann, 1998; Moore and Reynolds, 1989). The measured d spacings of the minerals compare well with literature, although the smectite d value falls within a range depending on the type of interlayer cations (dioctahedral vs. trioctahedral) and the swelling condition. For this reason the sample was glycolated and the scan repeated. The expected changes in diffraction characteristics of smectite and chlorite upon glycolation and heat treatment are given in table 15.

Table 13. Minerals identified by X-ray diffraction in the Cullinan TKB sample.

Mineral name (Mineral group name and probable identity)	Formula	d-values (Å) of most prominent peaks (range 3 – 30° 2θ)	2θ values of most prominent peaks (degrees 2θ)	Symbol used
CHLORITE (Clinochlore)	$Mg_5Al(Si_3Al)O_{10}(OH)_8$	14.1 7.2 4.8 3.6	6.3 12.3 18.5 24.7	C
Smectite	$(NaCaK)(MgAl_2Si_4O_{10})(OH)_2 \cdot nH_2O$	14.1 12.3	6.3 7.2	S
MICA (Phlogopite ?)	$KMg_3Al\ Si_3O_{10}(OH)_2$	10.1	8.8	M
Talc	$Mg_3Si_4O_{10}(OH)_2$	9.3	9.5	T
AMPHIBOLE (Tremolite)	$Ca_2\ Mg\ _5Si_8O_{22}(OH)_2$	8.4 3.2	10.5 27.9	A
PYROXENE (Diopside)	$Ca(Mg,Al)(Si,Al)_2O_6$	3.0	29.8	P
Quartz	SiO_2	3.3	27.0	Q

Table 14. Literature information on minerals in the Cullinan TKB sample in the 3 - 30 ° 2θ range.

Mineral name (Mineral group name and probable identity)	Formula	d-values (Å) of most prominent peaks (range 3 – 30° 2θ)	2θ values of most prominent peaks (degrees 2θ)	Symbol used
CHLORITE (Clinochlore)	$Mg_5Al(Si_3Al)O_{10}(OH)_8$	14.1 7.1 4.6 3.6	6.3 12.5 19.3 24.7	C
Smectite	$(NaCaK)(MgAl_2Si_4O_{10})(OH)_2 \cdot nH_2O$	13 - 18	6.8 – 4.9	S
MICA (Phlogopite ?)	$KMg_3Al\ Si_3O_{10}(OH)_2$	10.1	8.8	M
Talc	$Mg_3Si_4O_{10}(OH)_2$	9.3	9.5	T
AMPHIBOLE (Tremolite)	$Ca_2Mg\ _5Si_8O_{22}(OH)_2$	8.4 3.2	10.5 27.9	A
PYROXENE (Diopside)	$Ca(Mg,Al)(Si,Al)_2O_6$	3.0	29.8	P
Quartz	SiO_2	3.3	27.0	Q

Table 15. Changes recorded in diffraction characteristics of untreated and treated clay minerals. Numbers in the table refer to d-spacings in Å.

Clay mineral	Peak position at specific d-value and effect of treatment			
	Untreated	Ethylene glycol	2h heat treatment	4h heat treatment
CHLORITE (Clinochlore)	14.1 7.2 4.8 3.6	14.1 7.2 4.8 3.6	14.1 increases in RPH* 7.2 4.8 and 3.6 decrease in RPH*	14.1 increase further in RPH* 4.8 and 3.6 collapse
SMECTITE (Swelling clay)	14.1 12.3	~ 16.5	-	~ 10 Å

* RPH - Relative peak height
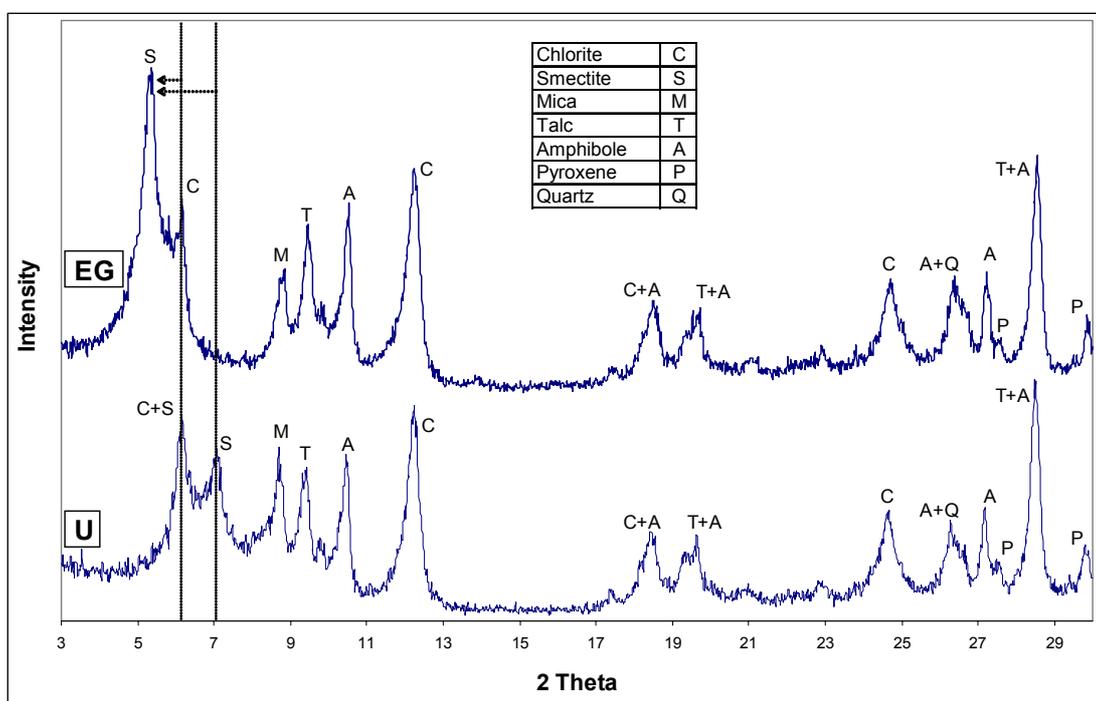
Figure 15. XRD scans of untreated (U) and ethylene glycol treated Cullinan TKB (EG), displaying the peak shift that characterizes smectite (swelling clay).

Figure 15 illustrates a peak shift after ethylene glycol treatment from 14.1 to 16.5 Å (with 2θ changing from 6.3° to 5.3°) and 12.3 to 16.5 Å (with 2θ changing from 7.2 to 5.3°), indicating the presence of a swelling clay (see table 16). For this study it was assumed that smectite as the swelling clay, as Cullinan brown or Type 2 TKB has been shown to be primarily saponite rich (Bartlett, 1994). The presence of two peaks could indicate the presence of two different types of smectite or otherwise two different swelling conditions. The peak at 12.3 Å (untreated sample) indicates the smectite has a monolayer of H_2O. More information, especially on the chemical composition of the clays, could be useful for a positive identification.
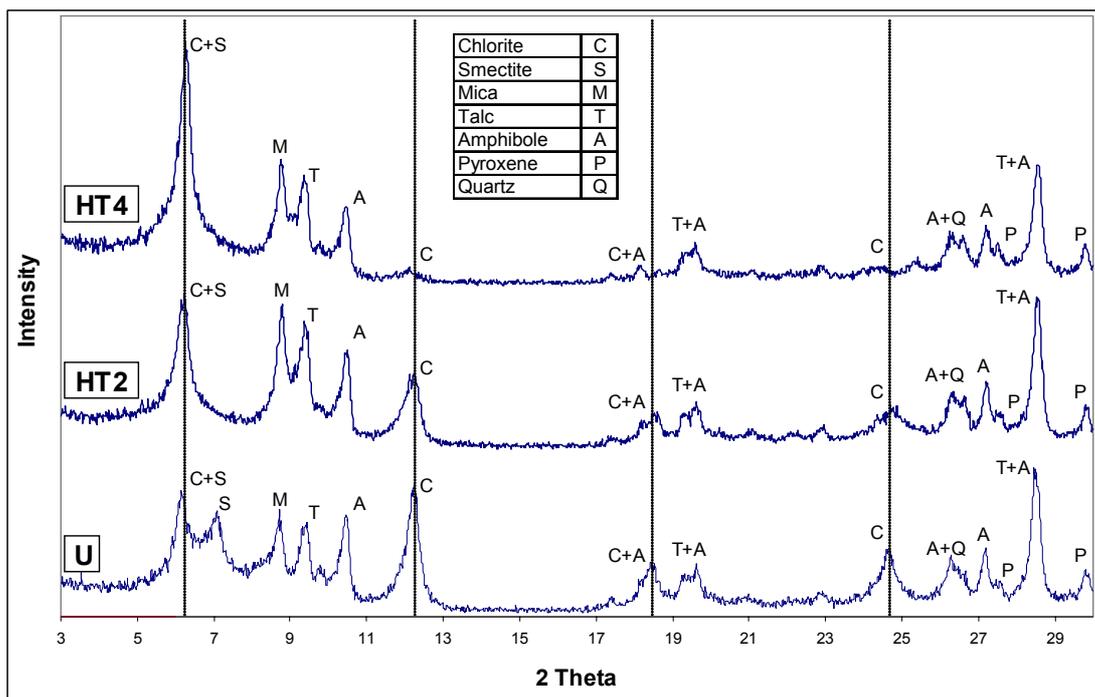
Figure 16. XRD-scans of Cullinan TKB for untreated (U), two-hour (HT2), and four-hour heat-treated (HT4) samples, displaying the effect on chlorite peaks (550 °C heat treatment temperature).

Chlorite was positively identified on the basis of the 14.1 Å ($2\theta=6.3°$) and 7.2 Å ($2\theta=12.3°$) peaks (figure 15), but not the specific mineral. The peak at 14.1 Å is positioned within a larger broad-based peak with uncertain identification. After the four-hour heat treatment, the 14.1 Å peak had increased in size whereas the other peaks collapsed (shown in figure 16). Table 15 summarizes the observed changes in diffraction characteristics of clay minerals. Note that the smectite peak at 12.3 Å ($2\theta = 7.2°$) also collapsed after the heat treatment. It is however possible that the heat treatment caused a structural change (loss of interlayer water) and could result in this behaviour.

During the experimental work it also became evident that the time allowed for the heat treatment is significant, as shown in figure 16. With the two hour heat treatment the chlorite peak at 14.1 Å increased in relative intensity while all the other chlorite peaks diminished to approximately half of their original size. With the four-hour heat treatment the 14.1 Å peak increased further in size while the other chlorite peaks disappeared, as expected. In addition to the changes to the clay minerals the mica and talc peaks also appeared to be affected by the heat treatment. This can possibly be explained by an increase in crystallinity of these two mineral species after heating.

A summary of the experimental d-values (measured at maximum peak height) as well as reference d-values (Thorez, 1975) obtained for smectite and chlorite with treatments is presented in tables 16 and 17. (The d-spacing scale in the table is only approximate).

Table 16.   Basal spacings (A) for smectite minerals.

Condition / treatment	Individual d-values measured experimentally or referred to in literature				
Air dried - experimental			14.2		12.3
Air dried – reference*					
Ethylene Glycol treated - experimental	16.5				
Ethylene Glycol treated - reference	17				
d-spacing scale	←17	←16	←15	←14	←13

* Depending on the type of smectite the d value can fall anywhere within this range

Table 17.   d- spacings (A) for chlorite minerals.

Condition / treatment	Individual d-values measured experimentally or referred to in literature											
Air dried - experimental	14.1							7.2			4.8	3.6
Air dried - reference	14.1							7.1			4.8	3.5
Ethylene Glycol treated -experimental	14.1							7.2			4.8	3.6
Heat-treated - reference	14.1							—			—	—
d-spacing scale	←15	←14	←13	←12	←11	←10	←9	←8	←7	←6	←5	←4

Clay minerals generally give intrinsically broad lines (peaks) because of small scattering domains, structural disorder, mixed layering, or some combination of these factors. Smectite minerals occur only as extremely small particles so that detailed diffraction data are difficult to obtain. The d-values as presented in the tables 16 and 17 were given at maximum peak value to be compared with data from literature. From this data saponite appears to be the best general fit when individual smectite minerals are considered to match the XRD-data. The basal peaks are broad and the d-values for certain saponite peaks (width at half height) are given in table 18. A more definitive chemical composition of the clay minerals in the Cullinan TKB could be very informative to make a more precise mineral identification. Electron microprobe determinations on these clay minerals could be very useful but it could also be difficult to locate a suitable specimen for analysis due to the small size of clay minerals in general.

Table 18.   d-value ranges for saponite after treatment (Thorez, 1975)

Smectite mineral	d-value range of basal reflection	Remarks
Saponite (13-0086)	17.5 to 15.5 Å	After EG-treatment
Saponite (13-0086)	14.5 to ~ 10 Å	After heat treatment

Comparison of XRD results from the three different institutions on Cullinan TKB is shown in table 19. The work by the University of Pretoria compares well with the results obtained by Mintek as the mineral groups and specific minerals identified correlate well. It is however a concern that the quantities are expressed as accurate numbers when in fact the error range is around 10 %. However, the semi-quantitative results also compare well with the work by Mintek. The only concern is the absence of serpentine from the University of Pretoria results. Mineral identification by Agricultural Research Council shows correlation with the other institutions but the quantitative results do not correlate with their results. Reporting of 50 % quartz in this sample shows the extent of errors that can occur during mineralogical characterization if critical evaluation of results is neglected.   However, the presence of xenoliths and poor sampling techniques can cause misleading results.   The point is that results like these should be cautiously evaluated and re-analysed.

The final results of Mintek were used although these were compared with the minerals identified at the University of Pretoria to ensure accurate peak identification. The results from Mintek were used as the mineralogist who did the interpretation was readily available and spent hours to ensure the quality of results. The mineralogist at the University of Pretoria did not have the time to discuss and continually work on the results. Mintek also provided semi-quantitative results using the combined methods of peak ratios and Topaz software. These results on all the kimberlites tested are given later in tables 21 and 22 (section 6.1.2).

Table 19. Comparison of XRD results from three different institutions, Mintek, Agricultural Research Council and University of Pretoria.

Mintek		Agricultural Research Council		University of Pretoria	
Mineral name (Mineral group name and probable identity)	Quantity	Mineral name (Mineral group name and probable identity)	Quantity	Mineral name (Mineral group name and probable identity)	Quantity
Chlorite (Clinochlore)	> 20	Quartz	50	Chlorite	34
Swelling Clay	10 - 20	Serpentine	16	Talc	16
Mica (Annite)	5 - 10	Smectite	11	Smectite (Montmorillonite)	13
Talc	10 - 20	Amphibole	9	Amphibole (Tremolite)	11
Amphibole (Tremolite)	10 - 15	Talc	8	Mica	8
Serpentine (Antigorite)	10 - 15	Mica	6	Quartz	6
Olivine (Forsterite)	< 10			Pyroxene	5
Pyroxene (Diopside)	~ 5			Dolomite	3
Magnetite	< 10			Calcite	2
Quartz	< 5			Orthoclase	1
Dolomite	< 5				

These results highlight the importance to evaluate mineralogical results critically and to ensure that interpretation is done by an experienced and professional individual or institution. In kimberlite the overlapping peaks of swelling clay and chlorites require further work to distinguish the one from the other (as shown in figures 15 and 16). The presence of quartz in predominance is very unlikely and should be further investigated if reported as such. Preferred orientation is a concern with clay rich samples, therefore micronizing of the sample is suggested. Preparation of the sample is very important e.g. the milling procedure and type of mounting used (see Schoen *et al*, 1973). Comparing the mineralogy and weathering behaviour could also show possible errors in mineralogical characterization, for example a hypabyssal kimberlite consisting mostly of minerals like mica, calcite and serpentine should not show any signs of degradation during weathering. Incorrect sampling could also cause unreliable results.

5.2 Weathering tests and conditions

5.2.1 Standard test

The kimberlite samples tested were all crushed in a laboratory jaw crusher to a size of –26.5 mm. The material was then screened into size fractions of –26.5 + 22.4, -22.4 + 19, -19 + 16, -16 + 13.2, -13.2 + 11.2, -11.2 + 9, – 9 + 8, -8 + 5.4 and –5.4 mm. Tests were done in size fractions so that if the size of the particles played a role in the weathering the effect could be eliminated. For the standard test 1.5 kg of the –26 + 22.4, -22.4 + 19 or –19 + 16 mm material was weathered in distilled water (pH 5.5) by immersion for 6 days and in some cases up to 15 days. Tests were performed at room temperature in 10 L flat bottomed plastic containers using 5 L solution. The particles were spread as a single layer, not touching. No dispersion took place. This was compared to the 0 days test which was a 1.5 kg sample that was milled in the unweathered state. The weathered samples were removed from the water after the specific weathering period and left to air dry for 1 day. The fine particles were filtered from the solution and added to the weathered sample after milling. The autogeneous batch mill test was used on the weathered sample. This involved autogeneous dry milling of the ore sample for 10 minutes in a 30 cm inner diameter, 30 cm in length stainless steel, rubber lined lab mill at around 60 rpm. The ore was subsequently removed from the mill and sized. The laboratory mill did not have lifter bars, unlike the autogeneous mill test discussed in the literature study. The weathering tests were performed in close proximity to the laboratory mill so that handling of the ore could be minimised. Some of the later test work did not utilise milling, as the degree of weathering was substantial enough and the size distribution after drying the sample was simply used as the output.

Sieving to determine the particle size distribution was done dry with manual shaking, utilising a single sieve at a time. The particle size distribution curves were plotted using the arithmetic mean sieve size and not the upper size limit as is the convention.

The other variables tested were:

- Time dependence of weathering
- Effect of cation species on weathering
- Effect of cation concentration on weathering
- Effect of temperature on the weathering process
- The influence of particle size
- The influence of anions

5.2.2 Koffiefontein

The standard test (6 or 15 days' weathering) was attempted on Koffiefontein ore but due to an inherently fast weathering rate, complete disintegration of the ore occurred and it could not be compared with the other samples. Instead a –26.5 + 22.4 mm sample was weathered for 1 and 3 hours to obtain results on the weathering rate.

5.2.3 Wesselton

On the Wesselton ore almost no weathering took place with the standard test utilising – 19 + 16 mm ore weathered for 6 and 15 days. More severe test conditions included immersion in acidified water at a pH ~ 3. The solution was prepared by adding sulphuric acid to the distilled water. A sodium chloride solution was also used for weathering tests at a concentration of 0.2 M. Cyclic wetting tests were performed by wetting the ore daily with 500 ml of distilled water. After further test results showed copper to be a very good accelerator for weatherable kimberlite, this was also used as a weathering solution at a concentration of   0.2 M, to test whether this ore maintains its non-weatherability under all the tested conditions. These weathering tests were done on – 26.5 + 22.4 mm particles for 6 days.

5.2.4   Cullinan TKB

The standard test was performed on Cullinan TKB utilising – 19 + 16 mm particles and further testing included using a sodium chloride solution (0.2 M).

5.2.5   Geluk Wes

The standard water test was done on the –19 + 16 mm fraction for 0 and 15 days. Further test work was done on the –22 + 19 mm fraction in sodium-, aluminium- and lithium-chloride solutions (all at 0.2 M concentration) for 6 days. This was done to test the effect of cations on the weathering process. It was specifically tested on this ore because although it has a slow weathering rate in water it does contain swelling clays and is therefore amenable to accelerated weathering by cations. A single test was done to test the effect of low pH (pH ~ 2.5) and cations by adding sulphuric acid to a sodium chloride solution. These tests showed interesting results. Due to limited availability of Geluk Wes ore, the effect of cations was then further investigated on the Dutoitspan sample.

5.2.6   Dutoitspan

The Dutoitspan sample was a large ore sample allowing more tests, specifically on the accelerated weathering of kimberlite by cations.

The standard test was performed on a 1.5 kg, – 26.5 + 22.4 mm sample for 6 days.

5.2.6.1   Influence of Mono-, Di- and Trivalent cations on weathering

This ore was used to finalise the test work to determine the effect of cations on an ore which is known to be weatherable. For monovalent cations the effect of lithium, sodium, potassium and ammonium on the weatherability was tested. Divalent cations included cupric, calcium, magnesium and ferrous. In the trivalent cation group the tests included aluminium and ferric. All these tests were done at 0.4 M cation concentration with kimberlite particles in the -26.5 + 22.4 mm size fraction.

5.2.6.2   Time dependence of weathering

Tests were done on 1.5 kg -26.5 + 22.4 mm Dutoitspan kimberlite samples in a 0.2 M magnesium chloride solution at 2, 6 and 15 days.

The tests were repeated in a 0.2 M copper sulphate solution for 6, 12, 24 and 144 hours, thus up to 6 days.

Another test with a copper sulphate solution was conducted at 0.5 M utilising 200 - 250 g of - 16 + 13.2 mm Dutoitspan kimberlite. This test was done at 4, 8, 24, 48, 168 hours (7 days), 360 hours (15 days) and 720 hours (30 days) to evaluate equilibrium conditions.

5.2.6.3   Influence of cation concentration on weathering

The effect of concentration of cations was tested in a copper solution as this was the most aggressive cation from the previous test work. Test work was done at 0.005, 0.025, 0.05, 0.1, 0.2 and 0.4 M concentrations for 6 days utilising particles sized – 26.5 + 22.4 mm.

5.2.6.4   Influence of temperature on weathering

Temperature tests were done to investigate the mechanism of cation weathering. The tests were performed in a water bath, which allows for temperature regulation. Containers with the ore spread out in the weathering media were placed in the bath and covered to limit the loss of water by evaporation. These tests were done on a 1.5 kg (size fraction – 19 + 16 mm) ore sample weathered in a distilled water and 0.2 M $MgCl_2$ solution at 40 °C for 6 days. The results were compared to room temperature tests.

5.2.6.5   Influence of anions on weathering

The influence of the type of anion was tested by comparing a 0.3 M cupric chloride and cupric sulphate solution weathered for 6 days using a 1.5 kg -26.5 + 22.4 mm sample.

5.2.6.6   Influence of particle size on weathering

The effect of particle size was tested with – 26.5 + 22.4, - 22.4 + 19, - 19 + 16 and - 16 + 13.2 mm size fractions in a 0.2 M $MgCl_2$ solution for 6 days. Magnesium chloride was chosen as the weathering medium because the test work on the influence of cations showed it to be a medium strength accelerator of the weathering process. Therefore the extent of weathering is limited and would enable clear determination of the effect of particle size on weathering.

5.2.6.7   Influence of milling on weathering results

The influence of employing an autogeneous milling test after the weathering procedure was investigated. The weathering tests were done in a 0.2 M copper sulphate solution (- 26.5 +

74

22.4 mm) for 12 hours with one sample milled and compared to the particle size distribution of the unmilled sample.

5.2.6.8 *The effect of a stabilising cation vs. swelling cation*

The effect of a stabilising cation (potassium) vs. a swelling cation (copper) and their effect on weathering was investigated. The test utilised 200 - 250 g of Dutoitspan kimberlite (- 16 + 13.2 mm) weathered in a 0.5 M potassium solution for 8, 48 and 144 hours. The tests were repeated in a 0.5 M copper solution at 4, 8, 24, 48, 168 (7 days) and 360 hours (15 days).

5.2.7 Venetia

The Venetia ores were obtained to validate the weathering mechanism. This ore was received as big lumps (~ 20 – 30 cm) and in limited amounts. Smaller lumps were broken from the bigger pieces and crushed to obtain a workable sample. The final tests were conducted on a 1 kg sample of the – 26.5 + 19 mm size fraction. The weathering was done in a copper sulphate solution (concentration 0.05 M) for a six days weathering period.

Venetia samples were labelled according to their sample position in the Venetia pit and the type of ore (see Doorgapershad *et al*, 2003). These include K1 Hypabyssal North East (K1 HYP NE), K1 Hypabyssal South (K1 HYP S), K1 Tuffisitic Kimberlite Breccia East (K1 TKB E), K2 North East (K2 NE), K2 South (K2 S), K2 West (K2 W), Red Kimberlite and K8.

Because weathering was performed in a copper solution, which caused significant breakdown of the ore, the mechanical test was not required. Therefore the output is just reported as the size distribution after weathering (unmilled).

5.3   Repeatability of results

Triplicate tests were done on Dutoitspan kimberlite to investigate repeatability of the results. 300 g of kimberlite (-16 + 13 mm) was weathered at 0.025, 0.1 and 0.5 M copper concentration for 2 days and the typical error range established. No milling was performed of these samples.

5.4   Kinetic evaluation of cation exchange

In trying to understand the cation exchange mechanism, the kinetics of this exchange reaction was investigated. The experimental work utilised 300 g of Dutoitspan kimberlite (-16 + 13 mm) weathered in 0.025, 0.1 and 0.5 M cupric chloride solutions at room temperature (20 °C). Solution samples (~ 40 ml) were removed at 0, 4 hours, 24 hours, 48 hours, 72 hours, 168 hours (7 days), 360 hours (15 days) and 720 hours (30 days) for ICP analysis.

The kinetic test was repeated on a 300 g Venetia Red kimberlite sample (-16 + 13 mm) weathered in 0.1, 0.5 and 1 M potassium chloride solutions at room temperature (20 °C). Solution samples were removed at 0, 4 hours, 8 hours, 24 hours, 48 hours, 72 hours and 216 hours (9 days) for ICP analysis.

5.5   Cation exchange behaviour

Cation exchange behaviour was investigated utilising 15 g of finely milled Venetia Red kimberlite. The cation solutions were prepared with 200 ml distilled water adding cation sulphate or chloride salts at 0.05 M concentration. The cations utilised included K^+, Li^+, NH_4^+, Ca^{2+}, Mg^{2+}, Ni^{2+}, Fe^{2+}, Cu^{2+}, Fe^{3+} and Al^{3+}. The solutions were sent for ICP analysis after 48 hours.

5.6   Correlation between cation weathering and interlayer spacing (from XRD)

The smectite interlayer spacing was investigated as a function of time to relate the swelling of smectite with the kinetics. Tests utilised 250 - 300 g of -16 + 13 mm Dutoitspan kimberlite, weathered in a 0.5 M solution of cupric chloride for 4 hours, 8 hours, 24 hours (1 day), 168 hours (7 days) and 720 hours (30 days). The kimberlite was removed, air dried for one day, milled to powder and sent for XRD analysis.

The collapsing of the interlayer spacing was investigated utilising 250 – 300 g of – 16 + 13.2 mm Venetia Red kimberlite treated in a 1.5 M potassium chloride solution for 4 hours. The treated and untreated kimberlite was sent for XRD analysis.

The smectite interlayer spacing was investigated with different cation species at 0.5 M concentration weathered for 6 days utilising Dutoitspan kimberlite sized – 16 + 13.2 mm. The cations included Ca^{2+}, Mg^{2+}, Cu^{2+}, Al^{3+}, K^+, NH_4^+, Na^+ and Li^+.

76

5.7   Mechanical test

As stated in section 2.3.1.5 the autogeneous batch-milling test was chosen to quantify the reduced bulk strength. The laboratory mill used was a 30 cm inner diameter, 30 cm in length stainless steel, rubber lined mill (figure 17). This mill did not have lifter bars. All samples were milled for 10 minutes before being removed and sized. The milling speed was fixed at ~ 60 rpm. The material was subsequently screened and a product size distribution determined. The sieve size of the milled unweathered product is the base case (termed 0 days weathering) and compared to the weathered milled product after a specific treatment. The sieve series used can be seen in Appendix C.

The mechanical test was incorporated to simulate typical mechanical forces to which kimberlite ore particles might be exposed to under plant conditions during or after weathering. This includes transport e.g. conveyers, stockpiling, scrubbing etc.

With hindsight it is clear that the mechanical test after weathering might not be required under relatively aggressive weathering conditions. When small differences in weathering behaviour are investigated milling is a useful tool (e.g. for weathering in water or other slow weathering media). However in more aggressive media and with highly weatherable ore, the weathering can be so rapid that a simple sieve analysis of the weathered product, without milling, is sufficient to characterise weathering.

Figure 17. Autogeneous batch mill used.

5.8   Agglomeration test

In order to investigate the stickiness of the kimberlite ore (the extent to which the ore becomes "claylike" and sticks to objects) a possible test for evaluating this property was developed. The test was done by employing a laboratory swing mill (Figure 18). A 200 g dry ore sample (- 9 + 8 mm) was milled for 3 minutes. The sample added to the swing mill container is shown in figure 19. The powder that agglomerated on the grinding surfaces of the metal milling units inside the container and the side walls of the container itself (which could not be removed by light brushing) was then weighed and expressed as a percentage of the total initial mass. The mass of the outer metal ring is 1407.2 g and the inner ring is 1505.6 g.

Figure 18. Swing mill used for agglomeration tests.
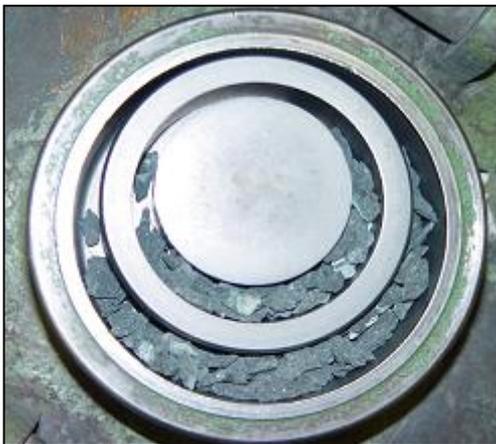
Figure 19. Ore added to the swing mill container for the agglomeration test showing the grinding metal pieces inside the container.

6.   EXPERIMENTAL RESULTS AND DISCUSSION

6.1   Geochemistry and Mineralogy

6.1.1 XRF Analysis

The XRF analysis was done at Mintek Analytical Services and the results shown in table 20. Kimberlite is a magnesium rich ore as discussed in section 2.1.1. The kimberlites also contain considerable amounts of calcium and iron and minor amounts of potassium. The other elements are not present in significant quantities. What is of particular interest is, firstly, K8, which was identified as a dolomite deposit which is supported by the high calcium content. The composition of K8 does not show the considerable carbonate component and therefore only adds up to ~ 67 %. In addition the high aluminium content of the red kimberlite should also be noted. The sum of elements does not equal 100 due to the loss of ignition not included in the table. The weathering indexes discussed in section 2.3.1.1.3 was fitted to the XRF data but no correlation could be found with weathering results reported later.

Table 20.   Results of XRF analysis done at Mintek Analytical Services on the ore samples tested (proportions by mass).

SAMPLE NAME	Na_2O	MgO	Al_2O_3	SiO_2	P_2O_5	K_2O	CaO	TiO_2	Fe_2O_3	MnO	SO_2
	%	%	%	%	%	%	%	%	%	%	ppm
DUTOITSPAN	2.33	25.3	5.94	46.6	0.63	2.03	5.82	0.81	8.45	0.12	< 60
GELUK WES	1.71	25.8	4.44	45.6	0.78	2.86	7.82	1.22	8.89	0.13	233
KOFFIEFONTEIN	1.17	26.3	5.52	49.4	0.33	0.98	5.17	0.75	8.35	0.11	795
CULLINAN	0.80	29.1	4.08	52.6	0.12	1.19	5.15	1.29	9.47	0.15	368
WESSELTON	0.36	32.4	2.07	35.1	1.24	1.86	8.63	1.33	9.83	0.16	244
K1 HYP NE	<300 ppm	32.7	1.6	35.4	0.47	1.57	8.44	0.72	8.25	0.13	346
K1 HYP S	<300 ppm	33.6	0.70	36.6	0.3	0.64	7.18	0.89	8.17	0.12	907
K1 TKB E	0.82	29.0	5.26	47.8	0.15	1.58	3.90	0.50	9.44	0.12	0.1
K2 NE	1.2	25.6	5.93	48.0	0.2	1.18	6.43	0.59	8.7	0.14	96
K2 S	0.6	21.7	5.78	46.5	0.28	1.69	9.88	0.76	8.68	0.19	509
K2 W	0.81	25.7	5.28	47.1	0.28	1.67	7.38	0.75	9.31	0.17	201
K8	<300 ppm	19.1	0.9	14.6	0.28	0.26	27.1	0.67	4.92	0.11	346
Red	1.09	19.6	8.37	51.1	0.18	1.86	4.46	0.72	8.79	0.10	< 60

6.1.2 XRD Analysis

As discussed in the experimental procedure the XRD analysis was done at three different institutions. The results from Mintek are reported in table 21 and 22, although the analysis by the University of Pretoria was used to confirm these results. The original XRD scans from Mintek and the University of Pretoria are shown in Appendix B.

Table 21. XRD Analysis results on Dutoitspan, Geluk Wes, Koffiefontein, Cullinan TKB and Wesselton kimberlites as done by Mintek.

Sample	Mineral group / mineral identified	Probable mineral	Estimated Quantity [Mass %]
Dutoitspan	Smectite	Dioctahedral	30 - 40
	Mica	Biotite / Phlogopite	~ 20
	Calcite		10 – 20
	Pyroxene	Diopside	10 – 20
	Serpentine	Antigorite ?	~ 10
	Magnetite		< 10
	Dolomite		~ 5
	Hematite		< 5
Geluk Wes	Smectite	Dioctahedral	30 - 40
	Calcite		> 20
	Mica	Biotite / Phlogopite	10 - 20
	Serpentine	Lizardite	~ 10
	Pyroxene	Diopside	~ 10
	Feldspar	Albite / Microcline	~ 10
	Magnetite		< 10
	Dolomite		~ 5
	Amphibole	Tremolite	< 5
	Hematite		< 5

Sample	Mineral group / mineral identified	Probable mineral	Estimated Quantity [Mass %]
Koffiefontein	Smectite	Dioctahedral	50 - 60
	Mica	Biotite / Phlogopite	~ 10
	Pyroxene	Augite	< 10
	Serpentine	Antigorite	5 - 10
	Feldspar	Microcline ?	5 - 10
	Dolomite		~ 5
	Calcite		< 5
	Magnetite		< 5
	Quartz		< 5
Cullinan TKB	Mica	Biotite / Hydrobiotite / Phlogopite	~ 25
	Chlorite	Chlinochlore	~ 20
	Magnetite		~ 20
	Talc		~ 15
	Amphibole	Tremolite	10 - 15
	Serpentine	Antigorite	< 10
	Pyroxene	Diopside	< 10
	Smectite	Trioctahedral	~ 5
	Hematite		< 5
	Olivine	Forsterite ?	< 5
	Quartz		< 5
Wesselton	Mica	Biotite	30 - 40
	Calcite		~ 20
	Serpentine	Antigorite ?	~ 20
	Olivine	Forsterite ?	~ 10
	Dolomite		< 10
	Magnetite		< 10
	Goethite		< 5
	Rectorite		~ 5

Table 22. XRD Analysis on Venetia Kimberlites as done by Mintek.

Sample	Mineral group / mineral identified	Probable mineral	Estimated Quantity [Mass %]
K1 HYP NE	Mica	Phlogopite	~ 30
	Calcite		~ 30
	Serpentine	Antigorite	20 - 30
	Magnetite		~ 10
	Chlorite	Chlinochlore	< 5
K1 HYP S	Serpentine	Lizardite	~ 60
	Calcite		20 - 30
	Mica	Biotite	< 10
	Magnetite		< 10
K1 TKB E	Smectite	Dioctahedral	~ 40
	Serpentine	Lizardite / Antigorite	20 - 30
	Mica	Phlogopite	10 - 20
	Amphibole	Tremolite	< 10
	Pyroxene	Diopside ?	< 10
	Dolomite		~ 5
	Magnetite		< 5
	Chlorite	Chlinochlore	< 5
	Calcite		< 5
K2 NE	Smectite	Dioctahedral	~ 45
	Mica	Phlogopite	20 - 30
	Pyroxene	Augite	10 - 20
	Serpentine	Antigorite	~ 10
	Magnetite		< 10
	Amphibole	Tremolite	~ 5
	Calcite		< 5
	Dolomite		< 5

Sample	Mineral group / mineral identified	Probable mineral	Estimated Quantity [Mass %]
K2 S	Smectite	Trioctahedral	~ 40
	Calcite		~ 30
	Mica	Biotite / Phlogopite	~ 20
	Amphibole	Tremolite	10 – 20
	Quartz		~ 10
	Magnetite		Trace
	Serpentine	Lizardite	Trace
K2 W	Smectite	Mixed layer	~ 30
	Pyroxene	Augite	< 30
	Mica	Biotite / Phlogopite	~ 25
	Serpentine	Antigorite	~ 10
	Calcite		~ 10
	Magnetite		< 10
	Dolomite		~ 5
RED KIMB	Smectite	Dioctahedral	~ 40
	Quartz		~ 25
	Calcite		~ 10
	Feldspar	Albite	~ 10
	Serpentine	Lizardite	< 10
	Mica	Phlogopite	~ 5
	Amphibole	Tremolite	< 5
	Magnetite		< 5
K8	Dolomite		> 90
	Calcite		< 10
	Unknown silicate		< 5

Initial test work used Koffiefontein and Wesselton ore. These ores show contrasting weathering behaviour as Koffiefontein weathered in minutes and Wesselton showed very little degradation even after fifteen days of exposure. XRD investigations showed Koffiefontein ore to contain predominantly swelling clays compared to Wesselton containing very little or no swelling clay (see table 21). Based on these preliminary results the hypothesis developed

84

around swelling clays and was refined through further test work and investigation. Cullinan TKB ore contains very little swelling clay resulting in a very low weathering rate. Geluk Wes contains 30 – 40 % swelling clay and therefore showed a medium to fast weathering behaviour depending on the weathering conditions. Similarly Dutoitspan contains 30 – 40 % swelling clay and shows similar weathering behaviour to Geluk Wes.

The position of the 060 reflection of smectite gives some information whether dioctahedral (montmorillonite, beidellite and nontronite) or trioctahedral (hectorite and saponite) smectites are present (Weaver, 1989). Dioctahedral smectites have reflections at 1.490 – 1.515 Å compared to trioctahedral smectites with reflections at 1.515 –   1.55 Å. This classification was done on the kimberlites used in this study and is given in tables 21 and 22. Note that the smectite was of the dioctahedral type in nearly all cases.

6.1.3 Visual observation of the kimberlite ores

Photographs were taken of all the kimberlites used for test work and these are shown in figure 20. The lumps are ~ 25 mm in size.

Dutoitspan	Geluk Wes
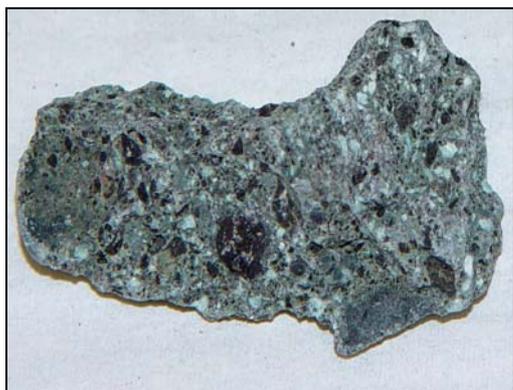
Koffiefontein	Wesselton

Venetia K1 Hypabyssal North East	Venetia K1 Hypabyssal South

| Venetia K1 TKB East | Venetia K2 North East |

| Venetia K2 South | Venetia K8 |

| Venetia Red |

Figure 20. Visual appearance of the untreated kimberlite lumps.

The kimberlite ores exhibit very different physical appearances as shown in figure 20. Colours range from grey, green, yellow, brown to blue and even red. Also the fine-grained matrix and larger xenoliths are easily identified.

87

6.1.4 Cation Exchange Capacity (CEC)

The cation exchange capacity (CEC) (procedure discussed in section 2.2.2.8) was determined at Agricultural Research Council (ARC) in Pretoria. A pulverised 300 g sample is used for this analysis. The CEC results are given in table 23 below.

Table 23. Cation Exchange Capacities for the kimberlites tested.

Sample Name	CEC cmol$_c$/kg
Dutoitspan	41.3
Geluk Wes	33.0
Koffiefontein	44.6
Cullinan TKB	18.7
Wesselton	5.4
V_K1 HYP NE	15.9
V_K1 HYP S	8.3
V_K1 TKB E	45.3
V_K2 NE	41.0
V_K2 S	31.1
V_K2 W	29.2
V_K8	10.4
V_Red	36.5

6.1.5 Conclusion

From the XRF and XRD results it is concluded that the kimberlites obtained for test work, vary extremely in geological and mineralogical properties. All the kimberlites contain considerable amounts of clay material. The predominant mineral species present are: amphibole, calcite, chlorite, feldspar, magnetite, mica, olivine, pyroxene, serpentine, smectite and talc. The smectite content and CEC values of all kimberlites used in this study are compared in figure 21. The cation exchange capacity is strongly influenced by the swelling clay content but also secondarily depends on the amounts of other minerals – for example, chlorite and mica - as they have different capacities to exchange cations. Therefore the ores with no swelling clay do have a non-zero and variable CEC. The cation exchange capacity is a property that can be used to complement the swelling clay content to provide information on the possible

weathering behaviour of a kimberlite. However due to the complexity and cost associated with XRD, CEC is the preferred property.
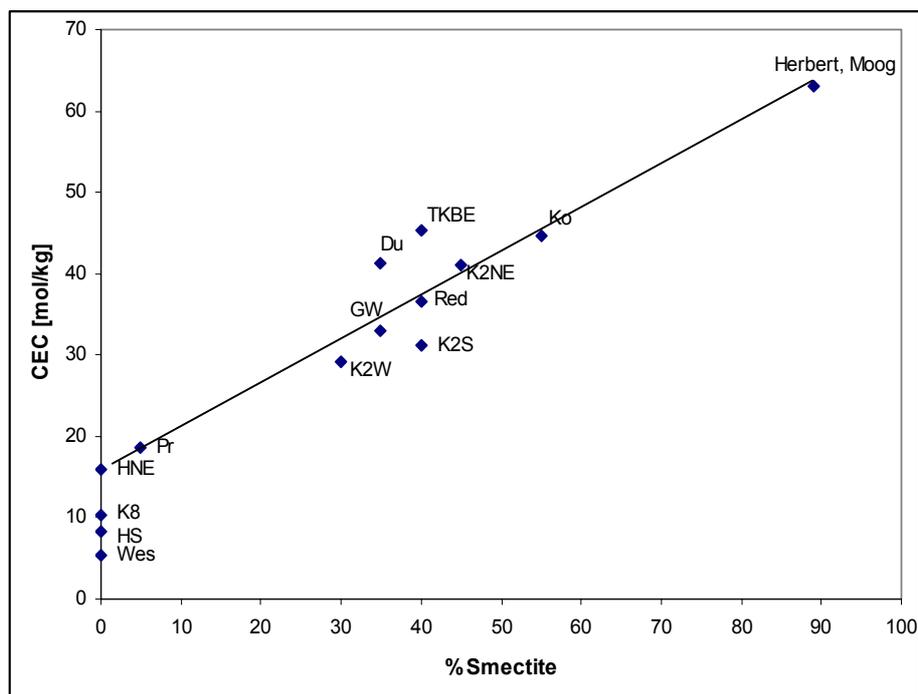
Figure 21. Comparison of the cation exchange capacity (CEC) and % smectite. Additionally a datapoint for a sodium bentonite from Herbert and Moog (1999) are presented.

The smectite - CEC relationship was plotted (figure 21) with the relationship $y = 0.57 x + 15.5$. A data point from the study of Herbert and Moog (1999) on bentonite clay was added to figure 21.

6.2   Weathering Results

Weathering results are given as the size distribution after milling. The unweathered ore was milled (labelled 0 days) and this size distribution given as the base case for comparison. The size distributions are given on linear scales on both axes as this was found to depict the results optimally. Weathering results at a later time did not utilise milling (as it was not required); the output of these tests is therefore given only as the size distribution after weathering and outdoor drying. The influence of milling on the size distribution is investigated in section 6.2.5.8. The repeatability of results was tested and is discussed in section 6.3.

6.2.1   Koffiefontein

The Koffiefontein sample was found to weather at a very high rate, as it forms fines within hours of contact with distilled water (figure 22).   This correlates with the mineralogical investigation reporting this ore to be very rich in swelling clays ~ 50 - 60 %. Figure 22 shows visual breakdown of this ore after 1 and 3 hours of exposure to distilled water.
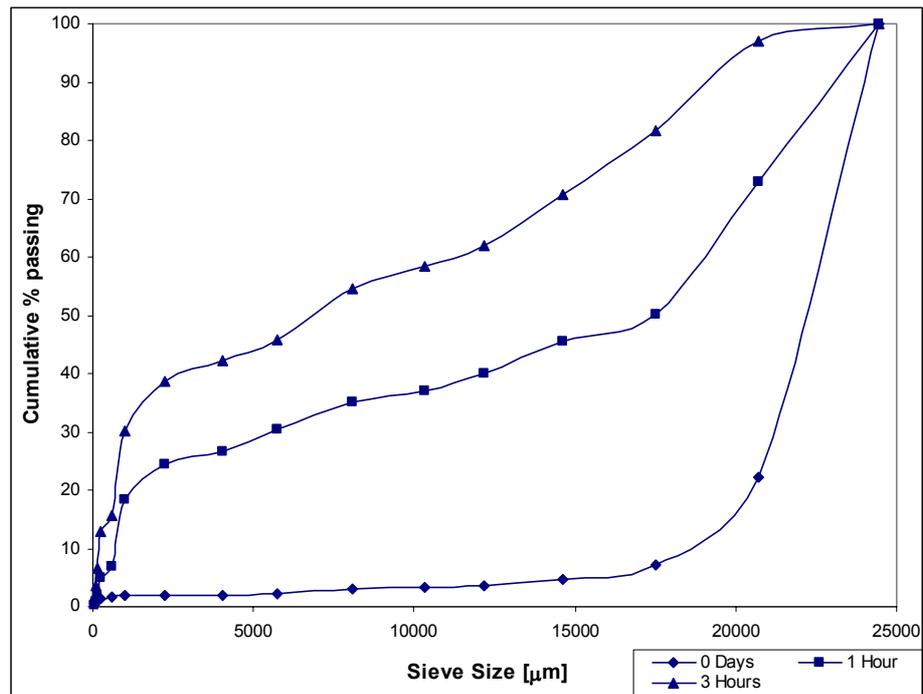
Figure 22. Results of a 1.5 kg (– 26.5 + 22.4 mm) Koffiefontein sample weathered for 1 and 3 hours respectively in distilled water.
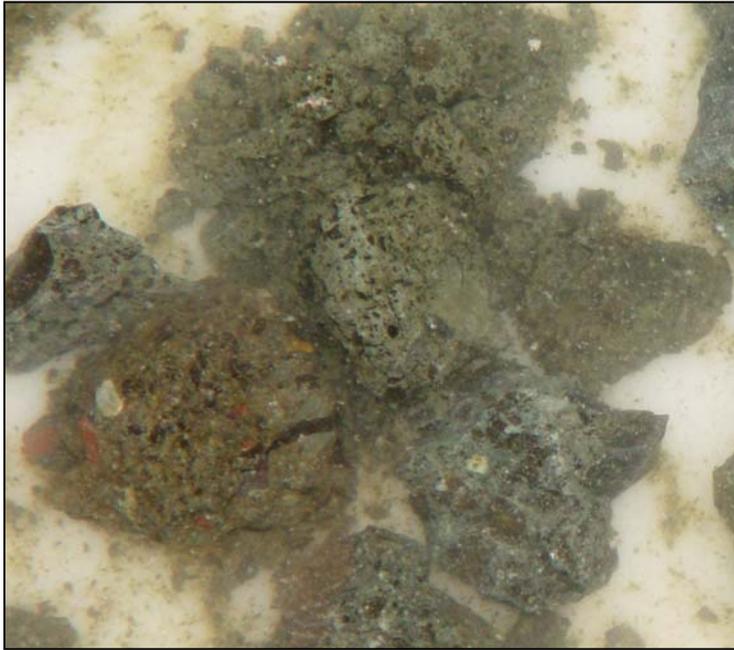
Figure 23.   Visual appearance of Koffiefontein ore (- 26.5 + 22.4 mm initial size fraction) weathered for 3 hours in distilled water.

Within 1 hour the cumulative % passing 17.5 mm has increased from 7 to 50 %, which is further increased to 82 % after 3 hours.   The particle size distribution shape remains similar but shifts to smaller size fractions. Figure 23 shows that the particles are cracked and some broken into fines already after 3 hours of weathering.

6.2.2   Wesselton

Wesselton ore was tested in different solutions namely water (figure 24), sodium chloride (figure 25), sulphuric acid (figure 26), cyclic wetting with distilled water (figure 27) and copper sulphate (figure 28). The visual appearance of the product of the standard weathering test is shown in figure 29.
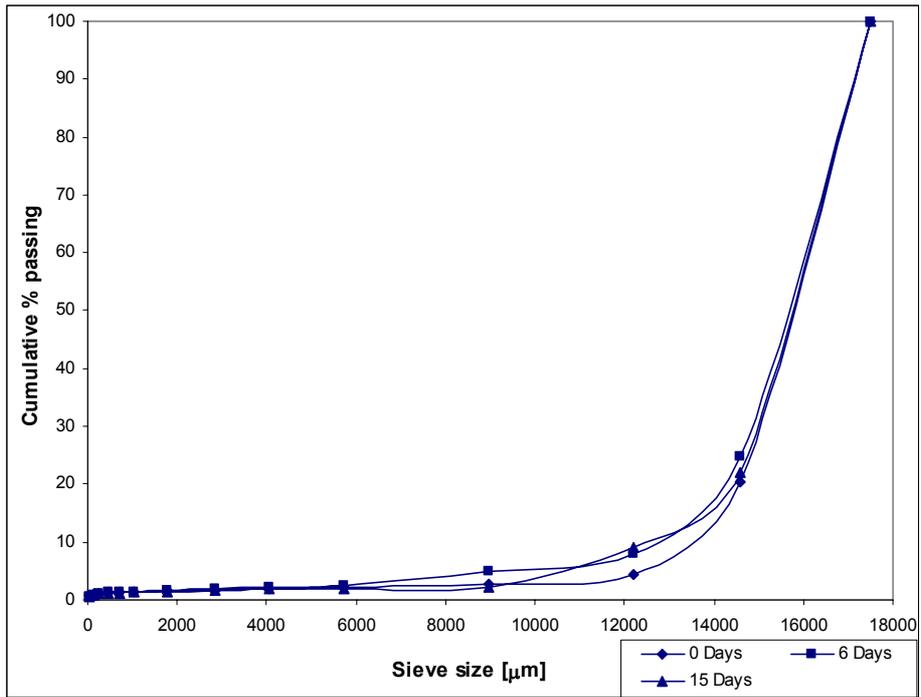
Figure 24. Weathering results from the standard test procedure; 1.5 kg (– 19 + 16 mm) Wesselton ore weathered in distilled water for 0, 6 and 15 days.
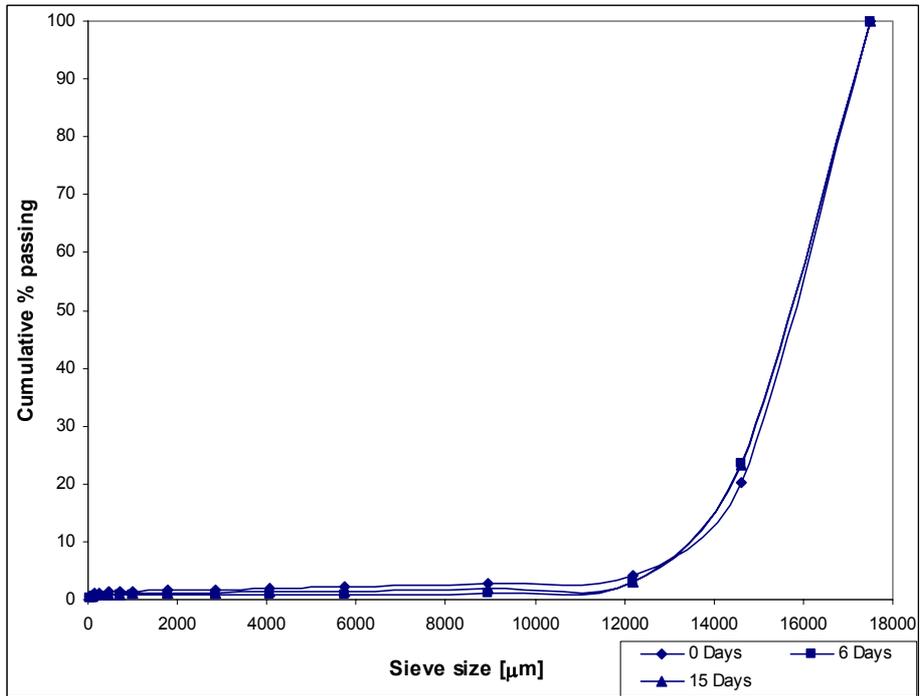
Figure 25. Weathering results from a 1.5 kg (– 19 + 16 mm) Wesselton ore sample weathered in sodium chloride solution (0.2 M) for 0, 6 and 15 days.
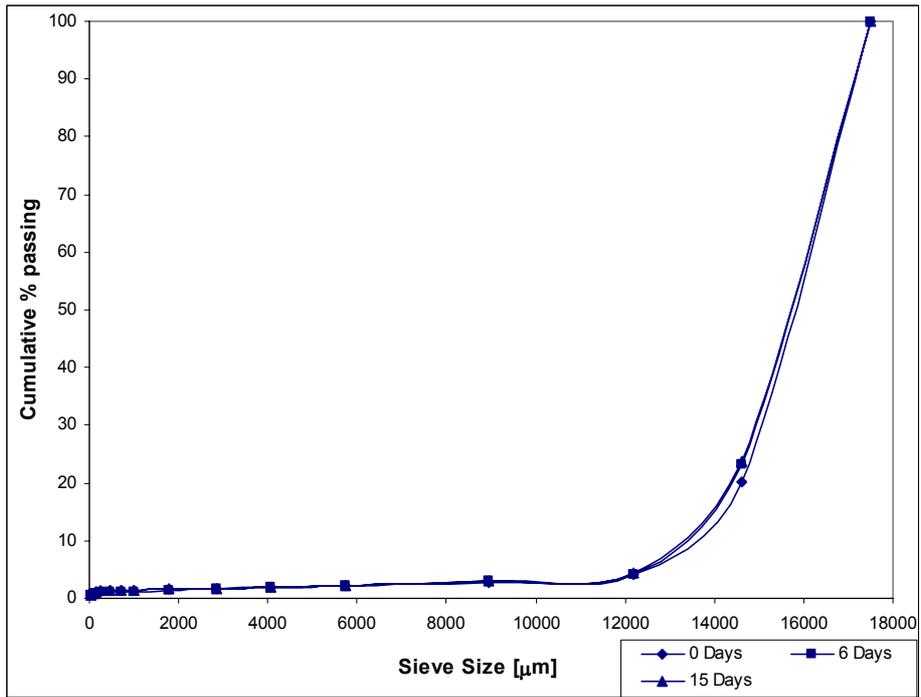
Figure 26.   Weathering results from a 1.5 kg (– 19 + 16 mm) Wesselton ore sample weathered in dilute sulphuric acid (pH ~ 3) for 0, 6 and 15 days.
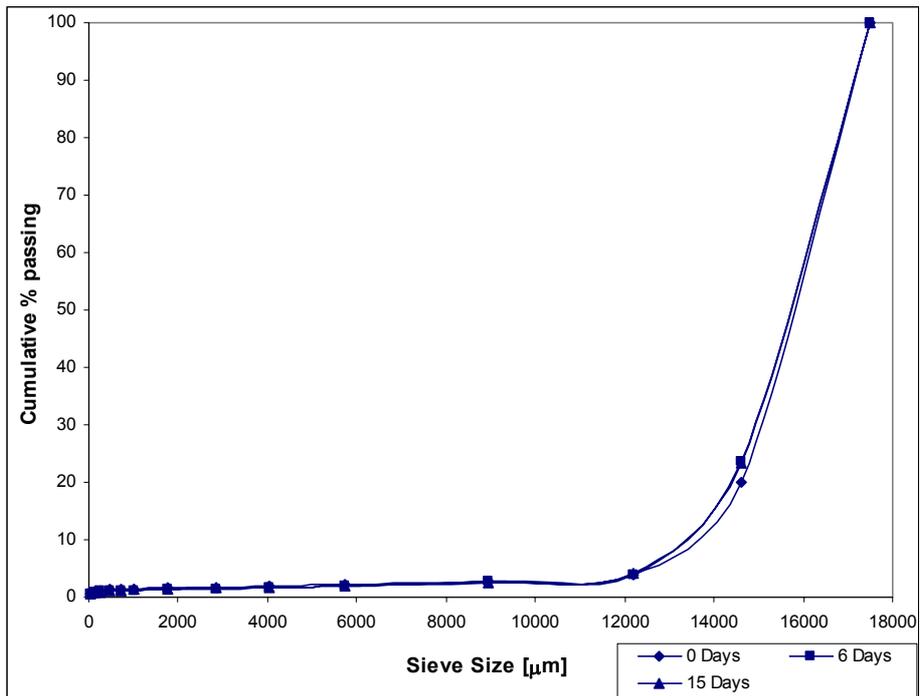
Figure 27.   Weathering results from a 1.5 kg (– 19 + 16 mm) Wesselton ore sample weathered by cyclic wetting with 500 ml of distilled water once a day for 0, 6 and 15 days.
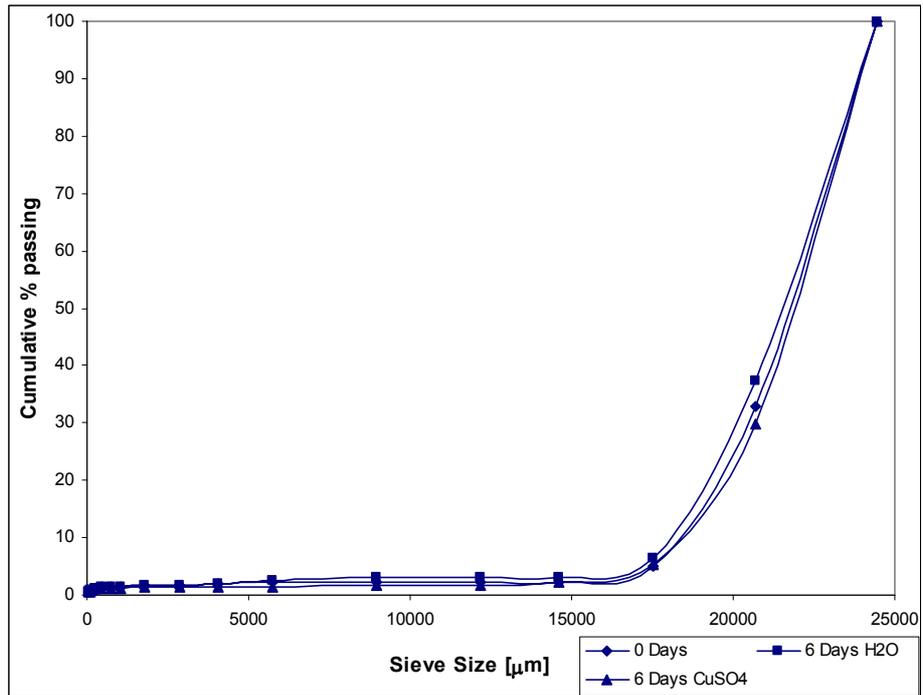
Figure 28.   Weathering results from a 1.5 kg (– 26.5 + 22.4 mm) Wesselton ore sample weathered in a 0.2 M copper sulphate solution for 0 and 6 days. The 6 days standard weathering test is shown for comparative purposes.

Figure 29.   Visual appearance of Wesselton ore after the standard weathering test (- 19 + 16 mm).

From the results of figures 24 to 27 it is concluded that this type of ore is not weatherable even under severely aggressive conditions. The absence of weathering is attributed to the fact that the ore does not contain any swelling clays (see section 6.1.2). Even the copper solution (figure 28), which showed severe attack on other ores made no significant impact on this ore.

6.2.3 Cullinan

Cullinan ore (- 19 + 16 mm) was weathered according to the standard weathering test (figure 30) and also in a 0.2 M sodium chloride solution (figure 31).
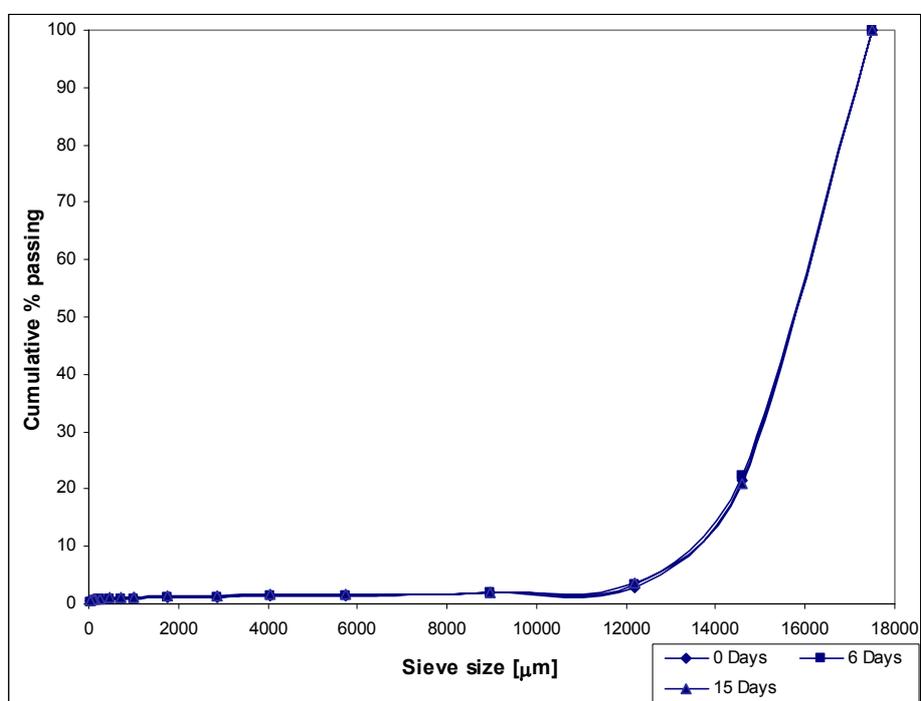
Figure 30. Weathering results from a 1.5 kg (– 19 + 16 mm) Cullinan TKB ore sample weathered by the standard test method for 0, 6 and 15 days.
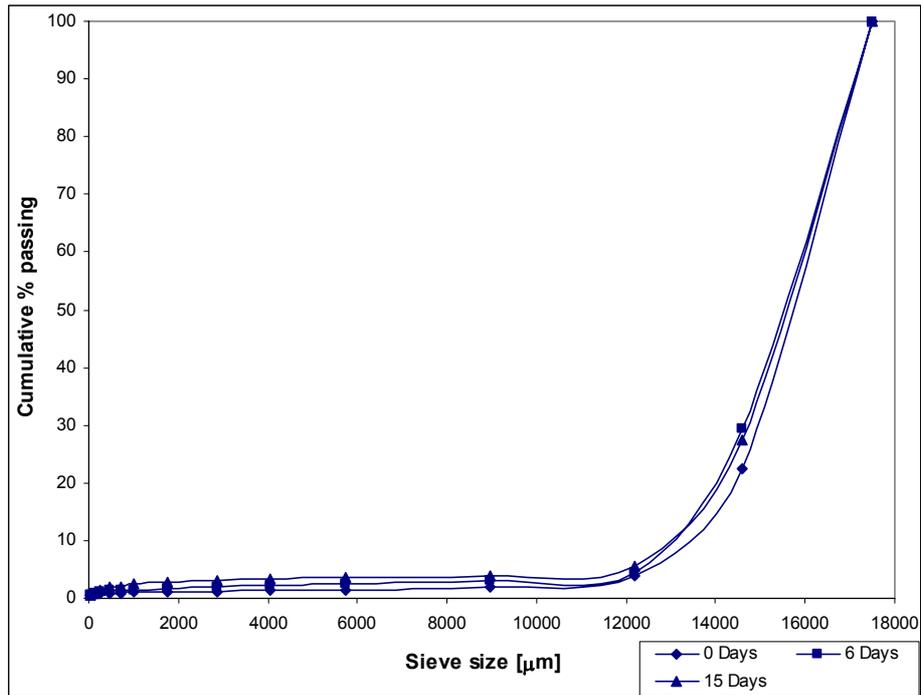
Figure 31. Weathering results from a 1.5 kg (– 19 + 16 mm) Cullinan TKB ore sample weathered in a 0.2 M sodium chloride solution for 0, 6 and 15 days.

Figure 32. Visual appearance of Cullinan TKB ore after the standard weathering test (-19 + 16 mm).

This ore also shows very little change when weathered (no change in particle size distribution). There is slightly enhanced weathering (~ 5 % increase in cumulative % passing 12.2 mm) in sodium chloride. This is however not a large enough increase to be considered a

96

significant influence. This ore contains less than five percent swelling clays, which is the presumed reason why weathering is very slow. The product of the standard weathering test is shown in figure 32.

6.2.4   Geluk Wes

This ore was weathered according to the standard conditions and then the effect of some cations (sodium, aluminium and lithium) was tested. The sodium chloride solution test was repeated with the addition of sulphuric acid to investigate the influence of pH.
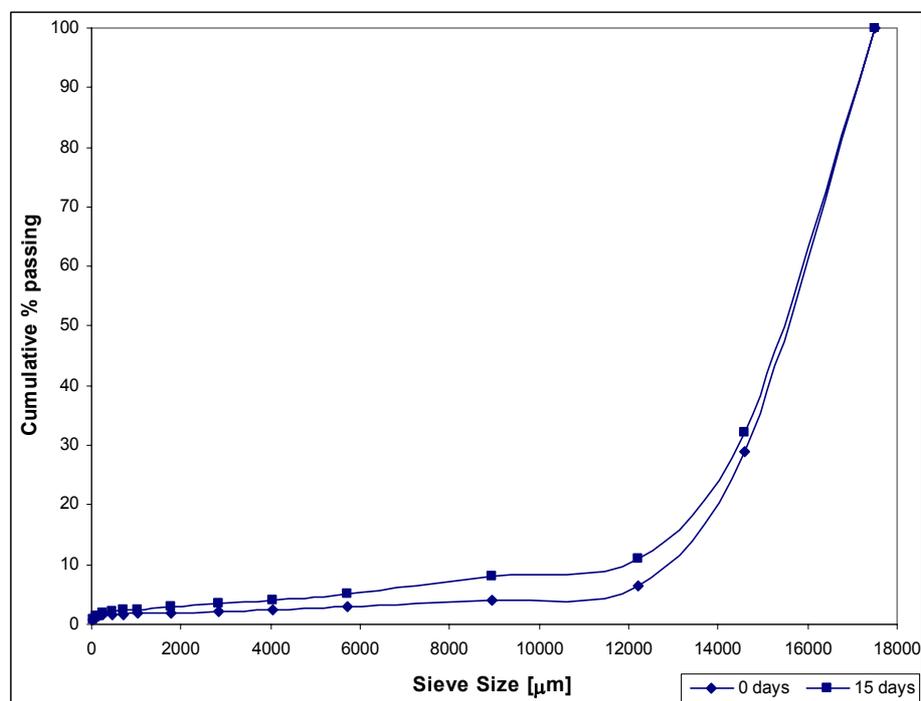
Figure 33.   Weathering results from a 1.5 kg (– 19 + 16 mm) Geluk Wes ore sample weathered by the standard test method for 0 and 15 days.
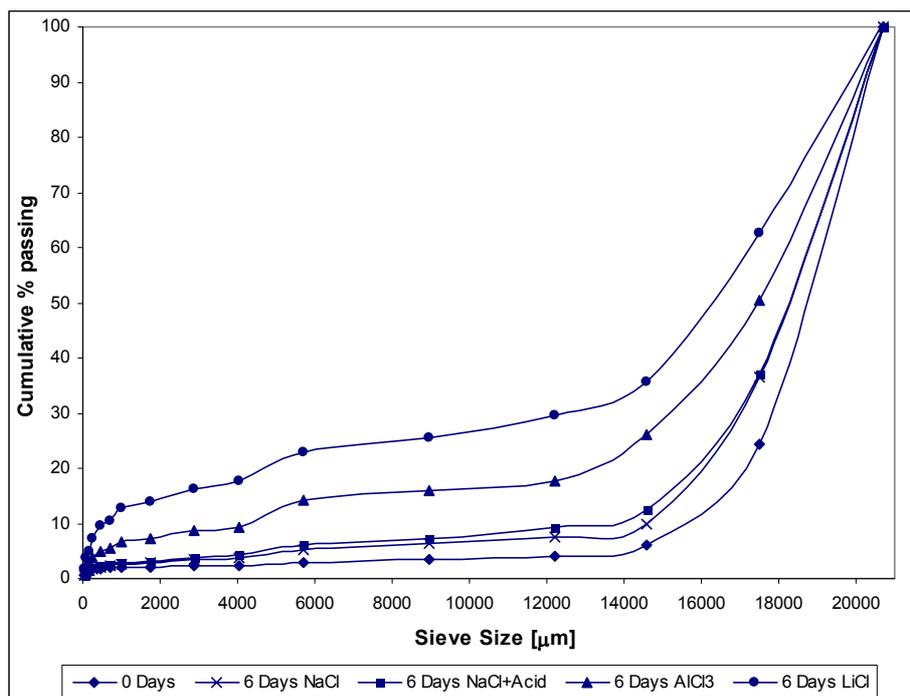
Figure 34. Weathering results from a 1.5 kg (– 22.4 + 19 mm) Geluk Wes ore sample weathered in 0.2 M sodium chloride, acidified sodium chloride at low pH (~ 2.5), aluminium chloride and lithium chloride solutions, all for 6 days.

Weathering of Geluk Wes ore in water shows a maximum of 5 % increase in cumulative % passing over the whole size range, after 15 days. Therefore under normal plant conditions this ore will show degradation to a limited extent.

Figure 34 shows the influence of cations on the weathering process. The results show a nominal increase (compared to water weathering) of 10 % in cumulative % passing 17.5 mm with the addition of sodium chloride, 25 % with aluminium chloride and 35 % with lithium chloride. It also shows that the addition of acid to the sodium medium did not enhance weathering and therefore acidification has no significant influence on weathering in this case. However the pH will influence the complex formation and precipitation reactions of cations. Figures 35, 36 and 37 show photographs of the weathered products using sodium chloride, aluminium chloride and lithium chloride solutions, respectively. Note the increase in broken material and fines from the sodium medium to the aluminium medium and then the lithium medium. These results led to further test work on the effect of cations using the Dutoitspan ore.
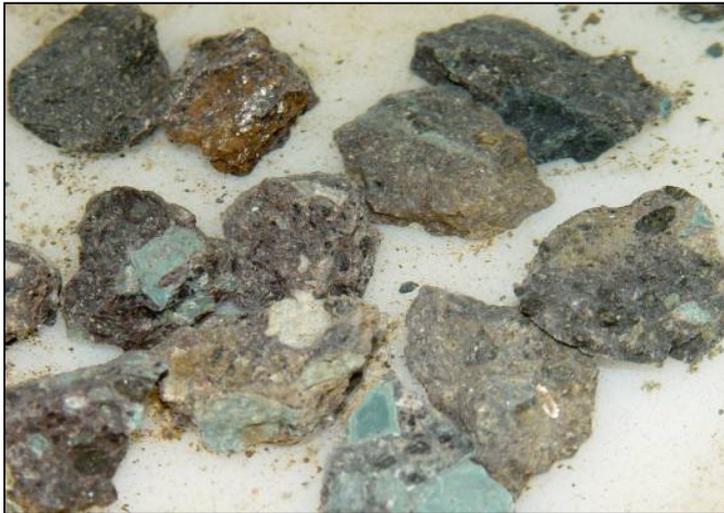
Figure 35. Visual appearance of Geluk Wes ore (initial size -22.4 + 19 mm) weathered in sodium chloride solution (0.2 M) for 6 days.

Figure 36. Visual appearance of Geluk Wes ore (initial size - 22.4 + 19 mm) weathered in aluminium chloride solution (0.2 M) for 6 days.

Figure 37. Visual appearance of Geluk Wes ore (initial size -22.4 + 19 mm) weathered in lithium chloride solution (0.2 M) for 6 days.

6.2.5 Dutoitspan

6.2.5.1   Standard weathering test
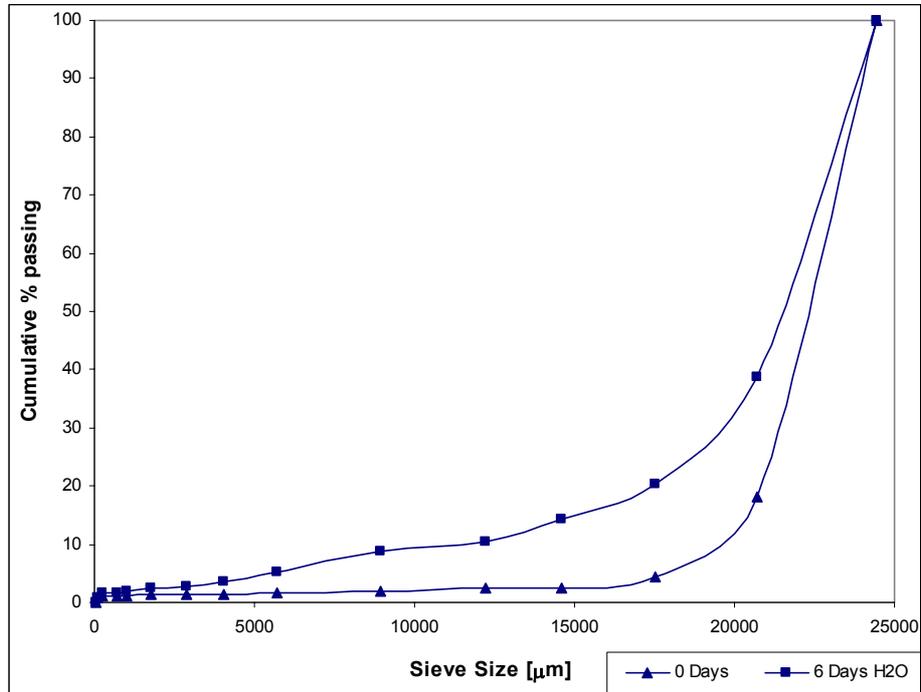
Figure 38. Weathering results from a 1.5 kg (– 26.5 + 22.4 mm) Dutoitspan ore sample weathered for 6 days in a distilled water medium.

Figure 38 shows the results of the standard weathering test on the Dutoitspan kimberlite. The unweathered sample, milled, gave 3.7 % passing 12.2 mm. The 6 days distilled water weathered sample resulted in 13 % passing 12.2 mm. The standard weathering test therefore gave a ~ 9 – 10 % change in the product size distribution. This test gives an indication of what might be expected under plant conditions from this ore, which again shows some degradation but not full disintegration.

6.2.5.2   Influence of cation species on weathering

Monovalent Cations

The results for weathering in a potassium-, sodium-, ammonium- and lithium chloride solution are shown in figure 43. Photos of the products are shown in figures 39-42.
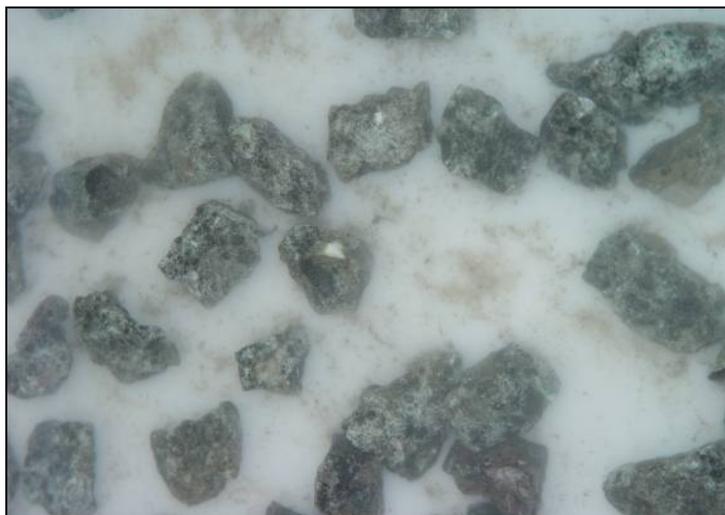
Figure 39. Visual appearance of Dutoitspan ore (initial size - 26.5 + 22.4 mm) weathered in potassium chloride solution (0.4 M) for 6 days.

Figure 40. Visual appearance of Dutoitspan ore (initial size - 26.5 + 22.4 mm) weathered in lithium chloride solution (0.4 M) for 6 days.

Figure 41. Visual appearance of Dutoitspan ore (initial size - 26.5 + 22.4 mm) weathered in ammonia chloride solution (0.4 M) for 6 days.

Figure 42. Visual appearance of Dutoitspan ore (initial size - 26.5 + 22.4 mm) weathered in sodium chloride solution (0.4 M) for 6 days.
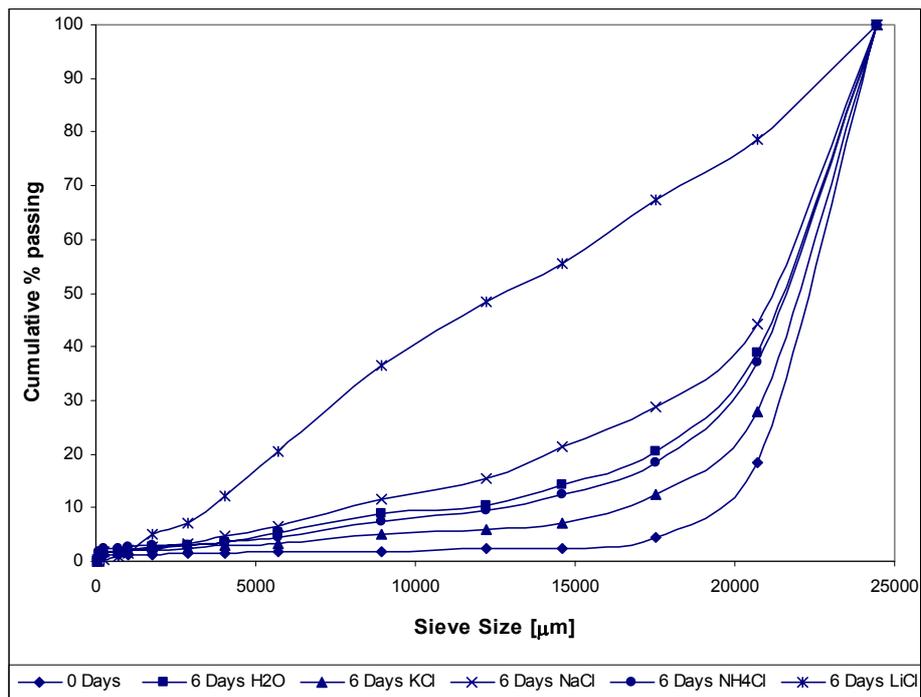
Figure 43. Results of the investigation on the influence of monovalent cations on the weathering behaviour of Dutoitspan ore. Tests were done utilising 1.5 kg (initial size – 26.5 + 22.4 mm) ore weathered in a 0.4 M cation solution for 6 days.

Visual appearances of the weathering tests are shown in figures 39 – 42 for the monovalent cations. The results of figure 43 show that, as suggested in literature (Vietti, 1994) the weathering behaviour can be decelerated by potassium, which in this case decreased the ore passing 17.5 mm by 6 %. Water and ammonium chloride showed similar weathering

103

behaviour, with sodium showing increased weathering of ~ 9 % compared to distilled water. Lithium showed the maximal weathering behaviour with 67 % ore passing 17.5 mm which is a substantial increase of ~ 50 %.

Divalent Cations

The results for weathering in a calcium-, cupric-, ferrous- and magnesium chloride solution are shown in figure 48. Photos of the products are shown in figures 44-47.

Figure 44. Visual appearance of Dutoitspan ore (initial size - 26.5 + 22.4 mm) weathered in calcium chloride solution (0.4 M) for 6 days.

Figure 45. Visual appearance of Dutoitspan ore (initial size - 26.5 + 22.4 mm) weathered in cupric chloride solution (0.4 M) for 6 days.
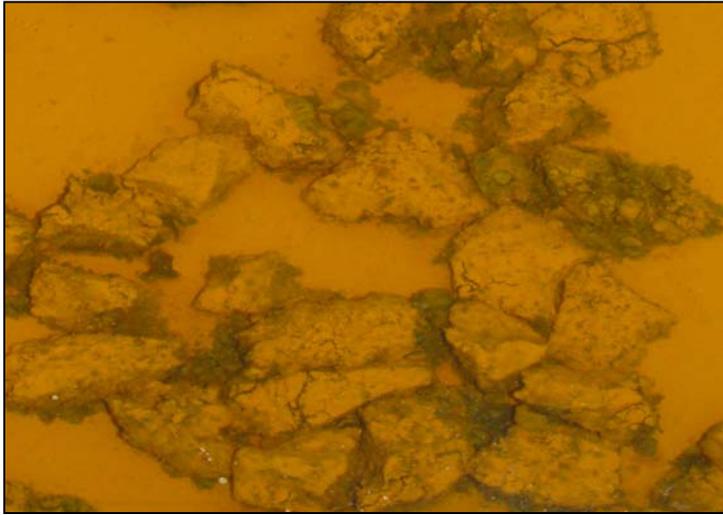
Figure 46. Visual appearance of Dutoitspan ore (initial size - 26.5 + 22.4 mm) weathered in ferrous chloride solution (0.4 M) for 6 days.

Figure 47. Visual appearance of Dutoitspan ore (initial size - 26.5 + 22.4 mm) weathered in magnesium chloride solution (0.4 M) for 6 days.
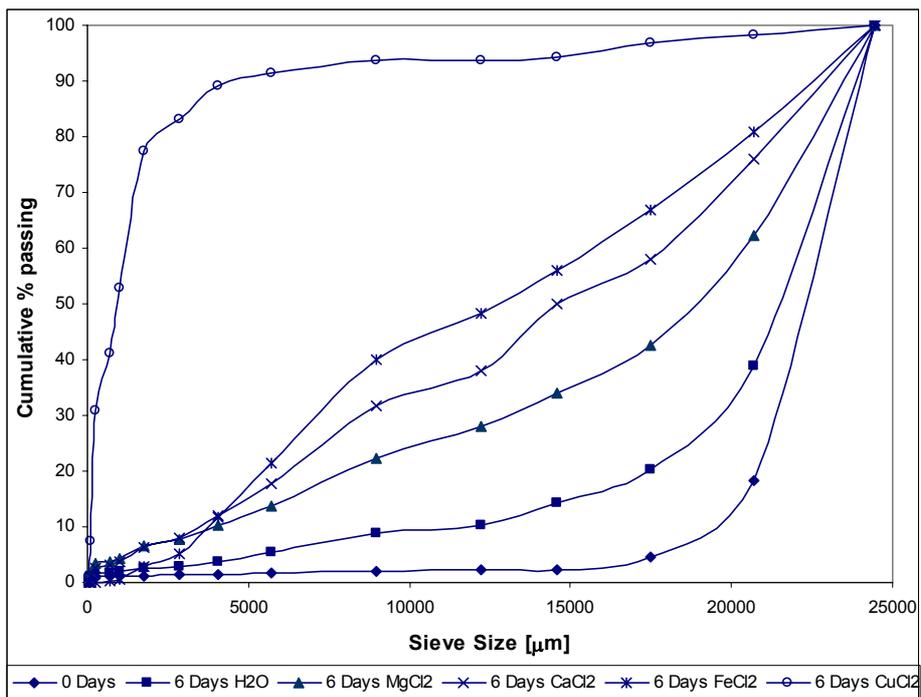
Figure 48. Results of the investigation on the influence of divalent cations on the weathering behaviour. Tests were done utilising 1.5 kg (initial size – 26.5 + 22.4 mm) Dutoitspan ore weathered in 0.4 M cation solution for 6 days.

Of the divalent cations copper was the most efficient cation, followed by iron, then calcium and lastly magnesium. Magnesium produced 42 % passing 17.5 mm, an increase of some 22 % relative to water weathering. Calcium results in 58 % passing 17.5 mm with ferrous iron giving 67 %. Copper showed unique weathering behaviour, moving the whole size distribution to the left to 90 % passing 4 mm. The shapes of the size distribution curves remain similar for unweathered, water, magnesium, calcium and ferrous iron, but copper produces a totally different form of size distribution.

Trivalent Cations

Tests on the influence of trivalent cations used aluminium and ferric ions at a 0.4 M concentration (with chloride as the anion).
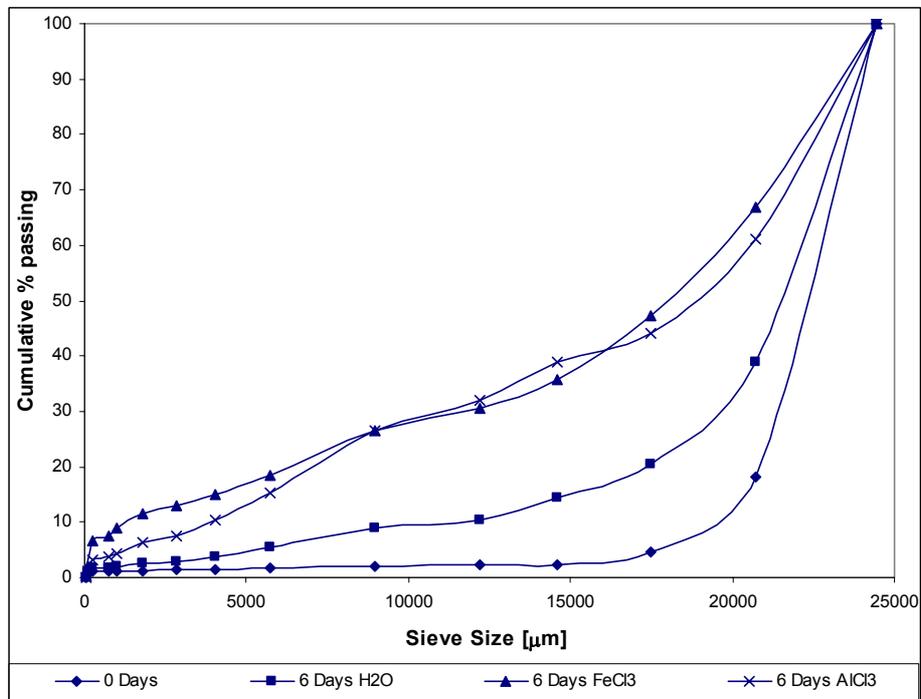
Figure 49. Results of the investigation on the influence of trivalent cations on the weathering behaviour. Tests were done utilising 1.5 kg (initial size – 26.5 + 22.4 mm) Dutoitspan ore weathered in a 0.4 M cation solution for 6 days.

Aluminium and ferric cation solutions showed similar weathering behaviour with ~ 45 % passing 17.5 mm.

Comparison of the weathering effect for differently charged cations is shown in figure 50.
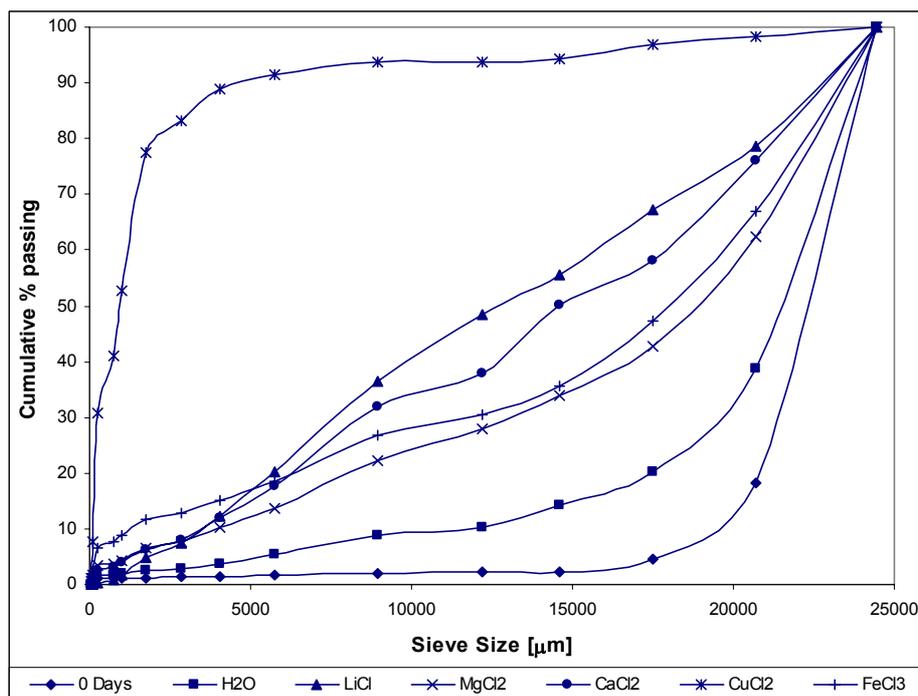
Figure 50. Comparing the influence of different charged cations on weathering behaviour. The tests were done on a 1.5 kg (- 26.5 + 22.4 mm) sample weathered for 6 days in a 0.4 M solution.

Comparison of differently charged cations yields the weathering series from most effective to least effective, as $Cu^{2+} > Li^+ > Ca^2 > Fe^{3+} > Mg^{2+}$. Newman (1987) showed that Mg^{2+} and Ca^{2+} hydrate to two sheet complexes under controlled humidity whereas Sr and Ba tend to form single layer complexes. All the cations Mg^{2+}, Ca^{2+}, Sr^{2+} and Ba^{2+} cause the clay to swell to 19 Å in water, but never swell macroscopically. Newman (1987) showed that K^+ easily dehydrates in the interlayer spacing, tending towards spacings of 12 – 13 Å in water. NH_4^+ behaves similar to K^+ with the exception that it can dissociate into H^+ and NH_3. Cs^+ and Rb^+ are large enough to prevent swelling and both form ~ 12 Å interlayer spacings independent of water content. Al^{3+} is shown by Newman (1987) to wet up to 19 Å but can increase to ~ 22 Å at high pH values due to the formation of Al-OH polymers.

The ionic potential (Z/r_{eff}) is an indication of the strength of hydration of cations of valency Z and effective ionic radius r_{eff}. Ferrage *et al* (2005) showed a correlation between the ionic potential and interlayer spacing (as measured by XRD). The ionic potential was therefore investigated for possible correlation with weathering results as shown in figure 51. The r_{eff} values were obtained from Shannon (1976), using the values for 6-fold coordination. Disregarding trivalent cations (which tend to form hydroxy interlayers, rather than simply exchanging into the interlayer), the relationship between observed weathering behaviour and ionic potential is strong. The weathering effects of Cu^{2+}, Fe^{2+} and Li^+ clearly lie above the trend formed by the other monovalent and divalent cations. It has been reported that all three

108

of these ions adsorb at other positions (such as crystal edges) in addition to exchanging into the interlayer (Strawn *et al*, 2004, Hofstetter *et al*, 2003, Anderson *et al*., 1989). This might explain the strong weathering effects of these three cations; it is argued later in this thesis that their strong weathering effect is probably related to a reduction in surface energy, so reducing the work required to generate fresh crack surfaces. The ionic potential correlation studied by Ferrage *et al* (2005) was not validated for trivalent cations as the clay structure was found to be very heterogeneous and assessment of the degree of saturation was difficult. Trivalent cations especially Al^{3+} and Fe^{3+} tend to form hydroxy species in the clay interlayer as utilised in pillared clay formation (Belver *et al*, 2004; Newman, 1987).   Polycation pillaring of smectites has also been investigated. This suggests that the mechanism of adsorption for trivalent cations are very different than mono- and divalent cation adsorption and could possible explain the poor correlation in figure 51.
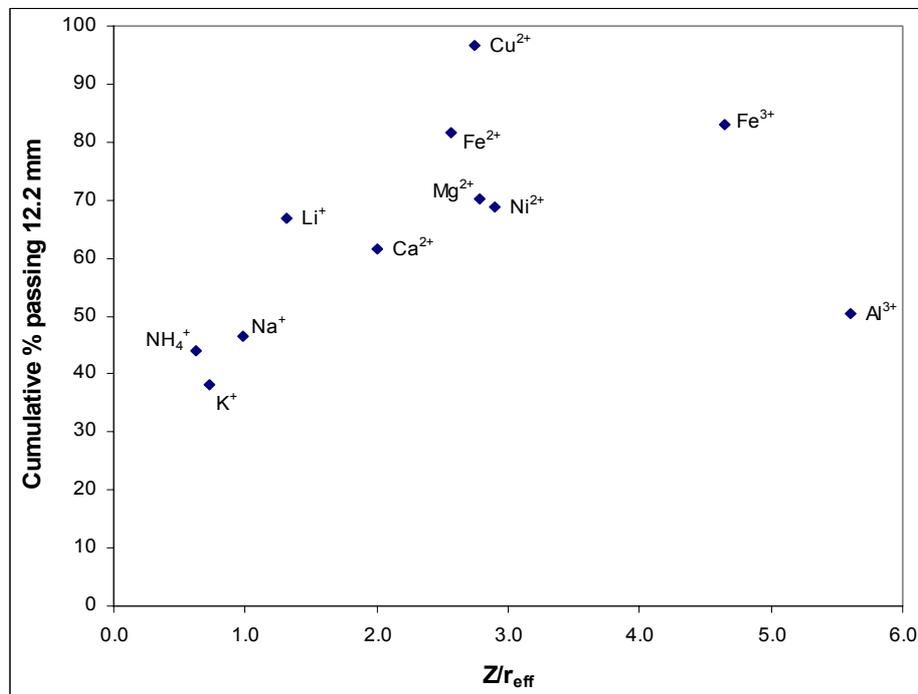
Figure 51. Weathering results of differently charged cations as a function of ionic potential. Weathering tests were performed with 300 g of – 16 + 13.2 mm Dutoitspan kimberlite, weathered in a 0.5 M cation solution for 6 days.

Based on the observed weathering acceleration, further tests were done on the concentration and time dependence when using cations in the weathering solution.

6.2.5.3   Time dependence of weathering

The time dependence of weathering was tested in magnesium and copper containing media.

Magnesium Chloride Medium

The time dependence of weathering was tested in a magnesium chloride solution (0.2 M) for 2, 6 and 15 days. Results are shown in figures 52 and 53.
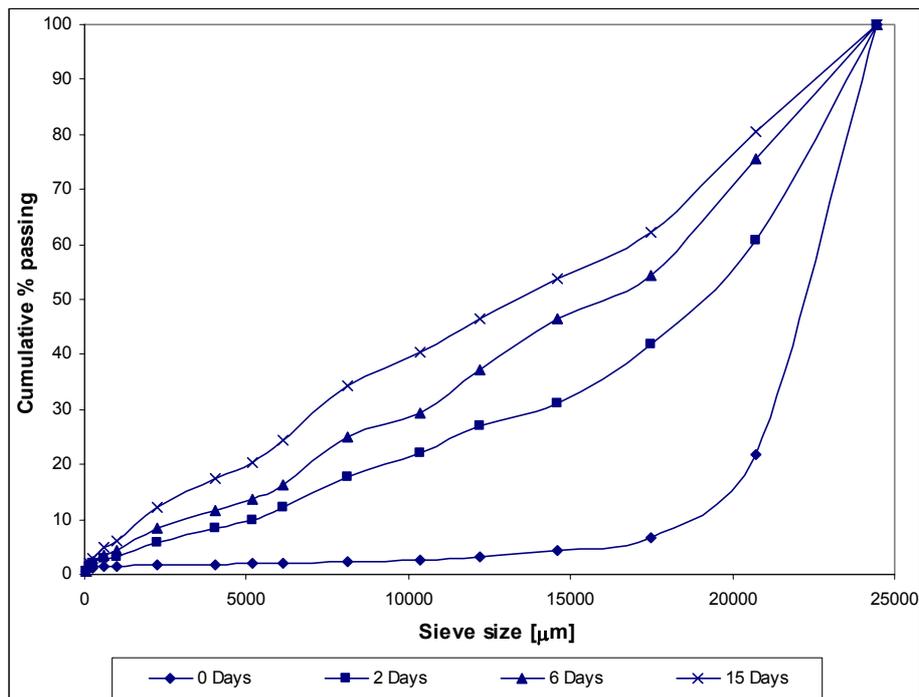
Figure 52. Weathering results from a 1.5 kg (initial size – 26.5 + 22.4 mm) Dutoitspan ore sample weathered in a 0.2 M magnesium chloride solution for 0, 2, 6 and 15 days.
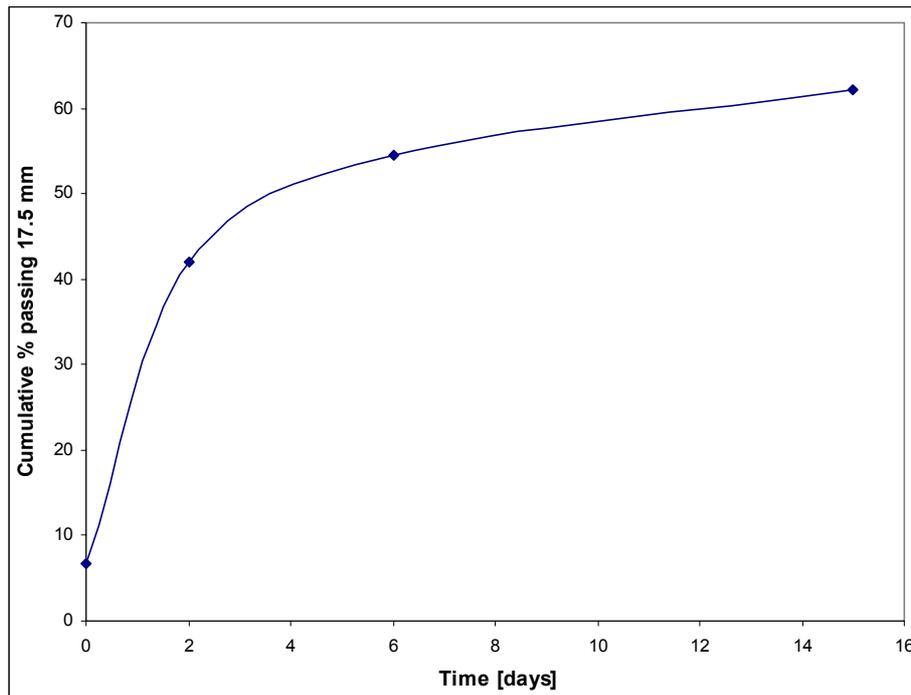
Figure 53. Summarised weathering results from a 1.5 kg (initial size – 26.5 + 22.4 mm) Dutoitspan ore sample weathered in a 0.2 M magnesium chloride solution for 0, 2, 6 and 15 days (from figure 52).

Figure 52 shows the results of time dependence tests done on Dutoitspan ore. Figure 53 was produced from figure 52 by plotting the cumulative % passing 17.5 mm vs. time. This graph shows a very high weathering rate for the first two days which subsequently decreases in rate. After 6 days the rate is considerably lower but not zero. Around 66 % of the total weathering for 15 days took place in the first two days and 88 % in the first six days.

Cupric Sulphate Medium

The time dependence of weathering was also tested in a cupric medium (0.2 M). Photos at 12, 24 and 144 hours clearly display the disintegration as time passes (figures 54 – 56).

Figure 54. Visual appearance of Dutoitspan ore (initial size - 26.5 + 22.4 mm) weathered in cupric sulphate solution (0.2 M) for 12 hours.

Figure 55. Visual appearance of Dutoitspan ore (initial size - 26.5 + 22.4 mm) weathered in cupric sulphate solution (0.2 M) for 24 hours.

Figure 56. Visual appearance of Dutoitspan ore (initial size - 26.5 + 22.4 mm) weathered in cupric sulphate solution (0.2 M) for 6 days (144 hours).
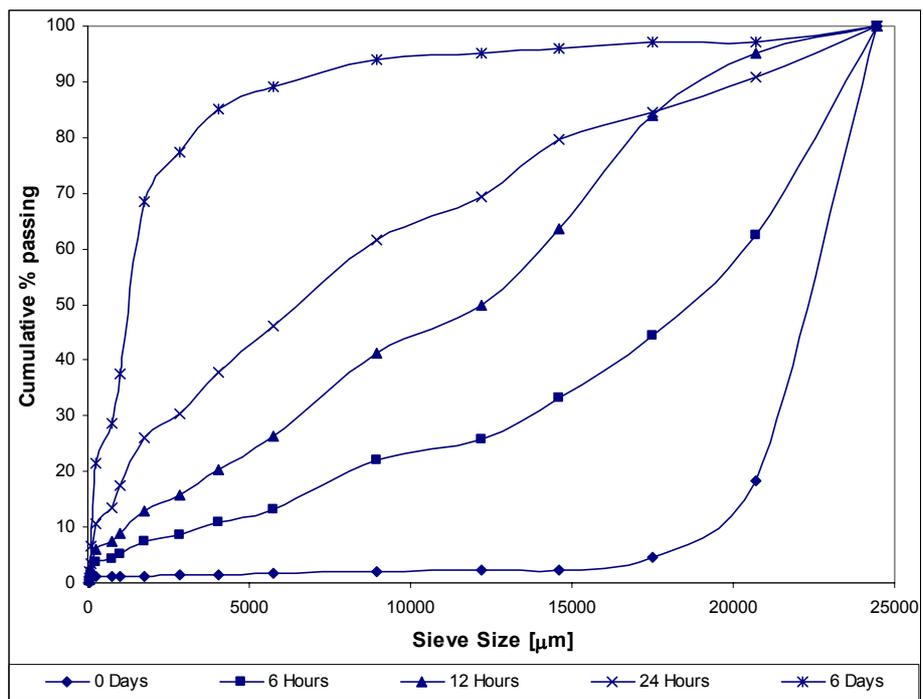
Figure 57. Weathering results from a 1.5 kg (initial size – 26.5 + 22.4 mm) Dutoitspan ore sample weathered in a 0.2 M cupric sulphate solution for 6, 12, 24 and 144 hours (6 days).
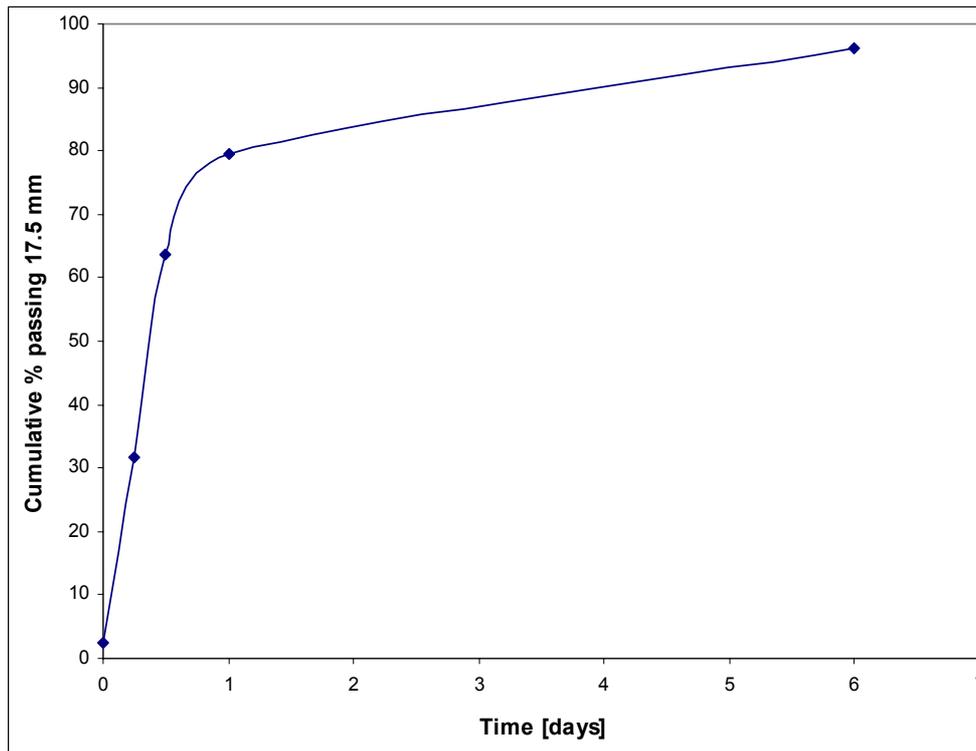
Figure 58. Results from the investigation of the time dependence of kimberlite weathering. Drawn from figure 57 as cumulative % passing 17.5 mm.

Results of time dependence tests using cupric suphate as weathering medium are shown in figures 57 and 58. Weathering is fast for the first 24 hours whereafter the rate decreases but does not seem to reach zero even in 6 days; this corresponds to the magnesium solution results. The results show that at this concentration of 0.2 M copper sulphate, 83 % of the weathering that took place over six days occurred within the first 24 hours.

Another test was done to investigate the effect of time, but the test was run for up to 30 days. The work was done with 250 – 300 g Dutoitspan kimberlite at 0.5 M copper concentration for 4 hours, 8 hours , 24 hours, 48 hours, 168 hours (7 days), 360 (15 days) and 720 hours (30 days). In this case a sample of – 16 + 13 mm kimberlite was used, as the -26 + 22.4 kimberlite fraction has all been utilised. The results are shown in figures 59 and 60. At a concentration of 0.5 M the weathering reached steady conditions after ~ 7 days. Again 80 % of the weathering took place in the first 24 hours. Comparison of figures 58 and 60 shows that concentration plays a role, which is discussed in the next section.

114
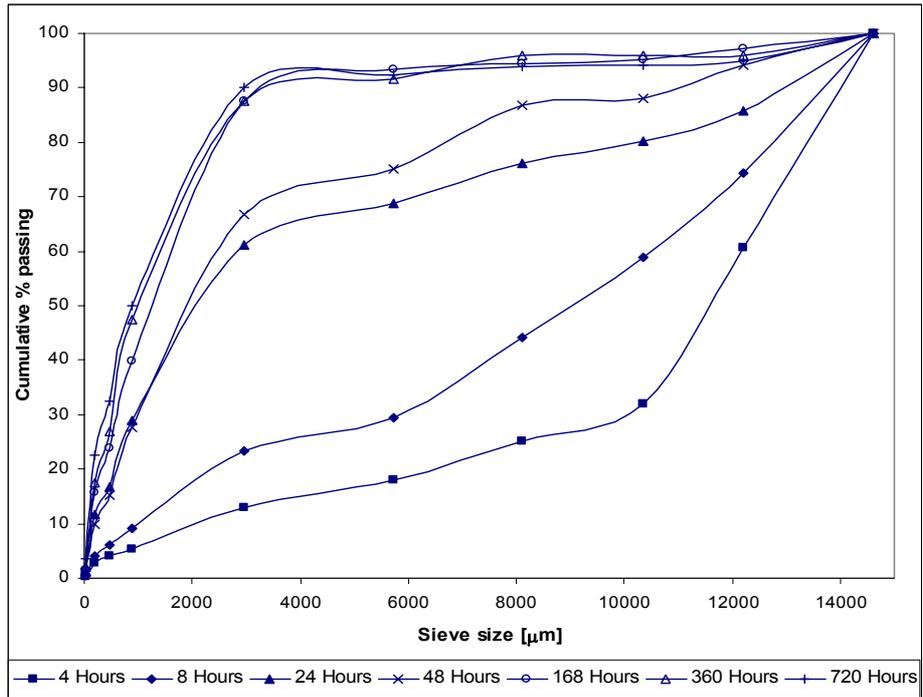
Figure 59. Weathering results from a 300 g (initial size – 16 + 13.2 mm) Dutoitspan ore sample weathered in a 0.5 M cupric sulphate solution for up to 30 days.
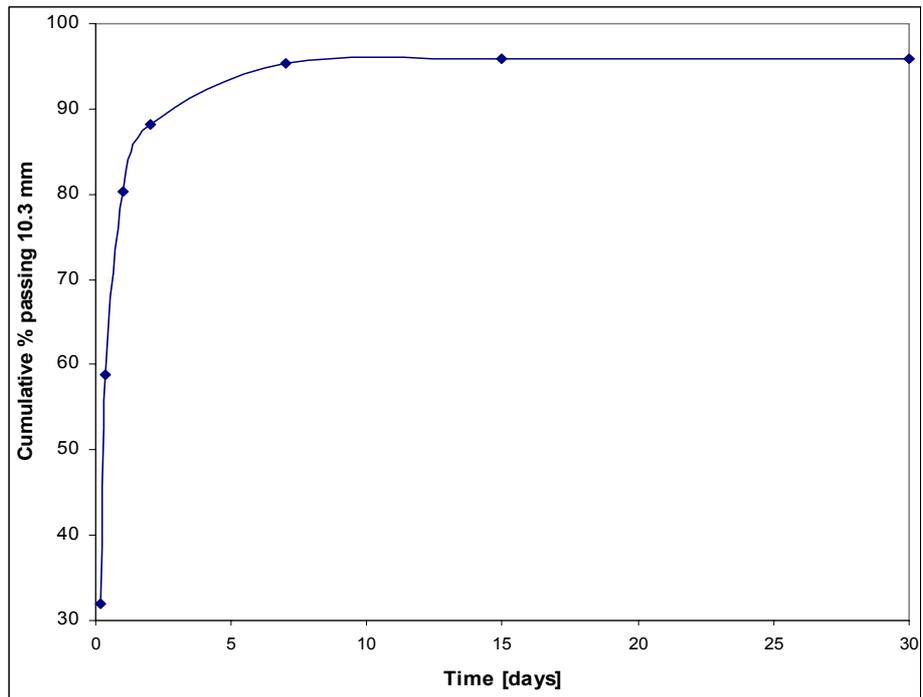
Figure 60. Results from the investigation of the time dependence of kimberlite weathering. Drawn from figure 59 as cumulative % passing 10.3 mm.

115

6.2.5.4   Influence of cation concentration on weathering

The influence of the cation concentration on accelerated weathering was tested in a cupric medium between 0.005 and 0.4 M concentration.

Figure 61. Visual appearance of Dutoitspan ore (initial size -26.5 + 22.4 mm) weathered in a 0.005 M cupric sulphate medium for 6 days.
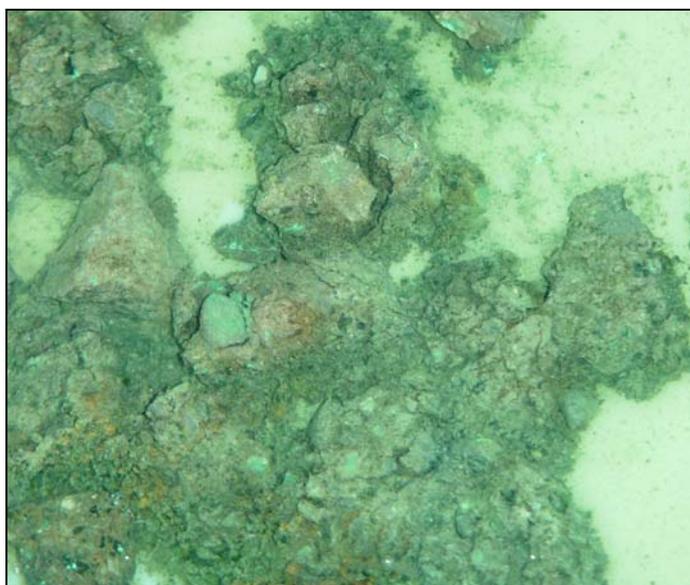
Figure 62. Visual appearance of Dutoitspan ore (initial size -26.5 + 22.4 mm) weathered in a 0.1 M cupric sulphate medium for 6 days.

116

Figure 63. Visual appearance of Dutoitspan ore (initial size -26.5 + 22.4 mm) weathered in a 0.4 M cupric sulphate media for 6 days.
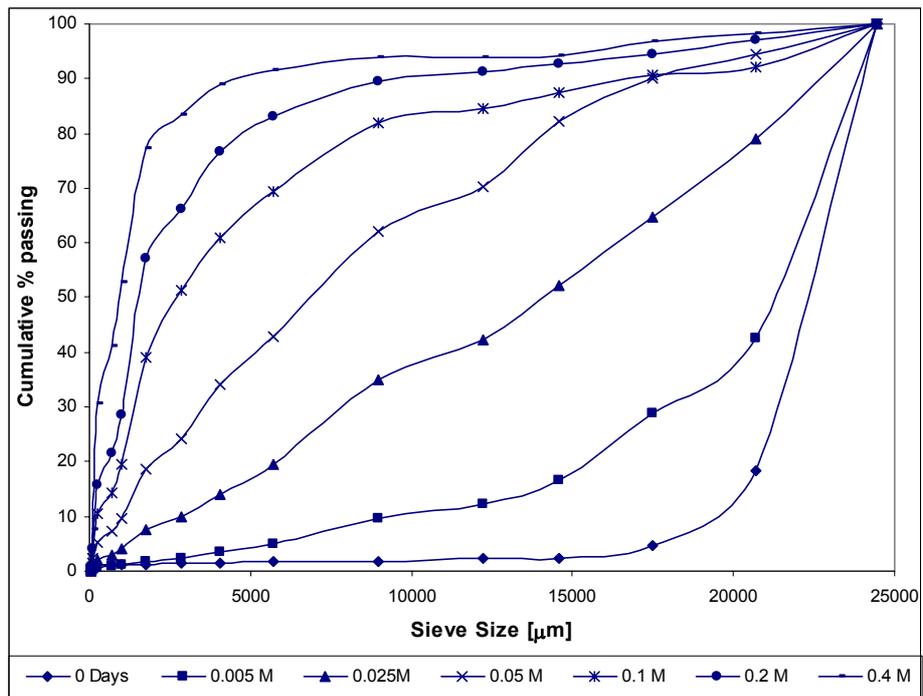
Figure 64. Results of the investigation to determine the influence of cation concentration. The tests were conducted on 1.5 kg of –26.5 +22.4 mm Dutoitspan ore. Copper sulphate concentrations were 0.005, 0.025, 0.05, 0.1, 0.2 and 0.4 M. The weathering time was constant at 6 days.

The influence of copper concentration on the efficiency of accelerated weathering was tested and results reported in figure 64 and 65. It is concluded from the tests that the concentration of cations is critical to the weathering of kimberlite. A very strong dependence is displayed up to 0.05 M whereafter the effect of concentration is less strong but still not negligible.
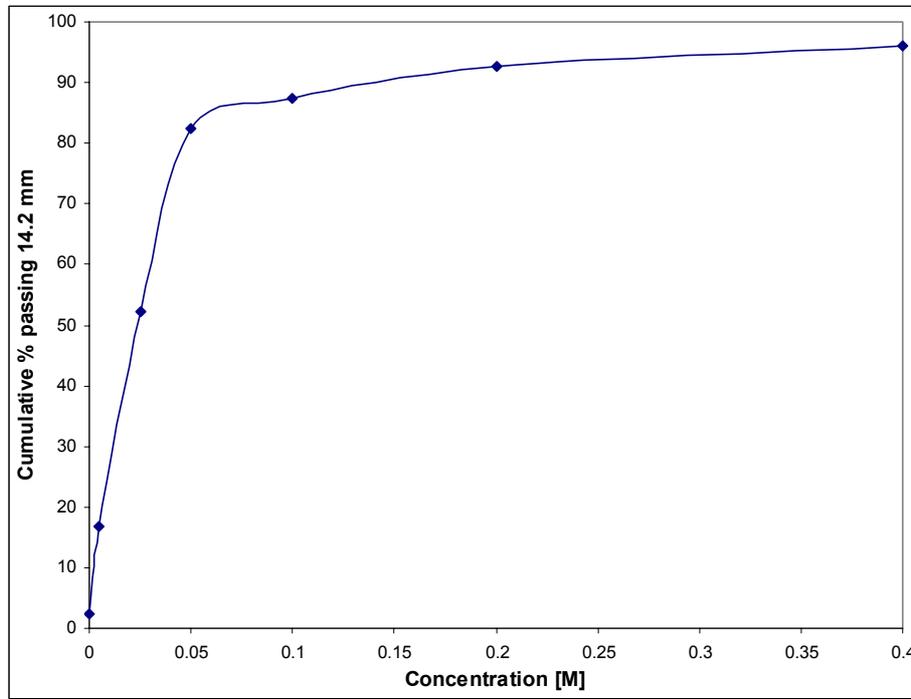
Figure 65. Weathering as a function of cation (cupric) concentration. The weathering is reported as the cumulative percent passing 14.2 mm from figure 64.

6.2.5.5   Influence of temperature on weathering

The influence of temperature was tested in a distilled water and magnesium chloride solution (0.2 M concentration) at 40 °C compared to room temperature (~ 20 °C). Results are shown in figure 66.
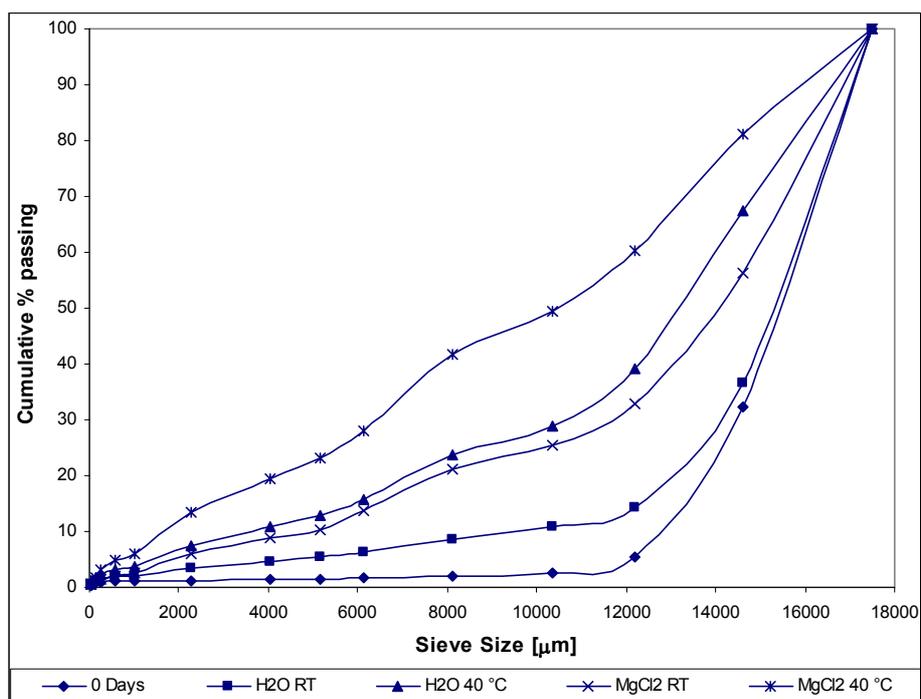
Figure 66. Results of the investigation of the influence of temperature on the weathering behaviour. The results include the standard test at room temperature and the standard test at 40 °C. The weathering tests in a 0.2 M $MgCl_2$ solution for 6 days at room temperature and 40 °C are also shown. All the tests were done on a 1.5 kg (initial size – 19 + 16 mm) Dutoitspan kimberlite sample.

Figure 66 shows the influence of higher temperature on the weathering process. The magnesium chloride solution was used as it shows limited accelerated weathering and therefore will allow for sensitive investigation of the effect of temperature. For the standard weathering test the higher temperature caused a 25 % increase in the cumulative mass % passing 12.2 mm. The influence of temperature is strong and comparable with that of cations in the weathering medium. The higher temperature combined with the magnesium chloride resulted in a further ~ 20 % increase in weathering over the room temperature magnesium chloride solution. The combination of 0.2 M $MgCl_2$ solution and 40 °C cause an increase of 55 % in the cumulative mass % passing at 12.2 mm compared to the unweathered material.

6.2.5.6   Influence of anions

The influence of anions was tested by comparing weathering results in a cupric chloride and cupric sulphate solution at 0.3 M for 6 days. From results shown in figure 67 it is concluded that the anion species does not influence the weathering process (an effect might be expected if the anion influences the solubility of the cation).

119
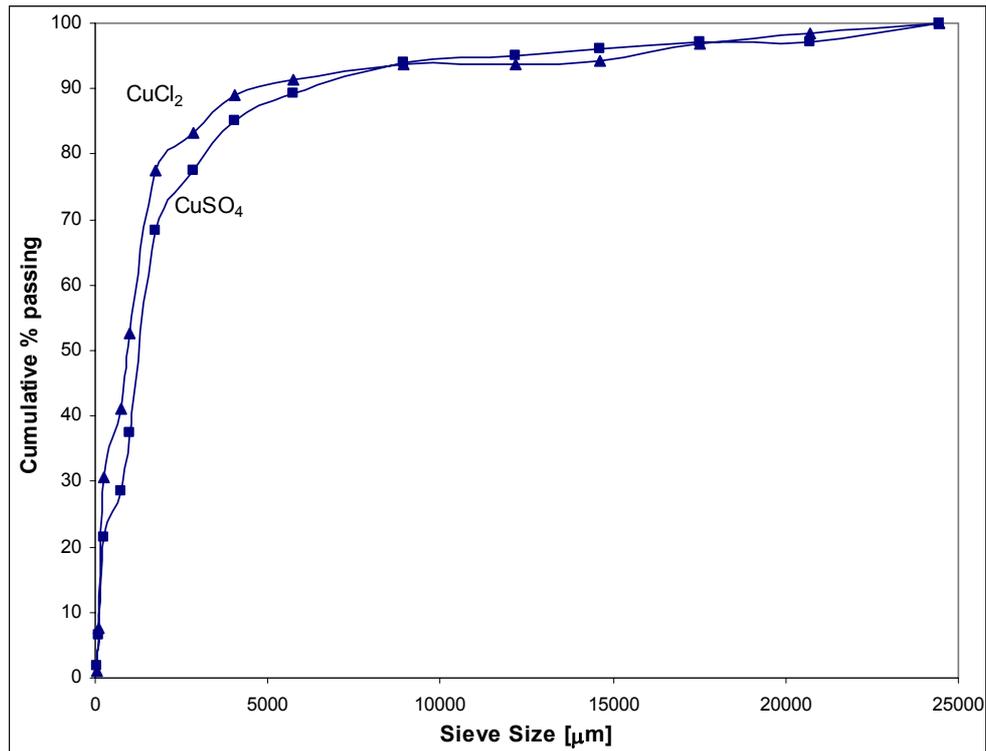
Figure 67.   Results of tests to determine the influence of the type of anion on weathering. Tests conducted on a 1.5 kg -26.5 + 22.4 mm Dutoitspan ore sample at 0.3 M cupric chloride and cupric sulphate solution for 6 days.

6.2.5.7   Influence of particle size

The influence of particle size was determined using 4 size intervals weathered for 6 days in a 0.2 M $MgCl_2$ solution.
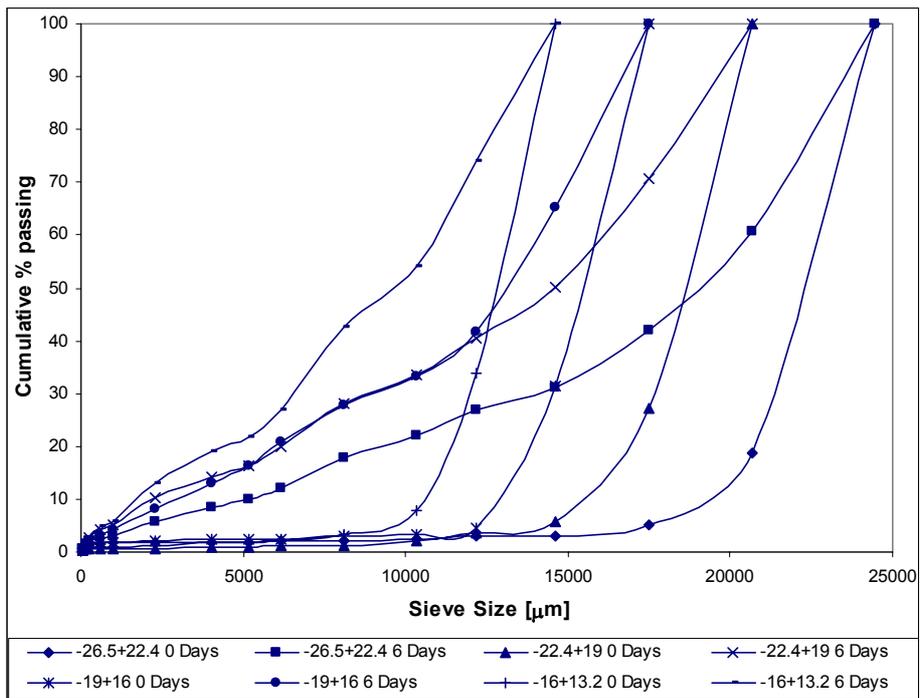
Figure 68. Results of the investigation to determine the influence of particle size. The tests were conducted in 0.2 M magnesium chloride solution for 6 days. The particle sizes used were –26.5 + 22.4, -22.4 + 19, -19 + 16 and -16 + 13.2 mm, using Dutoitspan ore.

The results are shown in figure 68 and comparative results in figure 69. The comparative results are shown at 70 % of the starting material size as this is the position in the size distribution curve where weathering is shown best. The conclusion from these results is that the starting size of the particles does not play a significant role in the efficiency of weathering. The starting particle sizes used in this test work are however similar in exposed surface area and work on finer size fractions (higher surface area) should be done for accurate conclusions.
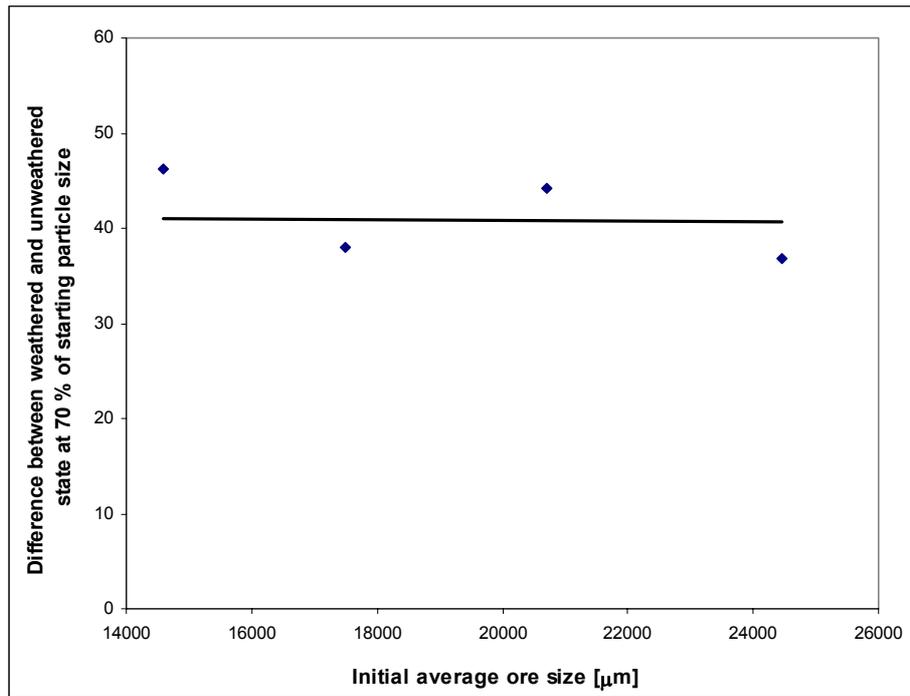
Figure 69. Results from the investigation of particle size. Comparison of the size distribution curves for the unweathered and weathered states at 70 % of the starting material size.

6.2.5.8   Influence of milling on weathering results

The usefulness of the autogeneous batch mill test was investigated and results are given in figure 70.   The results show that the milling test does increase the size reduction after weathering.   The milled sample seems to have less larger sized particles (> 15 mm) compared to the unmilled sample, which might be due to abrasion. Milling can increase the sensitivity of weathering tests especially in cases where small differences in weathering are investigated. With the copper medium the influence of weathering is so strong that the size degradation is large and no milling is required.
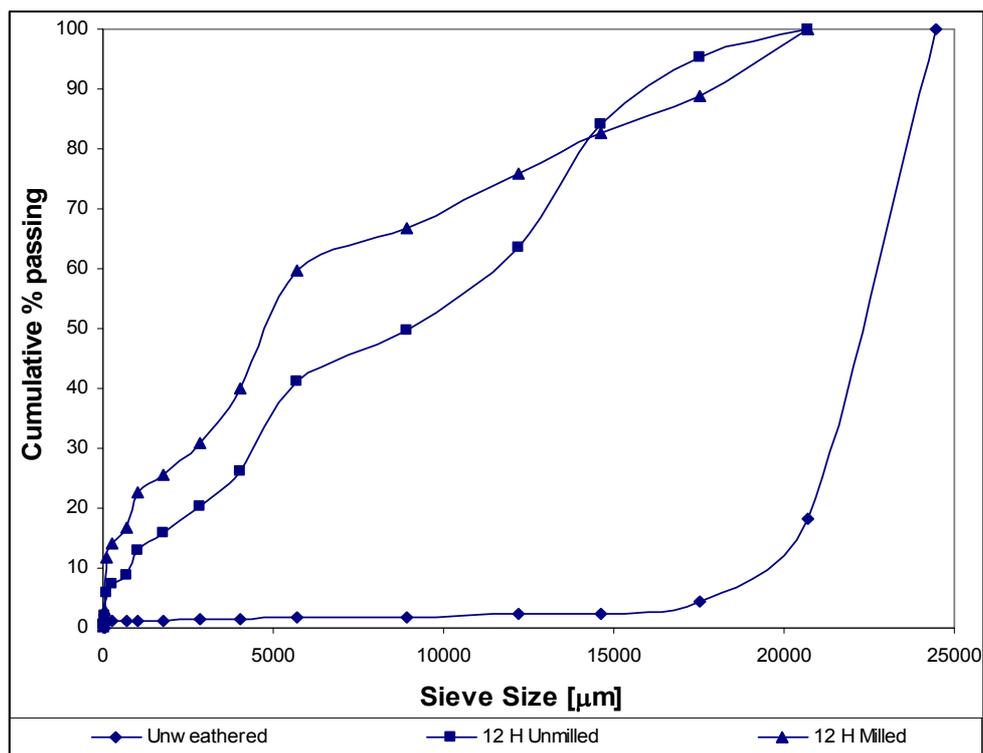
Figure 70.   Investigation of the influence of milling on weathering tests. Weathering tests were performed in a 0.2 M cupric sulphate solution (initial size - 26.5 + 22.4 mm) Dutoitspan ore for 12 hours and the unmilled and milled sample product size distributions compared.

6.2.5.9   The effect of a stabilising cation vs. swelling cation

The effects of a potassium (stabilising cation) and copper (a swelling cation) on weathering were investigated. The test utilised 200 - 250 g of Dutoitspan kimberlite (initial size - 16 + 13.2 mm) weathered in a 0.5 M potassium solution for 4, 8 and 144 hours. The tests were repeated in a 0.5 M copper solution at 4, 8, 24, 48, 168 (7 days) and 360 hours (15 days). The weathering results in the potassium medium are shown in figure 71. The results for copper are shown in figure 70. Photos of both products are shown in figure 73.

These results show that cations can be utilised to influence the weathering behaviour of kimberlite by either increasing the extent of weathering as with copper cations or alternatively decreasing the extent of weathering as is the case with potassium cations. It is compared in this section to show the extremes of the influence of cations on weathering behaviour.

123
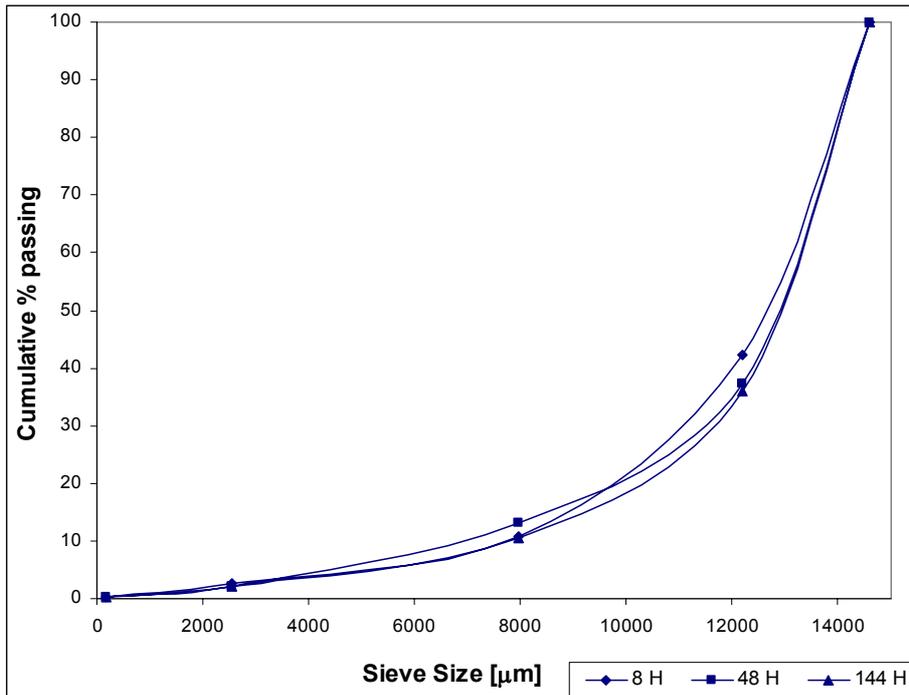
Figure 71. Investigation of the influence of potassium on weathering tests. Weathering tests were performed on a 250 - 300 g -16 + 13.2 mm Dutoitspan kimberlite in a 0.5 M potassium solution for 8, 48 and 144 hours.
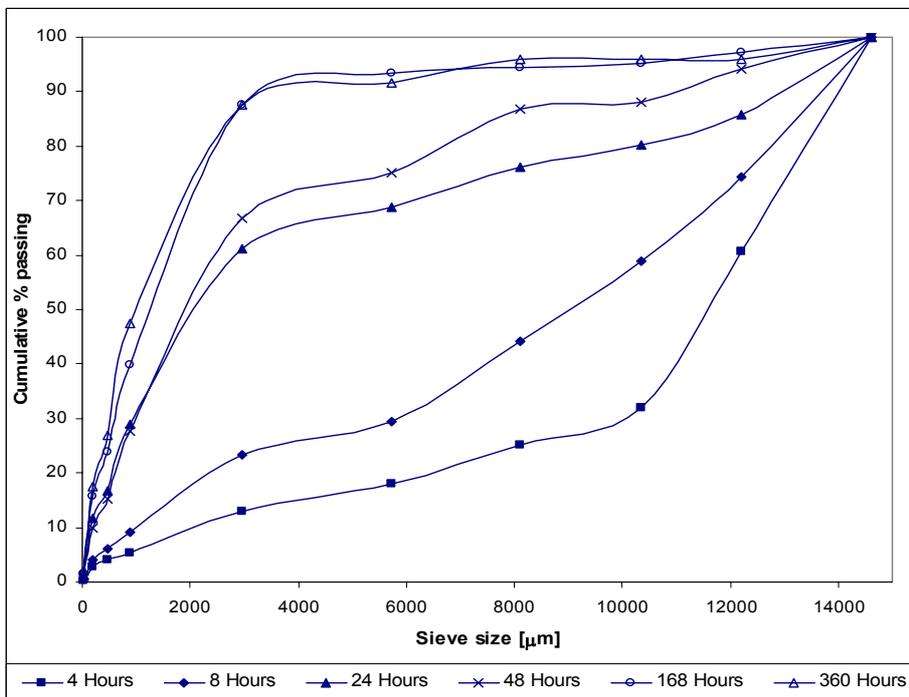
Figure 72. Investigation of the influence of copper on weathering tests. Weathering tests were performed on a 250 - 300 g -16 + 13.2 mm Dutoitspan kimberlite in a 0.5 M copper solution for up to 15 days.

Figure 73. Comparison of the effect of copper (swelling cation) on the left and potassium (stabilising cation) on the right and their effect on the weathering of kimberlite (photos taken after 6 days for potassium and 15 days for copper medium).

6.2.6 Venetia

The samples received from Venetia (- 26.5 + 22.4 mm) were weathered in a 0.05 M cupric sulphate solution for 6 days. The unweathered and weathered samples are shown for comparative purposes (figures 74 – 81).

K1 Hypabyssal North East

Figure 74. Venetia K1 Hypabyssal North East kimberlite unweathered (left) compared to the weathered product (right). Weathering was done in a 0.05 M cupric sulphate solution for 6 days.

K1 Hypabyssal South
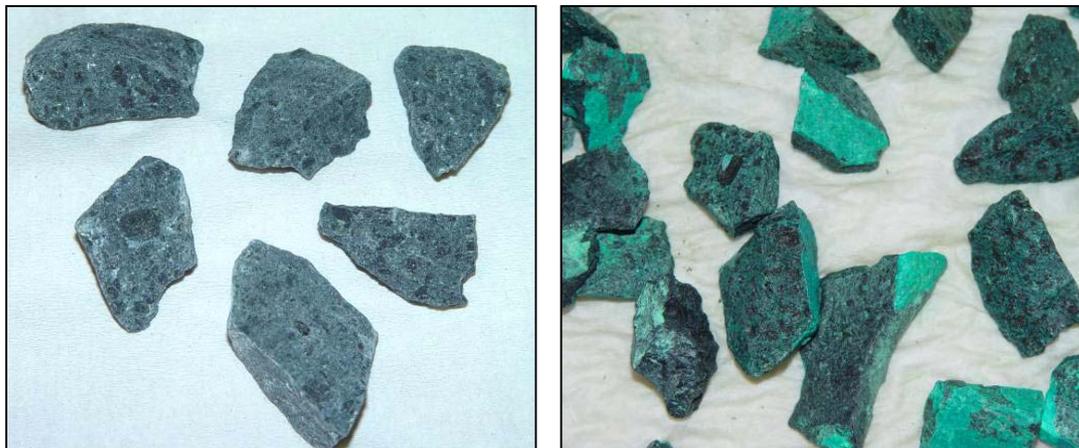
Figure 75. Venetia K1 Hypabyssal South kimberlite unweathered (left) compared to the weathered product (right). Weathering was done in a 0.05 M cupric sulphate solution for 6 days.

K1 TKB East

Figure 76. Venetia K1 TKB East kimberlite unweathered (left) compared to the weathered product (right). Weathering was done in a 0.05 M cupric sulphate solution for 6 days.

K2 South

Figure 77. Venetia K2 South kimberlite unweathered (left) compared to the weathered product (right). Weathering was done in a 0.05 M cupric sulphate solution for 6 days.

K2 North East
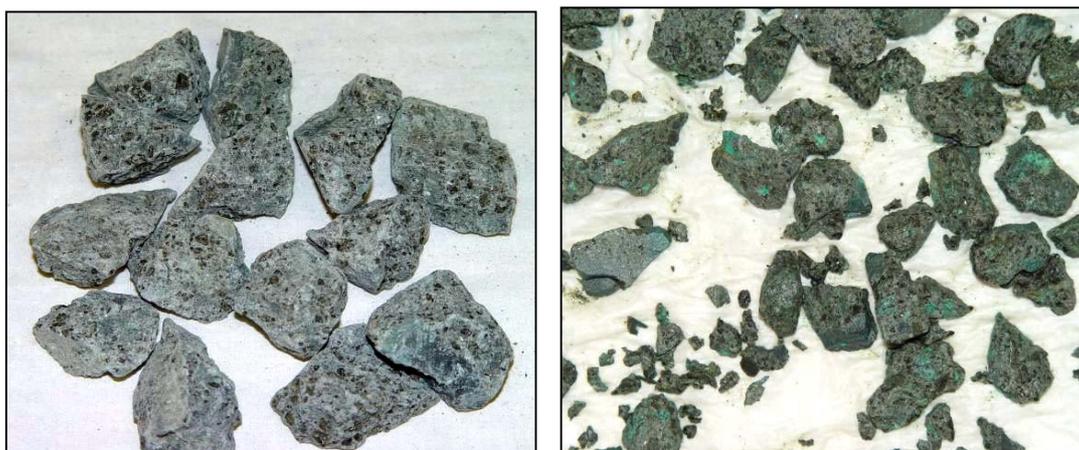
Figure 78. Venetia K2 North East kimberlite unweathered (left) compared to the weathered product (right). Weathering was done in a 0.05 M cupric sulphate solution for 6 days.

K2 West

Figure 79. Venetia K2 West kimberlite unweathered (left) compared to the weathered product (right). Weathering was done in a 0.05 M cupric sulphate solution for 6 days.

K8

Figure 80. Venetia K8 unweathered (left) compared to the weathered product (right). Weathering was done in a 0.05 M cupric sulphate solution for 6 days.

Red Kimberlite

Figure 81. Venetia Red kimberlite unweathered (left) compared to the weathered product (right). Weathering was done in a 0.05 M cupric sulphate solution for 6 days.
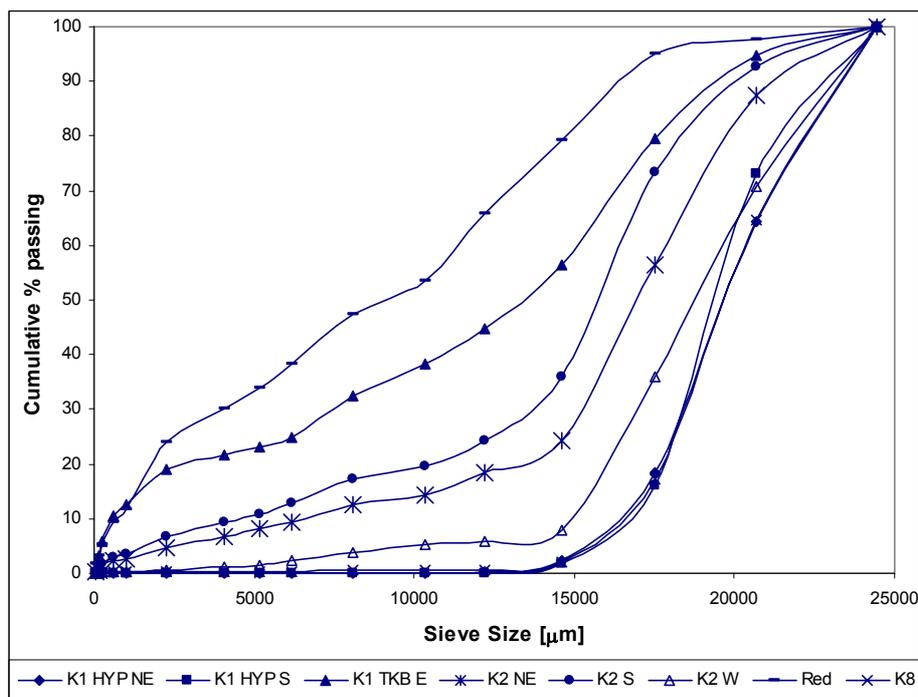
Figure 82. Results of weathering tests performed on Venetia kimberlites (- 26.5 + 22.4 mm) in a 0.05 M cupric sulphate solution for 6 days.

Both hypabyssal ores showed no weathering at all (figure 82), and both contained no swelling clay and had low CEC values, in line with the suggestion that the presence of swelling clay is the parameter that renders a kimberlite amenable to weathering. K8, although not classified as a kimberlite, also contains no swelling clay and has a correspondingly low CEC value, with

no weathering observed. Kimberlites with no swelling clay are concluded to be resistant to weathering even under aggressive conditions.

The K2W kimberlite displayed some signs of weathering with 8 % passing 14.6 mm after weathering. The K2NE kimberlite ranked next with 25 % passing 14.6 mm after weathering, followed by K2S with 36 %, K1 TKB E with 56 % and Red kimberlite with 80 %. The swelling clay content was the same (at 40 %) for the K1 TKB E, K2S and Red kimberlites even though these kimberlites behaved differently during weathering. Therefore, while the swelling clay content does give an indication of the expected weathering behaviour, it cannot give a fully quantitative prediction of weathering. This might be related to the inherent inaccuracy of the semi-quantitative phase determination by XRD analysis. In addition, when a kimberlite is rendered weatherable by the presence of swelling clay, other factors, such as the cations in the ore and weathering solution (and the associated hydration and complexation properties of the cations) play a role, as these will determine the amount of swelling.
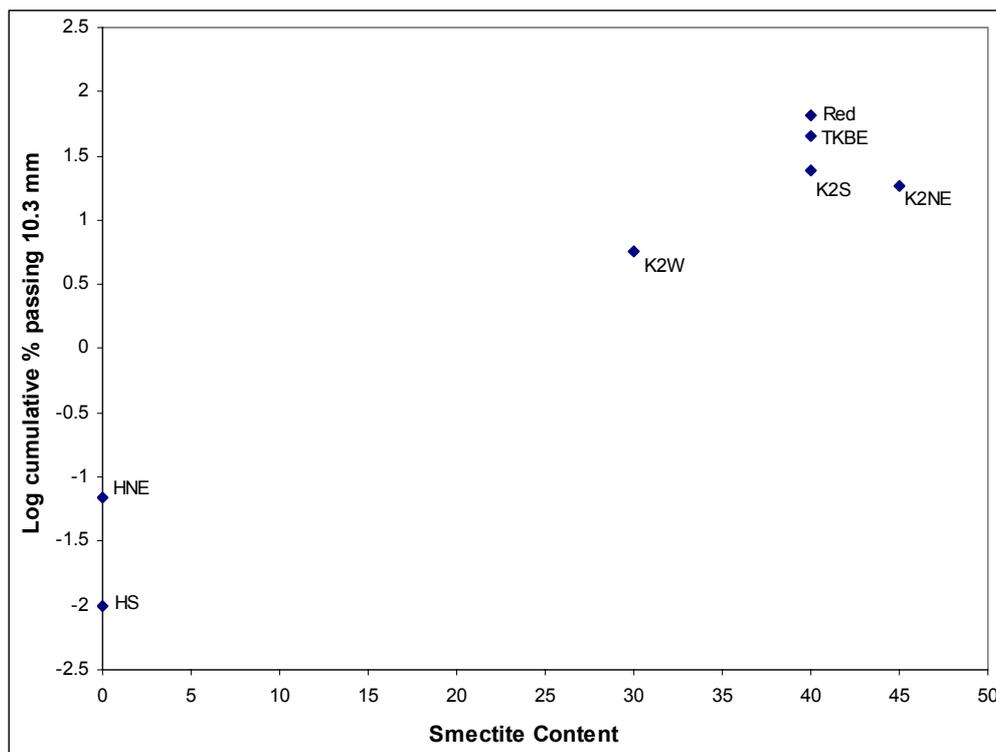
Figure 83a.   Comparing weathering results with the smectite content of Venetia ores. Weathering is shown as log cumulative % passing at 10.3 mm from figure 82 (6 days' weathering in 0.05 M copper sulphate).

130
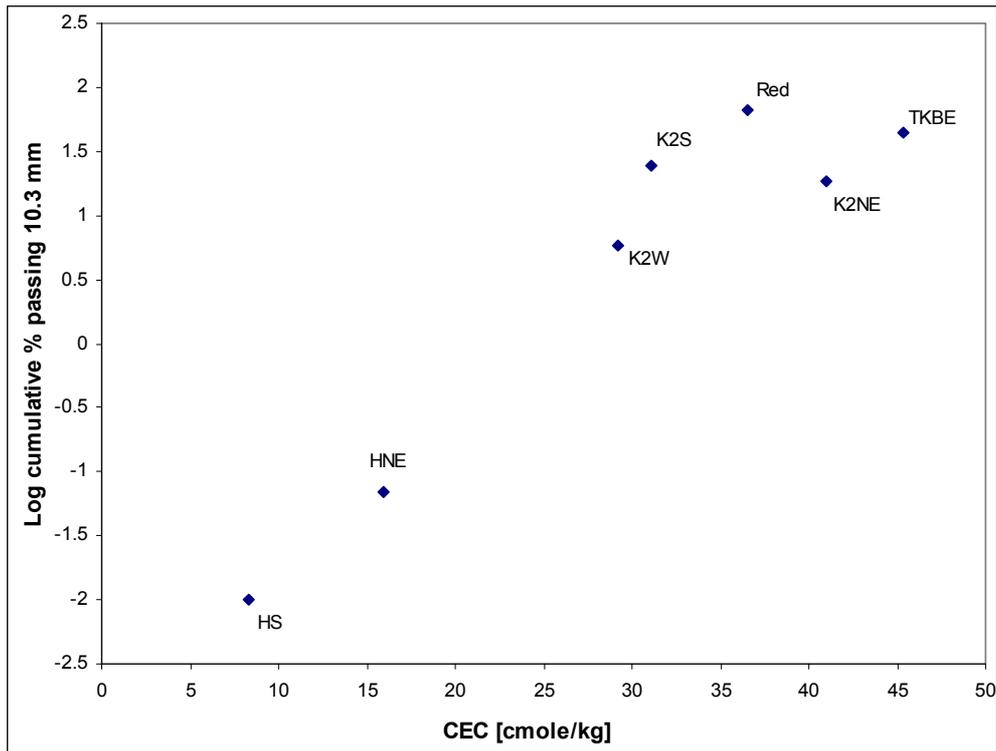
Figure 83b. Comparing weathering results with cation exchange capacity of Venetia ores. Weathering is shown as log cumulative % passing at 10.3 mm from figure 82 (6 days' weathering in 0.05 M copper sulphate).

The weathering behaviour correlates well with both the cation exchange capacity and the swelling clay content (figure 83 a and b). However, determination of the swelling clay content is tedious and expensive.   CEC is therefore the preferred parameter to characterise kimberlitic ores and their weathering behaviour.

6.3   Repeatability of results

The repeatability of the experimental results was tested by repeating test work in triplicate at 0.025, 0.1 and 0.5 M copper concentration. The tests were done on 300 g -16 +13.2 Dutoitspan kimberlite for 2 days. The results (figure 84) show that all results consistently fall in a 7 % interval. Statistical analysis of the results is shown in table 24, which includes the standard deviation and the 95 % confidence limits. The largest standard deviation value is 3.8 %. The largest difference between the 95 % confidence lower and upper limit is 19 %. This could be improved by increasing the number of tests.
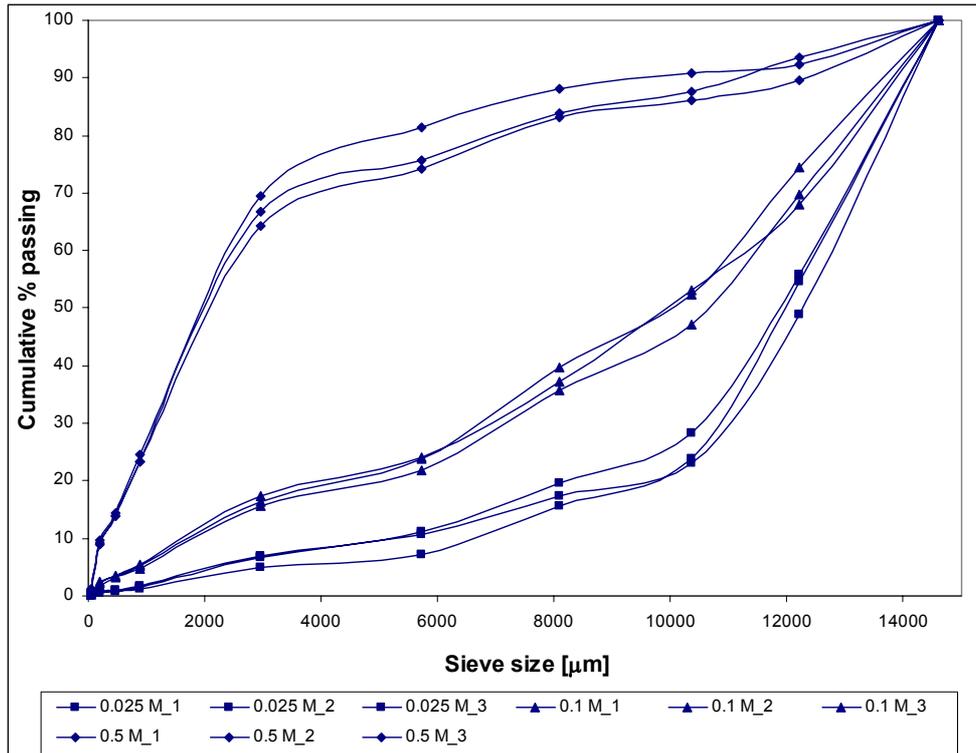
Figure 84. Repeatability of the weathering tests were evaluated by triplicate tests at 0.025, 0.1 and 0.5 M copper concentration. Tests were done on 300 g, -16 + 13.2 mm Dutoitspan kimberlite.

Table 24. Statistical evaluation of repeatability results.

2 Days 0.025 M Cu				
Ave particle size (μm)	Mean cum % passing	Standard deviation	95 % confidence lower limit	95 % Confidence higher limit
14600	100.00	0.00	100.00	100.00
12200	53.12	3.73	43.85	62.39
10350	25.12	2.82	18.11	32.14
8100	17.51	2.00	12.55	22.47
5725	9.59	2.16	4.22	14.96
2965	6.26	1.08	3.57	8.95
890	1.48	0.28	0.79	2.18
467.5	0.90	0.17	0.48	1.33
205	0.58	0.11	0.31	0.85
37.5	0.05	0.00	0.05	0.05
2 Days 0.1 M Cu				
Ave particle size (μm)	Mean cum % passing	Standard deviation	95 % confidence lower limit	95 % Confidence higher limit
14600	100.00	0.00	100.00	100.00
12200	70.73	3.38	62.34	79.11
10350	50.79	3.25	42.71	58.87
8100	37.53	1.94	32.72	42.34
5725	23.18	1.17	20.28	26.08
2965	16.45	0.82	14.42	18.49
890	5.11	0.28	4.41	5.81
467.5	3.38	0.09	3.15	3.61
205	2.21	0.31	1.44	2.97
37.5	0.39	0.03	0.32	0.45
2 Days 0.5 M Cu				
Ave particle size (μm)	Mean cum % passing	Standard deviation	95 % confidence lower limit	95 % Confidence higher limit
14600	100.00	0.00	100.00	100.00
12200	91.80	2.08	86.64	96.97
10350	88.17	2.48	82.01	94.32
8100	85.03	2.68	78.36	91.69
5725	77.09	3.80	67.65	86.53
2965	66.79	2.69	60.11	73.46
890	23.70	0.80	21.71	25.68
467.5	14.07	0.28	13.36	14.77
205	9.28	0.43	8.23	10.34
37.5	1.05	0.09	0.84	1.27

133

Table 25. ICP analysis results of copper weathering solution as a function of time.

0.025 M Copper					
Time	Cu	Na	K	Mg	Ca	Al
[hours]	mmol/l	mmol/l	mmol/l	mmol/l	mmol/l	mmol/l
0	23.60	0.57	0.069	0.014	0.052	0.000
3	15.11	15.66	0.921	0.041	0.127	0.000
24	3.93	38.28	1.662	0.086	0.187	0.000
48	1.57	41.76	1.816	0.103	0.195	0.000
72	0.77	42.19	1.842	0.111	0.195	0.000
168	0.41	43.50	1.944	0.132	0.187	0.000
360	0.007	43.50	2.072	0.156	0.217	0.000
720	0.004	47.85	2.200	0.202	0.185	0.000
0.1 M Copper					
Time	Cu	Na	K	Mg	Ca	Al
[hours]	mmol/l	mmol/l	mmol/l	mmol/l	mmol/l	mmol/l
0	95.99	0.48	0.02	0.02	0.13	0.005
3	83.40	24.79	1.56	0.13	0.47	0.009
24	51.93	69.60	3.84	0.45	1.37	0.089
48	39.34	82.65	4.35	1.03	1.90	0.010
72	34.62	87.00	5.63	0.86	2.30	0.025
168	25.18	100.04	5.63	1.73	2.74	0.141
360	18.88	104.39	6.14	2.43	4.24	0.289
720	14.48	104.39	6.65	3.17	6.24	0.070
0.5 M Copper					
Time	Cu	Na	K	Mg	Ca	Al
[hours]	mmol/l	mmol/l	mmol/l	mmol/l	mmol/l	mmol/l
0	448.49	0.43	0.00	0.02	0.09	0.01
3	432.76	28.71	2.10	0.31	1.02	0.05
24	393.42	95.69	7.16	2.39	5.49	0.27
48	379.25	108.74	8.44	3.13	8.73	0.48
72	372.96	108.74	8.18	3.54	10.48	0.52
168	346.21	113.09	9.72	6.58	16.72	2.85
360	336.76	113.09	9.21	9.87	21.21	1.07
720	330.47	121.79	10.49	14.81	27.45	2.82

Figure 85. ICP analysis results displaying the steady decrease of the concentration of copper in the weathering solution as a function of time. The lines are fitted curves for simple n^{th} - order kinetics (parameters of curve fits in table 25).

Figure 86. ICP analysis results displaying the release of sodium, potassium, calcium and the sum of minor cations (K^+, Ca^{2+}, Mg^{2+} and Al^{3+}) from the kimberlite into the 0.025 M copper solution.

136

Figure 87. ICP analysis results displaying the release of sodium, potassium, calcium and the sum of minor cations (K^+, Ca^{2+}, Mg^{2+} and Al^{3+}) from the kimberlite into the 0.1 M copper solution.

Figure 88. ICP analysis results displaying the release of sodium, potassium, calcium and the sum of minor cations (K^+, Ca^{2+}, Mg^{2+} and Al^{3+}) from the kimberlite into the 0.5 M copper solution.

6.4   Kinetic evaluation of cation exchange

Cupric Medium

The kinetics of the cation exchange reaction was investigated by utilising 300 g of Dutoitspan kimberlite (-16 + 13 mm) weathered in 0.025, 0.1 and 0.5 M cupric chloride solutions at room temperature (20 °C) with 1 L weathering solution. The Dutoitspan kimberlite showed medium weatherability compared to the other kimberlites (see section 6.2.5). Samples of the solution were removed (~ 50 ml) at 0, 4 hours, 24 hours, 48 hours, 72 hours, 168 hours (7 days), 360 hours (15 days) and 720 hours (30 days) for ICP analysis to follow the uptake of copper by the kimberlite. The release of other cations from the kimberlite into the solution was monitored simultaneously.   The ICP results are given in table 25 and include the concentration of copper, sodium, calcium, potassium, magnesium and aluminium.   The decrease in the concentration of copper in the three solutions is shown in figure 85. The decrease in copper concentration is rapid initially and then the reaction becomes slower at around 7 days; thereafter the concentration changes very little.   The expected initial concentrations compared well with the analyses for the 0.025 and 0.1 M concentrations but not for the 0.5 M concentration. The reason for the difference in initial concentration could be the fact that the samples removed initially were kept in storage and sent for analysis with the other samples taken up to 30 days later. This could results in minor precipitation of copper sulphate, especially for the high concentrations.   In some cases small flakes could be observed at the bottom of the sample holder.

The increase in sodium, potassium, calcium and sum of minor cations (the total of potassium, calcium, magnesium and aluminium) are shown in figure 86 for the 0.025 M copper solution, figure 87 for the 0.1 M copper solution and figure 88 for the 0.5 M copper solution. In the 0.025 M solution it is essentially only sodium that is replaced from the kimberlite (up to ~ 48 mmol/l) and the sum of minor cations remains lower at ~ 2.6 mmol/l. In the 0.1 M copper solution the amount of sodium replaced from the kimberlite is considerably higher (~ 104 mmol/l) but the concentration of other cations that are replaced is also significant (sum of minor cations ~ 16 mol/l).   The sodium concentration for the 0.5 M copper solution only increases up to ~ 122 mmol/l, but the concentration of the other cations increases significantly to ~ 56 mmol/l. This increase in concentration of other cations was primarily due to calcium and potassium that were being replaced from the kimberlite.

The release of sodium from the kimberlite into the three copper solutions is compared in figure 89, and also the sum of other cations in figure 90. It is concluded that sodium is the cation most easily replaced from the kimberlite.   Initially with the increase in copper concentration from 0.025 to 0.1 M, the release of sodium into the solution is increased from 48 to 104 mmol/l at long times.   The further increase in copper concentration does not increase the sodium concentration in solution drastically. The sum of minor cations (shown in figure 90) for the different copper solutions, show that the sum of minor cations for the 0.025 M solution is relatively low (2.6 mmol/l) which is increased to around 16 mmol/l for the 0.1 M copper solution and drastically increased to 56 mmol/l for the 0.5 M copper solution. Therefore at low weathering cation concentration it is primarily sodium that is replaced from the kimberlite, but as the concentration of cations in the weathering solution increases, so does the driving force for replacing other cations as well. Sodium is the smallest hydrated cation present in the kimberlite and the hydration energy is not as large as for di- or trivalent cations. Sodium is therefore assumed to be the most easily replaced although the quantities of different cations present in the kimberlite should also influence the observed cation exchange process.   Equilibrium exchange behaviour from literature is usually done on a single cation saturated clay and usually do not contain different cations as in this present case. Grim (1968) showed the selectivity order on Ba saturated clay as $Na^+ < K^+ < Mg^{2+} < Ca^{2+}$.   This agrees with the observed behaviour that sodium is the most easily replaced cation.
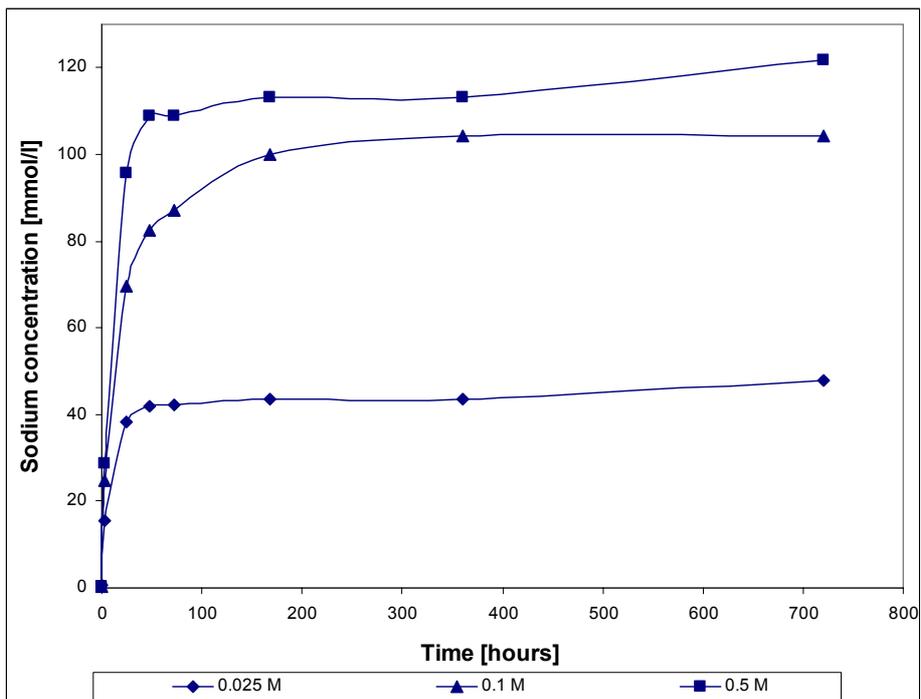
Figure 89. ICP analysis results displaying the release of sodium from the kimberlite into the solution at 0.025, 0.1 and 0.5 M copper concentration.
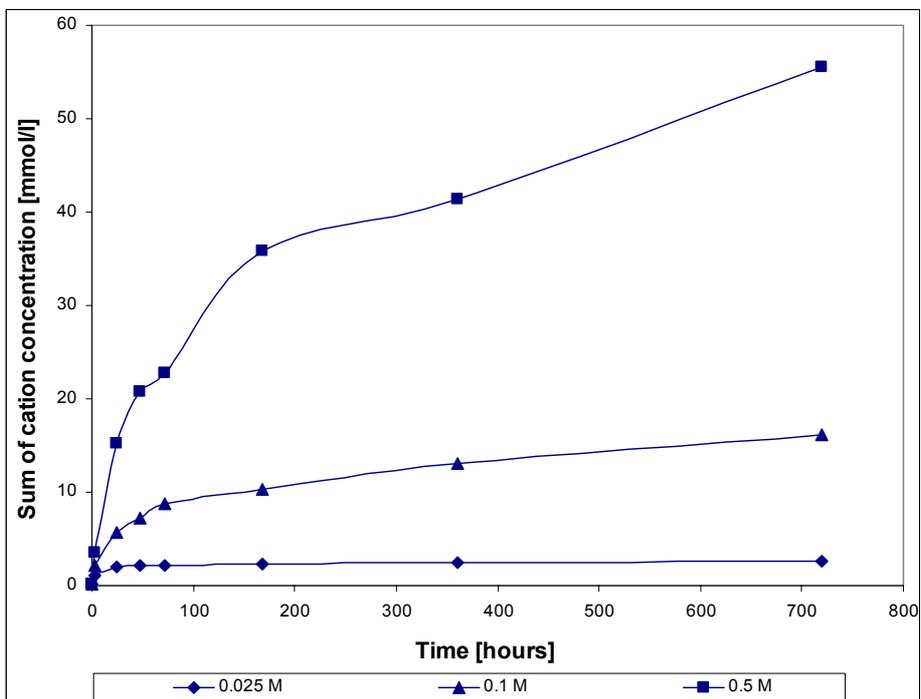
Figure 90. ICP analysis results displaying the release of the sum of other cations (K^+, Ca^{2+}, Mg^{2+} and Al^{3+}) from the kimberlite into the solution at 0.025, 0.1 and 0.5 M copper concentration.

The following simple n^{th}-order kinetic equation was used to fit the data for the change of copper concentration with time:

$$dC/dt = -k(C-C_\infty)^n \tag{32}$$

where C is the concentration in solution, k the rate constant, n the apparent reaction order, and C_∞ the equilibrium concentration. The integrated form of this equation, assuming C_∞, k and n to be constant with time, is as follows:

$$(C- C_\infty)^{(1-n)} – (C_0-C_\infty)^{(1-n)} = kt(n\text{-}1) \tag{33}$$

This equation was written with time as the subject, and fitted to the experimental data (measured concentrations at different times) by using the curve-fitting facility of the package SigmaPlot. The values of k, n, R^2 and the standard error for the three cases are given in table 26. The fitted curves are shown in figure 85.

Table 26.   Results of fitting kinetic equation 33 to weathering data.

Variable	Coefficient	Std. Error
0.025 M		
C_o (mmol/l)	23.6	-
C_∞ (mmol/l)	0.0042	1.57E-06
k	0.0316	0.0002
n	1.1342	0.0014
R^2	0.9806	-
0.1 M		
C_o (mmol/l)	96.0	-
C_∞ (mmol/l)	0.3382	0.6785
$10^7 k$	6.6642	5.5389
n	3.5313	0.0975
R^2	1.0000	
0.5 M		
C_o (mmol/l)	448.5	
C_∞ (mmol/l)	322.2862	2.4187
$10^4 k$	0.9486	2.0710
n	2.1790	0.2613
R^2	0.9988	

A graphical method was also used, plotting dC/dt against $(C-C_\infty)$ on logarithmic axes. A plot of log dC/dt vs log $|C-C_\infty|$ will enable calculation of n and k. The C_∞ values calculated from the Sigmaplot curve fits were used (table 26). The results are shown in figure 91 for the 0.025 M copper solution, figure 92 for 0.1 M copper solution and figure 93 for the 0.5 M copper solution. Fitted values of k and n are given in table 27.

dC/dt was determined by straight lines through to the data for the first and last pair of datapoints in each set. For the datapoints in between these, a parabola was fitted to every three consecutive datapoints and the differential of this parabola used to find dC/dt at the central datapoint.

Table 27.   Results of graphical fitting kinetic equation 32 to weathering data.

Copper concentration [M]	Equation of line	n	k
0.025	y=1.112x – 1.235	1.11	5.82E-2
0.1	y=3.409x – 5.936	3.41	1.159E-6
0.5	y=2.261x – 4.094	2.26	8.059E-5
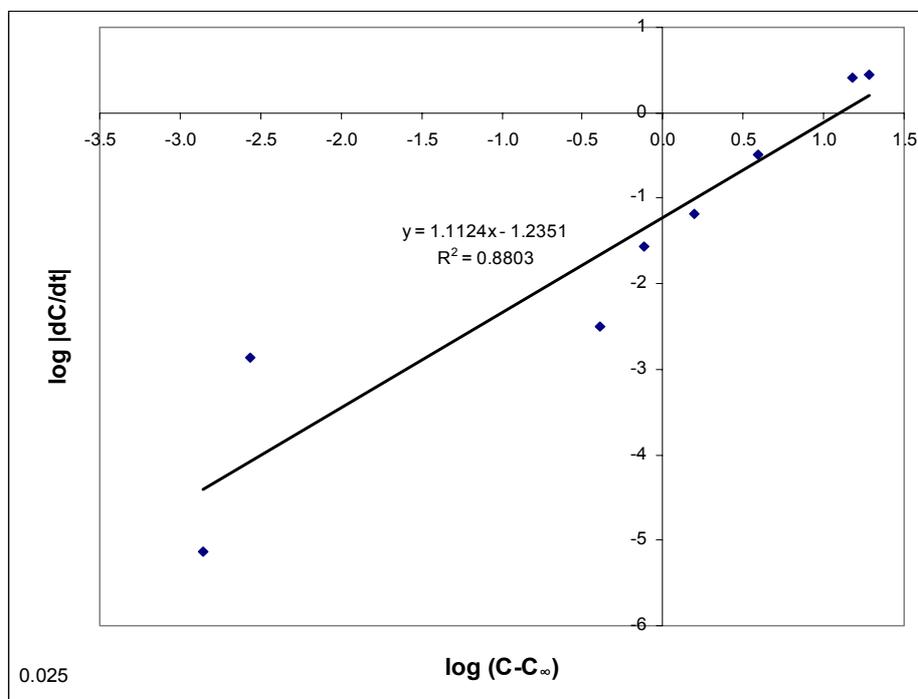
Figure 91. A plot of log dC/dt vs. log $(C-C_\infty)$ for the 0.025 M copper weathering test. Time in hours, $(C-C_\infty)$ in mmol/l and dC/dt in mmol/(lxh).
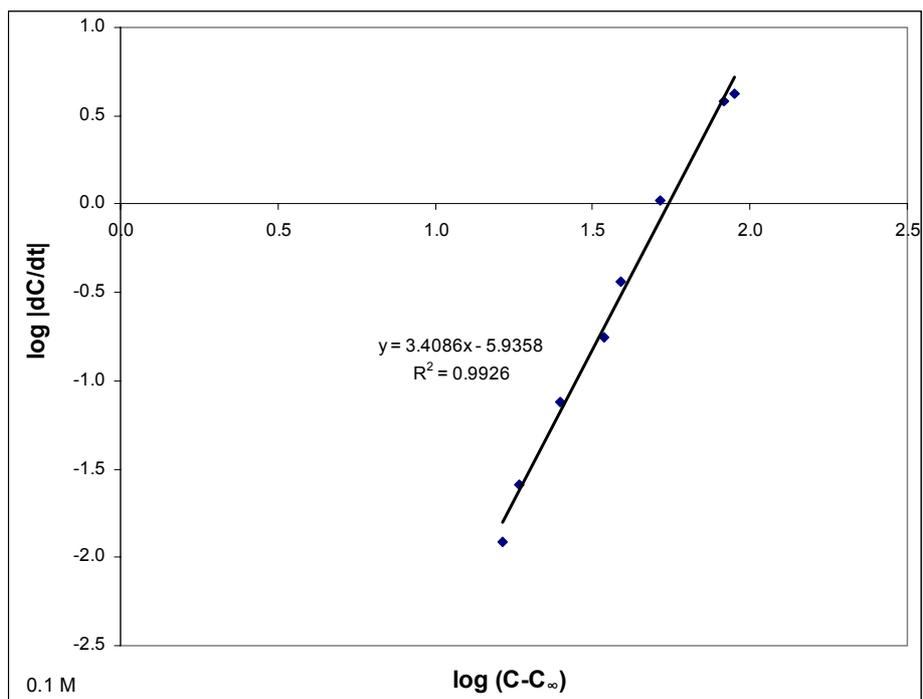
Figure 92. A plot of log dC/dt vs. log (C-C$_\infty$) for the 0.1 M copper weathering test. Time in hours, (C-C$_\infty$) in mmol/l and dC/dt in mmol/(lxh).
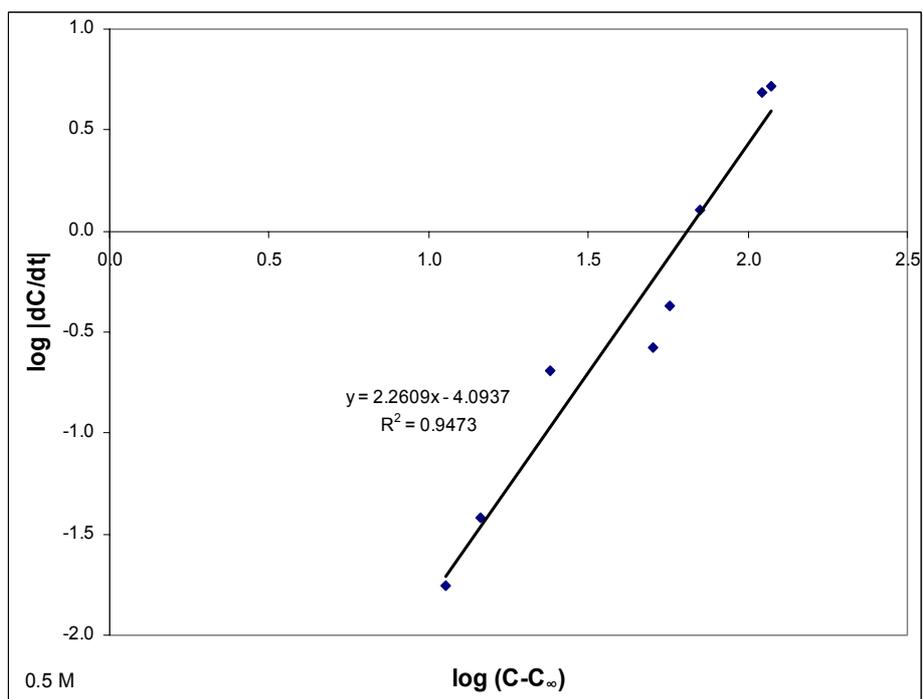
Figure 93. A plot of log dC/dt vs. log (C-C$_\infty$) for the 0.5 M copper weathering test. Time in hours, (C-C$_\infty$) in mmol/l and dC/dt in mmol/(lxh).

142

The two techniques used for interpretation of the data (graphical and by curve fitting) give very similar results for the apparent reaction order (within 5 %) and rate constants (taking into account the standard error as shown in table 26). The values for n and k are compared in table 28. The order of the reaction is close to 1 for the 0.025 M copper solution, which indicates a mass transfer control reaction. The apparent order is however considerably higher for the 0.1 and 0.5 M copper solutions indicating a different controlling mechanism of transfer due to the higher copper concentration. What reaction step determines the rate cannot be concluded. The dependence of apparent reaction order on initial concentration is unexpected, and cannot be explained at this stage.

Table 28.   Results of fitting n^{th} – order kinetic equation to copper weathering data.

	Cu concentration [M]	Curve fitting	Graphical method
	0.025	1.112	1.134
n	0.100	3.409	3.531
	0.500	2.261	2.179
	0.025	0.058	0.032
k	0.100	1.159E-06	6.664E-05
	0.500	8.059E-05	9.486E-05

Kinetic and thermodynamic studies of copper exchange on Na montmorillonite were performed by El-Batouti *et al* (2003). The study utilised an Orion Cu-ion specific electrode. This was repeated in water, methanol and ethanol media and utilised only the < 1 μm fraction of the clay. They found an apparent order of 2.7 for water at temperatures 20 – 40 °C. The exchange took place within 270 s in the study by El-Batouti *et al* (2003), which is very fast compared to the current study. The main reason is the difference in particle size. El-Batouti *et al* (2003) used only < 1 μm material where this study utilised fine rocks (-16 + 13 mm). The much higher concentration used in this present study could also influence the kinetics of the exchange reaction. The lower adsorption rate for copper and the lower reaction order (close to 1 for the 0.025 M concentration) in this present work suggest a degree of mass transfer control in this study. The higher apparent reaction order for the 0.1 and 0.5 M copper concentrations agree well with the study of El-Batouti *et al* (2003). Mass transfer control could be tested in principle by using different sizes of kimberlite particles, but break-up of these particles during weathering changes the diffusion distance as copper take-up proceeds, so the effect of particle size will not follow simple shrinking core kinetic behaviour.

Mass balance for the cupric medium

The total charge of cations absorbed by the kimberlite (expressed as Cu^{2+} equivalents) should equal the total charge of other cations released. For the three copper concentrations, the moles of copper taken up by the kimberlite and the moles of other cations released are compared in table 29. The charge balance over the cation exchange reaction is fairly good, although the 0.1 M copper concentration does not agree very well. A small pH difference did occur which could account for the discrepancies.

Table 29.   Mass balance of copper weathering tests.

Copper concentration	Moles of Cu taken up by ore	Moles of Na & K released	Moles of Mg & Ca released	Moles of Al released	Total equivalent moles of cations released*
0.025	**0.023601**	0.050046	0.000386	0.000000	**0.025409**
0.1	**0.081516**	0.111043	0.009406	0.000070	**0.065033**
0.5	**0.118025**	0.132279	0.042258	0.002817	**0.112623**

 *Total equivalent moles of cations released = K /2 + Na/ 2 + Ca + Mg + 3/2 * Al

Potassium Medium

The kinetic study of the cation exchange reaction was repeated in a different solution with a different kimberlite. The Venetia kimberlite was used in this case, as the effect of potassium on the weathering behaviour of Venetia was already studied and the kinetic data could be used for optimising and understanding the application thereof on underground tunnels. The test utilised a potassium solution and 300 g of Venetia kimberlite (-16 + 13 mm) weathered in 0.1, 0.5 and 1 M potassium chloride solutions at room temperature (20 °C), using 1 litre of weathering medium.   Solution samples were removed at 0, 4 hours, 8 hours, 24 hours, 48 hours, 72 hours and 216 hours (9 days) for ICP analysis to follow the uptake of potassium by the kimberlite. The ICP results are given in table 30 and include the concentration of sodium, calcium and magnesium.

The decrease in the concentration of potassium in the three solutions is shown in figure 94. The decrease in potassium concentration is initially rapid and then the reaction becomes slower at around 2-3 days and thereafter the concentration changes very little. This is faster than for copper, where exchange continued for up to 7 days.

The increase in sodium is shown in figure 95 and the increase in the sum of magnesium and calcium in figure 96. Similar to the copper kinetic evaluation it is essentially sodium that is replaced from the kimberlite for the 0.1 M potassium solution (up to ~ 48 mmol/l) while the

144

sum of calcium and magnesium is ~ 5 mmol/l. In the 0.5 M potassium solution the sodium replaced from the kimberlite goes up to 83 mmol/l and the sum of magnesium and calcium up to 30 mmol/l. For the 1 M solution the sodium goes up to 87 mmol/l and the sum of calcium and magnesium up to 39 mmol/l. The sum of calcium and magnesium replaced from kimberlite increases considerably with potassium concentration. (The detail of the cation exchange of the copper and potassium mediums cannot be compared directly as different kimberlites were used during these tests.)

Table 30. ICP analysis results of potassium weathering solution as a function of time.

0.1 M Potassium			
Time	K	Na	Ca	Mg
[hours]	mmol/l	mmol/l	mmol/l	mmol/l
0	99.75	0.96	0.05	0.03
4	69.06	24.36	2.12	0.53
8	63.94	29.58	2.74	0.74
24	53.71	37.84	3.24	1.03
48	48.60	43.50	3.24	1.11
72	43.48	47.85	3.49	1.15
216	40.92	47.85	3.49	1.19
0.5 M Potassium			
Time	K	Na	Ca	Mg
[hours]	mmol/l	mmol/l	mmol/l	mmol/l
0	485.95	3.35	0.04	0.09
4	434.80	38.28	9.73	1.73
8	409.22	52.20	13.47	2.55
24	383.65	65.25	17.71	3.37
48	358.07	73.95	21.21	4.11
72	352.96	78.30	22.95	4.94
216	350.40	82.65	24.20	5.35
1 M Potassium			
Time	K	Na	Ca	Mg
[hours]	mmol/l	mmol/l	mmol/l	mmol/l
0	946.33	6.52	0.05	0.13
4	895.18	38.28	10.73	1.65
8	856.81	60.90	18.71	2.88
24	818.45	73.95	23.45	3.66
48	818.45	82.65	28.69	4.53
72	805.66	87.00	32.44	5.35
216	792.87	87.00	32.44	6.17
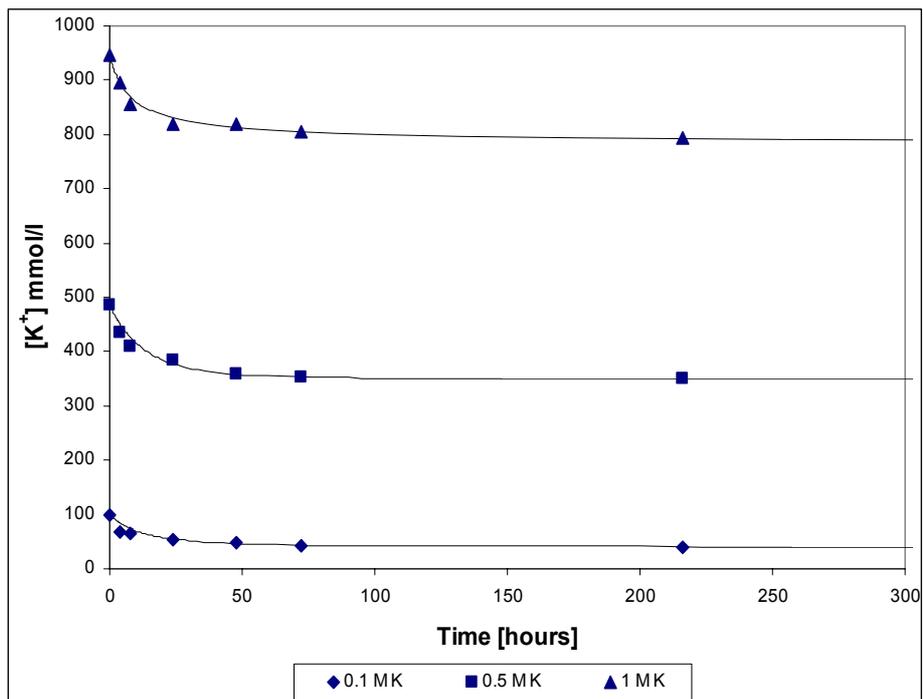
Figure 94.   ICP analysis results displaying the steady decrease of the concentration of potassium in the weathering solution as functions of time.   The lines are fitted curves for simple n[th] - order kinetics (parameters in table 30).
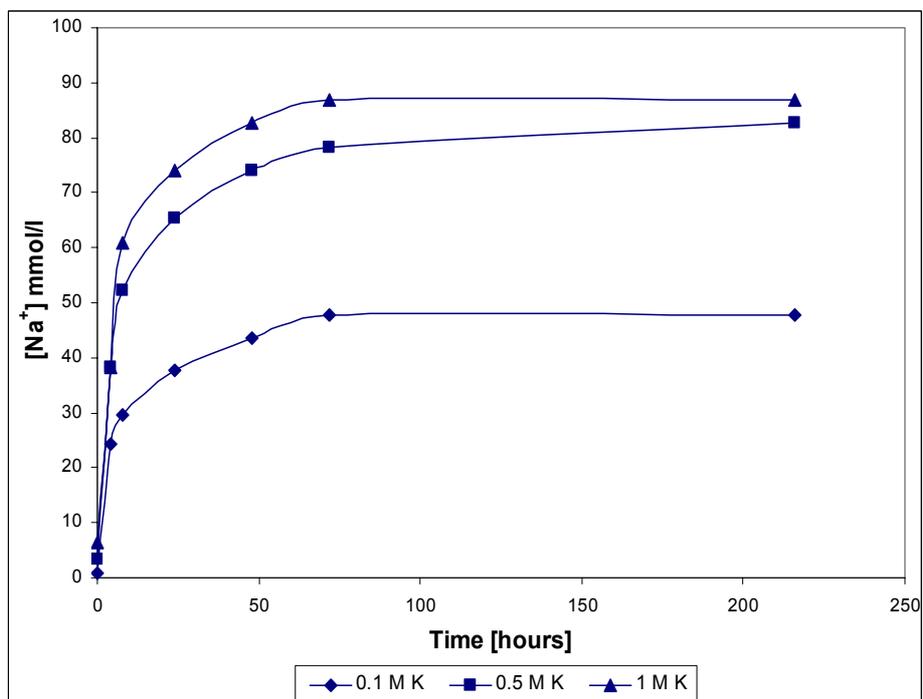
Figure 95. ICP analysis results displaying the increase in the concentration of sodium in the potassium weathering solution as functions of time.

146
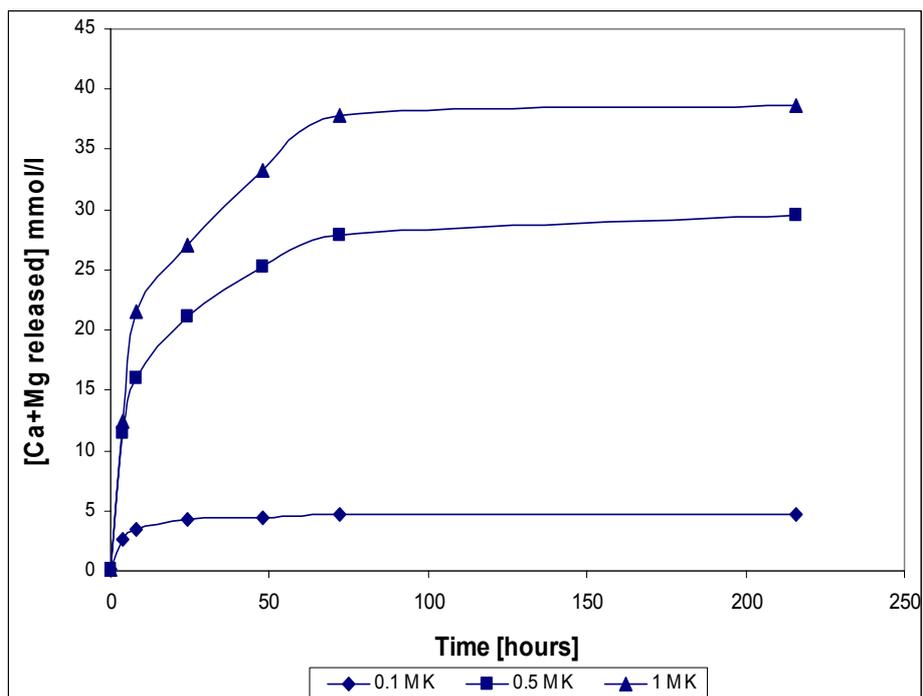
Figure 96. ICP analysis results displaying the increase in the concentration of the sum of calcium and magnesium in the potassium weathering solution as functions of time.

Table 31.   Results of fitting kinetic equation 33 to weathering data.

Variable	Coefficient	Std Error
0.1 M		
C_o (mmol/l)	99.749	-
C_∞ (mmol/l)	40.488	0.489
k	0.013	0.024
n	1.448	0.278
R^2	0.994	-
0.5 M		
C_o (mmol/l)	485.955	-
C_∞ (mmol/l)	350.348	0.026
k	0.034	0.018
n	1.169	0.081
R^2	0.999	-
1 M		
C_o (mmol/l)	946.333	-
C_∞ (mmol/l)	785.456	11.002
k	4.967E-04	4.644E-03
n	2.062	1.056
R^2	0.990	-

The potassium kinetic data was also fitted graphically and by Sigmaplot curve fitting. Results are given in tables 31 and 31. The apparent reaction order is ~ 1.5 for the 0.1 M solution, ~ 1 for the 0.5 M solution and ~ 2 for the 1 M potassium solution. The results of both these fitting methods are shown in table 33 for comparison.

Table 32.   Results of graphical fitting of kinetic equation 32 to potassium weathering data.

Potassium concentration	Equation of line	n	k
0.1	y=1.644x – 1.963	1.6	0.011
0.5	y=1.310x - 1.585	1.3	2.6E-02
1	y=2.194x – 3.425	2.2	3.8E-04
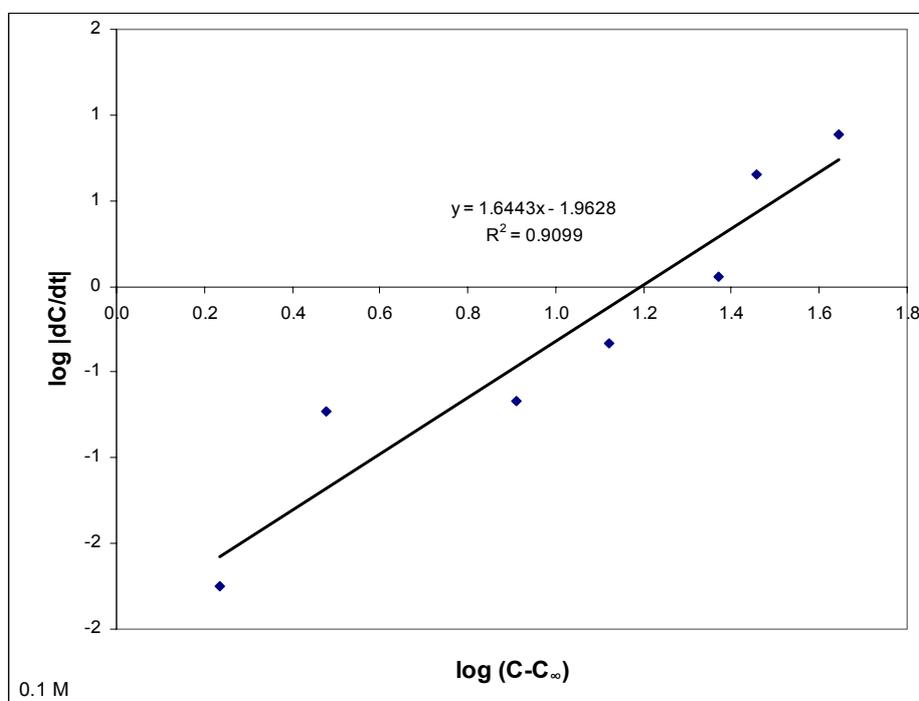
Figure 97. A plot of log dC/dt vs. log (C-C$_\infty$) for the 0.1 M potassium weathering test. Time in hours, (C-C$_\infty$) in mmol/l and dC/dt in mmol/(lxh).
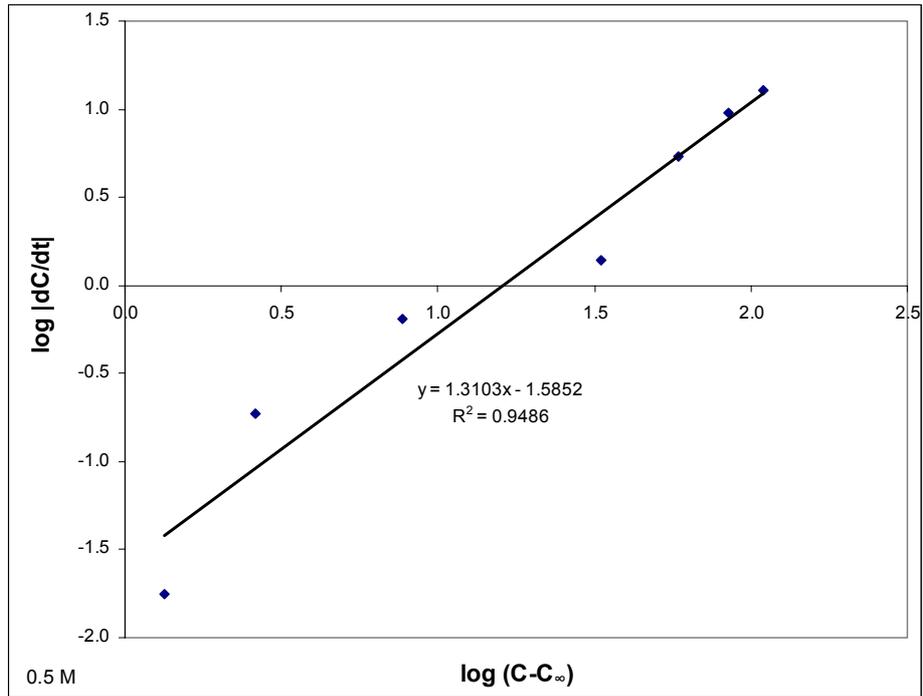
Figure 98. A plot of log dC/dt vs. log (C-C$_\infty$) for the 0.5 M potassium weathering test. Time in hours, (C-C$_\infty$) in mmol/l and dC/dt in mmol/(lxh).
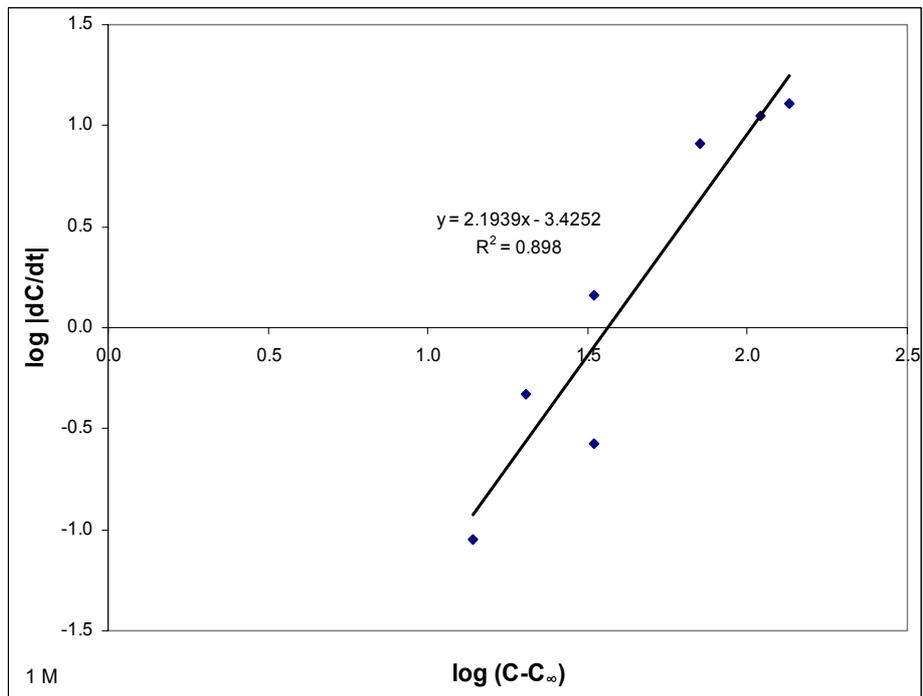
Figure 99. A plot of log dC/dt vs. log (C-C$_\infty$) for the 1 M potassium weathering test. Time in hours, (C-C$_\infty$) in mmol/l and dC/dt in mmol/(lxh).

Table 33.   Results of fitting n^{th} – order kinetic equation to potassium weathering data.

	Cu concentration [M]	Curve fitting	Graphical method
n	0.1	1.644	1.448
	0.5	1.310	1.169
	1.0	2.194	2.062
k	0.1	0.011	0.013
	0.5	0.026	0.034
	1.0	3.757E-04	4.967E-04

To enable comparison of the potassium and copper data, a plot of $t_{0.5}$ vs. $C_0 - C_\infty$ is given in figure 100. The value of $t_{0.5}$ represents the time to reduce the difference between the copper concentration in solution and its equilibrium concentration, to half the original difference.
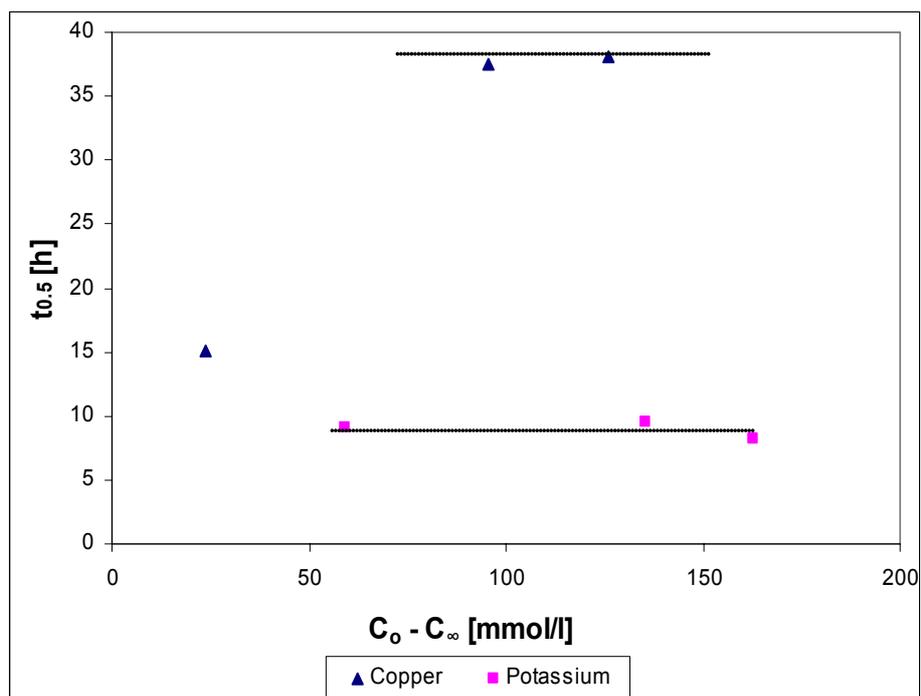
Figure 100.   A plot of $t_{0.5}$ (time to reduce the difference between the exchanging cation concentration and the equilibrium concentration to half of the original difference) vs. $\log C_0 - C_\infty$ for the copper and potassium data.

150

Figure 100 confirms the more rapid exchange of potassium, which is in line with its higher mobility: the room temperature diffusion coefficient for K^+ equals 1.957×10^{-5} cm^2 s^{-1} compared to 0.714×10^{-5} cm^2 s^{-1} for Cu^{2+} (Lide and Frederikse, 1994). For the case where k and n are not dependent on the initial concentration, it is expected that $t_{0.5}$ would be proportional to $(C_0 - C_\infty)^{n-1}$. For n > 1 (as in this case) it is hence expected that $t_{0.5}$ would decrease as C_0 increases, which is not the case in figure 100. This suggests that the exchange mechanism and reaction kinetics are not clearly understood at this stage.

Langmuir adsorption isotherms

The equilibrium data for copper and potassium can be plotted as adsorption isotherms as shown by Dahiya *et al* (2005), Herbert and Moog (1999) and Rytwo *et al* (1996). This is a plot of Qe (the quantity of cation uptake by the solid, units mol/l) vs. Ce (the final cation concentration in solution, units mol/l). Qe was not measured in this case but calculated from the cation concentration removed from the solution. The Langmuir equation is shown as equation 34 where Qe = X/M; X the amount of solute absorbed, M the weight of the solid, a and b are constants. A plot similar to Dahiya *et al* (2005) of Ce/Qe vs. Ce is shown in figure 100 for the three concentrations of copper and potassium. Note that Ce/Qe is dimensionless.

Langmuir equation: $\qquad \dfrac{Ce}{Qe} = \dfrac{Ce}{a} + \dfrac{1}{b}$ $\qquad\qquad\qquad\qquad$ (34)
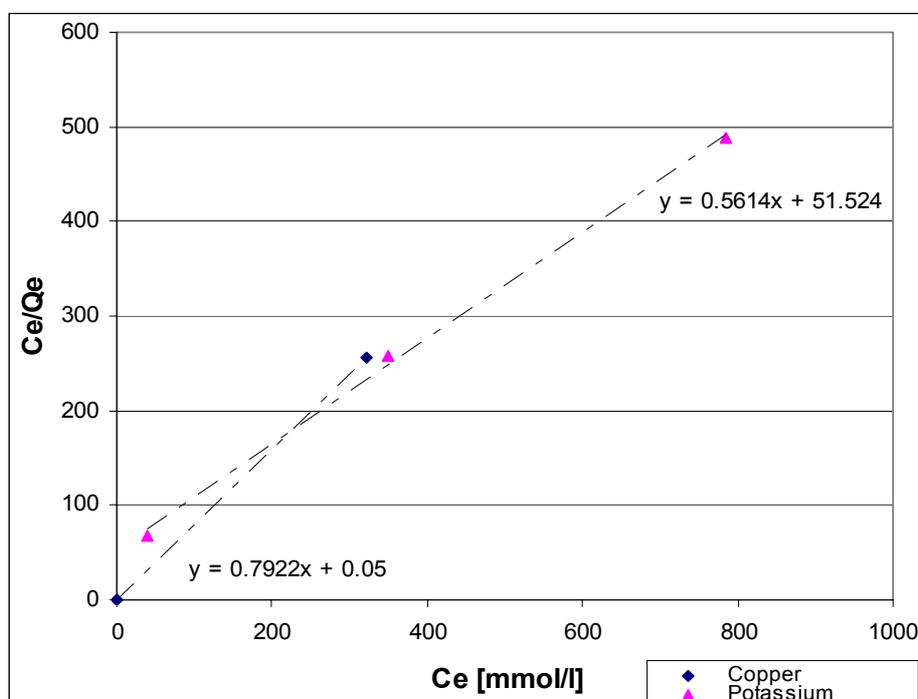
Figure 101. Langmuir adsorption isotherm for kimberlite treated with copper at 0.025, 0.1 and 0.5 M and treated with potassium at 0.1, 0.5 and 1 M.

Linear relationships are obtained in figure 101 according to the Langmuir equation although more data points would be useful. This is similar to zinc adsorption work by Dahiya *et al* (2005) on one specific soil they tested. Another soil tested in their work fitted the Freundlich adsorption equation. The concentration used in the present work is much higher and utilised copper rather than zinc. According to Dahiya *et al* (2005) the amount of zinc absorbed was determined by the type of soil (different clay minerals present), the initial concentration and temperature. The Langmuir equation represents the capacity of a soil to absorb a specific cation. In this case (figure 101) the capacity of absorption for copper is higher than for potassium (at higher concentrations), although this is difficult to compare directly as different kimberlites were used for the test work. Figure 101 also shows that the absorption is directly correlated with the cation concentration in solution (concentration of cations available for up-take). This correlates with the kinetic data which showed that as the cation concentration in solution increased, the amount of cations absorbed by the kimberlite increased.

6.5   Cation exchange behaviour

The cation exchange constant refers to the ease of replacing the interlayer cations with cations in the surrounding medium. The method used for calculation of the cation exchange constant (K_N) is discussed in section 3.2. The tabulated data by Bruggenwert and Kamphorst (1982) are compared with the ionic potential (as used in section 6.2.5.2) in figure 102. Note that the tendency to exchange monovalent Na^+ with other cations was compared by calculating the product $K_N\left(0.5c_B\right)^{(1/z_B - 1/z_A)}$, where constant K_N is the equilibrium constant for the exchange of cation A (taken to be Na^+) with cation B. For this calculation, an arbitrary (but realistic) value of 0.1 M equivalent concentration of cation B was used.   The Na-montmorillonite data was used for comparison, as experimental results (section 6.4) indicated that primarily Na^+ is replaced from the kimberlite, especially at low cation concentrations. No data is available for the iron species in Bruggenwert and Kamphorst (1982). Figure 102 shows that there is no correlation between the ionic potential and cation exchange constants.

The cation exchange constants were determined experimentally utilising finely milled Venetia Red kimberlite and 0.05 M K^+, Li^+, NH_4^+, Ca^{2+}, Mg^{2+}, Ni^{2+}, Fe^{2+}, Cu^{2+}, Fe^{3+} and Al^{3+} solutions. The cation exchange constants determined experimentally compared with the ionic potential are shown in figure 103. The experimental data were expressed simply as the ratio of the equilibrium concentration in the liquid of the exchanging cation B (raised to the power $1/z_B$) to that of the exhanged cation, Na^+ (with both concentrations expressed in mol/dm^3). There is a positive correlation between the experimental cation exchange behaviour and the ionic potential as shown in figure 103, with the exception of Fe^{2+} and Cu^{2+}.
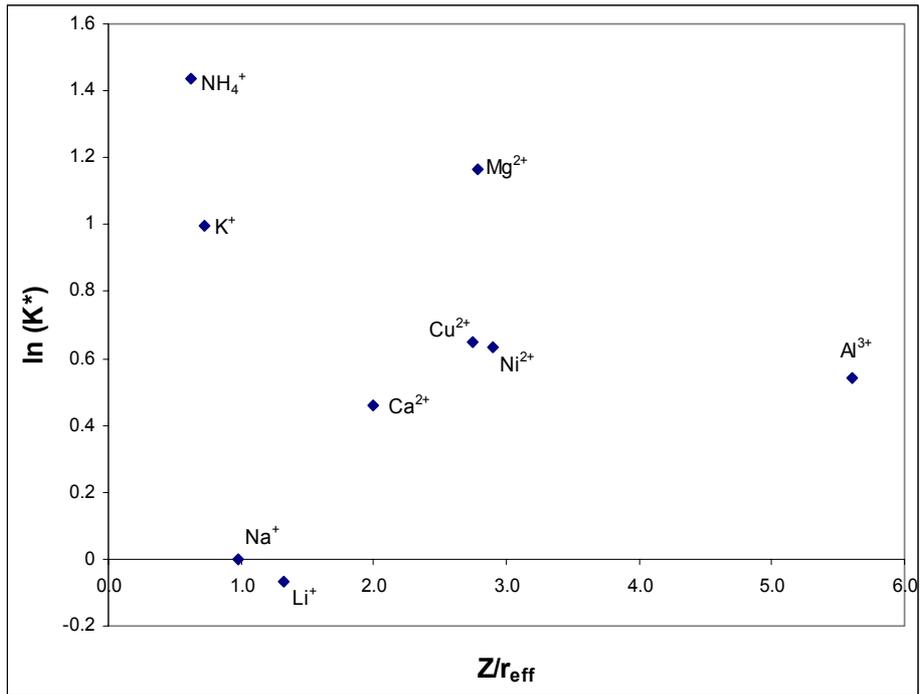
Figure 102. Cation exchange constants as published by Bruggenwert and Kamphorst (1982) as a function of ionic potential.
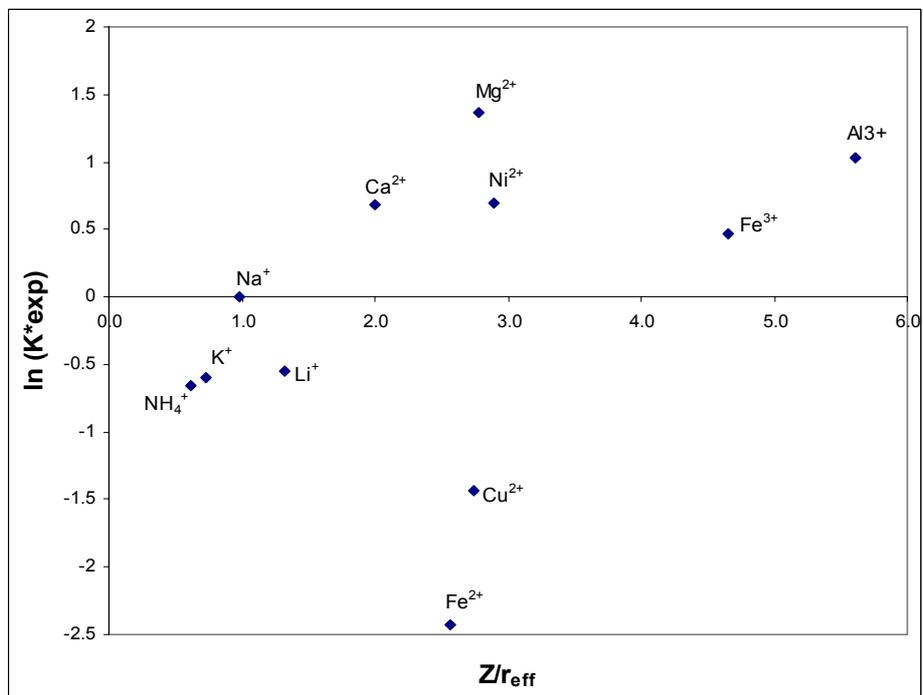
Figure 103.   Experimentally determined cation exchange constants as a function of ionic potential.

6.6   Correlation between cation weathering and interlayer spacing (from XRD)

The relationship between changes in interlayer spacing of the clay mineral (measured by XRD) and cation exchange was studied. Dutoitspan kimberlite (250 – 300 g of the – 16 + 13.2 mm size fraction) was weathered in a 0.5 M copper solution for 4 hours, 8 hours, 1 day, 7 days and 30 days utilising 1.5 litres of weathering medium.   XRD analysis was performed on the air dried kimberlite after weathering to determine the interlayer spacing (d value of the smectite peak). The results are shown in figure 104. The interlayer spacing is at 12.5 Å (7.1 ° 2 theta) after 4 and 8 hours exposure to the copper solution. At two days, two peaks are visible at 12.5 and 14.5 Å (6.1 ° 2 theta) indicating the presence of smectite with an interlayer spacings of both 12.5 and 14.5 Å, i.e. the smectite is in the process of swelling. After 7 days the 12.5 Å peak is totally collapsed and only the 14.5 Å peak is visible. All the smectite has therefore swollen to this value and it is shown that after 30 days the interlayer spacing is still at 14.5 Å. Only 2 spacing values are observed with no intermediate values. This could indicate stepwise swelling as suggested by Madsen and Müller-Vonmoos (1989). A spacing of 14.5 Å is associated with a double water layer.

The Venetia Red kimberlite interlayer spacing was determined on the untreated sample and then exposed to a 1.5 M potassium chloride solution for 4 hours before repeating the XRD scan (-16 + 13.2 mm). The untreated interlayer spacing is at 14 Å or 6.3 ° 2 theta (figure 105) and is collapsed to 12.5 Å (7.1 ° 2 theta) with the potassium chloride solution.

The d spacing was investigated as a function of the cation type by exposing Dutoitspan kimberlite to different 0.5 M cation solutions (sulphate and chloride anion) for six days. The final d spacings are shown in table 34. The weathering order for some of the cations are: $Cu^{2+} > Li^{1+} > Ca^2 > Mg^{2+}$. The table shows that there is no correlation between the interlayer spacing and the severity of weathering. The differences between the interlayer spacing for Ca^{2+}, Mg^{2+} and Cu^{2+} exchange are very small whilst the weathering results are very different. For K^+ the interlayer spacing relates to the collapsed form as expected. Ferrage *et al* (2005) showed that, for ambient conditions (room temperature and around 35 % relative humidity) montmorillonite with Mg^{2+} and Ca^{2+} in the interlayer had primarily 2 water layers in the interlayer. Na^+ and Li^+ on the other hand will display primarily 1 water layer spacings and K^+ predominantly 0 water layers.   The results for Ca^{2+}, Mg^{2+}, Li^+ and K^+ therefore agrees well with the work by Ferrage *et al* (2005). Cu^{2+} agrees with the Mg^{2+} and Ca^{2+} exchanged forms; a two water layer system under room temperature and humidity conditions.

Ferrage *et al* (2005) formulated equations for the interlayer thickness as a function of the ionic potential and relative humidy, which allows the quantification of the increase of layer thickness with increase in the relative humidity for single and double water layer systems. These formulations are given as equations 35 and 36 with ν the cation charge, r the effective radius and RH the relative humidity as a fraction. For room conditions these equations could predict the experimentally determined cation interlayer spacings within a 7 % interval as shown in table 34 (assuming 2 water layer systems for Cu^{2+} and Al^{3+} at room conditions).

$$\text{Layer thickness (1W)} = 12.556 + 0.3525 \times (\nu/r - 0.241) \times (\nu \times RH - 0.979) \qquad (35)$$

$$\text{Layer thickness (2W)} = 15.592 + 0.6472 \times (\nu/r - 0.839) \times (\nu \times RH - 1.412) \qquad (36)$$

From these results it is concluded that the interlayer spacing (swelling) can not in itself explain the weathering behaviour of kimberlite. The other factors for example cation charge, hydrated radius, type of clay mineral and layer charge all contribute towards the weathering mechanism.

Table 34. Interlayer spacing for Dutoitspan kimberlite weathered in solutions containing different cations.

Cation Type	Measured d spacing	Ferrage *et al* (2005) predicted spacing
	Å	Å
Ca^{2+}	15.1	15.06
Mg^{2+}	14.6	14.70
Cu^{2+}	14.9	14.72
Al^{3+}	14.6	14.47
K^+	10.1	10.00
NH_4^+	12.5	12.47
Na^+	13.3	12.40
Li^+	12.9	12.30
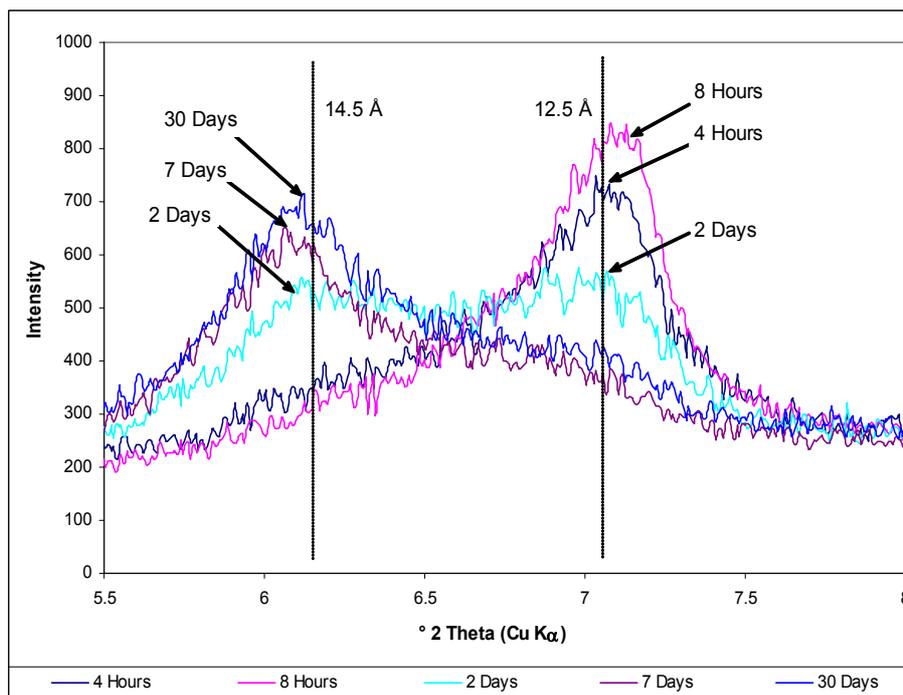
Figure 104. XRD scans (5.5 – 8 ˚ 2θ) of Dutoitspan kimberlite after exposure to copper solutions for 4 hours, 8 hours, 2 days, 7 days and 30 days.
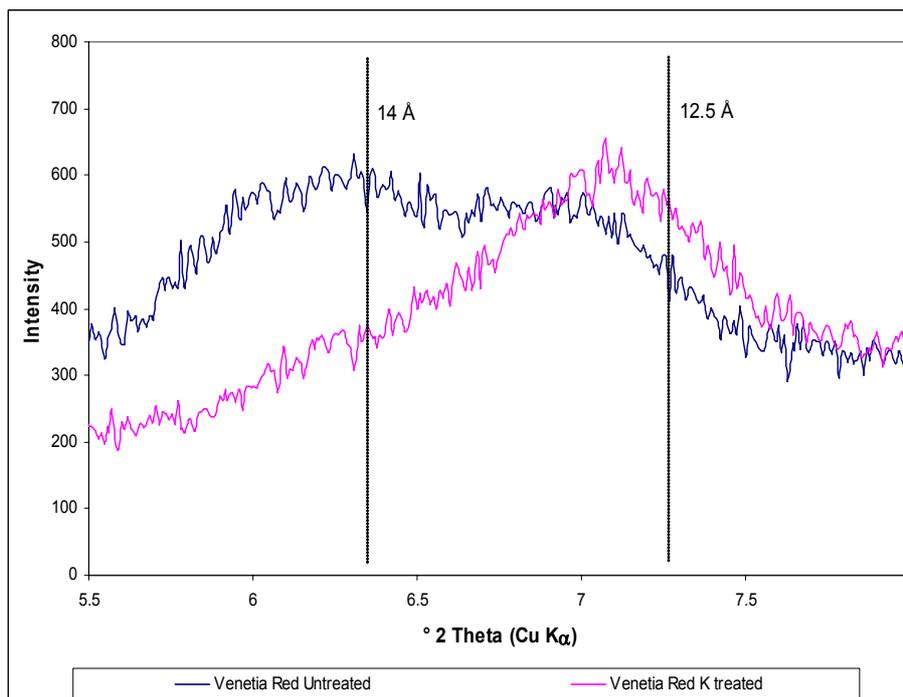
Figure 105. XRD scans (5.5 – 8 ˚ 2θ) of Venetia Red kimberlite after exposure to a 1.5 M potassium chloride solution for 4 hours.

156

The absence of an effect of cation type on the extent of smectite swelling is in apparent contradiction with the central role of swelling clay in kimberlite weathering which is proposed in this work. To state the apparent contradiction simply: swelling causes kimberlite weathering; kimberlite weathering is strongly affected by the identity of cations in the solution; yet cation identity has little effect on swelling.

This apparent contradiction can be resolved by invoking other elements of the failure process. Griffith-style fracture of brittle materials depends on defect length, applied stress and surface tension. Of these, the defect length is expected to depend on the kimberlite structure, and this does not change if the weathering solution is changed. The stress is applied by swelling; this can be seen to be little affected by cation identity. By elimination, this leaves an effect of cation identity on the surface energy of the crack; such an effect could arise from cation adsorption on the crack surface. The study of Cu^{2+} sorption on montmorillonite by Stadler et and Schindler (1993) suggested that for $3 < pH < 5$ the Cu^{2+} sorbs in the interlayer of montmorillonite through ion exchange, but for $pH > 5$ forms surface complexes with surface hydroxyl groups, which could influence the crack surface energy. This effect was not explored further in this study (careful study of fracture behaviour is severely impeded by the rapid disintegration of the kimberlite). However, it would be a worthwhile direction for future work, especially where solutions with more than one cation are used (perhaps the solution could be designed to contain one cation which exchanges with sodium to cause swelling and another cation/s which changes the crack surface energy).

The type of cation expressed as the ionic potential (cation valence and effective radius) show correlation with the observed weathering behaviour. The type of clay and layer charge will also influence the degree of weathering and the effect of cations. The adsorption mechanism has been shown to differ for different cations (section 6.2.5.2) which also influences the effect of cations on the clay structure and properties. In summary it was shown that Cu^{2+}, Fe^{2+} and Li^+ can absorb in different positions than only the interlayer rendering the adsorption very effective. Fe^{3+} and Al^{3+} on the other hand have the tendency to form hydroxy species in the interlayer and therefore exhibit a very different mechanism of adsorption. The relationship between ionic potential and observed weathering behaviour holds well for all cations except the trivalent species. It is suggested that the different adsorption mechanism accounts for the weak correlation observed in this case.

6.7 Agglomeration test results

The results of this test are given in table 35. Visual observations of the agglomeration effect were also recorded and shown in figure 106. The results broadly agreed with the weathering results. The Wesselton and Cullinan ores, that showed no and very little weathering, had very little ore agglomerated on the metal piece while Geluk Wes had 2.5 % and Koffiefontein 13.6 %. Figure 107 shows the correlation between this test and weathering results of the Venetia ores.

Table 35. Results of the agglomeration test.

Ore type	Mass retained on metal pieces	% Material retained on metal pieces
Dutoitspan	26.03	13.01
Geluk Wes	5.02	2.51
Koffiefontein	27.32	13.66
Cullinan	1.85	0.92
Wesselton	0.28	0.14
Venetia K1 HYP NE	0.17	0.09
Venetia K1 HYP S	0.81	0.41
Venetia K1 TKB E	2.25	1.13
Venetia K2 NE	6.82	3.41
Venetia K2 S	4.64	2.32
Venetia K2 W	4.76	2.38
Venetia K8	0.11	0.05
Venetia Red	8.59	4.29

| Koffiefontein | Dutoitspan |

| Geluk Wes | Cullinan TKB |

| Wesselton | Venetia K1 HYP NE |

Figure 106. Visual results of the agglomeration test showing the degree of agglomerated ore on the metal piece.

159

Venetia K1 HYP S	Venetia K1 TKB E
Venetia K2 NE	Venetia K2 S
Venetia K2W	Venetia K8

Figure 106. Visual results of the agglomeration test showing the degree of agglomerated ore on the metal piece.

Venetia Red

Figure 106. Visual results of the agglomeration test showing the degree of agglomerated ore on the metal piece.
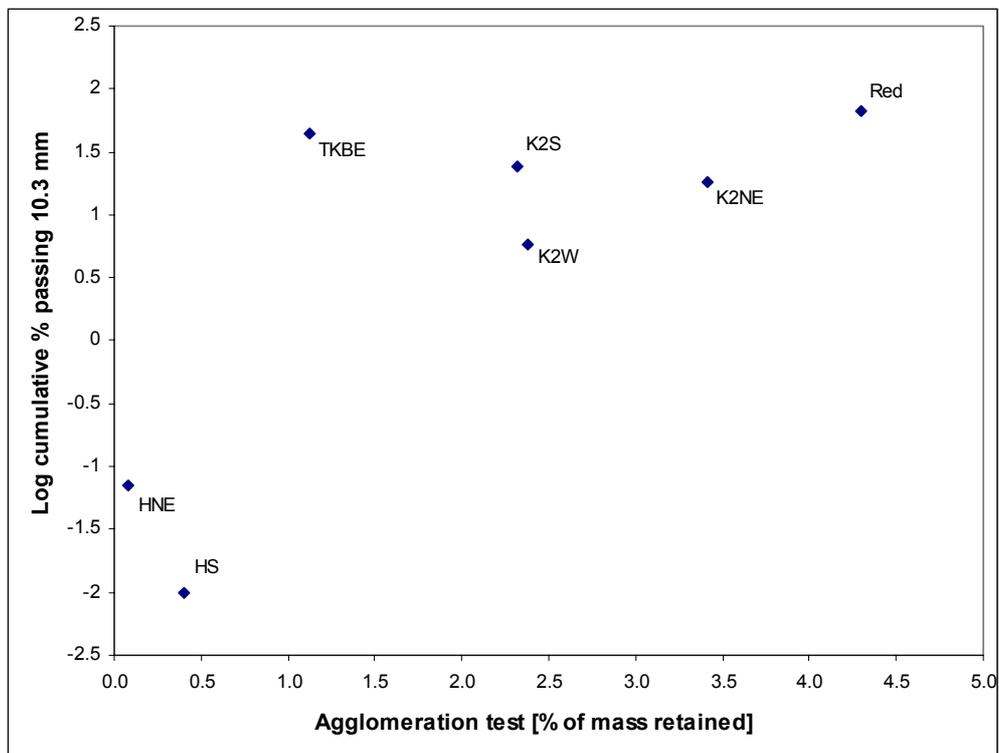
Figure 107. Comparing weathering results with the agglomeration test of Venetia ores. Weathering is shown as log cumulative % passing at 10.3 mm from figure 82 (6 days' weathering in 0.05 M copper sulphate).

Figure 107 shows the relationship between observed weathering behaviour and the agglomeration test for Venetia ores. The poor correlation is evident. This can be due to differences in inherent water content or differences in the histories of these samples, as the

161

samples were not dried prior to testing. It was therefore suggested that a standard test be developed based on this idea, which should include drying all samples so that it will allow for comparison. This was done as part of a final year undergraduate project (Morkel and Bronkhorst, 2005). The results showed that initial drying at 100 °C for 4 hours and then wetting in distilled water for 2 hours gave good results (figure 108). A R^2 of 0.91 was obtained. This is a simple test for prediction of an ore's likely behaviour during weathering.
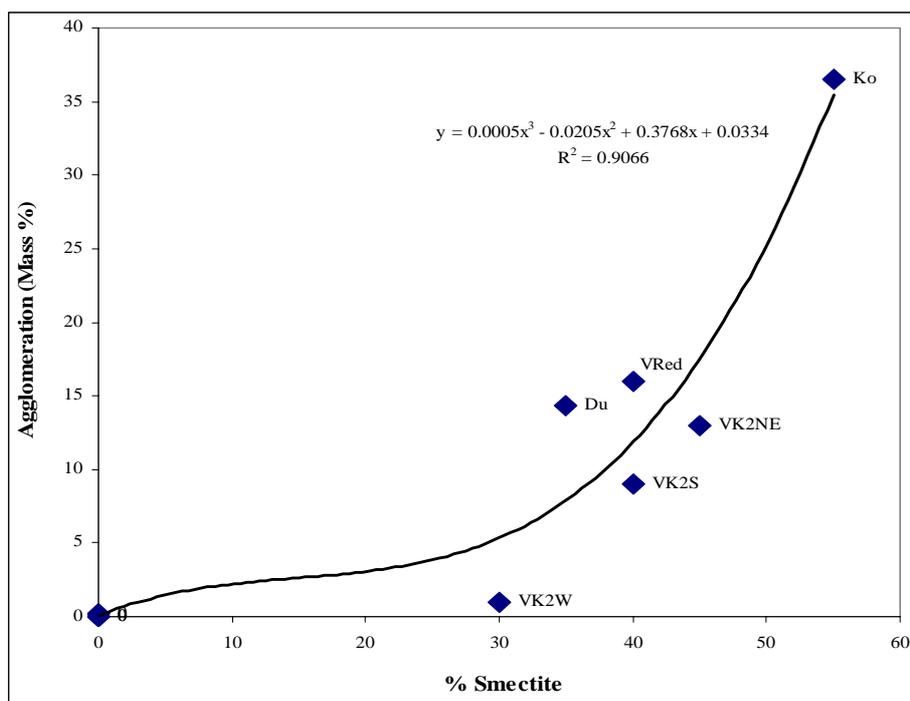
Figure 108. Agglomeration test results for kimberlites dried at 100 °C and then wetted in distilled water for 2 hours.

7   INDUSTRIAL APPLICATION

7.1   *% Smectite vs. CEC for some De Beers Mines*

Plots of the analysed % smectite and CEC for kimberlites from some De Beers mines are shown in figures 109 - 113. This data was obtained from the Ore Dressing Study group at De Beers Technical Services.   De Beers has previously determined their % smectite at Agricultural Research Council (ARC) and therefore the XRD analysis was done on the -2 μm fraction only. This data therefore can not be compared to data in this thesis. We expect a linear increase in CEC as % Smectite increases.
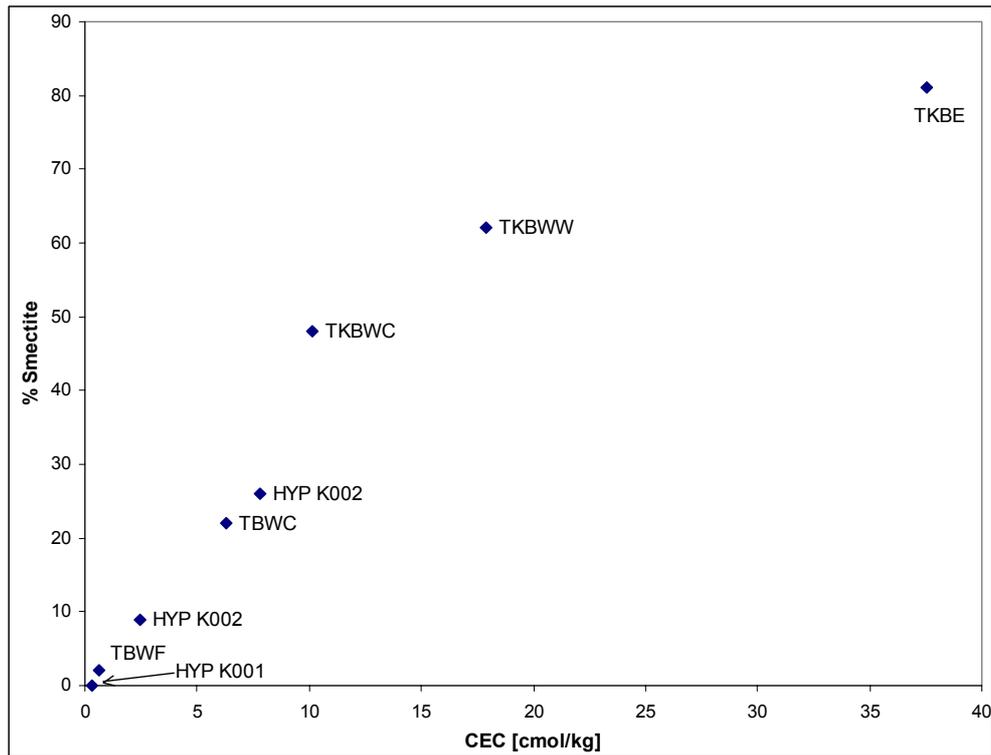
Figure 109. Smectite vs. CEC for Venetia ores / kimberlites from the De Beers geological database. Symbols of kimberlites shown in table 36.

Figure 109 shows the CEC and % smectite for Venetia kimberlites. Very good correlation between these parameters is observed. It is shown that Venetia has kimberlites over the whole spectrum from unweatherable (hypabyssal kimberlite) to highly weatherable (TKB East and West). No kimberlites in this group have a cation exchange capacity larger than 40 cmol/kg.

Table 36. Venetia ores / kimberlites from the De Beers Geological database.

Ore / Kimberlite type	Label
Hypabyssal K001	HYP K001
Tuffisitic Breccia West Fine	TBWF
Hypabyssal K002	HYP K002
Tuffisitic Breccia West Coarse	TBWC
Tuffisitic Kimberlite Breccia West Competent	TKBWC
Tuffisitic Kimberlite Breccia West Weathered	TKBWW
Tuffisitic Kimberlite Breccia East	TKBE
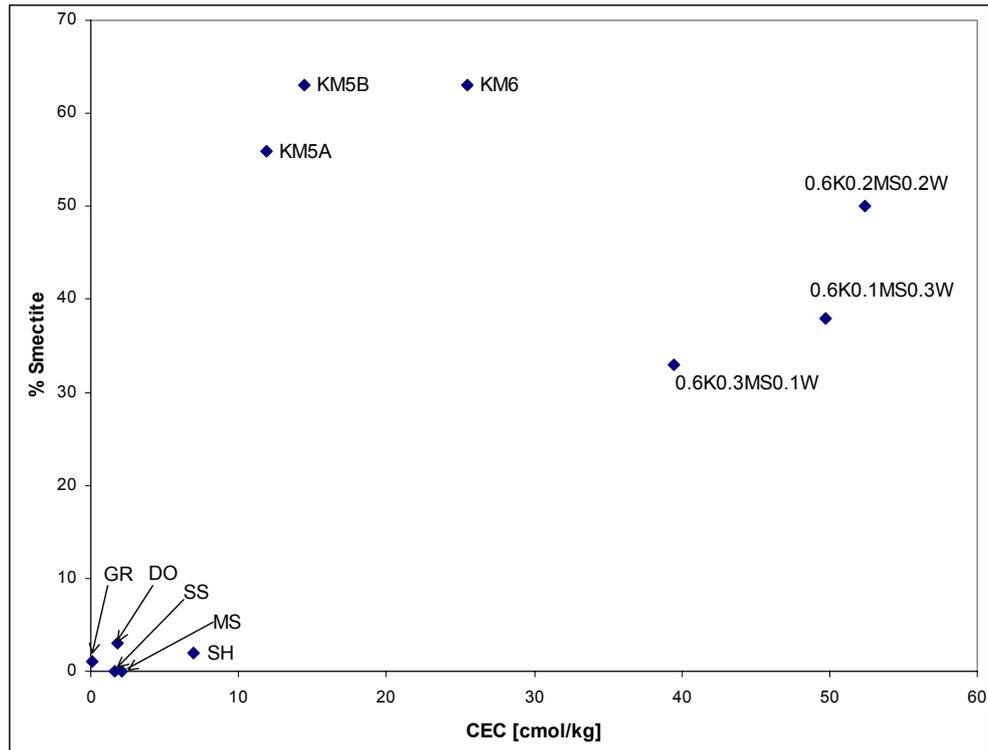
Figure 110. Smectite vs. CEC for Koffiefontein ores / kimberlites from the De Beers geological database. Symbols of ores / kimberlites shown in table 37.

Figure 110 shows the CEC and % Smectite for Koffiefontein ore / kimberlite. Although the correlation between the two parameters is not very good, a prediction of the behaviour of these kimberlites during weathering can be made based on the cation exchange capacity. There are a few ores / kimberlites that should show no weathering (granite, dolomite, mudstone, sandstone and shale) and then progressively the kimberlites will become more prone to weathering as the CEC increases with the kimberlite; mudstone and whittworth mixed ore being the most vulnerable. Note that the highest CEC value here is ~ 55 cmol/kg compared to the highest value for Venetia kimberlite which is below 40 cmol/kg.

164

Table 37. Koffiefontein ores / kimberlites from the De Beers Geological database.

Ore / Kimberlite type	Label
Granite	GR
Dolomite	DO
Sandstone	SS
Mudstone	MS
Shale	SH
Kimberlite KM5A	KM5A
Kimberlite KM5B	KM5B
Kimberlite KM6	KM6
60 % Kimberlite, 30 % Mudstone, 10 % Whittworth	0.6K0.3MS0.1W
60 % Kimberlite, 10 % Mudstone, 30 % Whittworth	0.6K0.1MS0.3W
60 % Kimberlite, 20 % Mudstone, 20 % Whittworth	0.6K0.2MS0.2W

Figure 111 shows the % smectite, CEC results for Cullinan kimberlites and slimes. The correlation between these two parameters is good. All four kimberlites present in the database have CEC values below 10 cmol/kg indicating these ores to be non weatherable. The CEC of C-Cut slimes is reported as 27 cmol/kg.

Table 38. Cullinan ores / kimberlites from the De Beers Geological database.

Ore / Kimberlite type	Label
Piebald Kimberlite	PBK
Tuffisitic Kimberlite Breccia	TKB
Black Kimberlite	Black
Brown Kimberlite	Brown
C-Cut Slimes	CSlimes
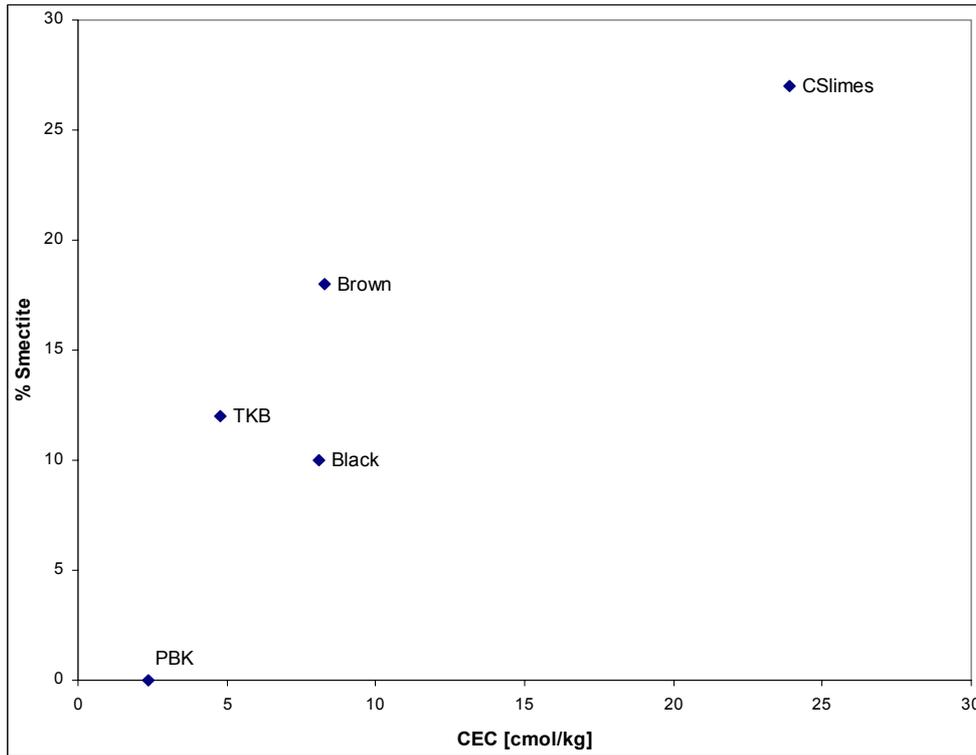
Figure 111. Smectite vs. CEC for Cullinan ores / kimberlites from the De Beers geological database. Symbols of ores / kimberlites given in table 38.
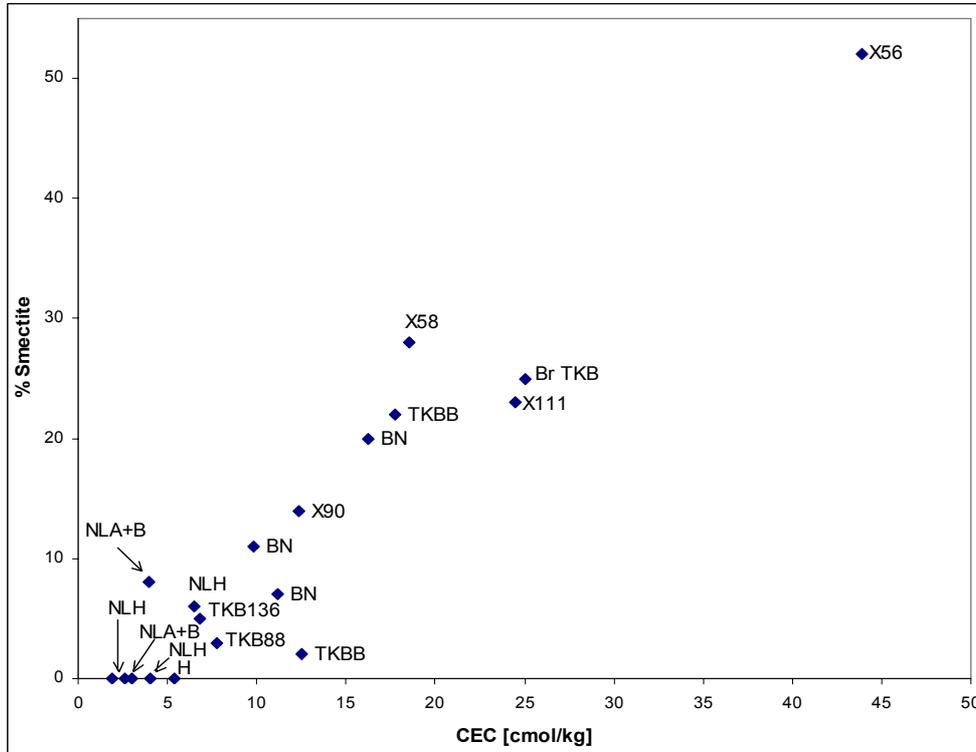
Figure 112. Smectite vs. CEC for Oaks ores / kimberlites from the De Beers geological database. Symbols used for the ores/ kimberlites are given in table 39.

166

Table 39. Oaks Kimberlite types from the De Beers Geological database.

Ore / Kimberlite type	Label
North Lobe Hypabyssal	NLH
North Lobe Amphibole and Biotite	NLA + B
Hypabyssal Kimberlite	H
TKBB136	TKB136
TKB88	TKB88
TKBB	TKBB
Breccia Neck (TKB)	BN
Xenolith (58 – 82 m)	X58
Xenolith (56 – 70 m)	X56
Xenolith (90 – 107 m)	X90
Xenolith (111 – 124 m)	X111
Br TKB (193 – 217 m)	Br TKB

The % smectite vs. CEC for the Oaks De Beers mine is shown in figure 112. The correlation between the parameters is also good with almost all the ores / kimberlites having CEC values below 30 cmol/kg. These ores therefore will mostly not be prone to weathering although some of the kimberlites (with CEC values close to 30 cmol/kg) might show some signs of degradation. There is however one data point at 43 cmol/kg which should be a kimberlite exhibiting degradation by weathering.

The data for these mines are combined in figure 113.
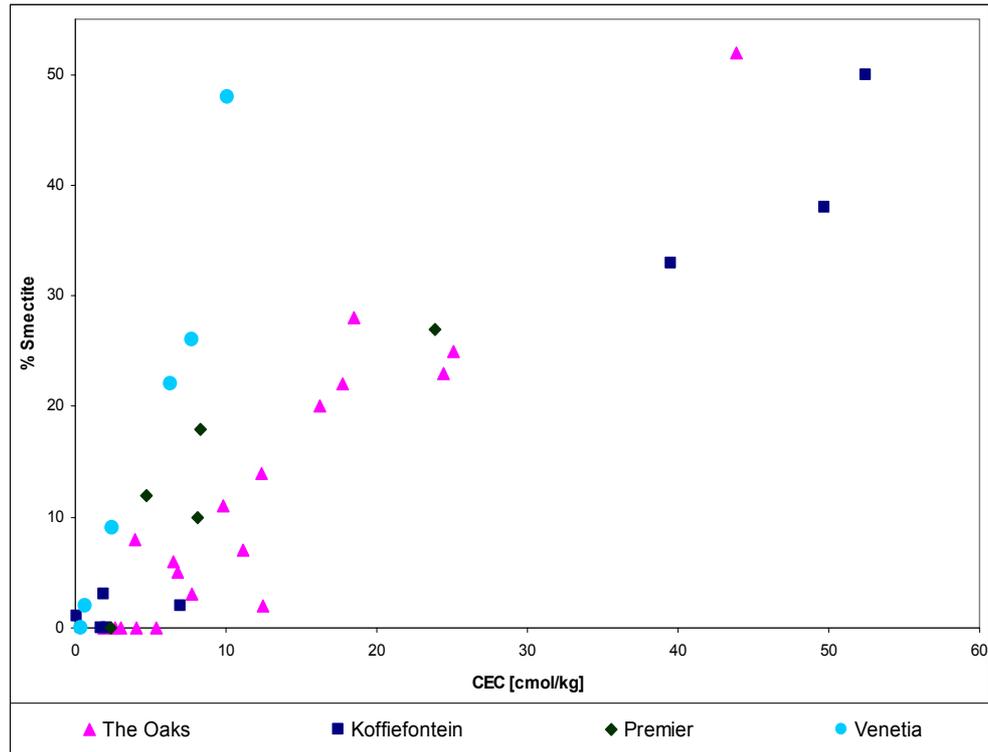
Figure 113. Smectite vs. CEC for the Oaks, Koffiefontein, Cullinan and Venetia mines from the De Beers geological database.

7.2   *Potassium as stabiliser of kimberlite*

7.2.1 Background

Understanding kimberlite weathering is also important in terms of underground mining techniques as De Beers currently experiences many problems with creating stable underground tunnels. Currently the kimberlite is sprayed with a sealant (commonly with an epoxy or polyurethane basis) and then sprayed with shotcrete (a concrete produced for underground mining). The function of the sealant is to seal off the kimberlite from the surroundings and the shotcrete is then applied to provide mechanical strength. The sealants however typically contain ~ 20 % of calcium sulphate and ~ 30 % water and therefore have been found to actually cause weathering of the kimberlite and then peel off. Typically adhesion tests are used to evaluate the adhesion property of sealants, and also allows for evaluation of whether the kimberlite has been affected by the sealant. This project looked at chemically altering the kimberlite to a more stable state, and also investigated altering the

sealant properties to minimise the effect on kimberlite. Some of the test results obtained during this study are shown in the next section.

7.2.2 Slake durability test results

The slake durability test discussed in section 2.3.1.4 was used to evaluate the weathering behaviour of the kimberlite. For these tests some Cullinan and Venetia kimberlites were obtained. Figure 114 shows the results for these kimberlites in distilled water (data are given in Appendix D).
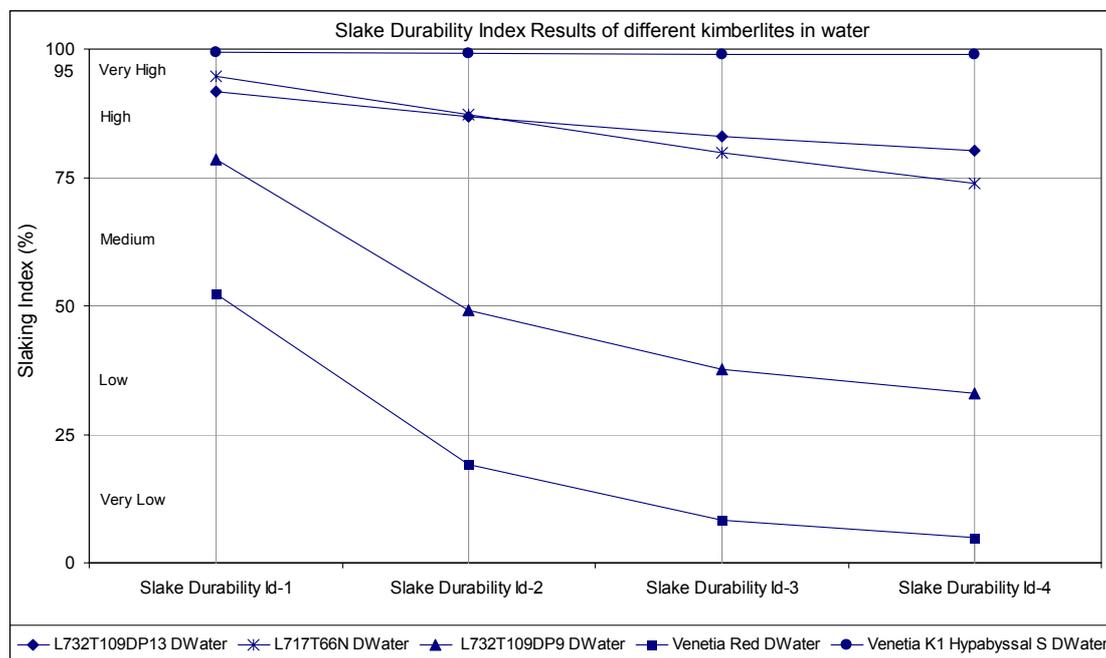
Figure 114.   Slake durability test results for three different Cullinan kimberlites (L732T109DP9, L717T66N, L732T109DP13) and Venetia Red and Venetia Hypabyssal kimberlites in distilled water.

The slake results for Cullinan and Venetia kimberlites in distilled water are shown in figure 114. Venetia Hypabyssal shows high slaking durability with almost all the mass retained after four cycles. Cullinan L732T109DP13 and L717T66N show strong slaking durability, whilst Cullinan L732T109DP9 kimberlite displays medium to low slaking durability. Venetia Red kimberlite has been shown to be very weatherable, which agrees with the very low slaking durability observed. The effect of utilising a potassium weathering medium was evaluated and results are shown in figure 115. Potassium has been shown a clay stabiliser (collapses swelling clays) and therefore is expected to provide more integrity to clay rich kimberlite. For these tests Venetia Red and Cullinan L732T109DP9 was chosen as these kimberlites showed the most slaking.

169
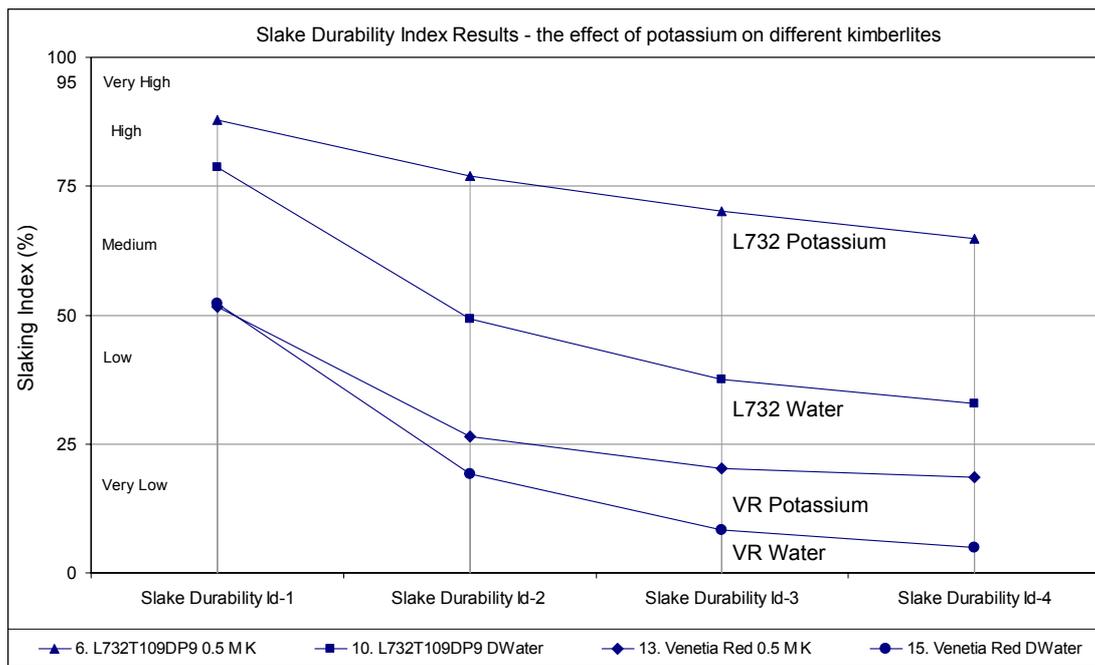
Figure 115. Slake durability test results for Venetia Red and Cullinan L732T109DP9 in a distilled water and a potassium chloride solution.

The addition of potassium to the weathering solution was investigated (0.5 M solution) and results shown in figure 116. Venetia Red was improved from a final slake durability index of 5 to 20 %. Similarly Cullinan kimberlite (L732) was improved from ~ 30 to 65 %. The weathering improvement obtainable depends on the abundance of smectite; Cullinan with less swelling clay can be improved more (35 %) that Venetia Red at 15 %.

8   POSSIBLE FUTURE WORK

The focus of this study was mainly on the understanding of what determines weathering in kimberlite. In the process a lot of work was done on the fundamentals of clays and cation exchange on clays. Possible future work could investigate better characterisation of the clay species especially the smectite minerals. Furthermore determining the layer charge of the smectites could provide useful information in understanding the properties and behaviour of clays. Investigation of the XRD interlayer spacing with different cations under controlled relative humidity could also shed more light on this topic. Petrograhical work including modal analysis of thin sections could estimate the degree of weathering and the source minerals of the weathering products.

Uniaxial compressive strength (UCS) tests to determine the strength of the kimberlite could not provide reproducible results. As an alternative, future work could investigate utilising the Block Punch Index (BPI) test. This test has been shown to be more applicable for clay bearing rocks (Sulukcu and Ulusay, 2001) and it uses disc shaped specimens in the point load testing frame. The UCS can be derived more precisely from the BPI result. It would be especially informative to test whether the strength of the rock increases with potassium treatment.

Other future work could include standardisation of weathering tests especially in terms of the particle size, experimental setup, weathering media and weathering output. This study found that milling is not required to evaluate the weathering behaviour of kimberlite.

Repeating some of the test work in this thesis in a stirred reactor, generating fresh surfaces continiously could also prove valuable. Especially for accelerated weathering e.g. cupric medium, concentration and temperature tests.

The influence of organic solvents on the swelling and collapsing of clays and kimberlite weathering is currently being investigated.

This study just started to investigate the mechanism of cation exchange and reaction kinetics. Future work to create a better understanding of the fundamental mechanisms should be performed. The suggestion that cation identity affects the microcrack surface energy should be examined to create a better understanding of the factors determining weathering.

Quantitative modelling can now be attempted incorporating the variables and knowledge generated in this study. The variables that should be included in experimental design are

171

smectite, CEC, weathering medium (cation, concentration, temperature), and particle size. The cation information can be incorporated into the modelling by utilising the ionic potential (valence and cation radius), as this showed correlation with weathering results. The trivalent cations and Cu^{2+}, Li^+ and Fe^{2+} however did not fit this correlation. The ionic potential data of these cations can be used as a first approximation or alternatively the ionic potential can be adjusted (corrected) to better fit the results obtained in this study.

9   CONCLUSION

XRD ANALYSIS

This study showed that XRD analysis of clay-containing ores such as kimberlite should include the sub treatments namely glycol and heat treatment to allow for more accurate identification of the clay minerals. The results should be critically reviewed before acceptance as correct and accurate. Verification can be performed by analysis of the same sample at different institutions and by performing sub treatments as discussed by Bühmann (1998) to ensure correct peak identification. Investigation of the ore by an experienced geologist will improve the overall understanding of the mineralogy. It is especially important to evaluate the results at overlapping peak positions e.g. smectite and chlorite (6.2º 2θ or d value of ~14.1 Å). The extent of errors in the estimated phase percentages can be up to 40 % and therefore special care should be taken in choosing appropriate institutions for analysis and evaluation of results.

The XRD interlayer spacing was investigated to gain more information on the swelling of clays. In the presence of potassium the interlayer spacing collapses to ~ 12 Å. The interlayer spacing of copper-weathered kimberlite as a function of time shows the increase in the interlayer spacing (to 14.5 Å), reaches the maximum after seven days and then stays constant up to thirty days. The interlayer spacing and the severity of weathering are not in correlation with cation weathering results. The interlayer spacing at relative humidity is shown by Ferrage *et al* (2005) as a two water layer system for Ca^{2+} and Mg^{2+}, a one water layer spacing for Na^+ and Li^+ and a zero water layer spacing for K^+. This agrees well with the observed spacings. It is suggested that is not only swelling that determines the weathering behaviour. The type of clay minerals, layer charge and cation properties influence weathering. When considering the Griffith-style of brittle material fracture, it depends on the defect length, applied stress and surface tension. The defect length depends on the kimberlite structure and is therefore not changed by the weathering solution. The stress is applied by swelling, which is little effected by cation identity. Therefore it is assumed that the cation identity influences the surface energy of the crack by adsorption on the crack surface.

SMECTITE CONTENT

It is concluded from this study that the weathering behaviour of kimberlite ores is directly affected by the mineralogy and specifically the swelling clay content. Kimberlites that contain no or very little swelling clay are not prone to weathering under any conditions. As the swelling clay content (smectite and vermiculite) increases the ore becomes more prone to weathering. Ores that contain around 30 % swelling clay may show slow weathering in distilled water but have the ability to weather rapidly in the presence of cations.

CATION EXCHANGE CAPACITY

The cation exchange capacity is a very useful parameter that correlates with the swelling clay content and can be used to predict kimberlite weathering behaviour. CEC might actually be preferred to the swelling clay content as XRD analysis is a cumbersome and expensive procedure in contrast to CEC, which can be determined easily.

AGGLOMERATION TEST

The agglomeration test is also shown as a simple test that gives an indication of an ore's 'stickiness'. Results show that heat treatment before wetting for a constant time, is required for improved results.

PRESENCE OF CATIONS IN WEATHERING MEDIUM

It is suggested by this study that the influence of the cations depends on a combination of cation charge and effective ionic radius (ionic potential), as well as the mechanism of cation absorption. Correlation between weathering results and ionic potential are good for all the cations except trivalent cations. Fe^{3+} and Al^{3+} have been shown to form hydroxy species in the interlayer and therefore are expected to behave differently. It has also been shown that the adsorption of Cu^{2+}, Fe^{2+} and Li^+ is not confined to the interlayer and therefore should influence the observed weathering. The type of smectite and layer charge also influences the effect of cations. If the original cations in the kimberlite are replaced by more 'active' cations, this will cause an increase in the observed weathering behaviour. The actual effect of some cations on accelerated weathering (from most to least aggressive) was found as follows: $Cu^{2+} > Li^+ > Fe^{2+} > Ca^{2+} > Fe^{3+} > Mg^{2+}$. Potassium was found to decelerate the weathering process. Li^+ increased the cumulative % passing 17.5 mm to 67 %, Fe^{2+} to 66 %, Ca^{2+} to 58 %, Fe^{3+} to 47 % and Mg^{2+} to 42 %. The weathering results did not show correlation with the XRD interlayer spacing.

CONCENTRATION OF CATIONS AND TIME OF WEATHERING

The weathering acceleration properties of copper show potential as the basis of a kimberlite processing, as treatment in a 0.4 M cupric solution causes breakdown of 25 mm kimberlite particles to 90 % passing 4 mm in 6 days. The concentration of the cation used for acceleration was shown to be a critical parameter as is the time allowed for weathering. The concentration was tested over a 0.005 M to 0.4 M interval and still showed improved weathering behaviour at 0.4 M. The time dependence tests at 0.5 M show very rapid weathering in the first 24 hours, with 85 % of the overall weathering obtained over thirty days taking place in the first 24 hours.

TEMPERATURE

Temperature tests were performed in a magnesium chloride medium and showed promising results. Weathering at 40 °C increased the cumulative % passing 17.5 mm by 25 % compared to room temperature. The results obtained with increased temperature are comparable with accelerated weathering obtained by the addition of a cation to the weathering medium.

KINETIC EVALUATION OF CATION EXCHANGE

The kinetics of cation exchange was investigated with a copper weathering medium at different concentrations. The data was fitted to the simple n^{th}-order kinetic equation to determine the apparent reaction order and rate constants utilising curve fitting and representing the data graphically. The apparent reaction order is between 1 and 3.5 depending on the concentration. The two methods used for interpreting the data correlate well. The apparent reaction order shows a dependence on initial copper concentration which is unexpected. The kinetics of cation exchange was repeated with a potassium weathering solution on a different kimberlite and again utilised the two methods of data interpretation. The apparent reaction order for potassium is between 1 and 2.2. The data cannot be correlated directly with copper data as different concentrations and types of kimberlites were utilised. It is shown that potassium exchange is more rapid in agreement with its higher mobility data. Both these data sets equilibrium values were plotted and fits the Langmuir conditions.

174

ANIONS

It is shown that the type of anion used does not influence kimberlite weathering. The type of anion can however influence the solubility and complexation of cations.

PARTICLE SIZE

Particle size did not show an effect on weathering in this case.

REPEATABILITY OF RESULTS

It is shown by triplicate tests that the size distribution weathering results consistently fell in a 7 % range. Standard deviation is always smaller than 3.8 % and the largest difference between 95 % confidence upper and lower limits are 18 %.

SLAKE DURABILITY TESTS

It is shown that slake durability tests is an alternative weathering testing method that provides the option of accelerating the weathering process due to the addition of the mechanical effect.

INDUSTRIAL APPLICATION

These results will firstly create a better understanding of the kimberlite weathering mechanism and how kimberlite might behave. It can be used in modelling, design and optimisation. The understanding is also used to prevent or decelerate weathering in an attempt to create underground tunnel wall stability and potassium (and other chemicals) show the potential of providing integrity to kimberlite. On the other hand using accelerated kimberlite weathering as a processing option is currently being investigated.

10   REFERENCES

Anderson, M.A., Bertsch, P.M., Miller, W.P., 1989, Exchange and apparent fixation of lithium in selected soils and clay minerals, Soil Science, Vol 148, No 1, p.p. 46 – 52.

Badreddine, R., Le Dred, R., Prost, R., 2002, Far infrared study of K^+, Rb^+ and Cs^+ during their exchange with Na^+ and Ca^{2+} in vermiculite, Clay Minerals, Vol 37, p.p. 71-81.

Bartlett, P.J., 1994, Geology of the Premier Diamond Pipe, XVTH CMMI Congress, South African Institute of Mining and Metallurgy, Vol 3, p.p. 201-213.

Belver C., Bonares-Munoz, M.A., Vicente M.A., 2004, Fe-saponite pillared and impregnated catalysts. I. Preparation and characterisation, Applied Catalysis B Environmental, Vol 50, Issue 2, p.p. 101-112.

Bland, W., Rolls, D., 1998, Weathering: An introduction to the scientific principles, Arnold Publishers.

Bond, F.C., 1954, Crushing and Grinding calculations, Canadian Mining and Metallurgical Bulletin, No 507, p.p. 466-472.

Brady, N.C., Weil, R.R., 1999, The nature and properties of soils, twelfth edition, Prentice Hall.

Brindly, G.W., 1955, Clays and Clay Technology, Division of Mines, Department of Natural Resources, Bulletin 169, p.p. 119 – 129.

Bruggenwert, M.G.M., Kamphorst, A., 1982, Survey of experimental information on cation exchange in soil systems, In Bolt, G.H., Soil Chemistry, B. Physico-Chemical Models, Elsevier, Amsterdam, p.p. 141 – 203.

Bühmann, D., 1998, Clay Workshop, The mineralogical Association of South Africa, Council for Geoscience.

Carson, C.D., Dixon, J.B., 1972, Potassium selectivity in certain montmorillonitic soil clays, Soil Science Society American Proceedings, Vol 36, p.p. 838 – 843.

Cases, J.M., Bérend, I., Francois, M., Uriot, J.P., Michot, L.J., Thomas, F., 1997, Mechanism of adsorption and desorption of water vapour by homoionic montmorillonite: 3. The Mg^{2+}, Ca^{2+}, Sr^{2+} and Ba^{2+} exchanged forms, Clays and Clay Minerals 45, no 1, p.p. 8 – 22.

Clark, I.H., 1982, The weathering of Venetia kimberlites after 1, 2, 4 and 6 months respectively, De Beers Research Laboratory, Report no. DRL 82/11/5 and DRL 82/12/3 and DRL 83/2/15 and DRL 83/6/1.

Czimerova, A., Jankovic, L., Bujdak, J., 2004, Effect of the exchangeable cations on the spectral properties of methylene blue in clay dispersions, Journal of colloid and interface science, Vol 274, p.p. 126 – 132.

Dahiya, S., Shanwal, A.V., Hegde, A.G., 2005, Studies on the sorption and desorption characteristics of Zn(II) on the surface soils of nuclear power plant sites in India using a radiotracer technique, Chemosphere, Volume 60, p.p. 1253-1261.

Dawson, J.B., 1980, Kimberlites and their Xenoliths, Springer-Verlag, Berlin Heidelberg New York.

Dawson, J.B. and Smith, J.V., 1977, The MARID (mica-amphibole-rutile-ilmenite-diopside) suite of xenoliths in kimberlite, Geochim Cosmochim Acta 41, p.p. 309-323.

Doorgapershad, A., Barnett, M., Twiggs, C., Martin, J., Millonig, L., Zenglein, R., Klemd, R., Barnett, W.P., Barton, J.R., September 2003, Recent studies of geology in and around Venetia kimberlite pipes, Limpopo belt, South Africa, South African Journal of Geology, Volume 106, p.p. 103 – 108.

Eberl, D.D., 1980, Alkali cation selectivity and fixation by clay minerals, Clays and Clay minerals, Vol 28, No 3, p.p. 161-172.

El-Batouti, M., Sadek, O.M., Assaad, F.F., 2003, Kinetics and thermodynamics studies of copper exchange on Na-montmorillonite clay mineral, Journal of Colloid and Interface Science 259, p.p. 223-227.

Erguler, Z.A., Ulusay, R., 2003, A simple test and predictive models for assessing swell potential of Ankara (Turkey) clay, Engineering geology 67, p.p. 331-352.

Ferrage, E., Lanson, B., Sakharov, B.A., Drits, V.A., 2005, Investigation of smectite hydration properties by modeling experimental X-ray diffraction patters: Part I. Montmorillonite hydration properties, American Mineralogist, Vol 90, p.p. 1358–1374.

Gökceoğlu, C., Ulusay, R., Sönmez, H., 2000, Factors affecting the durability of selected weak and clay-bearing rocks from Turkey, with particular emphasis on the influence of the number of drying and wetting cycles, Engineering Geology 57, p.p. 215–237.

Goldich, S.S., 1938, A study of rock weathering, Journal of Geology 46, p.p. 17-58.

Greenwood, N.N., Earnshaw, A., 1997, Chemistry of the elements, Second edition, Butterworth-Heinemann.

Grim, R.E., 1968, Clay Mineralogy, Mcgraw Hill.

Harlow, G.E., 1998, The nature of diamonds, Cambridge University Press in association with the Americal museum of Natural History.

Harnois, L., 1988, The CIW index: A new chemical index of weathering, Sediment. Geology, Vol 55,p.p. 319 – 322.

Herbert, H.J., Moog, H.C., 1999, Cation exchange, interlayer spacing and water content of MX-80 bentonite in high molar saline solutions, Engineering Geology 54, p.p. 55-65.

Hodgson, I.M.J., 1981, Hydrothermal Alteration of Kimberlite, Imperial College of Science and Technology (LONDON SW7 2BP), Thesis in fulfilment of degree of Doctor of Philosophy, Department of Mineral Resource Engineering.

Hofstetter, T.B., Schwarzebach, R.P., and Haderlein, S.B., 2003, Environ. Sci. Technol., Volume 37, p.p. 519 – 528.

Holtz, W.G., Gibbs, H., 1956, Engineering properties of expansive clays, Transactions of the Americal Society of Civil Engineers, volume 121, p.p. 641–677.

Hopwood, J.S., Webb, S.M., 1975, The accelerated weathering of kimberlite, De Beers Research Laboratory (DRL), Report no. DRL 75/9/2.

Klein, C., Hurlbut, C.S., 1993, Manual of Mineralogy, twenty-first edition, John Wiley and Sons.

Lide, D.R., Frederikse, H.P.R., 1994, CRC Handbook of Chemistry and Physics, 75 th edition, CRC Press.

Madsen, F.T., Müller-Vonmoos, M., 1989, The swelling behaviour of clays, Applied Clay Science 4, p.p. 143-156, Elsevier Science Publishers.

Malla, P.B., Douglas, L.A., 1985, Identification of expanding layer silicates: Layer charge vs. expansion properties, Proceedings of the International Clay Conference, Denver.

Mitchell, R.H., 1986, Kimberlites: Mineralogy, Geochemistry and Petrology, New York Plenum Press.

Moore, D. M., Reynolds, R.C., 1989, X-Ray Diffraction and the identification and analysis of Clay minerals, Oxford University Press.

Morkel, J., Bronkhorst, L., 2005, Developing a standard agglomeration test to predict the smectite content of kimberlitic ores, De Beers Technical Services, Technical Note 2005-11-09.

Napier-Munn, T.J., Morrell, S., Morrison, R.D., and Kojovic, T., 1996, Mineral Comminution circuits: Their operation and optimization, Julius Kruttschnitt Mineral Research Centre, University of Queensland.

Nesbitt, H.W. and Young G,M., 1982, Early Proterozoic climates and plate motions inferred from major element chemistry of lutites, Nature 299:p.p. 715 – 717.

Newman, A.C.D., 1987, Chemistry of clays and clay minerals, Longman Scientific & Technical.

Ollier, C.D., 1965, Some features of granite weathering in Australia. Zeitschrift fur Geomorphologie 9, p.p. 285-304.

Pettijohn F.J., 1941, Persistence of heavy minerals and geologic age, Journal of Geology 49, p.p. 610-625.

Poppe, L.J., Paskevich, J.C., Hathaway, J.C., Blackwood, D.S., 2001, A Laboratory Manual for X-Ray Powder Diffraction, http://pubs.usgs.gov/of/of01-041/.

Parker, A., 1970, An index of weathering for silicate rocks, Geological Magazine, Vol 107, No 6, p.p.501–504 (AIS no. 550)

Prost, R., 1981, Near Infrared properties of water in Na-Hectorite pastes, International Clay Conference, Published as Developments in Sedimentology, Vol. 35, Elsevier.

Richens, D.T., 1997, The Chemistry of Aqua Ions: Synthesis, structure and reactivity, John Wiley and Sons, United Kingdom.

Rytwo, G., Banin, A., Nir, S., 1996, Exchange reactions in the Ca-Mg-Na montmorillonite system, Clay Minerals, Vol. 44, No 2, p.p. 276-285.

Saydam, S., Onargan, T. and Deliormanli, A.H., 2003, The relationship between slake durability and geomechanical properties for upper rocks of Beypazari trona bed in Ankara, Turkey., South African Institute of Mining and Metallurgy, Volume 103, No. 4, p.p. 241-252.

Schoen, R., Foord, E., Wagner, D., 1973, Quantitative analysis of clays: Problems, achievements and outlook, Proceedings of the international clay conference, Division de Ciencias C.S.I.C., Madrid, p.p. 787-796.

Shannon, R.D., 1976, Revised effective ionic radii and systematic studies of interatomic distances in halides and chalcogenides, Acta Cryst, A32, p.p. 751–767.

Skinner, E.M.W., Clement, C.R., 1979, Mineralogical classification of southern African kimberlites, in Boyd, F.R., Meyer, H.O.A., eds., Kimberlites, Diatremes and Diamonds: Their geology, petrology and Geochemistry, American Geophysical Union, Washington.

Soil Science Society of South Africa, 1990, Handbook of standard soil testing methods for advisory purposes.

Stadler, M., Schindler, P.W., 1993, Modelling of H^+ and Cu^{2+} adsorption of calcium montmorillonite, Clays and Clay Mineralogy, Volume 41, p.p. 288-296.

Stephens, A.R., 1975, Quantitative analysis of kimberlite weathering, De Beers Research Laboratory (DRL), Report no. DRL 75/10/13.

Strawn, D.G., Palmer N.E., Furnare, L.J., Goodell, C., Amonette, J.E., Kukkadapu, R.K., 2004, Copper sorption mechanisms on smectites, Clays and Clay Minerals, Vol 52, No 3, p.p. 321-333.

Sulukcu, S., Ulusay, R., Evaluation of the block punch index test with particular reference to the size effect, failure mechanism and its effectiveness in predicting rock strength, International Journal of Rock Mechanics and Mining Sciences 38, p.p. 1091–1111.

Tessier, D., Saiyouri, N., Hicher, P.Y., 2004, Experimental study of swelling in unsaturated compacted clays, Clay minerals 39, p.p. 469-479.

Thorez, J., 1975, Phyllosilicates and clay minerals, Editions G.Lelotte, B4820 Dison, Belgique.

Vietti, A, J, 1994, Clay – Water – Flocculant Interaction, De Beers Diamond Research Laboratory, Report no. E66/005/006.

Vogel, A., 1973, Seismiche Prospektion, Earth-Science Reviews, Volume 9, Issue 3, p.p. 281

Weaver, C.E., 1989, Clays, Muds and Shales, Elsevier, Amsterdam.

Wilson, M.G.C., Anhaeusser, C.R., 1998, The mineral resources of South Africa, Sixth Edition, Handbook 16, Council for Geoscience, p.p. 232-258.

Wu, G., Li, L.. Y., 1998, Modelling of heavy metal migration in sand / bentonite and the leachate pH effect, Journal of Contaminant Hydrology 33, p.p., 313–336.

APPENDIX A: Specification on XRD work done at University of Pretoria and Mintek

The sample was prepared using standard Siemens sample holders and the powder was pressed into the holder using a glass slide.

TABLE 1: Instrument and data collection parameters

	Mintek	University of Pretoria
Instrument	Siemens D-500	Siemens D-501
Radiation	Cu *Kα*	Cu *Kα* (1.5418 Å)
Temperature	25°C	25°C
Specimen	Flat-plate, rotating (30 RPM)	flat-plate, rotating (30 RPM)
Power Setting	40 kV, 40 mA	40 kV, 40 mA
Soller slits	2°	2° (diffracted beam side)
Divergence slits	1°	1°
Receiving slits	0.05°	0.05°
Monochromator	Secondary, graphite	secondary, graphite
Detector	Scintillation counter	scintillation counter
Range of 2θ	5 – 80 ° 2θ	4 – 70 ° 2θ
Step width	0.02 ° 2θ	0.04° 2θ
Time per step	1 s	1.5s

APPENDIX B: ORIGINAL XRD DATA

B1: XRD of Dutoitspan

B2: XRD of Geluk Wes

B3: XRD of Koffiefontein

B4: XRD of Cullinan TKB

B5: XRD of Wesselton

B6: XRD of Venetia

B1:   XRD of Dutoitspan

DuToitspan kimberlite (side mounted) - File: DuToitspan.raw - Type: 2Th/Th locked - Start: 5.000 ° - E
Operations: Import
44-1447 (N) - Antigorite - Mg3Si2O5(OH)4 - Y: 20.83 % - d x by: 1. - WL: 1.5406 - Monoclinic - I/Ic Us
05-0586 (*) - Calcite, syn - CaCO3 - Y: 50.00 % - d x by: 1. - WL: 1.5406 - Rhombohedral - I/Ic PDF 2
74-1687 (C) - Dolomite - CaMg(CO3)2 - Y: 18.75 % - d x by: 1. - WL: 1.5406 - Rhombohedral - I/Ic P
33-0664 (*) - Hematite, syn - Fe2O3 - Y: 14.58 % - d x by: 1. - WL: 1.5406 - Rhombohedral - I/Ic PDF
19-0629 (*) - Magnetite, syn - Fe+2Fe2+3O4 - Y: 28.21 % - d x by: 1. - WL: 1.5406 - Cubic - I/Ic PDF
83-1817 (C) - Diopside - CaMgSi2O6 - Y: 47.83 % - d x by: 1. - WL: 1.5406 - Monoclinic - I/Ic PDF 1.

12-0204 (D) - Montmorillonite - Nax(Al,Mg)2Si4O10(OH)2·zH2O - Y: 28.93 % - d x by: 1. - WL: 1.540
24-0867 (I) - Biotite-1M, syn - KMg3(Si3Al)O10(OH)2 - Y: 35.42 % - d x by: 1. - WL: 1.5406 - Monocli
10-0493 (I) - Phlogopite-2M1 - KMg3(Si3Al)O10(OH)2 - Y: 33.85 % - d x by: 1. - WL: 1.5406 - Monocl

Figure 1. XRD Scan by Mintek on Dutoitspan

B2:   XRD of Geluk Wes

Geluk-Wes kimberlite - File: GelukwesB.raw - Type: 2Th/Th locked - Start: 5.000 ° - End: 80.000 ° - S
Operations: Import
05-0586 (*) - Calcite, syn - CaCO3 - Y: 85.42 % - d x by: 1. - WL: 1.5406 - Rhombohedral - I/Ic PDF 2
74-1687 (C) - Dolomite - CaMg(CO3)2 - Y: 22.92 % - d x by: 1. - WL: 1.5406 - Rhombohedral - I/Ic P
33-0664 (*) - Hematite, syn - Fe2O3 - Y: 26.74 % - d x by: 1. - WL: 1.5406 - Rhombohedral - I/Ic PDF
11-0654 (D) - Diopside - CaMg(SiO3)2 - Y: 42.02 % - d x by: 1. - WL: 1.5406 - Monoclinic - I/Ic PDF 1
19-0926 (*) - Microcline, ordered - KAlSi3O8 - Y: 15.28 % - d x by: 1. - WL: 1.5406 - Triclinic -
19-0629 (*) - Magnetite, syn - Fe+2Fe2+3O4 - Y: 39.58 % - d x by: 1. - WL: 1.5406 - Cubic - I/Ic PDF

13-0259 (Q) - Montmorillonite-14A - Na0.3(Al,Mg)2Si4O10(OH)2·xH2O - Y: 79.17 % - d x by: 1. - WL:
24-0867 (I) - Biotite-1M, syn - KMg3(Si3Al)O10(OH)2 - Y: 40.10 % - d x by: 1. - WL: 1.5406 - Monocli
10-0393 (*) - Albite, disordered - Na(Si3Al)O8 - Y: 37.50 % - d x by: 1. - WL: 1.5406 - Triclinic -
09-0444 (N) - Lizardite-6T - Mg3Si2O5(OH)4 - Y: 27.47 % - d x by: 1. - WL: 1.5406 - Hexagonal -
85-2157 (C) - Tremolite - (Na0.11K0.04)(Na0.04Ca1.67Mn0.03Mg3.65Fe1.40Al0.21)((Si7.38Al0. - Y:
10-0493 (I) - Phlogopite-2M1 - KMg3(Si3Al)O10(OH)2 - Y: 32.12 % - d x by: 1. - WL: 1.5406 - Monocl

Figure 1. XRD Scan by Mintek on Geluk Wes

185
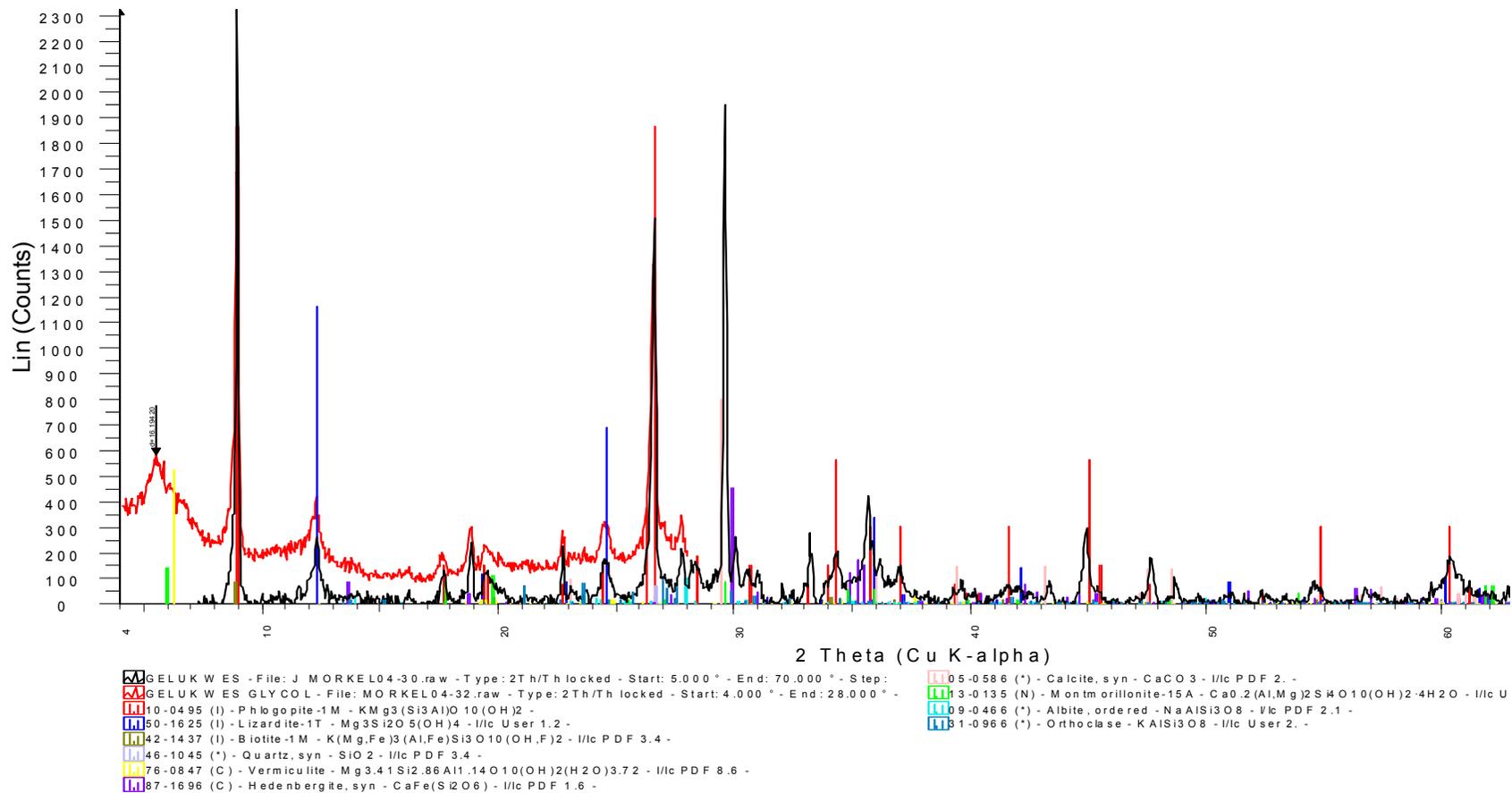
Figure 2. XRD Scan by University of Pretoria on Geluk Wes (Black shows air dry scan, red shows temperature treated scan)

B3:   XRD of Koffiefontein

Koffiefontein kimberlite - File: KoffiefonteinB.raw - Type: 2Th/Th locked - Start: 5.000 ° - End: 80.000
Operations: X Offset 0.050 | Import
05-0586 (*) - Calcite, syn - CaCO3 - Y: 19.96 % - d x by: 1. - WL: 1.5406 - Rhombohedral - I/Ic PDF 2
36-0426 (*) - Dolomite - CaMg(CO3)2 - Y: 16.67 % - d x by: 1. - WL: 1.5406 - Rhombohedral -
46-1045 (*) - Quartz, syn - SiO2 - Y: 14.59 % - d x by: 1. - WL: 1.5406 - Hexagonal - I/Ic PDF 3.4 -
29-1498 (Q) - Montmorillonite-15A - Na0.3(Al,Mg)2Si4O10(OH)2·4H2O - Y: 25.52 % - d x by: 1. - WL:
19-0926 (*) - Microcline, ordered - KAlSi3O8 - Y: 14.59 % - d x by: 1. - WL: 1.5406 - Triclinic -
24-0201 (I) - Augite - Ca(Fe,Mg)Si2O6 - Y: 27.08 % - d x by: 1. - WL: 1.5406 - Monoclinic - I/Ic PDF 0

19-0629 (*) - Magnetite, syn - Fe+2Fe2+3O4 - Y: 25.00 % - d x by: 1. - WL: 1.5406 - Cubic - I/Ic PDF
24-0867 (I) - Biotite-1M, syn - KMg3(Si3Al)O10(OH)2 - Y: 19.09 % - d x by: 1. - WL: 1.5406 - Monocli
44-1447 (N) - Antigorite - Mg3Si2O5(OH)4 - Y: 18.75 % - d x by: 1. - WL: 1.5406 - Monoclinic - I/Ic Us
10-0493 (I) - Phlogopite-2M1 - KMg3(Si3Al)O10(OH)2 - Y: 20.83 % - d x by: 1. - WL: 1.5406 - Monocl

Figure 1. XRD Scan by Mintek on Koffiefontein

187

Figure 2. XRD Scan by University of Pretoria on Koffiefontein (Black shows air dry scan, red shows temperature treated scan)

B4:   XRD of Cullinan TKB
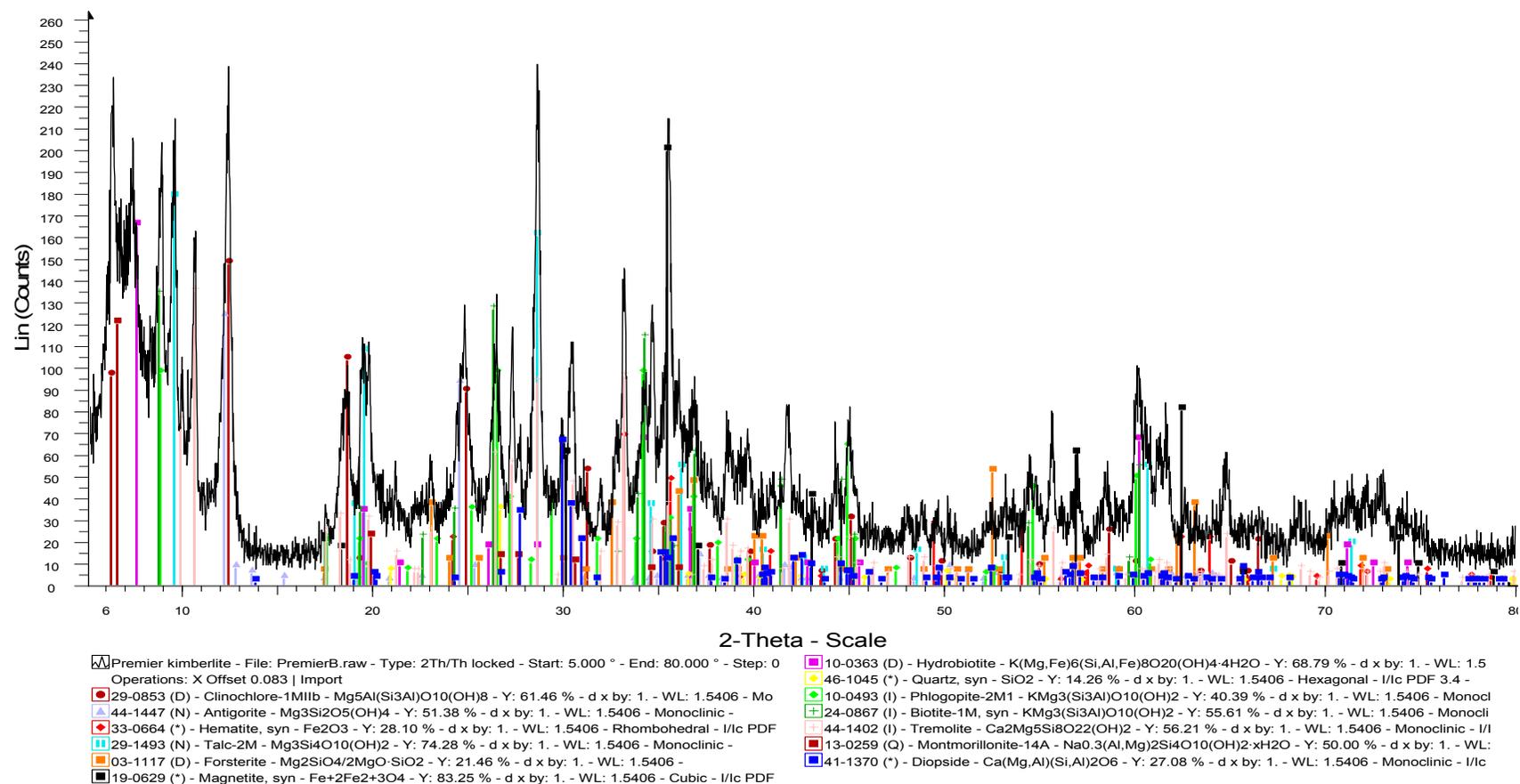
Figure 1. XRD Scan by Mintek on Cullinan TKB
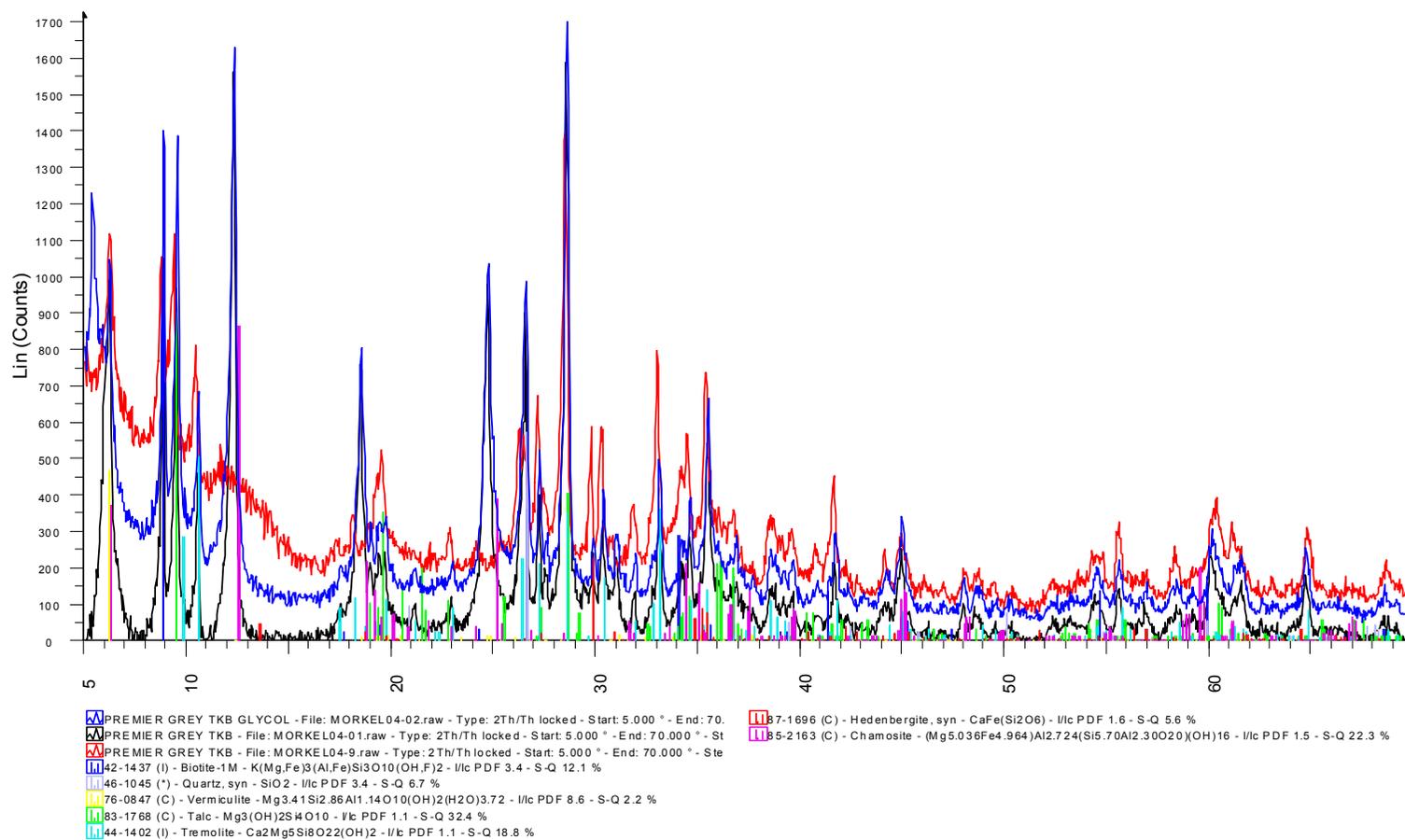
Figure 2. XRD Scan by University of Pretoria on Cullinan TKB (Black shows air dry scan, red shows temperature treated scan)

B5:   XRD of Wesselton
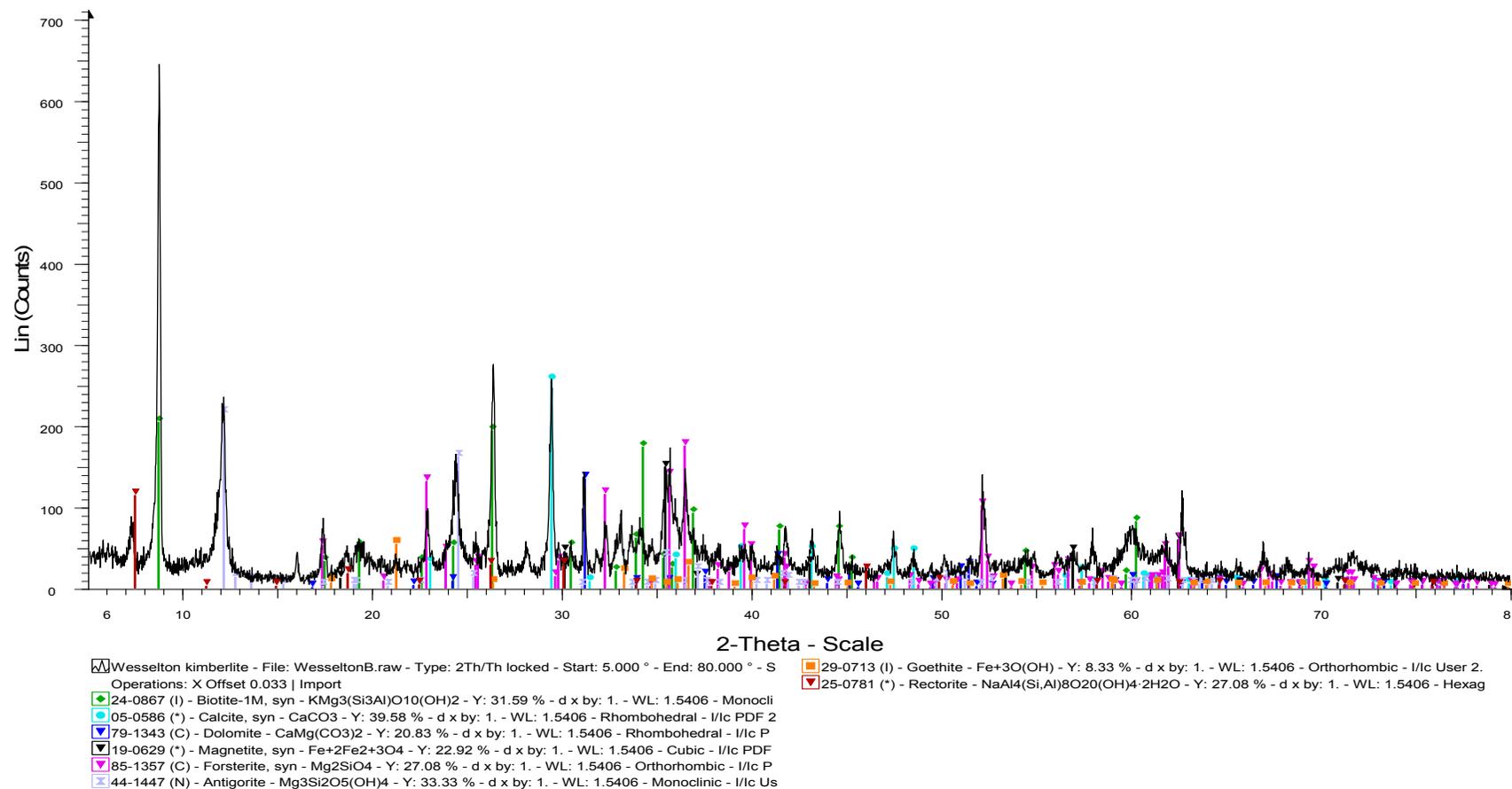
Figure 1. XRD Scan by Mintek on Wesselton
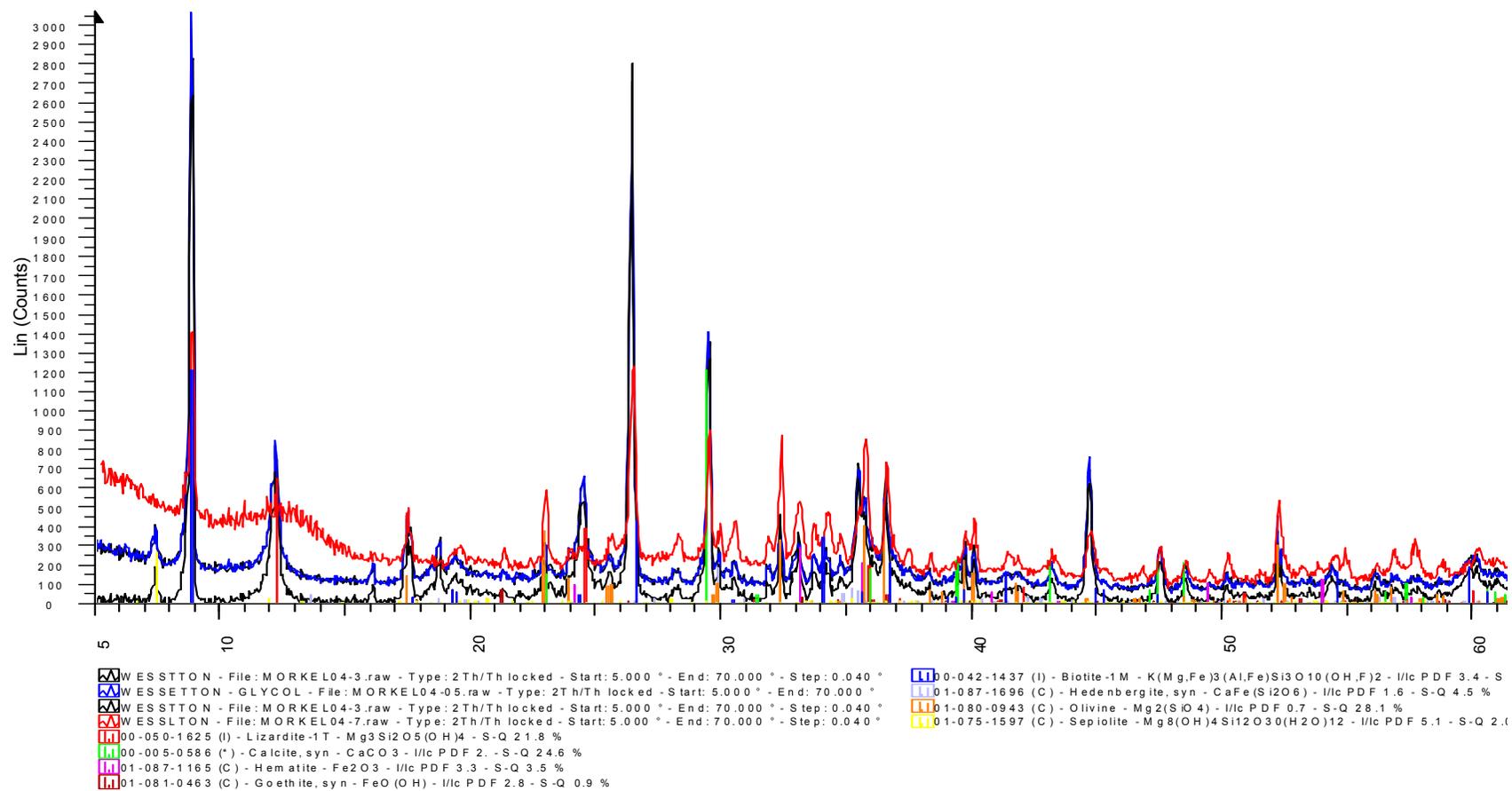
Figure 2. XRD Scan by University of Pretoria on Wesselton (Black shows air dry scan, red shows temperature treated scan)

B6   Venetia Kimberlites

B6.1   K1 Hypabyssal North East

Venetia K1 HYP NE - File: Venetia K1 HYP NE.raw - Type: 2Th/Th locked - Start: 5.000 ° - End: 80.000 ° - Step: 0.020 ° - Step time: 1. s - Temp.: 25 °C (Room) - Time Started: 0 s - 2-Theta: 5.000 ° - Theta: 2.5
Operations: Import
10-0493 (I) - Phlogopite-2M1 - KMg3(Si3Al)O10(OH)2 - Y: 35.25 % - d x by: 1. - WL: 1.5406 - Monoclinic -
44-1447 (N) - Antigorite - Mg3Si2O5(OH)4 - Y: 50.00 % - d x by: 1. - WL: 1.5406 - Monoclinic - I/Ic User 1.3 -
29-0853 (D) - Clinochlore-1MIIb - Mg5Al(Si3Al)O10(OH)8 - Y: 12.50 % - d x by: 1. - WL: 1.5406 - Monoclinic -
19-0629 (*) - Magnetite, syn - Fe+2Fe2+3O4 - Y: 33.33 % - d x by: 1. - WL: 1.5406 - Cubic - I/Ic PDF 4.9 -
05-0586 (*) - Calcite, syn - CaCO3 - Y: 75.00 % - d x by: 1. - WL: 1.5406 - Rhombohedral - I/Ic PDF 2. -

Figure 1. XRD Scan by Mintek on Venetia K1 Hypabyssal North East

B6.2   K1 Hypabyssal South
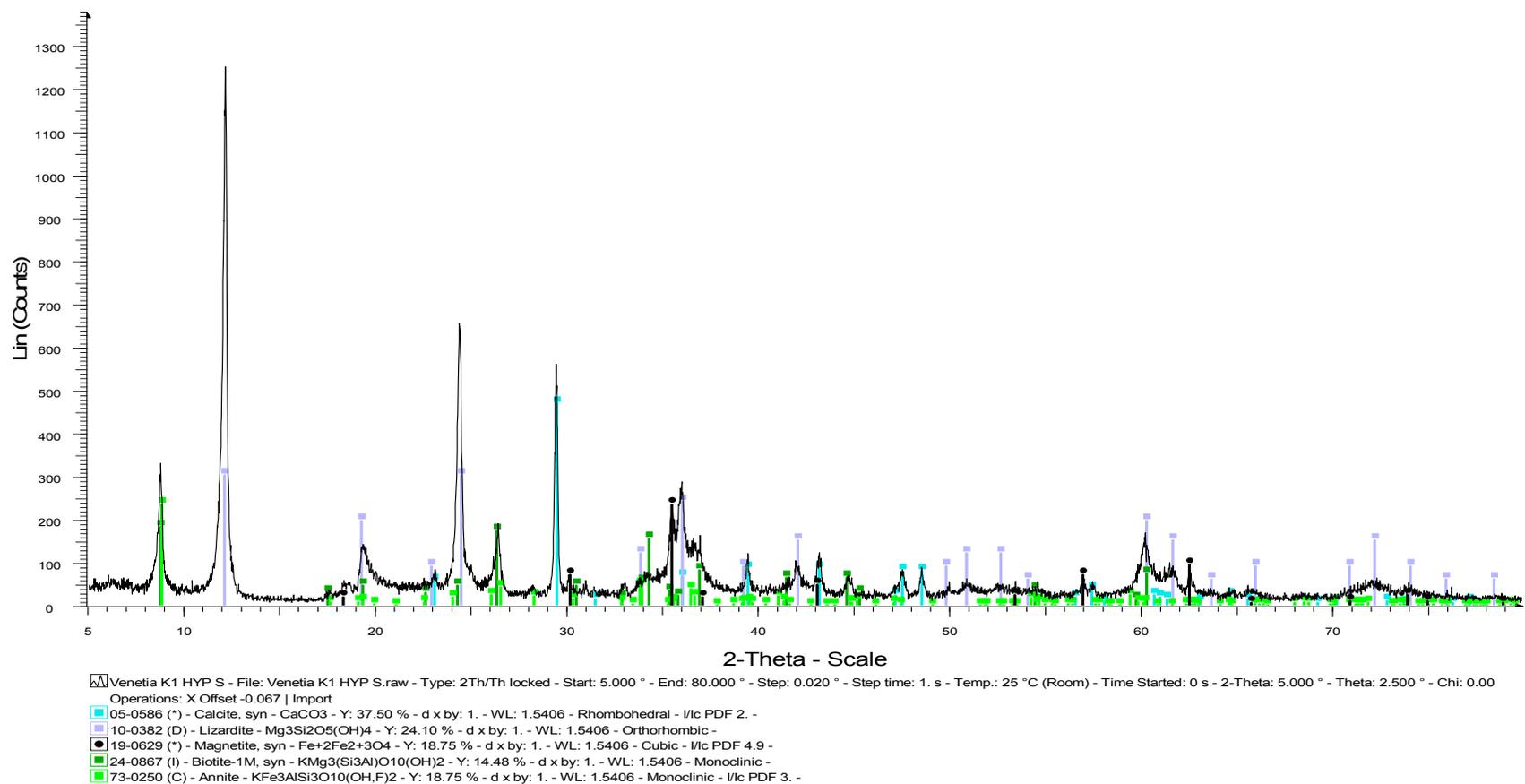
Figure 1. XRD Scan by Mintek on Venetia K1 Hypabyssal South

B6.3 K1 TKB East
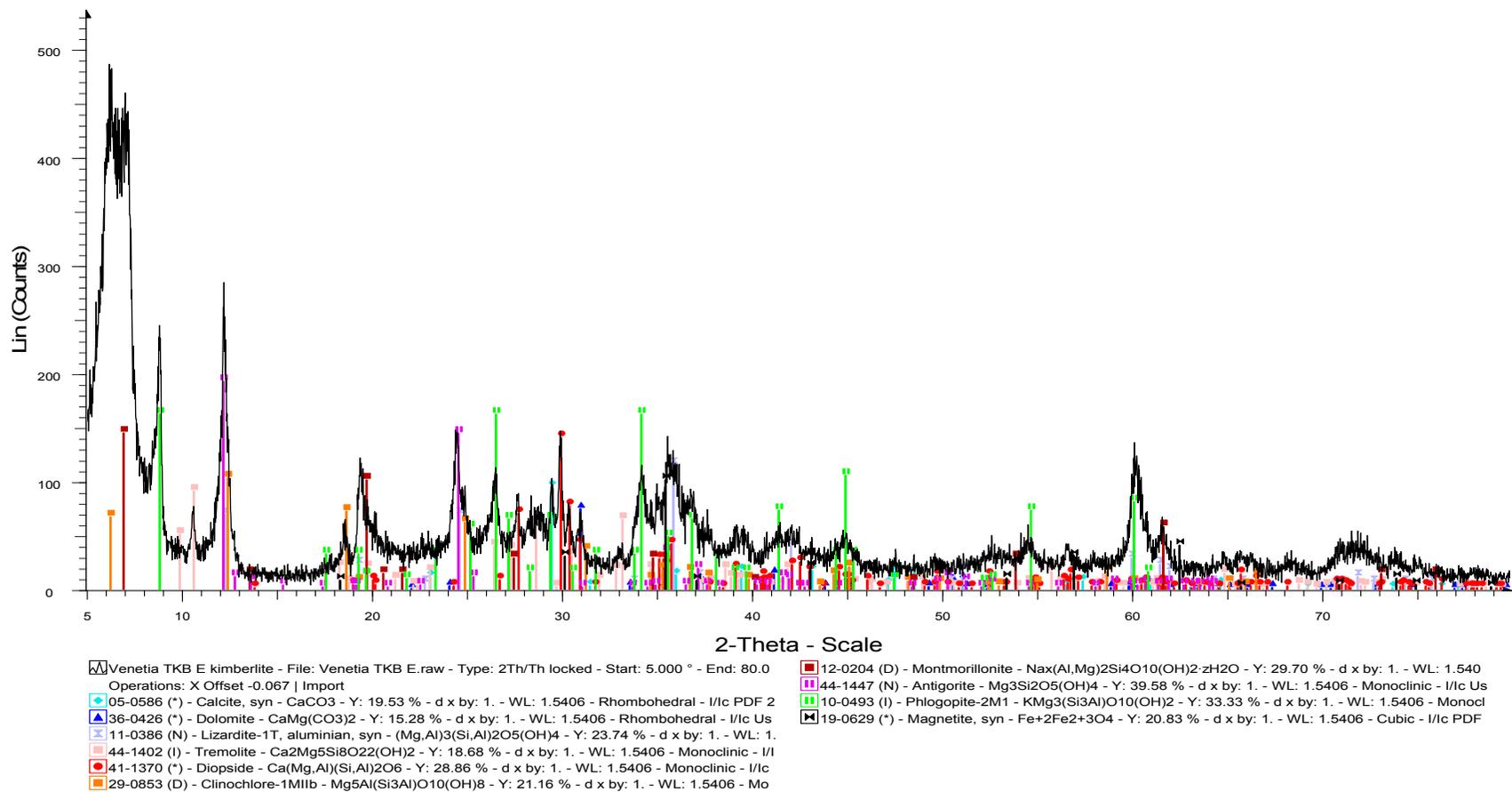
Figure 1. XRD Scan by Mintek on Venetia K1 TKB East

B6.4   K2 North East
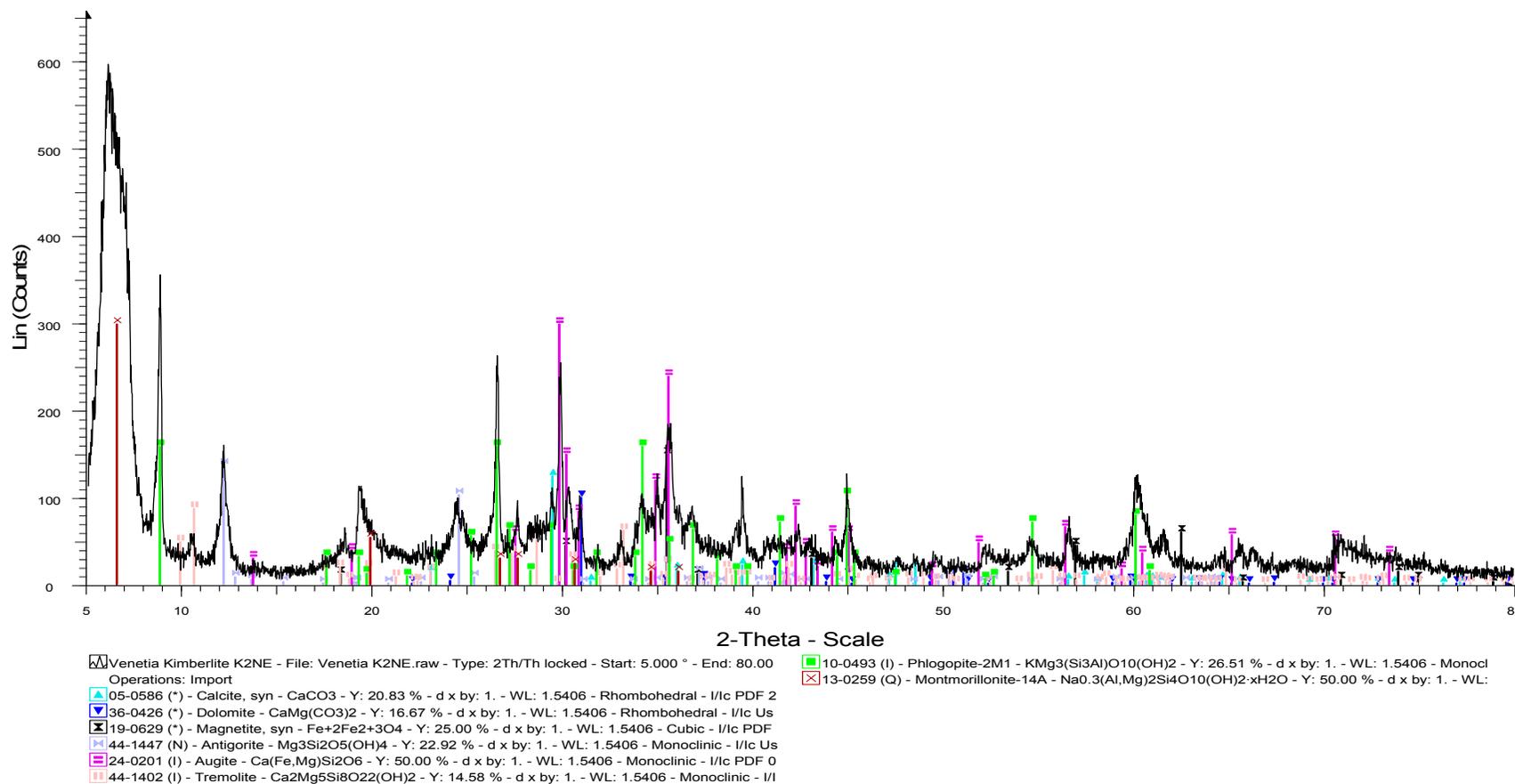
Figure 1. XRD Scan by Mintek on Venetia K2 North East

B6.5   K2 South
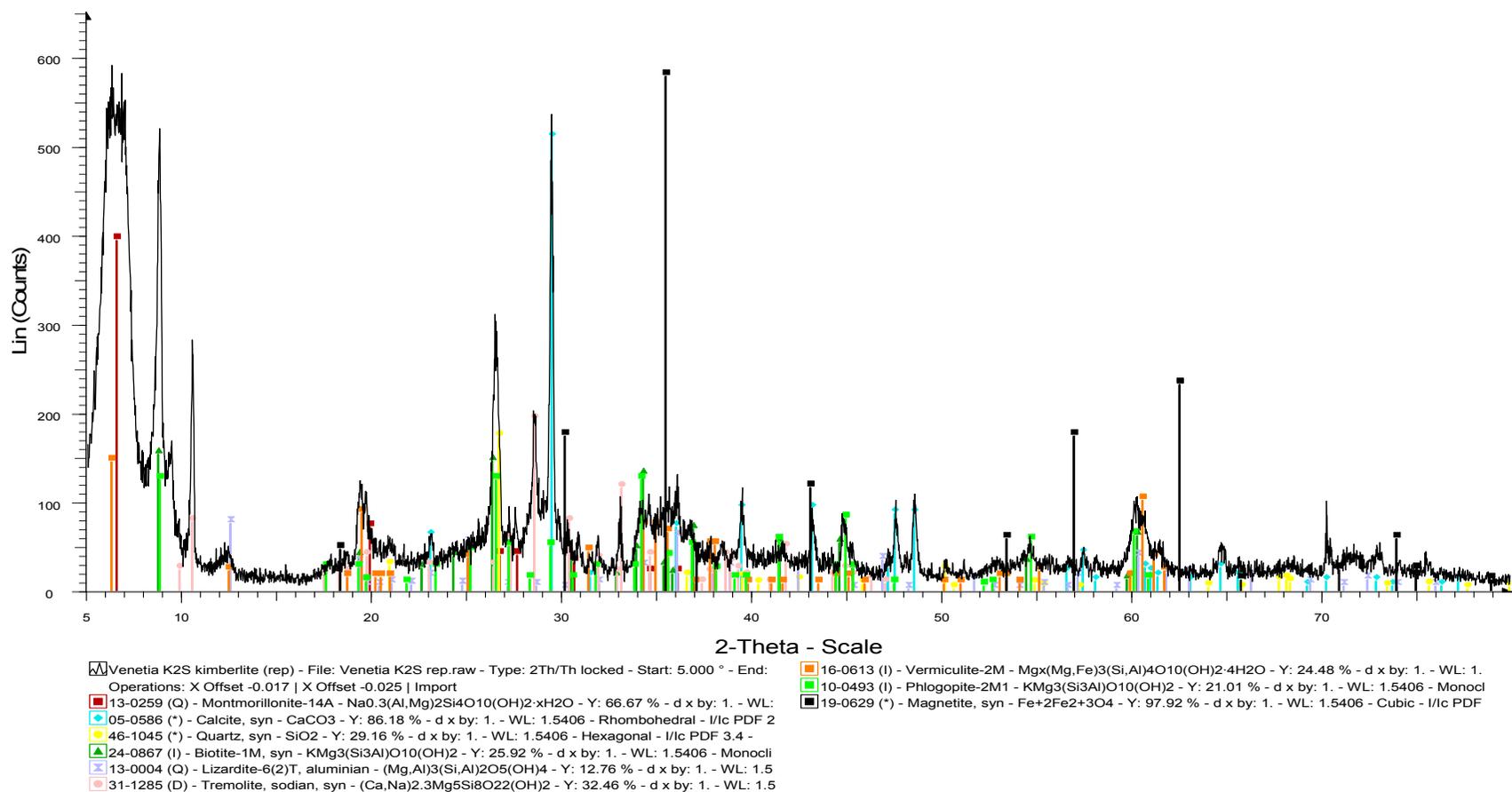
Figure 1. XRD Scan by Mintek on Venetia K2 South

197

B6.6   K2 West
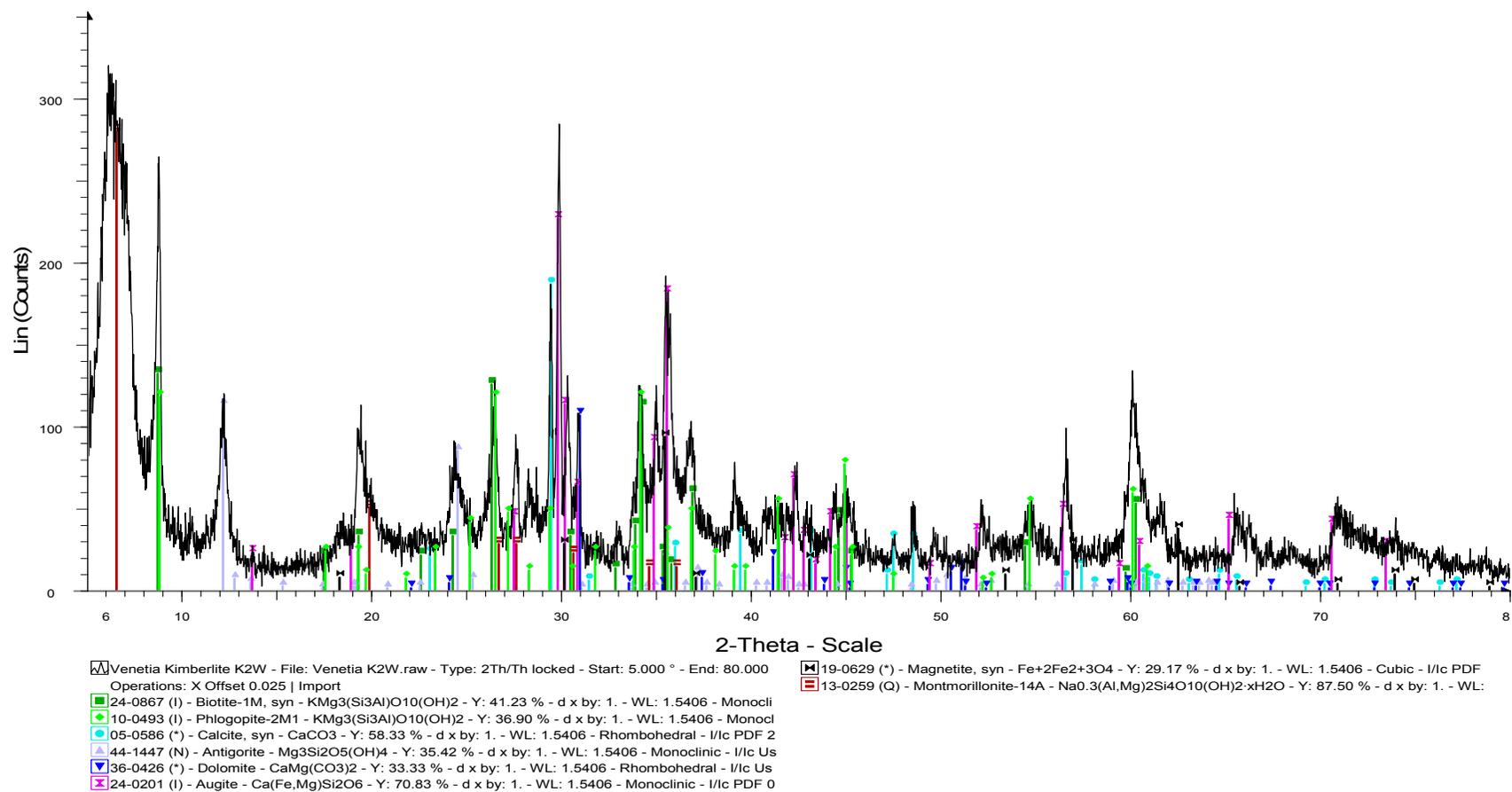
Figure 1. XRD Scan by Mintek on Venetia K2 West

B6.7   K8
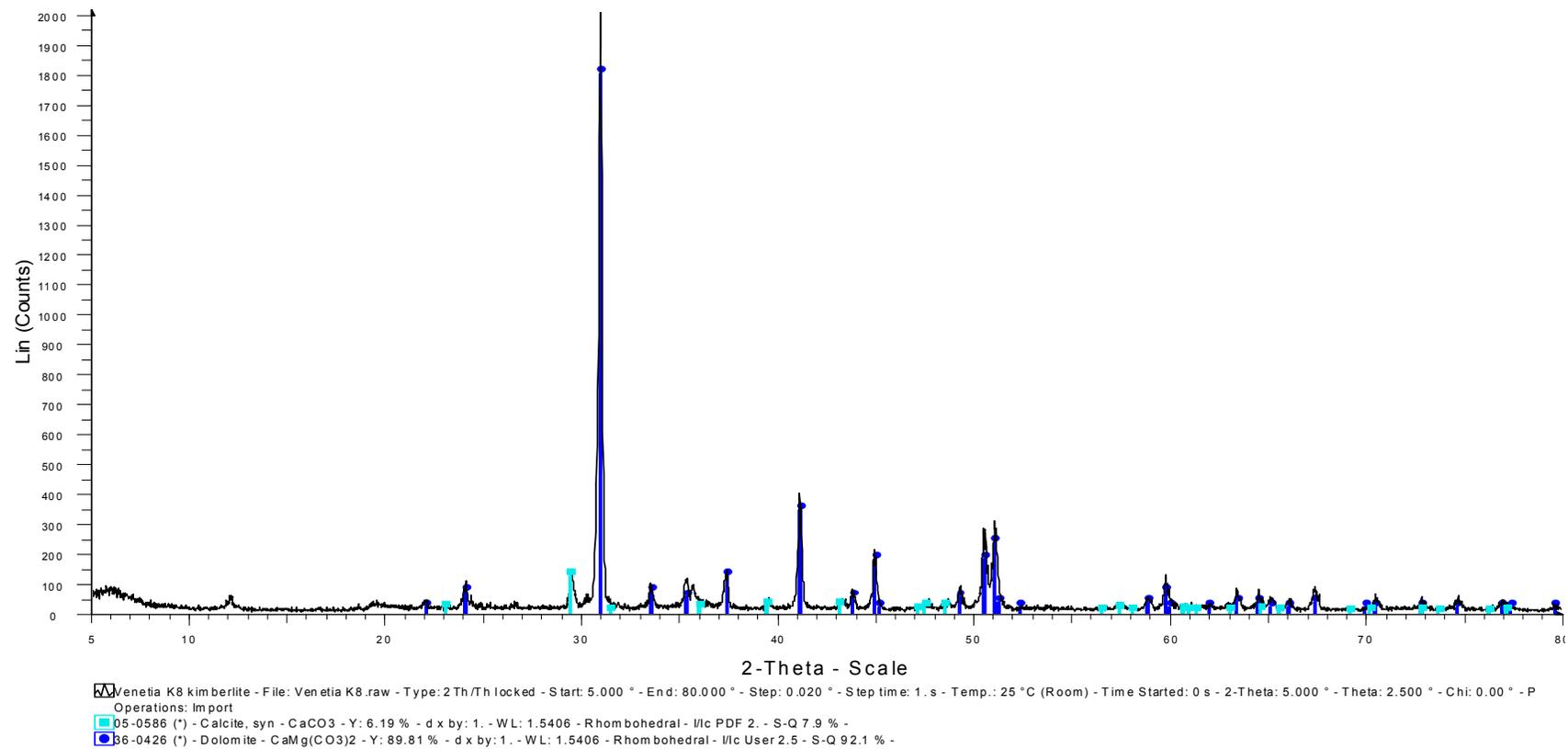
Figure 1. XRD Scan by Mintek on Venetia K8

B6.8   Red Kimberlite
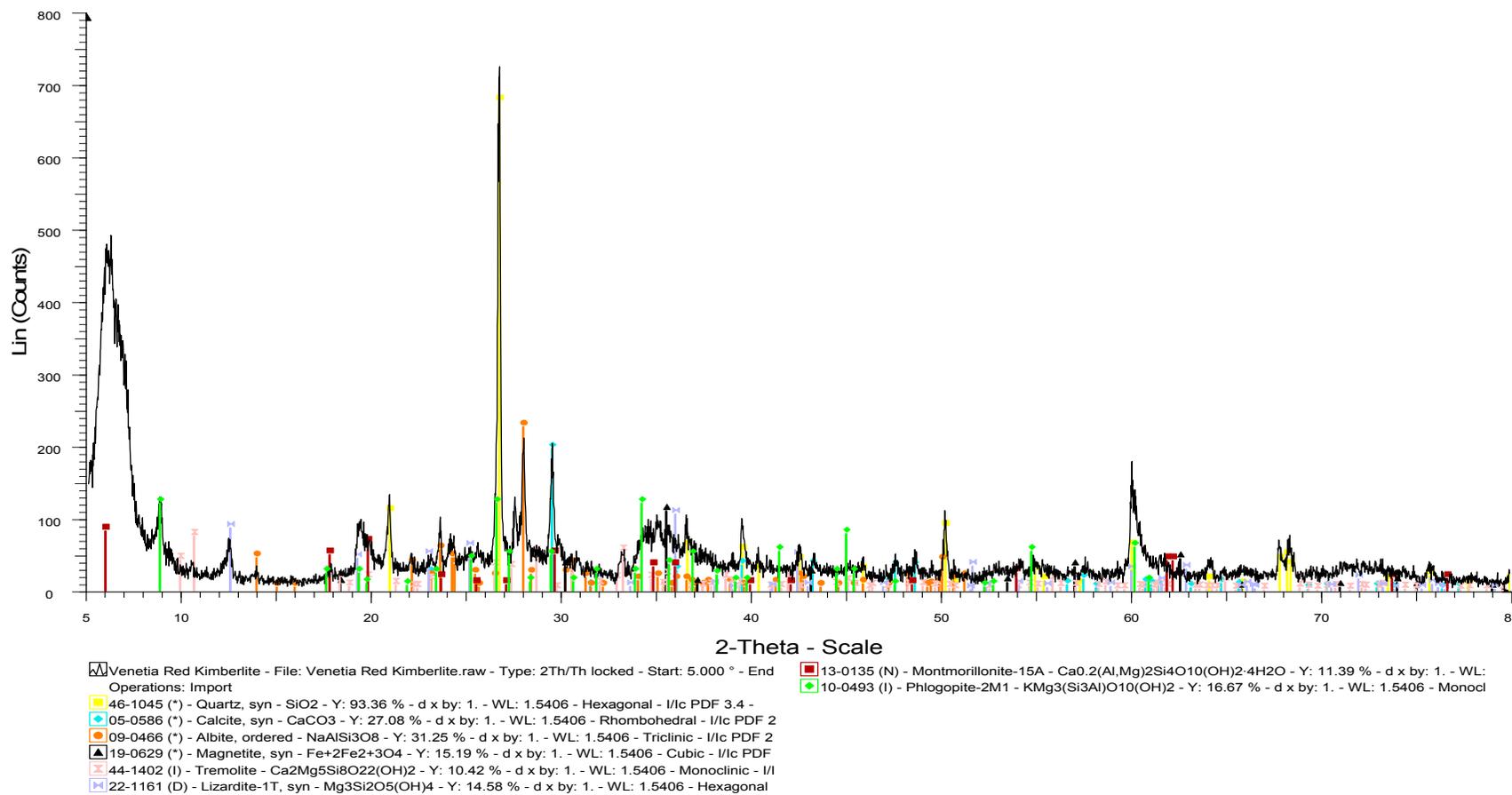
Figure 1. XRD Scan by Mintek on Venetia Red Kimberlite

200

APPENDIX C: SIZE DISTRIBUTION DATA

C1: Data of Dutoitspan

C2: Data of Geluk Wes

C3: Data of Koffiefontein

C4: Data of Cullinan TKB

C5: Data of Wesselton

C6: Data of Venetia

C1:   Data of Dutoitspan

C1.1   Standard Weathering test

Dutoitspan

Weathering Condition			Standard weathering test					
Weathering Time			0 Days			6 Days		
Min. size	Max. size	Ave size	Weight	% in fraction	Cum % passing	Weight	% in fraction	Cum % passing
-	+	μm	g			g		
26500	22400	24450	1237.00	81.74	100.00	905.21	61.21	100.00
22400	19000	20700	208.00	13.74	18.26	272.98	18.46	38.79
19000	16000	17500	31.80	2.10	4.52	87.92	5.95	20.33
16000	13200	14600	0.00	0.00	2.42	59.99	4.06	14.38
13200	11200	12200	8.10	0.54	2.42	21.02	1.42	10.33
11200	6700	8950	3.60	0.24	1.88	52.53	3.55	8.91
6700	4750	5725	2.70	0.18	1.65	25.56	1.73	5.35
4750	3350	4050	1.80	0.12	1.47	11.60	0.78	3.63
3350	2360	2855	1.00	0.07	1.35	5.77	0.39	2.84
2360	1180	1770	1.40	0.09	1.28	7.59	0.51	2.45
1180	850	1015	0.50	0.03	1.19	2.54	0.17	1.94
850	600	725	0.40	0.03	1.16	1.78	0.12	1.77
335	180	257.5	5.80	0.38	1.13	11.77	0.80	1.65
125	75	100	9.50	0.63	0.75	10.72	0.72	0.85
75	0	37.5	1.80	0.12	0.12	1.85	0.13	0.13
			1513.40			1478.83		

202

C1.2   Influence of cations on weathering: Monovalent cations

Dutoitspan

			Monovalent Cations								
Weathering Condition											
Weathering Time			0 Days			6 Days KCl			6 Days NaCl		
Min. size	Max. size	Ave size	Weight	% in fraction	Cum % passing	Weight	% in fraction	Cum % passing	Weight	% in fraction	Cum % passing
-	+	µm	g								
26500	22400	24450	1237.00	81.74	100.00	1054.80	72.25	100.00	811.10	55.75	100.00
22400	19000	20700	208.00	13.74	18.26	225.10	15.42	27.75	223.40	15.36	44.25
19000	16000	17500	31.80	2.10	4.52	77.32	5.30	12.34	109.70	7.54	28.90
16000	13200	14600	0.00	0.00	2.42	17.27	1.18	7.04	86.90	5.97	21.36
13200	11200	12200	8.10	0.54	2.42	11.20	0.77	5.86	53.30	3.66	15.38
11200	6700	8950	3.60	0.24	1.88	24.80	1.70	5.09	73.80	5.07	11.72
6700	4750	5725	2.70	0.18	1.65	8.06	0.55	3.39	29.50	2.03	6.65
4750	3350	4050	1.80	0.12	1.47	6.09	0.42	2.84	17.80	1.22	4.62
3350	2360	2855	1.00	0.07	1.35	3.02	0.21	2.42	9.00	0.62	3.40
2360	1180	1770	1.40	0.09	1.28	3.67	0.25	2.22	10.40	0.71	2.78
1180	850	1015	0.50	0.03	1.19	1.25	0.09	1.97	2.80	0.19	2.06
850	600	725	0.40	0.03	1.16	1.12	0.08	1.88	2.10	0.14	1.87
335	180	257.5	5.80	0.38	1.13	10.16	0.70	1.80	8.70	0.60	1.73
125	75	100	9.50	0.63	0.75	14.09	0.97	1.11	12.30	0.85	1.13
75	0	37.5	1.80	0.12	0.12	2.08	0.14	0.14	4.10	0.28	0.28
			1513.40			1460.03			1454.90		

Dutoitspan

			Monovalent Cations					
Weathering Condition								
Weathering Time			6 Days LiCl			6 Days NH$_4$Cl		
Min. size	Max. size	Ave size	Weight	% in fraction	Cum % passing	Weight	% in fraction	Cum % passing
-	+	µm						
26500	22400	24450	315.30	21.31	100.00	918.40	63.05	100.00
22400	19000	20700	169.40	11.45	78.69	269.70	18.51	36.95
19000	16000	17500	171.70	11.61	67.24	86.10	5.91	18.44
16000	13200	14600	105.50	7.13	55.63	43.00	2.95	12.53
13200	11200	12200	177.00	11.96	48.50	30.20	2.07	9.58
11200	6700	8950	239.50	16.19	36.54	43.00	2.95	7.50
6700	4750	5725	119.90	8.10	20.35	12.50	0.86	4.55
4750	3350	4050	73.60	4.97	12.24	9.00	0.62	3.69
3350	2360	2855	34.50	2.33	7.27	3.40	0.23	3.08
2360	1180	1770	49.60	3.35	4.93	3.80	0.26	2.84
1180	850	1015	11.60	0.78	1.58	1.30	0.09	2.58
850	600	725	6.20	0.42	0.80	0.80	0.05	2.49
335	180	257.5	5.30	0.36	0.38	10.40	0.71	2.44
125	75	100	0.20	0.01	0.02	21.00	1.44	1.72
75	0	37.5	0.10	0.01	0.01	4.10	0.28	0.28
			1479.40			1456.70		

C1.2   Influence of cations on weathering: Divalent cations

Dutoitspan

| Weathering Condition | | | Divalent Cations | | | | | | | | |
| Weathering Time | | | 0 Days | | | 6 Days CuCl$_2$ | | | 6 Days MgCl$_2$ | | |
Min. size	Max. size	Ave size	Weight	% in fraction	Cum % passing	Weight	% in fraction	Cum % passing	Weight	% in fraction	Cum % passing
-	+	μm	g								
26500	22400	24450	1237.00	81.74	100.00	25.20	1.61	100.00	561.50	37.63	100.00
22400	19000	20700	208.00	13.74	18.26	24.60	1.58	98.39	294.70	19.75	62.37
19000	16000	17500	31.80	2.10	4.52	40.60	2.60	96.81	130.60	8.75	42.61
16000	13200	14600	0.00	0.00	2.42	6.00	0.38	94.21	87.40	5.86	33.86
13200	11200	12200	8.10	0.54	2.42	1.10	0.07	93.82	85.40	5.72	28.00
11200	6700	8950	3.60	0.24	1.88	35.40	2.27	93.75	127.90	8.57	22.28
6700	4750	5725	2.70	0.18	1.65	38.50	2.47	91.49	53.00	3.55	13.71
4750	3350	4050	1.80	0.12	1.47	89.80	5.75	89.02	35.60	2.39	10.15
3350	2360	2855	1.00	0.07	1.35	92.10	5.90	83.27	19.80	1.33	7.77
2360	1180	1770	1.40	0.09	1.28	384.40	24.63	77.37	31.20	2.09	6.44
1180	850	1015	0.50	0.03	1.19	180.70	11.58	52.74	8.90	0.60	4.35
850	600	725	0.40	0.03	1.16	162.60	10.42	41.17	6.90	0.46	3.75
335	180	257.5	5.80	0.38	1.13	362.00	23.19	30.75	22.70	1.52	3.29
125	75	100	9.50	0.63	0.75	100.00	6.41	7.56	19.90	1.33	1.77
75	0	37.5	1.80	0.12	0.12	18.00	1.15	1.15	6.50	0.44	0.44
			1513.40			1561.00			1492.00		

Dutoitspan

| Weathering Condition | | | Divalent Cations | | | | | |
| Weathering Time | | | 6 Days CaCl$_2$ | | | 6 Days FeCl$_2$ | | |
Min. size	Max. size	Ave size	Weight	% in fraction	Cum % passing	Weight	% in fraction	Cum % passing
-	+	μm						
26500	22400	24450	359.10	24.04	100.00	291.40	19.17	100.00
22400	19000	20700	266.70	17.86	75.96	213.20	14.03	80.83
19000	16000	17500	119.50	8.00	58.10	165.60	10.90	66.80
16000	13200	14600	180.70	12.10	50.10	113.90	7.49	55.90
13200	11200	12200	92.50	6.19	38.00	129.80	8.54	48.41
11200	6700	8950	211.50	14.16	31.80	280.80	18.47	39.87
6700	4750	5725	85.20	5.70	17.64	148.20	9.75	21.40
4750	3350	4050	58.60	3.92	11.94	98.10	6.45	11.65
3350	2360	2855	26.50	1.77	8.01	37.00	2.43	5.19
2360	1180	1770	35.60	2.38	6.24	34.90	2.30	2.76
1180	850	1015	10.00	0.67	3.86	3.80	0.25	0.46
850	600	725	7.40	0.50	3.19	1.40	0.09	0.21
335	180	257.5	22.80	1.53	2.69	1.20	0.08	0.12
125	75	100	14.90	1.00	1.17	0.40	0.03	0.04
75	0	37.5	2.50	0.17	0.17	0.20	0.01	0.01
			1493.50			1519.90		

C1.2   Influence of cations on weathering: Trivalent cations

Dutoitspan											
Weathering Condition			Trivalent Cations								
Weathering Time			0 Days			6 Days FeCl$_3$			6 Days AlCl$_3$		
Min. size	Max. size	Ave size	Weight	% in fraction	Cum % passing	Weight	% in fraction	Cum % passing	Weight	% in fraction	Cum % passing
-	+	μm	g								
26500	22400	24450	1237.00	81.74	100.00	490.50	33.11	100.00	595.62	38.98	100.00
22400	19000	20700	208.00	13.74	18.26	288.80	19.50	66.89	260.05	17.02	61.02
19000	16000	17500	31.80	2.10	4.52	173.64	11.72	47.39	77.36	5.06	44.00
16000	13200	14600	0.00	0.00	2.42	75.89	5.12	35.67	105.46	6.90	38.94
13200	11200	12200	8.10	0.54	2.42	57.71	3.90	30.55	85.42	5.59	32.03
11200	6700	8950	3.60	0.24	1.88	122.32	8.26	26.65	169.50	11.09	26.44
6700	4750	5725	2.70	0.18	1.65	50.02	3.38	18.39	77.97	5.10	15.35
4750	3350	4050	1.80	0.12	1.47	31.40	2.12	15.02	43.00	2.81	10.25
3350	2360	2855	1.00	0.07	1.35	19.82	1.34	12.90	18.40	1.20	7.43
2360	1180	1770	1.40	0.09	1.28	39.84	2.69	11.56	29.41	1.92	6.23
1180	850	1015	0.50	0.03	1.19	18.91	1.28	8.87	10.33	0.68	4.30
850	600	725	0.40	0.03	1.16	15.62	1.05	7.59	7.70	0.50	3.63
335	180	257.5	5.80	0.38	1.13	66.04	4.46	6.54	30.28	1.98	3.12
125	75	100	9.50	0.63	0.75	24.53	1.66	2.08	16.02	1.05	1.14
75	0	37.5	1.80	0.12	0.12	6.28	0.42	0.42	1.44	0.09	0.09
			1513.40			1481.32			1527.96		

C1.3   Time dependence tests: Mg time tests (0.2 M)

Dutoitspan														
Weathering Condition			Time tests											
Weathering Time			0 Days			2 Days			6 Days			15 Days		
Min. size	Max. size	Ave size	Weight	% in fraction	Cum % passing	Weight	% in fraction	Cum % passing	Weight	% in fraction	Cum % passing	Weight	% in fraction	Cum % passing
-	+	μm	g			g			g			g		
26500	22400	24450	1173.44	78.19	100.00	578.75	39.29	100.00	362.5	24.33	100.00	290.5	19.50	100.00
22400	19000	20700	225.87	15.05	21.81	276.65	18.78	60.71	316.46	21.24	75.67	273	18.32	80.50
19000	16000	17500	34.2	2.28	6.76	159.01	10.80	41.92	116.8	7.84	54.43	126.7	8.50	62.18
16000	13200	14600	17.67	1.18	4.49	62.27	4.23	31.13	140.2	9.41	46.59	108.7	7.30	53.67
13200	11200	12200	10.72	0.71	3.31	69.57	4.72	26.90	117.08	7.86	37.19	90.8	6.09	46.38
11200	9500	10350	3.64	0.24	2.59	63.99	4.34	22.17	64.76	4.35	29.33	87.6	5.88	40.28
9500	6700	8100	5.39	0.36	2.35	83.74	5.69	17.83	130.19	8.74	24.98	149	10.00	34.40
6700	5600	6150	1.07	0.07	1.99	32.49	2.21	12.14	39.25	2.63	16.24	62.2	4.18	24.40
5600	4750	5175	1.9	0.13	1.92	22.55	1.53	9.94	28.93	1.94	13.61	40.8	2.74	20.22
4750	3350	4050	2.5	0.17	1.79	37.1	2.52	8.41	50.17	3.37	11.67	76.5	5.13	17.49
3350	1180	2265	2.84	0.19	1.63	40.15	2.73	5.89	59.56	4.00	8.30	95.2	6.39	12.35
1180	850	1015	0.62	0.04	1.44	5.78	0.39	3.16	10.06	0.68	4.30	16.4	1.10	5.96
850	335	592.5	1.63	0.11	1.40	10.65	0.72	2.77	17.99	1.21	3.63	27.4	1.84	4.86
335	180	257.5	3.15	0.21	1.29	8.75	0.59	2.05	13.43	0.90	2.42	16.7	1.12	3.02
180	75	127.5	9.4	0.63	1.08	14.22	0.97	1.45	14.68	0.99	1.52	17.7	1.19	1.90
75	0	37.5	6.8	0.45	0.45	7.18	0.49	0.49	7.97	0.53	0.53	10.6	0.71	0.71
			1500.84			1472.85			1490.03			1489.8		

C1.3   Time dependence tests: Cu time tests (0.2 M)

Dutoitspan

Weathering Condition			Time								
Weathering Time			0 Days			6 Hours CuSO$_4$			12 Hours CuSO$_4$		
Min. size	Max. size	Ave size	Weight	% in fraction	Cum % passing	Weight	% in fraction	Cum % passing	Weight	% in fraction	Cum % passing
-	+	µm	g			g			g		
26500	22400	24450	1237.00	81.74	100.00	554.60	38.37	100.00	71.00	4.73	100.00
22400	19000	20700	208.00	13.74	18.26	268.80	18.60	61.63	168.00	11.19	95.27
19000	16000	17500	31.80	2.10	4.52	163.40	11.30	43.04	308.40	20.54	84.08
16000	13200	14600	0.00	0.00	2.42	111.50	7.71	31.73	207.40	13.81	63.55
13200	11200	12200	8.10	0.54	2.42	57.40	3.97	24.02	128.40	8.55	49.73
11200	6700	8950	3.60	0.24	1.88	129.70	8.97	20.05	223.60	14.89	41.18
6700	4750	5725	2.70	0.18	1.65		0.00	11.08	91.10	6.07	26.29
4750	3350	4050	1.80	0.12	1.47	33.70	2.33	11.08	67.00	4.46	20.23
3350	2360	2855	1.00	0.07	1.35	16.80	1.16	8.74	41.20	2.74	15.76
2360	1180	1770	1.40	0.09	1.28	32.60	2.26	7.58	61.30	4.08	13.02
1180	850	1015	0.50	0.03	1.19	12.90	0.89	5.33	23.60	1.57	8.94
850	600	725	0.40	0.03	1.16	10.80	0.75	4.43	20.10	1.34	7.37
335	180	257.5	5.80	0.38	1.13	32.80	2.27	3.69	57.80	3.85	6.03
125	75	100	9.50	0.63	0.75	15.90	1.10	1.42	24.30	1.62	2.18
75	0	37.5	1.80	0.12	0.12	4.60	0.32	0.32	8.40	0.56	0.56
			1513.40			1445.50			1501.60		

Dutoitspan

Weathering Condition			Time					
Weathering Time			24 Hours CuSO$_4$			6 Days CuSO$_4$		
Min. size	Max. size	Ave size	Weight	% in fraction	Cum % passing	Weight	% in fraction	Cum % passing
-	+	µm	g			g		
26500	22400	24450	132.60	9.04	100.00	43.30	2.92	100.00
22400	19000	20700	94.60	6.45	90.96	0.00	0.00	97.08
19000	16000	17500	72.80	4.96	84.51	15.10	1.02	97.08
16000	13200	14600	149.30	10.18	79.55	15.00	1.01	96.07
13200	11200	12200	115.60	7.88	69.37	15.40	1.04	95.06
11200	6700	8950	226.30	15.43	61.49	71.90	4.84	94.02
6700	4750	5725	119.50	8.15	46.07	61.70	4.16	89.18
4750	3350	4050	109.60	7.47	37.92	113.70	7.66	85.02
3350	2360	2855	64.10	4.37	30.45	132.60	8.93	77.36
2360	1180	1770	127.30	8.68	26.08	459.30	30.94	68.43
1180	850	1015	58.20	3.97	17.40	133.30	8.98	37.50
850	600	725	42.30	2.88	13.44	106.40	7.17	28.52
335	180	257.5	103.80	7.08	10.55	220.20	14.83	21.35
125	75	100	36.40	2.48	3.48	68.90	4.64	6.52
75	0	37.5	14.60	1.00	1.00	27.90	1.88	1.88
			1467.00			1484.70		

C1.3   Time dependence tests: Cu time tests (0.5 M)

Dutoitspan

Weathering Condition			Time dependance								
Weathering Time			4 Hours			8 Hours			24 Hours		
Min. size	Max. size	Ave size	Weight	% in fraction	Cum % passing	Weight	% in fraction	Cum % passing	Weight	% in fraction	Cum % passing
-	+	µm	g			g			g		
16000	13200	14600	64.2	39.29	100.00	65.2	25.76	100.00	24.1	14.16	100.00
13200	11200	12200	47.0	28.76	60.71	39.1	15.45	74.24	9.5	5.58	85.84
11200	9500	10350	11.3	6.92	31.95	37.3	14.74	58.79	6.8	4.00	80.26
9500	6700	8100	11.3	6.92	25.03	37.0	14.62	44.05	12.7	7.46	76.26
6700	4750	5725	8.6	5.26	18.12	15.7	6.20	29.44	12.9	7.58	68.80
4750	1180	2965	12.1	7.41	12.85	35.9	14.18	23.23	55.1	32.37	61.22
1180	600	890	2.4	1.47	5.45	7.8	3.08	9.05	20.4	11.99	28.85
600	335	467.5	1.9	1.16	3.98	5.1	2.02	5.97	9.0	5.29	16.86
335	75	205	4.2	2.57	2.82	9.0	3.56	3.95	17.6	10.34	11.57
	-75	37.5	0.4	0.24	0.24	1.0	0.40	0.40	2.1	1.23	1.23
			163.4			253.1			170.2		

Dutoitspan

Weathering Condition			Time dependance												
Weathering Time			48 Hours			168 Hours			360 Hours			720 Hours		
Min. size	Max. size	Ave size	Weight	% in fraction	Cum % passing	Weight	% in fraction	Cum % passing	Weight	% in fraction	Cum % passing	Weight	% in fraction	Cum % passing
-	+	µm	g			g			g					
16000	13200	14600	15.8	5.88	100.00	5.0	2.67	100.00	6.7	4.16	100.00	13.5	5.10	100.00
13200	11200	12200	16.0	5.96	94.12	3.8	2.03	97.33	0.0	0.00	95.84	1.7	0.65	94.90
11200	9500	10350	3.7	1.38	88.16	1.5	0.80	95.30	0.0	0.00	95.84	1.0	0.38	94.26
9500	6700	8100	31.4	11.69	86.78	1.9	1.01	94.50	6.8	4.22	95.84	3.9	1.47	93.88
6700	4750	5725	22.5	8.38	75.09	11.1	5.92	93.49	6.7	4.16	91.61	6.4	2.42	92.40
4750	1180	2965	105.1	39.13	66.72	89.5	47.76	87.57	64.5	40.06	87.45	106.0	40.01	89.99
1180	600	890	33.3	12.40	27.59	29.8	15.90	39.81	33.1	20.56	47.39	46.0	17.36	49.98
600	335	467.5	14.4	5.36	15.19	15.4	8.22	23.91	14.9	9.25	26.83	26.8	10.12	32.61
335	75	205	23.4	8.71	9.83	26.5	14.14	15.69	25.2	15.65	17.58	50.3	18.99	22.50
	-75	37.5	3.0	1.12	1.12	2.9	1.55	1.55	3.1	1.93	1.93	9.3	3.51	3.51
			268.6			187.4			161.0			264.9		

C1.4   Cation concentration

Dutoitspan

Weathering Condition			Concentration								
Weathering Time			0 Days			6 Days CuSO$_4$ (0.005 M)			6 Days CuSO$_4$ (0.025 M)		
Min. size	Max. size	Ave size	Weight	% in fraction	Cum % passing	Weight	% in fraction	Cum % passing	Weight	% in fraction	Cum % passing
-	+	µm	g			g			g		
26500	22400	24450	1237.00	81.74	100.00	857.10	57.37	100.00	309.10	21.02	100.00
22400	19000	20700	208.00	13.74	18.26	206.80	13.84	42.63	211.00	14.35	78.98
19000	16000	17500	31.80	2.10	4.52	180.40	12.07	28.79	183.10	12.45	64.63
16000	13200	14600	0.00	0.00	2.42	68.30	4.57	16.71	144.20	9.81	52.18
13200	11200	12200	8.10	0.54	2.42	39.30	2.63	12.14	108.10	7.35	42.37
11200	6700	8950	3.60	0.24	1.88	66.30	4.44	9.51	227.20	15.45	35.02
6700	4750	5725	2.70	0.18	1.65	24.50	1.64	5.07	81.80	5.56	19.57
4750	3350	4050	1.80	0.12	1.47	17.20	1.15	3.43	58.10	3.95	14.01
3350	2360	2855	1.00	0.07	1.35	7.50	0.50	2.28	35.20	2.39	10.06
2360	1180	1770	1.40	0.09	1.28	10.80	0.72	1.78	54.60	3.71	7.66
1180	850	1015	0.50	0.03	1.19	2.90	0.19	1.06	15.30	1.04	3.95
850	600	725	0.40	0.03	1.16	2.50	0.17	0.86	11.30	0.77	2.91
335	180	257.5	5.80	0.38	1.13	7.20	0.48	0.70	23.00	1.56	2.14
125	75	100	9.50	0.63	0.75	2.60	0.17	0.21	7.00	0.48	0.58
75	0	37.5	1.80	0.12	0.12	0.60	0.04	0.04	1.50	0.10	0.10
			1513.40			1494.00			1470.50		

Dutoitspan

Weathering Condition			Concentration											
Weathering Time			6 Days CuSO$_4$ (0.05 M)			6 Days CuSO$_4$ (0.1 M)			6 Days CuSO$_4$ (0.2 M)			6 Days CuSO$_4$ (0.4 M)		
Min. size	Max. size	Ave size	Weight	% in fraction	Cum % passing	Weight	% in fraction	Cum % passing	Weight	% in fraction	Cum % passing	Weight	% in fraction	Cum % passing
-	+	µm	g			g			g			g		
26500	22400	24450	81.30	5.58	100.00	117.20	7.78	100.00	43.50	2.86	100.00	43.30	2.92	100.00
22400	19000	20700	61.80	4.24	94.42	22.70	1.51	92.22	38.60	2.54	97.14	0.00	0.00	97.08
19000	16000	17500	114.20	7.84	90.17	48.40	3.21	90.71	29.70	1.96	94.59	15.10	1.02	97.08
16000	13200	14600	174.10	11.96	82.33	45.70	3.03	87.50	21.90	1.44	92.64	15.00	1.01	96.07
13200	11200	12200	119.40	8.20	70.37	38.20	2.54	84.46	27.10	1.78	91.20	15.40	1.04	95.06
11200	6700	8950	283.00	19.44	62.17	190.50	12.65	81.93	96.20	6.33	89.41	71.90	4.84	94.02
6700	4750	5725	127.40	8.75	42.73	123.60	8.21	69.28	97.10	6.39	83.08	61.70	4.16	89.18
4750	3350	4050	141.80	9.74	33.98	145.90	9.69	61.07	160.10	10.54	76.69	113.70	7.66	85.02
3350	2360	2855	81.30	5.58	24.24	187.60	12.46	51.38	135.70	8.93	66.15	132.60	8.93	77.36
2360	1180	1770	130.20	8.94	18.66	291.60	19.36	38.93	435.60	28.68	57.21	459.30	30.94	68.43
1180	850	1015	36.90	2.53	9.72	78.00	5.18	19.57	106.50	7.01	28.53	133.30	8.98	37.50
850	600	725	28.40	1.95	7.18	57.60	3.82	14.39	86.00	5.66	21.52	106.40	7.17	28.52
335	180	257.5	55.50	3.81	5.23	124.50	8.27	10.56	179.50	11.82	15.86	220.20	14.83	21.35
125	75	100	17.30	1.19	1.42	32.00	2.12	2.30	49.60	3.27	4.04	68.90	4.64	6.52
75	0	37.5	3.40	0.23	0.23	2.60	0.17	0.17	11.80	0.78	0.78	27.90	1.88	1.88
			1456.00			1506.10			1518.90			1484.70		

209

C1.5   Temperature tests

Dutoitspan

Weathering Condition			Temperature tests								
				0 Days		6 Days Water Room Temperature			6 Days MgCl$_2$ Room Temperature		
Weathering Time											
Min. size	Max. size	Ave size	Weight	% in fraction	Cum % passing	Weight	% in fraction	Cum % passing	Weight	% in fraction	Cum % passing
-	+	µm	g			g			g		
19000	16000	17500	1036.28	67.81	100.00	958.99	63.36	100.00	619.34	43.61	100.00
16000	13200	14600	409.33	26.79	32.19	338.21	22.34	36.64	335.27	23.61	56.39
13200	11200	12200	44.06	2.88	5.40	50.08	3.31	14.30	106.32	7.49	32.79
11200	9500	10350	6.41	0.42	2.52	35.68	2.36	10.99	60.89	4.29	25.30
9500	6700	8100	7.83	0.51	2.10	36.37	2.40	8.63	105.33	7.42	21.01
6700	5600	6150	1.59	0.10	1.58	12.06	0.80	6.23	46.15	3.25	13.60
5600	4750	5175	0.78	0.05	1.48	12.74	0.84	5.43	21.28	1.50	10.35
4750	3350	4050	2.52	0.16	1.43	17.30	1.14	4.59	42.31	2.98	8.85
3350	1180	2265	2.80	0.18	1.26	19.92	1.32	3.45	47.74	3.36	5.87
1180	850	1015	0.49	0.03	1.08	3.03	0.20	2.13	6.03	0.42	2.51
850	335	592.5	1.16	0.08	1.05	6.31	0.42	1.93	8.79	0.62	2.08
335	180	257.5	1.80	0.12	0.97	5.05	0.33	1.52	5.94	0.42	1.46
180	75	127.5	8.06	0.53	0.86	9.52	0.63	1.18	8.24	0.58	1.05
75	0	37.5	5.02	0.33	0.33	8.39	0.55	0.55	6.61	0.47	0.47
			1528.13			1513.65			1420.24		

Dutoitspan

Weathering Condition			Temperature tests					
			6 Days Water 40 °C			6 Days MgCl$_2$ 40 °C		
Weathering Time								
Min. size	Max. size	Ave size	Weight	% in fraction	Cum % passing	Weight	% in fraction	Cum % passing
-	+	µm	g			g		
19000	16000	17500	482.30	32.52	100.00	280.40	18.72	100.00
16000	13200	14600	422.00	28.46	67.48	314.10	20.97	81.28
13200	11200	12200	151.00	10.18	39.02	161.20	10.76	60.31
11200	9500	10350	77.70	5.24	28.84	118.60	7.92	49.55
9500	6700	8100	115.40	7.78	23.60	205.10	13.69	41.64
6700	5600	6150	44.70	3.01	15.81	73.60	4.91	27.94
5600	4750	5175	28.90	1.95	12.80	53.60	3.58	23.03
4750	3350	4050	50.30	3.39	10.85	91.80	6.13	19.45
3350	1180	2265	54.30	3.66	7.46	108.60	7.25	13.32
1180	850	1015	7.80	0.53	3.80	17.30	1.15	6.07
850	335	592.5	13.10	0.88	3.27	28.00	1.87	4.92
335	180	257.5	10.40	0.70	2.39	18.30	1.22	3.05
180	75	127.5	14.50	0.98	1.69	18.60	1.24	1.83
75	0	37.5	10.50	0.71	0.71	8.80	0.59	0.59
			1482.90			1498.00		

C1.6   Influence of anions

Dutoitspan											
Weathering Condition			**Anion Effect**								
Weathering Time			0 Days			6 Days CuCl$_2$			6 Days CuSO$_4$		
Min. size	Max. size	Ave size	Weight	% in fraction	Cum % passing	Weight	% in fraction	Cum % passing	Weight	% in fraction	Cum % passing
-	+	μm	g			g			g		
26500	22400	24450	1237.00	81.74	100.00	25.20	1.61	100.00	43.30	2.92	100.00
22400	19000	20700	208.00	13.74	18.26	24.60	1.58	98.39	0.00	0.00	97.08
19000	16000	17500	31.80	2.10	4.52	40.60	2.60	96.81	15.10	1.02	97.08
16000	13200	14600	0.00	0.00	2.42	6.00	0.38	94.21	15.00	1.01	96.07
13200	11200	12200	8.10	0.54	2.42	1.10	0.07	93.82	15.40	1.04	95.06
11200	6700	8950	3.60	0.24	1.88	35.40	2.27	93.75	71.90	4.84	94.02
6700	4750	5725	2.70	0.18	1.65	38.50	2.47	91.49	61.70	4.16	89.18
4750	3350	4050	1.80	0.12	1.47	89.80	5.75	89.02	113.70	7.66	85.02
3350	2360	2855	1.00	0.07	1.35	92.10	5.90	83.27	132.60	8.93	77.36
2360	1180	1770	1.40	0.09	1.28	384.40	24.63	77.37	459.30	30.94	68.43
1180	850	1015	0.50	0.03	1.19	180.70	11.58	52.74	133.30	8.98	37.50
850	600	725	0.40	0.03	1.16	162.60	10.42	41.17	106.40	7.17	28.52
335	180	257.5	5.80	0.38	1.13	362.00	23.19	30.75	220.20	14.83	21.35
125	75	100	9.50	0.63	0.75	100.00	6.41	7.56	68.90	4.64	6.52
75	0	37.5	1.80	0.12	0.12	18.00	1.15	1.15	27.90	1.88	1.88
			1513.40			1561.00			1484.70		

C1.7   Particle size tests

Dutoitspan											
Weathering Condition			**Particle size investigation**								
Weathering Time			0 Days			2 Days MgCl$_2$			6 Days MgCl$_2$		
Particle Size			- 26.5 + 22.4 mm			- 26.5 + 22.4 mm			- 26.5 + 22.4 mm		
Min. size	Max. size	Ave size	Weight	% in fraction	Cum % passing	Weight	% in fraction	Cum % passing	Weight	% in fraction	Cum % passing
-	+	μm	g			g			g		
26500	22400	24450	1237	81.30	100.00	578.75	39.29	100.00	362.5	24.33	100.00
22400	19000	20700	208	13.67	18.70	276.65	18.78	60.71	316.46	21.24	75.67
19000	16000	17500	31.8	2.09	5.03	159.01	10.80	41.92	116.8	7.84	54.43
16000	13200	14600	0	0.00	2.94	62.27	4.23	31.13	140.2	9.41	46.59
13200	11200	12200	8.1	0.53	2.94	69.57	4.72	26.90	117.08	7.86	37.19
11200	9500	10350	3.6	0.24	2.41	63.99	4.34	22.17	64.76	4.35	29.33
9500	6700	8100	2.7	0.18	2.17	83.74	5.69	17.83	130.19	8.74	24.98
6700	5600	6150	1.8	0.12	1.99	32.49	2.21	12.14	39.25	2.63	16.24
5600	4750	5175	1	0.07	1.88	22.55	1.53	9.94	28.93	1.94	13.61
4750	3350	4050	1.4	0.09	1.81	37.1	2.52	8.41	50.17	3.37	11.67
3350	1180	2265	0.5	0.03	1.72	40.15	2.73	5.89	59.56	4.00	8.30
1180	850	1015	0.4	0.03	1.69	5.78	0.39	3.16	10.06	0.68	4.30
850	335	592.5	5.8	0.38	1.66	10.65	0.72	2.77	17.99	1.21	3.63
335	180	257.5	9.5	0.62	1.28	8.75	0.59	2.05	13.43	0.90	2.42
180	75	127.5	1.8	0.12	0.65	14.22	0.97	1.45	14.68	0.99	1.52
75	0	37.5	8.14	0.53	0.53	7.18	0.49	0.49	7.97	0.53	0.53
			1521.54			1472.85			1490.03		

Dutoitspan

Weathering Condition			Particle size investigation												
Weathering Time			0 Days			6 Days MgCl$_2$			0 Days			6 Days MgCl$_2$		
Particle Size			- 22.4 + 19 mm			- 22.4 + 19 mm			- 19 + 16 mm			- 19 + 16 mm		
Min. size	Max. size	Ave size	Weight	% in fraction	Cum % passing	Weight	% in fraction	Cum % passing	Weight	% in fraction	Cum % passing	Weight	% in fraction	Cum % passing
-	+	μm	g			g			g			g		
22400	19000	20700	1078.00	72.82	100.00	437.28	29.30	100.00						
19000	16000	17500	315.30	21.30	27.18	308.88	20.69	70.70	1036.28	68.46	100.00	519.34	34.62	100.00
16000	13200	14600	33.40	2.26	5.88	142.65	9.56	50.01	409.33	27.04	31.54	355.27	23.68	65.38
13200	11200	12200	23.00	1.55	3.62	104.77	7.02	40.45	16.74	1.11	4.50	126.32	8.42	41.70
11200	9500	10350	12.50	0.84	2.07	81.44	5.46	33.43	6.41	0.42	3.39	80.89	5.39	33.28
9500	6700	8100	2.10	0.14	1.22	119.38	8.00	27.98	7.83	0.52	2.97	105.33	7.02	27.89
6700	5600	6150	2.50	0.17	1.08	54.36	3.64	19.98	1.59	0.11	2.45	66.15	4.41	20.87
5600	4750	5175	1.50	0.10	0.91	29.89	2.00	16.34	0.78	0.05	2.35	51.28	3.42	16.46
4750	3350	4050	1.50	0.10	0.81	60.48	4.05	14.33	2.52	0.17	2.30	72.31	4.82	13.04
3350	1180	2265	0.20	0.01	0.71	78.05	5.23	10.28	2.80	0.18	2.13	57.74	3.85	8.22
1180	850	1015	0.10	0.01	0.70	12.92	0.87	5.05	0.49	0.03	1.94	20.03	1.34	4.37
850	335	592.5	0.30	0.02	0.69	21.12	1.41	4.19	1.16	0.08	1.91	12.79	0.85	3.04
335	180	257.5	1.80	0.12	0.67	16.59	1.11	2.77	14.71	0.97	1.84	9.94	0.66	2.19
180	75	127.5	2.13	0.14	0.55	16.36	1.10	1.66	8.06	0.53	0.86	12.24	0.82	1.52
75	0	37.5	5.98	0.40	0.40	8.44	0.57	0.57	5.02	0.33	0.33	10.61	0.71	0.71
			1480.31			1492.61			1513.72			1500.24		

Du Toit Span

Weathering Condition			Particle size investigation					
Weathering Time			0 Days			6 Days MgCl$_2$		
Particle Size			- 16 + 13.2 mm			- 16 + 13.2 mm		
Min. size	Max. size	Ave size	Weight	% in fraction	Cum % passing	Weight	% in fraction	Cum % passing
-	+	μm	g			g		
16000	13200	14600	990.22	66.06	100.00	390.22	26.03	100.00
13200	11200	12200	391.74	26.13	33.94	299.19	19.96	73.97
11200	9500	10350	65.82	4.39	7.80	171.08	11.41	54.01
9500	6700	8100	17.83	1.19	3.41	234.35	15.63	42.60
6700	5600	6150	3.94	0.26	2.22	76.77	5.12	26.96
5600	4750	5175	3.24	0.22	1.96	42.56	2.84	21.84
4750	3350	4050	6.87	0.46	1.74	90.33	6.03	19.00
3350	1180	2265	5.25	0.35	1.29	106.27	7.09	12.98
1180	850	1015	0.70	0.05	0.94	17.86	1.19	5.89
850	335	592.5	1.35	0.09	0.89	27.45	1.83	4.70
335	180	257.5	1.44	0.10	0.80	16.85	1.12	2.87
180	75	127.5	6.08	0.41	0.70	15.93	1.06	1.74
75	0	37.5	4.46	0.30	0.30	10.18	0.68	0.68
			1498.94			1499.04		

213

C1.8   Influence of milling on weathering results

Dutoitspan											
Weathering Condition			Influence of milling								
Weathering Time			0 Days			12 Hours CuSO$_4$			12 Hours CuSO$_4$ MILLED		
Min. size	Max. size	Ave size	Weight	% in fraction	Cum % passing	Weight	% in fraction	Cum % passing	Weight	% in fraction	Cum % passing
-	+	µm	g			g			g		
26500	22400	24450	1237.00	81.74	100.00	71.00	4.73	100.00	168.4	11.21	100.00
22400	19000	20700	208.00	13.74	18.26	168.00	11.19	95.27	92.6	6.17	88.79
19000	16000	17500	31.80	2.10	4.52	308.40	20.54	84.08	102.9	6.85	82.62
16000	13200	14600	0.00	0.00	2.42	207.40	13.81	63.55	135.4	9.02	75.77
13200	11200	12200	8.10	0.54	2.42	128.40	8.55	49.73	106.5	7.09	66.75
11200	6700	8950	3.60	0.24	1.88	223.60	14.89	41.18	296.7	19.76	59.66
6700	4750	5725	2.70	0.18	1.65	91.10	6.07	26.29	135.5	9.02	39.90
4750	3350	4050	1.80	0.12	1.47	67.00	4.46	20.23	78	5.19	30.88
3350	2360	2855	1.00	0.07	1.35	41.20	2.74	15.76	43.6	2.90	25.68
2360	1180	1770	1.40	0.09	1.28	61.30	4.08	13.02	89.6	5.97	22.78
1180	850	1015	0.50	0.03	1.19	23.60	1.57	8.94	40.1	2.67	16.81
850	600	725	0.40	0.03	1.16	20.10	1.34	7.37	37.5	2.50	14.14
335	180	257.5	5.80	0.38	1.13	57.80	3.85	6.03	128.6	8.56	11.65
125	75	100	9.50	0.63	0.75	24.30	1.62	2.18	41.4	2.76	3.08
75	0	37.5	1.80	0.12	0.12	8.40	0.56	0.56	4.9	0.33	0.33
			1513.40			1501.60			1501.7		

C1.9   The effect of a stabilising cation vs. a swelling cation

Dutoitspan

Weathering Condition			Copper (swelling medium)								
Weathering Time			4 Hours			8 Hours			24 Hours		
Min. size	Max. size	Ave size	Weight	% in fraction	Cum % passing	Weight	% in fraction	Cum % passing	Weight	% in fraction	Cum % passing
-	+	µm	g			g			g		
16000	13200	14600	64.2	39.29	100.00	65.2	25.76	100.00	24.1	14.16	100.00
13200	11200	12200	47.0	28.76	60.71	39.1	15.45	74.24	9.5	5.58	85.84
11200	9500	10350	11.3	6.92	31.95	37.3	14.74	58.79	6.8	4.00	80.26
9500	6700	8100	11.3	6.92	25.03	37.0	14.62	44.05	12.7	7.46	76.26
6700	4750	5725	8.6	5.26	18.12	15.7	6.20	29.44	12.9	7.58	68.80
4750	1180	2965	12.1	7.41	12.85	35.9	14.18	23.23	55.1	32.37	61.22
1180	600	890	2.4	1.47	5.45	7.8	3.08	9.05	20.4	11.99	28.85
600	335	467.5	1.9	1.16	3.98	5.1	2.02	5.97	9.0	5.29	16.86
335	75	205	4.2	2.57	2.82	9.0	3.56	3.95	17.6	10.34	11.57
	-75	37.5	0.4	0.24	0.24	1.0	0.40	0.40	2.1	1.23	1.23
			163.4			253.1			170.2		

Dutoitspan

Weathering Condition			Copper (swelling medium)											
Weathering Time			48 Hours			168 Hours			360 Hours			720 Hours		
Min. size	Max. size	Ave size	Weight	% in fraction	Cum % passing	Weight	% in fraction	Cum % passing	Weight	% in fraction	Cum % passing	Weight	% in fraction	Cum % passing
-	+	µm	g			g			g					
16000	13200	14600	15.8	5.88	100.00	5.0	2.67	100.00	6.7	4.16	100.00	13.5	5.10	100.00
13200	11200	12200	16.0	5.96	94.12	3.8	2.03	97.33	0.0	0.00	95.84	1.7	0.65	94.90
11200	9500	10350	3.7	1.38	88.16	1.5	0.80	95.30	0.0	0.00	95.84	1.0	0.38	94.26
9500	6700	8100	31.4	11.69	86.78	1.9	1.01	94.50	6.8	4.22	95.84	3.9	1.47	93.88
6700	4750	5725	22.5	8.38	75.09	11.1	5.92	93.49	6.7	4.16	91.61	6.4	2.42	92.40
4750	1180	2965	105.1	39.13	66.72	89.5	47.76	87.57	64.5	40.06	87.45	106.0	40.01	89.99
1180	600	890	33.3	12.40	27.59	29.8	15.90	39.81	33.1	20.56	47.39	46.0	17.36	49.98
600	335	467.5	14.4	5.36	15.19	15.4	8.22	23.91	14.9	9.25	26.83	26.8	10.12	32.61
335	75	205	23.4	8.71	9.83	26.5	14.14	15.69	25.2	15.65	17.58	50.3	18.99	22.50
	-75	37.5	3.0	1.12	1.12	2.9	1.55	1.55	3.1	1.93	1.93	9.3	3.51	3.51
			268.6			187.4			161.0			264.9		

Dutoitspan

Weathering Condition			K (collapsing medium)								
Weathering Time			8 Hours			2 Days			6 Days		
Min. size	Max. size	Ave size	Weight	% in fraction	Cum % passing	Weight	% in fraction	Cum % passing	Weight	% in fraction	Cum % passing
-	+	µm	g								
16000	13200	14600	135.5	57.64	100.00	176.0	62.86	100.00	211.0	63.96	100.00
13200	11200	12200	74.5	31.69	42.36	66.9	23.89	37.14	84.2	25.52	36.04
6700	4750	5725	19.0	8.08	10.68	31.1	11.11	13.25	28.1	8.52	10.52
600	335	467.5	5.2	2.21	2.59	5.4	1.93	2.14	6.0	1.82	2.00
335	0	167.5	0.9	0.38	0.38	0.6	0.21	0.21	0.6	0.18	0.18
			235.1			280.0			329.9		

C1.10 Repeatability of results

Dutoitspan

Weathering Condition			Repeatability								
Weathering Time			2 Days 0.025 M Cu			2 Days 0.025 M Cu			2 Days 0.025 M Cu		
Min. size	Max. size	Ave size	Weight	% in fraction	Cum % passing	Weight	% in fraction	Cum % passing	Weight	% in fraction	Cum % passing
-	+	μm	g								
16000	13200	14600	89.40	45.38	100.00	86.20	44.14	100.00	99.40	51.13	100.00
13200	11200	12200	60.70	30.81	54.62	53.70	27.50	55.86	49.90	25.67	48.87
11200	9500	10350	16.10	8.17	23.81	17.10	8.76	28.37	11.50	5.92	23.20
9500	6700	8100	16.80	8.53	15.63	16.70	8.55	19.61	13.00	6.69	17.28
6700	4750	5725	4.10	2.08	7.11	8.50	4.35	11.06	6.90	3.55	10.60
4750	1180	2965	7.60	3.86	5.03	10.00	5.12	6.71	10.40	5.35	7.05
1180	600	890	0.90	0.46	1.17	1.20	0.61	1.59	1.30	0.67	1.70
600	335	467.5	0.50	0.25	0.71	0.70	0.36	0.97	0.70	0.36	1.03
335	75	205	0.80	0.41	0.46	1.10	0.56	0.61	1.20	0.62	0.67
	-75	37.5	0.10	0.05	0.05	0.10	0.05	0.05	0.10	0.05	0.05
			197.00			195.30			194.40		

Dutoitspan

Weathering Condition			Repeatability								
Weathering Time			2 Days 0.1 M Cu			2 Days 0.1 M Cu			2 Days 0.1 M Cu		
Min. size	Max. size	Ave size	Weight	% in fraction	Cum % passing	Weight	% in fraction	Cum % passing	Weight	% in fraction	Cum % passing
-	+	μm	g								
16000	13200	14600	61.70	30.22	100.00	49.80	25.53	100.00	62.9	32.08	100.00
13200	11200	12200	46.40	22.72	69.78	43.30	22.19	74.47	29.2	14.89	67.92
11200	9500	10350	23.00	11.26	47.06	24.70	12.66	52.28	31.10	15.86	53.03
9500	6700	8100	28.50	13.96	35.80	31.00	15.89	39.62	25.90	13.21	37.17
6700	4750	5725	12.50	6.12	21.84	14.50	7.43	23.73	13.00	6.63	23.97
4750	1180	2965	22.30	10.92	15.72	21.70	11.12	16.30	23.50	11.98	17.34
1180	600	890	3.10	1.52	4.80	3.50	1.79	5.18	3.70	1.89	5.35
600	335	467.5	2.90	1.42	3.28	2.10	1.08	3.38	2.00	1.02	3.47
335	75	205	3.00	1.47	1.86	3.80	1.95	2.31	4.00	2.04	2.45
	-75	37.5	0.80	0.39	0.39	0.70	0.36	0.36	0.80	0.41	0.41
			204.20			195.10			196.1		

Dutoitspan

Weathering Condition			Repeatability								
Weathering Time			2 Days 0.5 M Cu			2 Days 0.5 M Cu			2 Days 0.5 M Cu		
Min. size	Max. size	Ave size	Weight	% in fraction	Cum % passing	Weight	% in fraction	Cum % passing	Weight	% in fraction	Cum % passing
-	+	μm	g								
16000	13200	14600	12.60	6.41	100.00	20.10	10.48	100.00	14.7	7.70	100.00
13200	11200	12200	11.80	6.00	93.59	6.70	3.49	89.52	2.7	1.42	92.30
11200	9500	10350	7.40	3.76	87.59	5.50	2.87	86.03	5.30	2.78	90.88
9500	6700	8100	16.00	8.14	83.83	17.20	8.97	83.16	12.80	6.71	88.10
6700	4750	5725	17.80	9.05	75.69	19.20	10.01	74.19	22.60	11.84	81.39
4750	1180	2965	82.60	42.01	66.63	78.50	40.93	64.18	88.40	46.33	69.55
1180	600	890	20.10	10.22	24.62	17.90	9.33	23.25	17.80	9.33	23.22
600	335	467.5	9.10	4.63	14.39	9.20	4.80	13.92	9.40	4.93	13.89
335	75	205	17.20	8.75	9.77	15.60	8.13	9.12	14.90	7.81	8.96
	-75	37.5	2.00	1.02	1.02	1.90	0.99	0.99	2.20	1.15	1.15
			196.60			191.80			190.8		

C2:   Data on Geluk Wes

C2.1   Standard Weathering test

Geluk Wes								
Weathering Condition			**Standard weathering test**					
Weathering Time			0 Days			15 Days		
Min. size	Max. size	Ave size	Weight	% in fraction	Cum % passing	Weight	% in fraction	Cum % passing
-	+	μm	g			g		
19000	16000	17500	1094.34	71.02	100.00	1012.00	67.72	100.00
16000	13200	14600	347.96	22.58	28.98	318.03	21.28	32.28
13200	11200	12200	35.02	2.27	6.40	42.72	2.86	11.00
11200	6700	8950	19.54	1.27	4.13	44.50	2.98	8.14
6700	4750	5725	5.74	0.37	2.86	15.11	1.01	5.16
4750	3350	4050	4.88	0.32	2.49	11.04	0.74	4.15
3350	2360	2855	2.61	0.17	2.17	5.25	0.35	3.41
2360	1180	1770	3.47	0.23	2.00	8.05	0.54	3.06
1180	850	1015	0.89	0.06	1.77	3.26	0.22	2.52
850	600	725	0.89	0.06	1.72	2.68	0.18	2.31
600	335	467.5	1.36	0.09	1.66	4.24	0.28	2.13
335	180	257.5	2.40	0.16	1.57	5.70	0.38	1.84
180	125	152.5	2.13	0.14	1.42	3.26	0.22	1.46
125	75	100	5.47	0.35	1.28	6.09	0.41	1.24
75	0	37.5	14.21	0.92	0.92	12.48	0.84	0.84
			1540.91			1494.41		

C2.2 Sodium-, lithium-, aluminium- chloride media (0.2 M)

Geluk Wes

Weathering Condition			Investigating the weathering media								
Weathering Time			0 Days			6 Days H$_2$O			6 Days NaCl		
Min. size	Max. size	Ave size	Weight	% in fraction	Cum % passing	Weight	% in fraction	Cum % passing	Weight	% in fraction	Cum % passing
-	+	μm	g			g			g		
22400	19000	20700	1107.75	75.73	100.00	942.64	62.52	100.00	962.44	63.56	100.00
19000	16000	17500	267.30	18.27	24.27	440.80	29.24	37.48	400.39	26.44	36.44
16000	13200	14600	28.56	1.95	6.00	15.80	1.05	8.25	39.43	2.60	10.00
13200	11200	12200	10.21	0.70	4.05	15.75	1.04	7.20	16.82	1.11	7.40
11200	6700	8950	5.05	0.35	3.35	19.60	1.30	6.15	17.06	1.13	6.28
6700	4750	5725	8.36	0.57	3.00	21.23	1.41	4.85	21.05	1.39	5.16
4750	3350	4050	1.28	0.09	2.43	3.36	0.22	3.45	4.15	0.27	3.77
3350	2360	2855	2.94	0.20	2.35	7.53	0.50	3.22	8.56	0.57	3.49
2360	1180	1770	1.26	0.09	2.14	4.07	0.27	2.72	3.90	0.26	2.93
1180	850	1015	2.00	0.14	2.06	5.24	0.35	2.45	5.42	0.36	2.67
850	600	725	0.80	0.05	1.92	2.16	0.14	2.11	2.19	0.14	2.31
600	335	467.5	2.11	0.14	1.87	5.76	0.38	1.96	4.95	0.33	2.17
335	180	257.5	3.67	0.25	1.72	6.40	0.42	1.58	5.57	0.37	1.84
180	125	152.5	2.97	0.20	1.47	4.65	0.31	1.16	4.24	0.28	1.47
125	75	100	8.99	0.61	1.27	6.61	0.44	0.85	9.18	0.61	1.19
75	0	37.5	9.57	0.65	0.65	6.17	0.41	0.41	8.90	0.59	0.59
			1462.82			1507.77			1514.25		

Geluk Wes

Weathering Condition			Investigating the weathering media								
Weathering Time			6 Days NaCl + Acid			6 Days AlCl$_3$			6 Days LiCl		
Min. size	Max. size	Ave size	Weight	% in fraction	Cum % passing	Weight	% in fraction	Cum % passing	Weight	% in fraction	Cum % passing
-	+	μm	g			g			g		
22400	19000	20700	950.58	62.95	100.00	738.62	49.65	100.00	564.78	38.10	100.83
19000	16000	17500	370.67	24.55	37.05	359.04	24.13	50.35	396.30	27.09	62.74
16000	13200	14600	46.59	3.09	12.50	127.97	8.60	26.22	90.96	6.22	35.65
13200	11200	12200	30.94	2.05	9.41	25.18	1.69	17.61	55.60	3.80	29.43
11200	6700	8950	20.57	1.36	7.37	26.85	1.80	15.92	38.47	2.63	25.63
6700	4750	5725	26.98	1.79	6.00	71.87	4.83	14.12	78.60	5.37	23.00
4750	3350	4050	4.78	0.32	4.22	10.53	0.71	9.29	18.89	1.29	17.62
3350	2360	2855	10.13	0.67	3.90	19.28	1.30	8.58	36.16	2.47	16.33
2360	1180	1770	3.76	0.25	3.23	9.71	0.65	7.28	16.87	1.15	13.86
1180	850	1015	6.62	0.44	2.98	17.45	1.17	6.63	33.58	2.30	12.71
850	600	725	2.50	0.17	2.54	6.70	0.45	5.46	12.99	0.89	10.41
600	335	467.5	5.65	0.37	2.38	16.45	1.11	5.01	33.47	2.29	9.52
335	180	257.5	6.57	0.44	2.00	15.73	1.06	3.90	32.05	2.19	7.24
180	125	152.5	3.96	0.26	1.57	8.64	0.58	2.84	19.78	1.35	5.05
125	75	100	10.80	0.72	1.30	14.09	0.95	2.26	28.41	1.94	3.69
75	0	37.5	8.90	0.59	0.59	19.55	1.31	1.31	25.61	1.75	1.75
			1510.00			1487.66			1482.52		

C3:   Data on Koffiefontein

Koffiefontein											
Weathering Condition			**Standard weathering test**								
Weathering Time			0 Days			1 Hour			3 Hours		
Min. size	Max. size	Ave size	Weight	% in fraction	Cum % passing	Weight	% in fraction	Cum % passing	Weight	% in fraction	Cum % passing
-	+	μm	g			g			g		
26500	22400	24450	1151.10	77.91	100.00	411.78	27.08	100.00	44.90	3.01	100.00
22400	19000	20700	221.80	15.01	22.09	345.33	22.71	72.92	228.70	15.32	96.99
19000	16000	17500	37.00	2.50	7.08	72.61	4.78	50.20	165.60	11.10	81.67
16000	13200	14600	16.00	1.08	4.58	84.30	5.54	45.43	129.80	8.70	70.57
13200	11200	12200	2.70	0.18	3.49	42.23	2.78	39.88	53.50	3.58	61.87
11200	9500	10350	4.50	0.30	3.31	29.69	1.95	37.10	57.80	3.87	58.29
9500	6700	8100	11.90	0.81	3.01	71.93	4.73	35.15	128.30	8.60	54.42
6700	4750	5725	2.20	0.15	2.20	60.13	3.95	30.42	55.80	3.74	45.82
4750	3350	4050	1.50	0.10	2.05	33.32	2.19	26.47	51.30	3.44	42.08
3350	1180	2265	2.20	0.15	1.95	89.79	5.91	24.27	125.20	8.39	38.64
1180	850	1015	3.90	0.26	1.80	176.95	11.64	18.37	216.40	14.50	30.25
850	335	592.5	0.90	0.06	1.54	29.09	1.91	6.73	44.10	2.95	15.75
335	180	257.5	1.90	0.13	1.48	43.94	2.89	4.82	93.80	6.29	12.80
180	75	127.5	3.00	0.20	1.35	18.12	1.19	1.93	44.20	2.96	6.51
125	75	100	8.60	0.58	1.14	9.08	0.60	0.74	28.60	1.92	3.55
75	0	37.5	8.30	0.56	0.56	2.10	0.14	0.14	24.40	1.63	1.63
			1477.50			1520.39			1492.40		

219

C4: Data on Cullinan TKB

C4.1 Standard Weathering test

Premier TKB

Weathering Condition			Standard weathering test								
Weathering Time			0 Days			6 Days			15 Days		
Min. size	Max. size	Ave size	Weight	% in fraction	Cum % passing	Weight	% in fraction	Cum % passing	Weight	% in fraction	Cum % passing
-	+	μm	g			g			g		
19000	16000	17500	1188.07	77.49	100.00	1174.07	77.68	100.00	1194.93	79.01	100.00
16000	13200	14600	283.86	18.51	22.51	285.99	18.92	22.32	263.03	17.39	20.99
13200	11200	12200	32.83	2.14	4.00	20.72	1.37	3.40	23.70	1.57	3.60
11200	6700	8950	7.36	0.48	1.86	9.01	0.60	2.03	5.21	0.34	2.03
6700	4750	5725	1.58	0.10	1.38	1.65	0.11	1.43	1.87	0.12	1.69
4750	3350	4050	1.89	0.12	1.28	2.66	0.18	1.32	3.06	0.20	1.57
3350	2360	2855	0.89	0.06	1.15	1.04	0.07	1.15	1.10	0.07	1.36
2360	1180	1770	1.52	0.10	1.09	2.09	0.14	1.08	2.52	0.17	1.29
1180	850	1015	0.60	0.04	1.00	0.66	0.04	0.94	0.83	0.05	1.12
850	600	725	0.47	0.03	0.96	0.53	0.04	0.90	0.60	0.04	1.07
600	335	467.5	0.71	0.05	0.93	0.83	0.05	0.86	0.99	0.07	1.03
335	180	257.5	1.42	0.09	0.88	1.86	0.12	0.81	1.99	0.13	0.96
180	125	152.5	1.18	0.08	0.79	1.06	0.07	0.68	1.67	0.11	0.83
125	75	100	1.92	0.13	0.71	3.16	0.21	0.61	3.25	0.21	0.72
75	0	37.5	8.96	0.58	0.58	6.12	0.40	0.40	7.66	0.51	0.51
			1533.26			1511.45			1512.41		

C4.2   Sodium chloride media

Premier TKB											
Weathering Condition			Sodium Chloride Media									
Weathering Time			0 Days			6 Days			15 Days		
Min. size	Max. size	Ave size	Weight	% in fraction	Cum % passing	Weight	% in fraction	Cum % passing	Weight	% in fraction	Cum % passing
-	+	µm	g			g			g		
19000	16000	17500	1188.07	79.10	100.00	1041.39	70.54	100.00	1084.90	72.61	100.00
16000	13200	14600	283.86	18.90	20.90	370.04	25.06	29.46	327.30	21.91	27.39
13200	11200	12200	1.59	0.11	2.00	19.38	1.31	4.40	22.40	1.50	5.48
11200	6700	8950	7.36	0.49	1.90	10.24	0.69	3.09	5.40	0.36	3.98
6700	4750	5725	1.58	0.11	1.41	3.32	0.22	2.39	2.50	0.17	3.62
4750	3350	4050	1.89	0.13	1.30	3.17	0.21	2.17	5.20	0.35	3.45
3350	2360	2855	0.89	0.06	1.18	2.62	0.18	1.95	3.00	0.20	3.11
2360	1180	1770	1.52	0.10	1.12	4.05	0.27	1.78	7.90	0.53	2.90
1180	850	1015	0.60	0.04	1.02	1.58	0.11	1.50	4.50	0.30	2.38
850	600	725	0.47	0.03	0.98	1.59	0.11	1.40	4.00	0.27	2.07
600	335	467.5	0.71	0.05	0.94	2.58	0.17	1.29	5.20	0.35	1.81
335	180	257.5	1.42	0.09	0.90	3.69	0.25	1.11	6.30	0.42	1.46
180	125	152.5	1.18	0.08	0.80	1.97	0.13	0.86	2.50	0.17	1.04
125	75	100	1.92	0.13	0.72	3.71	0.25	0.73	4.80	0.32	0.87
75	0	37.5	8.96	0.60	0.60	7.06	0.48	0.48	8.20	0.55	0.55
			1502.02			1476.39			1494.10		

C5:   Data on Wesselton

C5.1   Standard Weathering test

Wesselton											
Weathering Condition			Standard weathering test								
Weathering Time			0 Days			6 Days			15 Days		
Min. size	Max. size	Ave size	Weight	% in fraction	Cum % passing	Weight	% in fraction	Cum % passing	Weight	% in fraction	Cum % passing
-	+	μm	g								
19000	16000	17500	1209.45	79.53	100.00	1130.68	75.08	100.00	1169	78.09	100.00
16000	13200	14600	244.34	16.07	20.47	253.76	16.85	24.92	192.25	12.84	21.91
13200	11200	12200	26.61	1.75	4.40	46.41	3.08	8.07	102.22	6.83	9.07
11200	6700	8950	6.62	0.44	2.65	37.66	2.50	4.99	4.73	0.32	2.25
6700	4750	5725	5.26	0.35	2.21	5.18	0.34	2.49	1.63	0.11	1.93
4750	3350	4050	2.87	0.19	1.87	3.79	0.25	2.14	4.13	0.28	1.82
3350	2360	2855	1.999	0.13	1.68	3.48	0.23	1.89	1.54	0.10	1.54
2360	1180	1770	2.35	0.15	1.55	3.84	0.25	1.66	2.31	0.15	1.44
1180	850	1015	0.99	0.07	1.39	0.84	0.06	1.40	0.72	0.05	1.29
850	600	725	0.84	0.06	1.33	1.35	0.09	1.35	0.83	0.06	1.24
600	335	467.5	1.55	0.10	1.27	1.73	0.11	1.26	1.36	0.09	1.18
335	180	257.5	2.4	0.16	1.17	2.81	0.19	1.14	2.48	0.17	1.09
180	125	152.5	1.6	0.11	1.01	1.79	0.12	0.96	1.38	0.09	0.93
125	75	100	3.31	0.22	0.91	3.38	0.22	0.84	3.25	0.22	0.83
75	0	37.5	10.5	0.69	0.69	9.24	0.61	0.61	9.25	0.62	0.62
			1520.694			1505.94			1497.08		

C5.2   Acid water media

Wesselton											
Weathering Condition			Acid media								
Weathering Time			0 Days			6 Days			15 Days		
Min. size	Max. size	Ave size	Weight	% in fraction	Cum % passing	Weight	% in fraction	Cum % passing	Weight	% in fraction	Cum % passing
-	+	μm	g								
19000	16000	17500	1209.45	79.78	100.00	1191.33	76.91	100.00	1153.02	76.13	100.00
16000	13200	14600	244.34	16.12	20.22	294.06	18.99	23.09	294.97	19.47	23.87
13200	11200	12200	21.86	1.44	4.10	17.80	1.15	4.10	22.19	1.46	4.40
11200	6700	8950	6.62	0.44	2.66	12.95	0.84	2.95	12.16	0.80	2.93
6700	4750	5725	5.26	0.35	2.22	4.64	0.30	2.11	2.75	0.18	2.13
4750	3350	4050	2.87	0.19	1.87	4.22	0.27	1.81	2.88	0.19	1.95
3350	2360	2855	1.999	0.13	1.68	2.01	0.13	1.54	2.26	0.15	1.76
2360	1180	1770	2.35	0.16	1.55	3.08	0.20	1.41	2.21	0.15	1.61
1180	850	1015	0.99	0.07	1.40	1	0.06	1.21	0.79	0.05	1.47
850	600	725	0.84	0.06	1.33	1.01	0.07	1.15	0.88	0.06	1.41
600	335	467.5	1.55	0.10	1.28	1.01	0.07	1.08	1.54	0.10	1.35
335	180	257.5	2.4	0.16	1.17	2.48	0.16	1.02	2.68	0.18	1.25
180	125	152.5	1.6	0.11	1.02	1.42	0.09	0.86	4.22	0.28	1.08
125	75	100	3.31	0.22	0.91	2.91	0.19	0.77	3.32	0.22	0.80
75	0	37.5	10.5	0.69	0.69	8.97	0.58	0.58	8.76	0.58	0.58
			1515.934			1548.892			1514.625		

C5.3   Sodium chloride media

Wesselton											
Weathering Condition			Sodium Chloride Media								
Weathering Time			0 Days			6 Days			15 Days		
Min. size	Max. size	Ave size	Weight	% in fraction	Cum % passing	Weight	% in fraction	Cum % passing	Weight	% in fraction	Cum % passing
-	+	μm	g								
19000	16000	17500	1209.45	79.70	100.00	1161.23	76.38	100.00	1164.5	76.77	100.00
16000	13200	14600	244.34	16.10	20.30	313.44	20.62	23.62	306.8	20.23	23.23
13200	11200	12200	23.45	1.55	4.20	28.91	1.90	3.00	16.90	1.11	3.00
11200	6700	8950	6.62	0.44	2.65	2.86	0.19	1.10	7.5	0.49	1.89
6700	4750	5725	5.26	0.35	2.22	1.95	0.13	0.91	1.6	0.11	1.39
4750	3350	4050	2.87	0.19	1.87	0.61	0.04	0.78	2.5	0.16	1.29
3350	2360	2855	1.999	0.13	1.68	0.12	0.01	0.74	0.9	0.06	1.12
2360	1180	1770	2.35	0.15	1.55	0.09	0.01	0.73	1.3	0.09	1.06
1180	850	1015	0.99	0.07	1.40	0.03	0.00	0.73	0.5	0.03	0.98
850	600	725	0.84	0.06	1.33	1.11	0.07	0.73	0.4	0.03	0.94
600	335	467.5	1.55	0.10	1.28	0.76	0.05	0.65	0.9	0.06	0.92
335	180	257.5	2.4	0.16	1.17	2.5	0.16	0.60	1.9	0.13	0.86
180	125	152.5	1.6	0.11	1.02	1.34	0.09	0.44	1.6	0.11	0.73
125	75	100	3.31	0.22	0.91	3.21	0.21	0.35	2.9	0.19	0.63
75	0	37.5	10.5	0.69	0.69	2.12	0.14	0.14	6.6	0.44	0.44
			1517.526			1520.278			1516.8		

C5.4   Cyclic water wetting

Wesselton											
Weathering Condition			**Cyclic Water wetting**								
Weathering Time			0 Days			6 Days			15 Days		
Min. size	Max. size	Ave size	Weight	% in fraction	Cum % passing	Weight	% in fraction	Cum % passing	Weight	% in fraction	Cum % passing
-	+	μm	g								
19000	16000	17500	1209.45	79.87	100.00	1134.24	76.49	100.00	1160.7	76.58	100.00
16000	13200	14600	244.34	16.13	20.13	290.15	19.57	23.51	291.22	19.22	23.42
13200	11200	12200	20.28	1.34	4.00	19.01	1.28	3.94	25.83	1.70	4.20
11200	6700	8950	6.62	0.44	2.66	11.16	0.75	2.66	6.87	0.45	2.50
6700	4750	5725	5.26	0.35	2.22	4.04	0.27	1.90	4.62	0.30	2.04
4750	3350	4050	2.87	0.19	1.88	2.93	0.20	1.63	3.15	0.21	1.74
3350	2360	2855	1.999	0.13	1.69	1.54	0.10	1.43	2.25	0.15	1.53
2360	1180	1770	2.35	0.16	1.55	2.03	0.14	1.33	1.95	0.13	1.38
1180	850	1015	0.99	0.07	1.40	0.79	0.05	1.19	0.77	0.05	1.25
850	600	725	0.84	0.06	1.33	0.73	0.05	1.14	1.3	0.09	1.20
600	335	467.5	1.55	0.10	1.28	1.19	0.08	1.09	2.24	0.15	1.12
335	180	257.5	2.4	0.16	1.18	2.43	0.16	1.01	1.48	0.10	0.97
180	125	152.5	1.6	0.11	1.02	1.24	0.08	0.85	1.5	0.10	0.87
125	75	100	3.31	0.22	0.91	2.44	0.16	0.76	2.8	0.18	0.77
75	0	37.5	10.5	0.69	0.69	8.88	0.60	0.60	8.89	0.59	0.59
			1514.362			1482.8			1515.574		

C5.5 Copper sulphate media

Wesselton

Weathering Condition			Copper media weathering								
Weathering Time			0 Days			6 Days Water			6 Days CuSO$_4$		
Min. size	Max. size	Ave size	Weight	% in fraction	Cum % passing	Weight	% in fraction	Cum % passing	Weight	% in fraction	Cum % passing
-	+	μm	g								
26500	22400	24450	1028.08	67.20	100.00	952.83	62.66	100.00	1089.30	70.08	100.00
22400	19000	20700	425.40	27.80	32.80	470.48	30.94	37.34	382.80	24.63	29.92
19000	16000	17500	44.21	2.89	5.00	50.36	3.31	6.40	46.97	3.02	5.30
16000	13200	14600	0.00	0.00	2.11	0.00	0.00	3.09	10.90	0.70	2.28
13200	11200	12200	0.00	0.00	2.11	2.20	0.14	3.09	0.00	0.00	1.58
11200	6700	8950	0.00	0.00	2.11	6.58	0.43	2.94	1.40	0.09	1.58
6700	4750	5725	3.86	0.25	2.11	9.09	0.60	2.51	1.00	0.06	1.49
4750	3350	4050	2.55	0.17	1.86	2.41	0.16	1.91	1.60	0.10	1.42
3350	2360	2855	1.68	0.11	1.69	2.21	0.15	1.75	0.00	0.00	1.32
2360	1180	1770	1.53	0.10	1.58	2.95	0.19	1.61	2.10	0.14	1.32
1180	850	1015	1.68	0.11	1.48	0.84	0.06	1.42	0.60	0.04	1.18
850	600	725	0.67	0.04	1.37	1.22	0.08	1.36	1.00	0.06	1.15
600	335	467.5	1.74	0.11	1.33	2.07	0.14	1.28	1.00	0.06	1.08
335	180	257.5	3.51	0.23	1.21	3.67	0.24	1.14	2.80	0.18	1.02
180	125	152.5	2.04	0.13	0.98	2.25	0.15	0.90	6.30	0.41	0.84
125	75	100	4.25	0.28	0.85	3.89	0.26	0.75	0.00	0.00	0.43
75	0	37.5	8.78	0.57	0.57	7.58	0.50	0.50	6.70	0.43	0.43
			1529.98			1520.63			1554.47		

C6:   Data on Venetia ores

Venetia											
Weathering Condition			Cu^{2+} weathering tests								
Kimberlite Name			K1 HYP NE			K1 HYP S			K1 TKB E		
Min. size	Max. size	Ave size	Weight	% in fraction	Cum % passing	Weight	% in fraction	Cum % passing	Weight	% in fraction	Cum % passing
-	+	μm	g			g			g		
26500	22400	24450	358.38	35.72	100.00	275.74	27.04	100.00	54.00	5.40	100.00
22400	19000	20700	460.77	45.92	64.28	580.83	56.96	72.96	151.58	15.15	94.60
19000	16000	17500	161.41	16.09	18.36	144.76	14.20	16.00	229.47	22.94	79.45
16000	13200	14600	19.38	1.93	2.27	17.45	1.71	1.80	117.28	11.72	56.52
13200	11200	12200	2.67	0.27	0.34	0.80	0.08	0.09	63.49	6.35	44.79
11200	9500	10350	0.70	0.07	0.07	0.10	0.01	0.01	59.92	5.99	38.45
9500	6700	8100	0.00	0.00	0.00	0.00	0.00	0.00	76.75	7.67	32.46
6700	5600	6150	0.00	0.00	0.00	0.00	0.00	0.00	17.59	1.76	24.79
5600	4750	5175	0.00	0.00	0.00	0.00	0.00	0.00	14.33	1.43	23.03
4750	3350	4050	0.00	0.00	0.00	0.00	0.00	0.00	26.97	2.70	21.60
3350	1180	2265	0.00	0.00	0.00	0.00	0.00	0.00	64.30	6.43	18.90
1180	850	1015	0.00	0.00	0.00	0.00	0.00	0.00	18.41	1.84	12.47
850	335	592.5	0.00	0.00	0.00	0.00	0.00	0.00	47.70	4.77	10.63
335	180	257.5	0.00	0.00	0.00	0.00	0.00	0.00	27.96	2.79	5.87
180	75	127.5	0.00	0.00	0.00	0.00	0.00	0.00	22.23	2.22	3.07
75	0	37.5	0.00	0.00	0.00	0.00	0.00	0.00	8.51	0.85	0.85
			1003.31			1019.68			1000.49		

Venetia

Weathering Condition			Cu^{2+} weathering tests								
Kimberlite Name			K2 NE			K2 S			K2 W		
Min. size	Max. size	Ave size	Weight	% in fraction	Cum % passing	Weight	% in fraction	Cum % passing	Weight	% in fraction	Cum % passing
-	+	μm	g			g			g		
26500	22400	24450	126.69	12.54	100.00	74.54	7.37	100.00	293.59	29.27	99.92
22400	19000	20700	313.29	31.00	87.46	193.80	19.16	92.63	347.80	34.67	70.65
19000	16000	17500	325.89	32.25	56.47	378.77	37.44	73.47	282.59	28.17	35.98
16000	13200	14600	58.81	5.82	24.22	119.44	11.81	36.03	20.78	2.07	7.80
13200	11200	12200	40.84	4.04	18.40	47.37	4.68	24.22	5.83	0.58	5.73
11200	9500	10350	16.83	1.67	14.36	23.35	2.31	19.54	14.35	1.43	5.15
9500	6700	8100	33.34	3.30	12.69	43.06	4.26	17.23	15.08	1.50	3.72
6700	5600	6150	13.50	1.34	9.40	21.35	2.11	12.98	7.87	0.78	2.21
5600	4750	5175	14.01	1.39	8.06	15.83	1.56	10.87	4.02	0.40	1.43
4750	3350	4050	19.89	1.97	6.67	27.41	2.71	9.30	4.21	0.42	1.03
3350	1180	2265	19.79	1.96	4.71	31.86	3.15	6.59	2.86	0.29	0.61
1180	850	1015	3.93	0.39	2.75	5.80	0.57	3.44	0.40	0.04	0.32
850	335	592.5	9.72	0.96	2.36	12.35	1.22	2.87	0.85	0.08	0.28
335	180	257.5	7.03	0.70	1.40	7.98	0.79	1.65	0.81	0.08	0.20
180	75	127.5	5.28	0.52	0.70	6.10	0.60	0.86	0.83	0.08	0.12
75	0	37.5	1.81	0.18	0.18	2.59	0.26	0.26	0.36	0.04	0.04
			1010.65			1011.60			1002.23		

Venetia

Weathering Condition			Cu^{2+} weathering tests					
Kimberlite Name			K8			RED		
Min. size	Max. size	Ave size	Weight	% in fraction	Cum % passing	Weight	% in fraction	Cum % passing
-	+	μm	g			g		
26500	22400	24450	353.47	35.24	100.00	23.26	2.27	100.00
22400	19000	20700	476.13	47.47	64.76	27.97	2.73	97.73
19000	16000	17500	153.37	15.29	17.29	161.05	15.72	95.00
16000	13200	14600	14.14	1.41	2.00	136.98	13.37	79.28
13200	11200	12200	1.52	0.15	0.59	128.21	12.51	65.91
11200	9500	10350	0.00	0.00	0.44	61.72	6.02	53.40
9500	6700	8100	0.40	0.04	0.44	94.14	9.19	47.37
6700	5600	6150	0.00	0.00	0.40	44.94	4.39	38.19
5600	4750	5175	0.00	0.00	0.40	37.18	3.63	33.80
4750	3350	4050	0.00	0.00	0.40	64.56	6.30	30.17
3350	1180	2265	1.02	0.10	0.40	123.87	12.09	23.87
1180	850	1015	0.87	0.09	0.30	24.92	2.43	11.78
850	335	592.5	0.66	0.07	0.21	42.16	4.11	9.35
335	180	257.5	0.42	0.04	0.14	21.84	2.13	5.23
180	75	127.5	0.65	0.06	0.10	13.60	1.33	3.10
75	0	37.5	0.38	0.04	0.04	18.17	1.77	1.77
			1003.03			1024.57		

APPENDIX D: SLAKE DURABILITY DATA

Sample Name	Slake Durability Id-1	Slake Durability Id-2	Slake Durability Id-3	Slake Durability Id-4
Venetia-Red Distilled Water	52.3	19.2	8.3	5
L732 T109 D9 Distilled Water	78.6	49.2	37.6	32.9
L732 T109 D13 Distilled Water	91.7	86.9	82.9	80.2
717L T66N Distilled Water	94.64	87.17	79.83	73.76
Venetia Hypabassal Distilled Water	99.32	99.08	98.99	98.90
Venetia-Red Potassium	51.6	26.4	20.2	18.5
L732 T109 D9 Potassium	87.8	77	70.1	64.8